Polymorphisms in Nitric Oxide Regulatory Enzymes and Effects on Vascular Function

Lisa Clare Jones

A thesis submitted in fulfillment of the requirements of the University of London for the Degree of Doctor of Philosophy

October 2003

Centre for Clinical Pharmacology
Department of Medicine
University College London

ProQuest LLC
789 East Eisenhower Parkway
P.O. Box 1346
Ann Arbor, MI 48106-1346

Abstract

Nitric oxide (NO) is an important signalling molecule of the central nervous system (CNS), immune system and vascular endothelium. In the vascular system NO acts as a vasodilator as well as having anti-thrombotic and atheroprotective functions. The development of cardiovascular disease (CVD) is a complex multifactorial process known to have a heritable component. The aim of this study therefore was to investigate the role of three candidate genes involved in regulation of NO synthesis and susceptibility to CVD.

This study investigated the association between cardiovascular risk factors and polymorphisms in the p22phox subunit of NADPH oxidase, GTPCH1 and DDAH2. This study showed the previously identified C242T polymorphism in p22phox was associated with endothelium-dependent vasodilation in healthy subjects. Individuals homozygous for the T allele exhibited increased endothelium-dependent vasodilation compared to C allele carriers. Single strand conformational polymorphism analysis (SSCP) identified four polymorphisms within the *GCH1* gene, three in the promoter (-577G/A, -741T/C and -796G/A) and one in intron 1 (599C/G). Genotyping of 2390 healthy men revealed an association between the -796 and -577 polymorphisms and circulating levels of neopterin. An association was also found between –796 genotype and endothelial function in a second cohort of 246 healthy subjects. SSCP of the *DDAH2* gene identified six polymorphisms. Five in the promoter region at position -1415G/A, -1151C/A, -1020C/G, -871 6G/7G and -449C/G and the sixth at position 618C/T within intron 4. No significant associations were identified between *DDAH2*

genotype and ADMA, SDMA ADMA/SDMA ratio or other cardiovascular disease risk factors in healthy subjects, renal failure patients or diabetics.

In conclusion, this study has identified common polymorphisms in enzymes affecting NO synthesis or inactivation. Polymorphisms in the p22phox gene and GTPCH1 gene were associated with risk factors for cardiovascular disease including endothelium-dependent vasodilation and plasma neopterin (a marker of BH_4).

Acknowledgements

Firstly, I would like to thank my supervisors Dr. Aroon Hingorani and Professor Patrick Vallance for giving me the opportunity to carry out this Ph.D, and for all their support and advice throughout my studies.

I am very grateful for all the help and advice given to me by members of the Department of Clinical Pharmacology, in particular Dr. James Leiper and Dr. Lucy Tran for help with making the DDAH2 constructs and Miss Rachel Jackson for the measurement of methylarginines by HPLC. I am also grateful to Dr. Noor Jeerooburkhan for help with the SSCP and Miss Jackie Cooper and Miss Shona Livingstone for help with the statistical analysis. I would also like to thank Professor Steve Humphries (Centre for Cardiovascular Genetics, UCL), Professor Rainer Boger (Department of Clinical Pharmacology, University of Hamburg), Professor John Deanfield and Dr. Paul Leeson (Vascular Physiology Unit, Great Ormond Street Hospital), Dr. Jenny Cross (Centre for Clinical Pharmacology, UCL), Dr. Carmine Zoccali (IBIM-CNR, Italy), Dr. Helen Colhoun (Department of Epidemiology, UCL) and Dr. Makrina Savvidou (Harris Birthright Research Centre for Fetal Medicine, King's College Hospital) for access to all the patient cohorts.

Many thanks go to my family and friends with whom I have shared my disappointments and successes over the past four years. A huge thankyou especially goes to my partner Nicholas for all his love and encouragement throughout. Finally, I would like to dedicate this thesis to my Grandpa, who sadly did not see its completion.

Publications

Jeerooburkhan N, **Jones LC**, Bujac S, Cooper JA, Miller GJ, Vallance P, Humphries SE, Hingorani AD. Genetic and environmental determinants of plasma nitrogen oxides and risk of ischemic heart disease. *Hypertension.* 2001 Nov;38(5):1054-61.

Jones LC, Leeson CPM, Jeerooburkhan N, Cooper JA, Deanfield JE, Humphries SE, Vallance P, Hingorani AD. Genetic variation in GTP cyclohydrolase-1 is associated with neopterin levels and endothelial function. *Submitted to Arteriosclerosis Thrombosis and Vascular Biology.*

Jones LC, Tran CTL, Leiper JM, Hingorani AD, Vallance P. Common genetic variation in a basal promoter element alters DDAH2 expression in endothelial cells. *Biochemical and Biophysical Research Communications Journal.* 2003;310(3):836-843.

Presentations

Poster presentation: 2nd International Conference of Biology, Chemistry and Therapeutic Applications of Nitric Oxide. Prague, Czech Republic, June 2002.

Poster presentation: UCL Postgraduate School, poster competition, March 2002.

Abbreviations

6-FAM	6-carboxyfluorescein
7,8-NH2-TP	7,8-dihydroneopterin triphosphate
ACh	Acetylcholine
ADMA	Asymmetric dimethylarginine
ANOVA	Analysis of variance
AP-1	Activating protein 1
ApoE	Apolipoprotein E
At-RA	All-trans retinoic acid
BH_2	dihydroneopterin
BH_4	Tetrahydrobiopterin
BK	Bradykinin
BMI	Body mass index
Ca^{2+}	Calcium
CAC	Coronary artery calcification
CAD	Coronary artery disease
CaM	Calmodulin
C/EBP	CCAAT box/enhancer binding protein
CGD	Chronic granulatomous disease
CHD	Coronary heart disease
CREED	Cardiovascular risk extended evaluation dialysis study
CRP	C-reactive protein
CVD	Cardiovascular disease
dATP	deoxyadenosine triphosphate
DBP	Diastolic blood pressure
dCTP	deoxycytidine triphosphate
DDAH	Dimethylarginine dimethylaminohydrolase
ddATP	di-deoxyadenosine triphosphate
ddCTP	di-deoxycytidine triphosphate
ddGTP	di-deoxyguanosine triphosphate
ddTTP	di-deoxythymidine triphosphate
dGTP	deoxyguanosine triphosphate
DNA	Deoxyribose nucleic acid
DRD	Dopa-responsive dystonia
dTTP	deoxythymidine triphosphate
EDHF	Endothelium derived hyperpolarizing factor
EDRF	Endothelium derived relaxant factor
EDTA	Ethylenediaminetetraacetic acid
EGM	Endothelial cell growth media
eNOS	endothelial nitric oxide synthase
FAD	Flavine adenine dinucleotide
FH	Familial hypercholesterolaemia
FMD	Flow-mediated dilatation
FMN	Flavine mononucleotide
GRE	glucocortoid response element
GTN	Glyceryl trinitrate

GTPCH1	GTPcyclohydrolase 1
H_2O_2	Hydrogen peroxide
Hb	Haemoglobin
HCL	Hydrochloric acid
HDL	High density lipoprotein
HNF	Hepatic nuclear factor
HPLC	High performance liquid chromatography
HUVEC	Human umbilical vein endothelial cell
IFNγ	Interferon γ
IHD	Ischeamic heart disease
iNOS	inducible nitric oxide synthase
Km	Michaelis constant
LDL	Low density lipoprotein
LNMMA	Ng-monomethyl-L-arginine
LSS	Laminar shear stress
$MgCl_2$	Magnesium chloride
MHC	Major histocompatability complex
MI	Myocardial infarction
mRNA	Messanger ribose nucleic acid
NA	Noradrenaline
NADPH	Nicotinamide adenine dinucleotide phosphate
NCBI	National center for biotechnology information
NFκB	Nuclear factor κB
NGF	Nerve growth factor
nNOS	neuronal nitric oxide synthase
NO	Nitric oxide
$NO2^-$	Nitrite
$NO3^-$	Nitrate
NOS	Nitric oxide synthase
O_2^-	Superoxide
$ONOO^-$	Peroxynitrite
OxLDL	Oxidized low density lipoprotein
PBS	Phosphate buffered saline
PCR	Polymerase chain reaction
PRMT	Protein arginine methyltransferase
PTPS	6-pyruvoyl tetrhydrobiopterin synthase
ROS	Reactive oxygen species
SBP	Systolic blood pressure
SD	Standard deviation
SDMA	Symmetric dimethylarginine
sGC	Soluble guanylate cyclase
SNP	Single nucleotide polymorphism
SOD	Superoxide dismutase
SR	Sepiapterin reductase
SRF	Serum response factor
SSCP	Single strand conformation polymorphism
SSRE	Shear stress response element
TBE	Tris borate/EDTA
TE	Tris-EDTA

TEMED	N,N,N',N'-Tetramethylethylenediamine
USF	Upstream stimulating factor
UTR	Untranslated region
VSMC	Vascular smooth muscle cell

Table of Contents

Title 1
Abstract 2
Acknowledgements 4
Publications 5
Abbreviations 6
Table of contents 7
List of tables and figures 13
CHAPTER 1: INTRODUCTION 20
1.1 Cardiovascular diseases and endothelial function 21
1.1.1 Background 21
1.1.2 Maintenance of a healthy vasculature-role of the endothelium 23
1.1.3 Heritability of vascular disease 27
1.1.3.1 Evidence for a heritable basis for atherosclerosis 29
1.1.4 Candidate genes for CVD 30
1.2 The L-Arginine→NO system 34
1.2.1 Discovery of Nitric Oxide 34
1.2.2 Different isoforms of NO exist 34
1.2.3 Physiological actions of eNOS 37
1.3 Decreased NO availability, endothelial dysfunction and cardiovascular disease 38
1.3.1 Decreased NOS expression or activity-studies of the eNOS gene (*NOS 3*) 39
1.3.2 Decreased L-arginine availability 40
1.3.3 Limited availability of BH_4 for NOS enzyme activity 41
1.3.3.1 Multiple functions of BH_4-essential NOS cofactor 42
1.3.3.2 Synthesis of BH_4 43
1.3.4 Inhibitors of nitric oxide synthase 45
1.3.4.1 Reduced DDAH expression or activity could account for elevated ADMA 47
1.3.5 Inactivation of NO by superoxide (O_2^-) 48
1.3.5.1 NADPH oxidase is a major source of ROS in the vasculature 49
1.4 Hypothesis 51
1.5 Aims 52
CHAPTER 2: MATERIALS AND METHODS 53
2.1 Materials 54
2.1.1 General reagents 54
2.1.2 Enzymes used for PCR and restriction digests 54
2.1.3 Oligonucleotides 55
2.1.4 DNA ladders for agarose gel electrophoresis and genescan 55
2.1.5 Gel loading buffers 55
2.1.6 Cell culture reagents 56
2.1.7 Kits 56
2.2 Methods 59
2.2.1 Extraction of DNA from whole blood samples 59
2.2.1.1 Salting out method 59
2.2.1.2 DNA purification kit method (*QiAmp blood minikit*) 60
2.2.2 DNA amplification by PCR 60
2.2.3 Agarose gel electrophoresis 61
2.2.4 Single-strand conformation polymorphism analysis (SSCP) 61
2.2.4.1 Radioactive SSCP 61
2.2.4.2 Non-radioactive SSCP (*PhastSystem*) 62
2.2.5 DNA sequencing 63
2.2.5.1 Template preparation 63
2.2.5.2 Sequencing reaction 63
2.2.5.3 Gel loading and electrophoresis of sequencing products 64
2.2.6 Genotyping 65
2.2.6.1 Genotyping by PCR-RFLP analysis 65
2.2.6.2 Genotyping by Genescan analysis 65

2.2.7 Search of the National Center for Biotechnology Information (NCBI) SNP database for polymorphisms 66
2.2.8 Search of the MatInspector database for putative transcription factor binding sites 67
2.2.9 Measurement of plasma nitrite and nitrate (*NOx*) 67
2.2.10 Measurement of plasma neopterin 68
2.2.11 Luciferase reporter gene assay 69
2.2.11.1 Cell culture and transfection 69
2.2.11.2 Cell lysis and luciferase assay 70
2.2.12 Populations collected for vascular phenotyping/disease studies 71
2.2.12.1 Healthy Subjects 71
2.2.12.2 Renal Failure patients 75
2.2.12.3 Diabetic patients and controls (EBCT cohort) 77
2.2.12.4 Pregnant Females 79
2.2.13 Measures of vascular function 80
2.2.13.1 Venous occlusion plethysmography 80
2.2.13.2 Flow mediated dilatation (FMD) 80
2.2.14 Statistical analysis 81
CHAPTER 3: ASSOCIATION STUDIES OF THE NADPH OXIDASE p22PHOX C242T POLYMORPHISM AND ENDOTHELIAL FUNCTION 82
3.1 Aim 83
3.2 Background 83
3.2.1 NADPH oxidase generates O_2^- in both phagocytic and non-phagocytic cells 84
3.2.2 Vasculature NADPH oxidase is distinct from phagocytic NADPH oxidase 85
3.2.3 Common Genetic variation in p22phox 87
3.3 Subjects and Methods 89
3.3.1 Subjects 89
3.3.2 DNA extraction 90
3.3.3 Genotyping by PCR-RFLP analysis 90
3.3.4 Data analysis 91
3.4 Results 92
3.4.1 Genotype and allele frequencies of the p22phox (*CYBA*) C242T polymorphism 92
3.4.2 p22phox genotype and CVD risk factors in the Cambridge Young Adults cohort 93
3.4.3 Relationship between p22phox genotype and vascular function in the Cambridge Young Adults cohort 94
3.4.4 p22phox genotype and cardiovascular risk factors in the EBCT cohort 96
3.4.5 Relationship between p22phox genotype and vascular function in the EBCT cohort 97
3.5 Discussion 99
CHAPTER 4: IDENTIFICATION OF POLYMORPHISMS IN THE HUMAN GTP-CYCLOHYDROLASE 1 GENE (*GCH1*) 104
4.1 Aim 105
4.2 Background 105
4.3 Subjects and Methods 110
4.3.1 Subjects 110
4.3.2 Oligonucleotide design and amplification of genomic DNA 110
4.3.3 Screening for polymorphisms by SSCP analysis 111
4.3.4 DNA sequencing to define the nature of variants detected by SSCP 111
4.3.5 Search of the National Center for Biotechnology Information (NCBI) SNP database for *GCH1* polymorphisms 114
4.3.6 Search of the MatInspector promoter database for putative *GCH1* transcription factor binding sites 114
4.4 Results 115
4.4.1 Polymorphisms identified in *GCH* 115
4.4.2 Analysis of the *GCH1* promoter and comparison of polymorphisms in the NCBI SNP database and those identified by SSCP 121
4.5 Discussion 124
4.5.1 *GCH1* promoter polymorphisms 124
4.5.2 Polymorphisms within *GCH1* exons 125
4.5.3 Future work 126

CHAPTER 5: *GCH 1* POLYMORPHISMS AND THEIR FUNCTIONAL IMPACT ON PTERIN METABOLISM AND ENDOTHELIAL FUNCTION 128
5.1 Aims 129
5.2 Background 129
5.3 Subjects and Methods 132
5.3.1 Subjects investigated for association between *GCH1* genotype and neopterin 132
5.3.2 Subjects investigated for association between *GCH1* genotype and endothelial function 133
5.3.3 Measurement of plasma neopterin in the NPHSII cohort 134
5.3.4 Genotyping studies 135
5.3.5 Statistical Analysis 135
5.4 Results 136
5.4.1 Genotype and allele frequency of *GCH1* polymorphisms 136
5.4.2 Baseline demographics of NPHSII study participants 138
5.4.3 Distribution and determinants of plasma neopterin 139
5.4.4 Relationship between *GCH1* genotype and plasma neopterin in the NPHSII cohort 140
5.4.5 *GCH1* polymorphism, and CVD risk 142
5.4.6 Baseline demographics of Cambridge Young Adults Study participants 143
5.4.7 Relationship between *GCH1* genotype and endothelial function 144
5.5 Discussion 146
CHAPTER 6: IDENTIFICATION OF POLYMORPHISMS IN THE HUMAN DIMETHYLARGININE DIMETHYLAMINOHYDROLASE GENE (*DDAH2*) 149
6.1 Aim 150
6.2 Background 150
6.3 Subjects and Methods 154
6.3.1 Subjects 154
6.3.2 Oligonucleotide design and amplification of genomic DNA 154
6.3.3 Screening for polymorphisms by SSCP analysis 157
6.3.4 DNA sequencing to define the nature of variants detected by SSCP 157
6.3.5 Search of the National Center for Biotechnology Information (NCBI) SNP database for *DDAH2* polymorphisms 157
6.3.6 Search of the MatInspector promoter database for putative *DDAH2* transcription factor binding sites 158
6.3.7 Identification of restriction enzyme sequences and genotyping of *DDAH2* Polymorphisms 158
6.4 Results 160
6.4.1 Polymorphisms in *DDAH2* 160
6.4.2 Analysis of the *DDAH2* promoter and comparison of polymorphisms in the National Center for Biotechnology Information (NCBI) SNP database with those identified by SSCP 170
6.4.3 Genotype and allele frequencies of *DDAH2* polymorphisms 174
6.5 Discussion 178
6.5.1 *DDAH2* promoter polymorphisms 178
6.5.2 Polymorphisms within *DDAH2* coding exons 182
CHAPTER 7: INFLUENCE OF *DDAH2* POLYMORPHISMS ON PROMOTER FUNCTION 183
7.1 Aims 184
7.2 Background 184
7.3 Materials and Methods 189
7.3.1 Identification of *DDAH2* transcripts in HUVEC 189
7.3.2 Cloning of human *DDAH2* promoter/reporter constructs containing allelic variants 190
7.3.2.1 Site-directed mutagenesis 190
7.3.2.2 TOPO TA cloning of allele-specific PCR products 192
7.3.2.3 Cloning allele-specific constructs into pGL3basic vector 192
7.3.2.4 Transformation of DH5α competent cells 193
7.3.3 Luciferase reporter gene assay 195
7.3.3.1 Cell culture and transfection 195
7.3.3.2 Cell lysis and luciferase assay 195
7.3.3.3 Statistical analysis 195
7.4 Results 196
7.4.1 Identification of *DDAH2* transcripts in HUVEC 196
7.4.2 Effect of *DDAH2* polymorphisms on promoter activity 197

7.5 Discussion ... 200
CHAPTER 8: *DDAH2* POLYMORPHISMS AND CIRCULATING METHYLARGININE CONCENTRATION ... 203
8.1 Aims ... 204
8.2 Background ... 204
8.3 Subjects and Methods ... 206
8.3.1 Subjects investigated for association between *DDAH2* polymorphisms and ADMA, SDMA and ADMA/SDMA ratio ... 206
8.3.2 Genotyping *DDAH2* polymorphisms ... 209
8.3.3 Measurement of plasma ADMA and SDMA by HPLC analysis ... 209
8.3.4 Statistical Analysis ... 210
8.4 Results ... 211
8.4.1 Genotype and allele frequencies of *DDAH2* polymorphisms in study cohorts ... 211
8.4.2 Relationship between *DDAH2* genotype, ADMA and SDMA concentration and ADMA/SDMA ratio in the German population screen ... 212
8.4.3 Relationship between *DDAH2* genotype, ADMA and SDMA concentration and ADMA/SDMA ratio in the London Renal Failure Cohort ... 218
8.4.4 Relationship between *DDAH2* genotype and ADMA, SDMA and ADMA/SDMA ratio in the CREED cohort ... 224
8.5 Discussion ... 229
CHAPTER 9: *DDAH2* POLYMORPHISMS, ENDOTHELIAL FUNCTION AND PLASMA NITROGEN OXIDES (NO_X) ... 232
9.1 Aims ... 233
9.2 Background ... 233
9.3 Subjects and Methods ... 237
9.3.1 Subjects investigated for association between *DDAH2* polymorphisms, plasma NO_X and blood pressure ... 237
9.3.2 Subjects investigated for association between *DDAH2* polymorphisms and endothelial function ... 238
9.3.3 Genotyping *DDAH2* polymorphisms ... 241
9.3.4 Measurement of plasma nitrite and nitrate (NOx) ... 241
9.3.5 Statistical Analysis ... 241
9.4 Results ... 243
9.4.1 Genotype and allele frequencies of *DDAH2* polymorphisms in each study cohort ... 243
9.4.2 Relationship between *DDAH2* genotype and plasma NOx in the NPHSII cohort ... 244
9.4.2.1 *DDAH2* genotype and blood pressure in the NPHSII cohort ... 245
9.4.3 Relationship between *DDAH2* genotype and endothelial function in the Cambridge Young Adults Study ... 249
9.4.3.1 Baseline demographic details of the Cambridge Young Adults Study ... 249
9.4.3.2 *DDAH2* genotype and endothelial function ... 249
9.4.4 Relationship between *DDAH2* genotype and endothelial function in women with normal pregnancies ... 252
9.4.4.1 Baseline demographics of the pregnancy cohort ... 252
9.4.4.2 *DDAH2* genotype and endothelial function ... 252
9.4.5 Relationship between *DDAH2* genotype and endothelial function in the EBCT cohort ... 255
9.4.5.1 Baseline demographics of the EBCT cohort ... 255
9.4.5.2 *DDAH2* genotype and endothelial function ... 259
9.5 Discussion ... 262
9.5.1 *DDAH2* genotype and plasma concentrations of NOx in the NPHSII cohort ... 262
9.5.2 *DDAH2* genotype and endothelial function ... 263
CHAPTER 10: GENERAL CONCLUSIONS ... 267
Appendix I Hardy-Weinberg Principle ... 272
Appendix II Linkage disequilibrium ... 273
Appendix III The difference in vascular responses between genotypes for Diabetics and non-diabetics and smokers and non-smokers ... 274
References ... 278

Tables and Figures

CHAPTER 1: INTRODUCTION

Table 1.1 Monogenic diseases.

Table 1.2 Examples of some of the genes investigated for association with CVD.

Figure 1.1 Schematic illustration of an atherosclerotic plaque within an artery.

Figure 1.2 Diagrammatic representation of the vascular endothelium and underlying smooth muscle cells.

Figure 1.3 Diagrammatic representation of endothelial nitric oxide synthase (eNOS).

Figure 1.4 Regulation of NO synthesis.

Figure 1.5 Synthesis of BH_4.

Figure 1.6 Synthesis and metabolism of ADMA.

Figure 1.7 NADPH oxidase enzyme complex.

CHAPTER 2: MATERIALS AND METHODS

Table 2.1 Restriction endonucleases used for PCR-RFLP analysis.

Table 2.2 Number of men recruited from each of the 9 UK clinics for the NPHSII study cohort.

Table 2.3 Demographic characteristics of the NPHSII study cohort.

Table 2.4 Demographic characteristics of the German population screen cohort.

Table 2.5 Demographic characteristics of the Cambridge Young Adults Study.

Table 2.6 Demographic characteristics of the London Renal Failure cohort.

Table 2.7 Demographic characteristics of the Italian Renal Failure cohort (CREED).

Table 2.8 Demographic characteristics of the Diabetic patients and controls.

Table 2.9 Demographic characteristics of the pregnancy cohort.

CHAPTER 3: ASSOCIATION STUDIES OF THE NADPH OXIDASE p22PHOX C242T POLYMORPHISM AND ENDOTHELIAL FUNCTION

Table 3.1 Genotype and allele frequencies of the p22phox C242T polymorphism.

Table 3.2 Phenotypic characteristics of the Cambridge Young Adults cohort according to p22phox C242T genotype

Table 3.3 Phenotypic characteristics of individuals from the EBCT study according to p22phox C242T genotype.

Table 3.4 Results of multiple regression analysis of endothelial function according to p22phox genotype in diabetics, non-diabetics, smokers and non-smokers.

Figure 3.1 FMD according to p22phox genotype in the Cambridge Young Adults Study.

Figure 3.2 % change in brachial artery diameter in response to GTN (endothelium-independent response) according to p22phox genotype in the Cambridge Young Adults Study.

Figure 3.3 p22phox genotype and vascular function in the EBCT study cohort.

Figure 3.4 Endothelial dysfunction as a manifestation of depleted NO caused by ROS generation.

CHAPTER 4: IDENTIFICATION OF POLYMORPHISMS IN THE HUMAN GTP-CYCLOHYDROLASE 1 GENE (*GCH1*)

Table 4.1 Oligonucleotides designed to amplify the *GCH1* promoter.

Table 4.2 Oligonucleotides designed to amplify *GCH1* exons.

Table 4.3 Human *GCH1* promoter polymorphisms identified in the NCBI SNP database.

Figure 4.1 Synthesis of BH_4 and its regulation by GFRP.

Figure 4.2 *GCH1* gene structure.

Figure 4.3 DNA sequence (of the reverse strand) confirming a G→A substitution at position –796 in the *GCH1* promoter.

Figure 4.4 DNA sequence (of the reverse strand) confirming a T→C substitution at position –741 in the *GCH1* promoter.

Figure 4.5 DNA sequence electropherogram confirming a G→A substitution at position –577 in the *GCH1* promoter.

Figure 4.6 SSCP gel image (*Phastsystem*) and DNA sequence of *GCH1* Exon 1b PCR.

Figure 4.7. Nucleotide sequence of the human *GCH1* promoter region.

CHAPTER 5: *GCH 1* POLYMORPHISMS AND THEIR FUNCTIONAL IMPACT ON PTERIN METABOLISM AND ENDOTHELIAL FUNCTION

Table 5.1 Genotype and allele frequencies of *GCH1* polymorphisms in the NPHSII cohort (top panel) and the Cambridge Young Adults Study cohort (bottom panel).

Table 5.2a Demographic details of subjects in the NPHSII cohort according to *GCH1* –577G/A genotype.

Table 5.2b Demographic details of subjects in the NPHSII cohort according to *GCH1* –796G/A genotype.

Table 5.3 Correlation of neopterin with risk factors for cardiovascular disease in the NPHSII cohort by stepwise multiple regression.

Table 5.4 Neopterin and neopterin/creatinine according to *GCH1* –577G/A (top panel) and –796G/A genotype (bottom panel).

Table 5.5 *GCH1* genotype and IHD risk in the NPHSII cohort.

Table 5.6a Demographic characteristics of the Cambridge Young Adults Study cohort according to *GCH1* –577G/A genotype.

Table 5.6b Demographic characteristics of the Cambridge Young Adults Study cohort according to *GCH1* –796G/A genotype.

Table 5.7 Endothelial function according to *GCH1* –577G/A (top panel) and –796G/A (bottom panel) genotype in the Cambridge Young Adults Study cohort.

CHAPTER 6: IDENTIFICATION OF POLYMORPHISMS IN THE HUMAN DIMETHYLARGININE DIMETHYLAMINOHYDROLASE GENE (*DDAH2*)

Table 6.1 Oligonucleotides used for PCR amplification of the human *DDAH2* gene.

Table 6.2 *DDAH2* polymorphisms – restriction enzymes and digestion products.

Table 6.3 Human *DDAH2* promoter polymorphisms identified in the NCBI SNP database.

Table 6.4 Genotype and allele frequencies of *DDAH2* polymorphisms in the NPHSII cohort (top panel) and the German Population Screen cohort (bottom panel).

Table 6.5 Pairwise linkage disequilibrium coefficients (Δ) for *DDAH2* polymorphisms.

Figure 6.1 *DDAH2* gene structure and polymorphisms identified by SSCP.

Figure 6.2a SSCP gel of *DDAH2* promoter 3 PCR.

Figure 6.2b SSCP gel of *DDAH2* exon 1 PCR.

Figure 6.2c SSCP gel of *DDAH2* Exon 2 PCR.

Figure 6.2d SSCP gel of *DDAH2* Exon 4+5 PCR.

Figure 6.3a DNA sequence confirming a G→A substitution at position –1415 in *DDAH2* promoter 2 PCR.

Figure 6.3b DNA sequence confirming a C→A substitution a position –1151 in the *DDAH2* promoter 3 PCR.

Figure 6.3c DNA sequence confirming a C→G substitution at position –1020 in *DDAH2* exon1.

Figure 6.3d DNA sequence electropherogram confirming the presence of an extra G at position –871 in the *DDAH2* promoter.

Figure 6.3e DNA sequence electropherogram confiming the presence of a C→G polymorphism within the *DDAH2* exon2 PCR.

Figure 6.3f. DNA sequence eletropherogram confirming the presence of a C→T polymorphism within the exon 4+5 PCR product.

Figure 6.4 DNA sequence of the *DDAH2* 5' untranslated region.

Figure 6.5 Restriction digest gel images.

Figure 6.6 Genescan trace produced upon genotyping the *DDAH2* –871 6G/7G bi-allelic length variation.

CHAPTER 7: INFLUENCE OF *DDAH2* POLYMORPHISMS ON PROMOTER FUNCTION

Table 7.1 Allele-specific and vector oligonucleotides used for site directed mutagenesis to generate *DDAH2* promoter constructs.

Figure 7.1 Diagrammatic representation of the vector pGL3basic.

Figure 7.2 Bioluminescent reactions of the firefly and *Renilla* luciferases.

Figure 7.3 A diagrammatic representation of the steps involved in cloning *DDAH2* promoter/reporter constructs containing allelic variants.

Figure 7.4 *DDAH2* transcripts identified in HUVEC.

Figure 7.5 Effect of different promoter variants on DDAH2 expression.

Figure 7.6 Promoter activity of 6G constructs compared to 7G constructs.

Figure 7.7 Effect of *at*-RA treatment on *DDAH2* promoter activity.

CHAPTER 8: *DDAH2* POLYMORPHISMS AND CIRCULATING METHYLARGININE CONCENTRATION

Table 8.1 Summary of cohorts genotyped for association between *DDAH2* polymorphisms and various risk factors for CVD.

Table 8.2 Allele frequencies, χ^2 and P values of each *DDAH2* polymorphism.

Table 8.3a Demographic characteristics of the German Population Screen cohort according to –1020C/G genotype.

Table 8.3b Demographic characteristics of the German Population Screen cohort according to –1151A/C genotype.

Table 8.3c Demographic characteristics of the German Population Screen cohort according to –871 6G/7G genotype.

Table 8.4a Demographic characteristics of the London Renal Failure Cohort according to –1020C/G genotype.

Table 8.4b Demographic characteristics of the London Renal Failure Cohort according to –1151A/C genotype.

Table 8.4c Demographic characteristics of the London Renal Failure Cohort according to –871 6G/7G genotype.

Table 8.5a Demographic characteristics of the CREED cohort according to –1151A/C genotype.

Table 8.5b Demographic characteristics of the CREED cohort according to –871 6G/7G genotype.

Figure 8.1a ADMA and SDMA concentrations and ADMA/SDMA ratio according to –1020C/G genotype in the German Population Screen.

Figure 8.1b ADMA and SDMA concentration, and ADMA/SDMA ratio according to –1151A/C genotype in the German Population Screen.

Figure 8.1c ADMA and SDMA concentration, and ADMA/SDMA ratio according to –871 6G/7G genotype in the German Population Screen.

Figure 8.2a ADMA and SDMA concentration, and ADMA/SDMA ratio according to –1020C/G genotype in the London Renal Failure cohort.

Figure 8.2b ADMA and SDMA concentration, and ADMA/SDMA ratio according to –1151A/C genotype in the London Renal Failure cohort.

Figure 8.2c ADMA and SDMA concentration, and ADMA/SDMA ratio according to –871 6G/7G genotype in the London Renal Failure cohort.

Figure 8.3a ADMA and SDMA concentration, and ADMA/SDMA ratio according to –1151A/C genotype in the CREED cohort.

Figure 8.3b ADMA and SDMA concentrations, and ADMA/SDMA ratio according to –871 6G/7G genotype in the CREED cohort.

CHAPTER 9: *DDAH2* POLYMORPHISMS, ENDOTHELIAL FUNCTION AND PLASMA NITROGEN OXIDES (NO_X)

Table 9.1 Summary of cohorts genotyped for association between DDAH2 polymorphisms and various risk factors for CVD.

Table 9.2 Allele frequencies, χ^2 and P values for each *DDAH2* polymorphism.

Table 9.3a Plasma NOx, systolic blood pressure (SBP), diastolic blood pressure (DBP) and cholesterol according to –449 G/C genotype for the Chesterfield (top) and North Mymms (bottom) NPHSII clinics.

Table 9.3b Plasma NOx, systolic blood pressure (SBP), diastolic blood pressure (DBP) and cholesterol according to –1020 C/G genotype for the Chesterfield (top) and North Mymms (bottom) NPHSII clinics.

Table 9.3c Plasma NOx, systolic blood pressure (SBP), diastolic blood pressure (DBP) and cholesterol according to –1151 A/C genotype for the Chesterfield (top) and North Mymms (bottom) NPHSII clinics.

Table 9.3d Plasma NOx, systolic blood pressure (SBP), diastolic blood pressure (DBP) and cholesterol according to –449G/C (top), -1020C/G (middle) and –1151 A/C (bottom) genotype for the combined Chesterfield and North Mymms NPHSII clinics.

Table 9.4a Endothelium-dependent and independent FMD and other CVD risk factors according to –1020C/G genotype in the Cambridge Young Adults Study cohort.

Table 9.4b Endothelium-dependent and independent FMD and other CVD risk factors according to –1151A/C genotype in the Cambridge Young Adults Study cohort.

Table 9.4c Endothelium-dependent and independent FMD and other CVD risk factors according to –871 6G/7G genotype in the Cambridge Young Adults Study cohort.

Table 9.5a Endothelium-dependent FMD and other CVD risk factors according to – 1020C/G genotype in the Pregnancy cohort.

Table 9.5b Endothelium-dependent FMD and other CVD risk factors according to – 1151A/C genotype in the Pregnancy cohort.

Table 9.5c Endothelium-dependent FMD and other CVD risk factors according to – 871 6G/7G genotype in the Pregnancy cohort.

Table 9.6a Demographic characteristics of the EBCT cohort according to –1151A/C genotype.

Table 9.6b Demographic characteristics of the EBCT cohort according to –1020C/G genotype.

Table 9.7 Distribution of –1151A/C and –1020C/G alleles according to diabetic status.

Figure 9.1a Endothelium-dependent and independent vascular responses according to –1151A/C genotype in the EBCT cohort.

Figure 9.1b Endothelium-dependent and independent vascular responses according to –1020C/G genotype in the EBCT cohort.

CHAPTER 1

INTRODUCTION

1.1 Cardiovascular diseases and endothelial function

1.1.1 Background

Atherosclerosis leads to stroke, coronary heart disease (CHD) and peripheral vascular disease and is a major cause of death and morbidity. In the developed world it accounts for over four million deaths every year in Europe (British Heart Foundation, www.dphpc.ox.ac.uk), and as a disease it is assuming greater importance in the developing world (Perret et al., 2000). Atherosclerosis is characterized by the development of atherosclerotic plaques in large and medium sized arteries. Early plaques are evident by the second decade of life (McGill et al., 2000) and their development is initiated and accelerated by damage to the endothelium. Atherosclerotic plaques consist of a core rich in cholesterol and other lipids, which are surrounded by smooth muscle cells and fibrous tissue (Figure 1.1). The formation of plaques is preceded initially by damage to the endothelium mediated by factors such as increased blood pressure, products of cigarette smoke, high levels of cholesterol, circulating oxidized low density lipoprotein (oxLDL) cholesterol and inflammatory cytokines (Ross et al., 1993). This leads to the adhesion of leukocytes to the vessel wall, their migration into the sub-endothelial space and the uptake of cholesterol rich lipid particles by macrophages (Libby, 2000). Proliferation of the underlying smooth muscle cells triggered by the release of growth factors eventually leads to a decrease in the size of the vessel lumen. Plaque fissure or rupture results in the exposure of plaque contents to the circulating blood, thrombus formation and occlusion of the vessel, which is responsible for myocardial infarction and some forms of stroke. The risk of developing vascular disease is highly increased in the presence of renal failure (Foley, 1998a;

Foley, 1998b) and diabetes (Ginsberg, 2000; Haffner et al., 1999), however onset cannot always be solely attributed to environmental factors. The genetic makeup of an individual is now being recognized as having a vital role in vascular disease risk (Boerwinkle et al., 1996). The past 20 years have seen huge developments in the field of genetics and molecular biology, in particular the advance of the human genome project (International Human Genome Sequencing Consortium, 2001), which has made possible the identification, isolation and characterization of a multitude of genes implicated in medical disorders including cardiovascular disease (CVD).

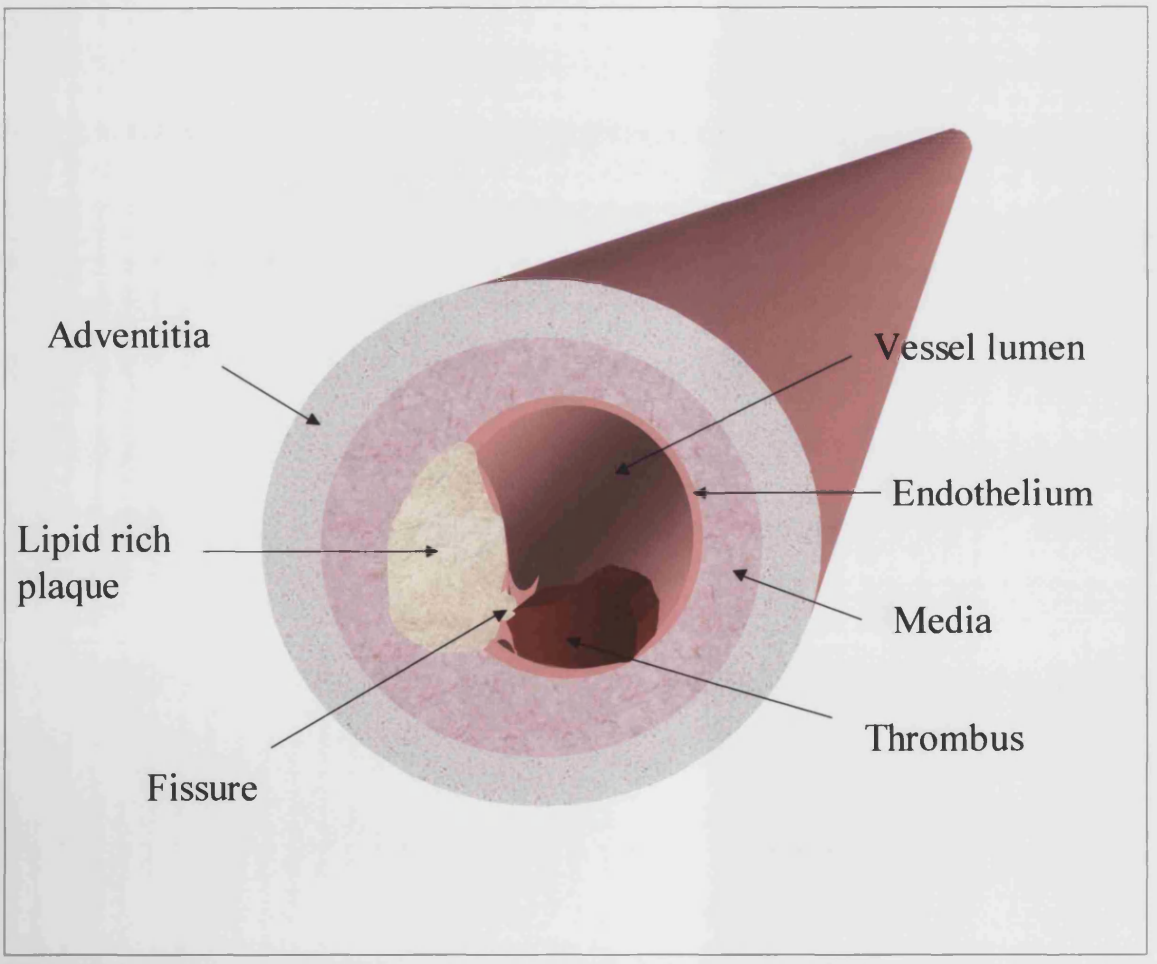

Figure 1.1. Schematic illustration of an atherosclerotic plaque within an artery. The lumen of the vessel is narrowed by the presence of the plaque, which contains cholesterol and other lipids. Rupture of the fibrous cap results in thrombus formation leading ultimately to occlusion of the vessel.

1.1.2 Maintenance of a healthy vasculature-role of the endothelium

The endothelium consists of a monolayer of cells lining all blood vessels. It serves as a permeability barrier between the circulating blood and the vessel wall. However, its role is not simply that of an inert barrier. Receptors on the endothelial cell surface act as sensors of the biochemical and physical environment of the blood, responding to chemical signals such as serotonin, bradykinin, and shear stress, which prompts this single layer of cells to release anti-adhesive, anti-thrombotic, vasoconstrictor and vasorelaxant mediators, thereby ensuring a state of vascular homeostasis.

The involvement of the endothelium in the process of atherosclerotic disease had been suggested as early as the 1800s (Virchow, 1856), but the mechanisms involved have only recently been identified. The essential role of the endothelium for vascular relaxation was first discovered by Furchgott and Zawadski in a series of experiments in which they demonstrated that removal of the endothelium completely inhibited relaxation of rabbit thoracic aorta to acetylcholine (Furchgott and Zawadski, 1980). This observation led to the discovery of a highly potent vasodilator originally named endothelium-derived relaxant factor (EDRF). EDRF was subsequently identified as nitric oxide (NO) (Ignarro et al., 1987), which is capable of exerting many athero-protective, anti-thrombotic and anti-inflammatory actions upon the vasculature and is discussed in more detail in section 1.2. The endothelium also releases other vasodilator molecules, for example prostacyclin and endothelium-derived hyperpolarizing factor (EDHF) as well as vasoconstrictors such as endothelin and angiotensin II (Figure 1.2). Production of these mediators is stimulated by physical factors (e.g. increased flow at the endothelial surface) as well as the binding of agonists including acetylcholine (ACh)

and bradykinin (Bk) to receptors on the endothelial cell surface. However, in the presence of a dysfunctional endothelium some of these agonists (e.g. ACh) are also capable of inducing vasoconstriction by binding to receptors on underlying vascular smooth muscle cells (VSMC).

Atherosclerotic plaques form predominantly at the sites of arterial branch points where there is disturbed laminar flow (Cornhill et al., 1976). This led to the theory that external forces upon endothelial cells such as shear stress (generated by the flow of blood over the endothelium) play a part in regulating endothelial cell function. Subsequent studies revealed that a number of genes expressed by the endothelium (including the gene encoding the enzyme for NO synthesis), are upregulated by shear stress (Resnick et al., 1995), suggesting that the hemodynamic forces generated by blood flow can indeed direct endothelial function.

Vascular homeostasis is therefore maintained through the balanced production of a range of vasoactive substances. Dysfunction of the endothelium caused by elevated blood cholesterol, hyperglycemia and hypertension are known to increase endothelial cell permeability, the expression of adhesion molecules and restrict the release of vasodilators such as NO. This ultimately manifests in the development of atherosclerosis and vascular disease.

Endothelial function in humans *in vivo* is often measured using one of two techniques- venous occlusion plethysmography which measures endothelial function in small resistance vessels and flow mediated dilatation (FMD) which measures endothelial function in the brachial artery, a conduit vessel. Venous occlusion plethysmography

measures the change in blood flow in the forearm in response to endothelium-dependent agonists. A cuff is placed on the upper arm and periodically inflated to prevent venous return. A strain-gauge placed around the forearm measures the change in forearm circumference in millimetres per minute which is proportional to arterial blood inflow during the period of occlusion (Benjamin et al., 1995). Insertion of a needle into the brachial artery allows administration of endothelium-dependent vasodilators such as ACh or Bk, and endothelium-independent control dilators such as GTN. FMD measures brachial artery diameter in response to increased blood flow. A cuff placed around the forearm is inflated to suprasystolic pressure to make the arm ischemic. When the cuff is deflated, the flow of blood into the ischemic arm and the resulting shear stress produced in the brachial artery causes NO release and dilatation. This dilatation is endothelium-dependent and can be measured using an ultrasound device (Celermajer et al., 1992). Endothelial dysfunction determined by venous occlusion plethysmography or FMD correlates with coronary endothelial dysfunction and is indicative of vascular disease (Vita et al., 1990). Endothelial dysfunction also correlates with cardiovascular risk factors as assessed by the Framingham risk score (Chan et al., 2001) and predicts cardiovascular outcome (Suwaidi et al., 2000; Schachinger et al., 2000).

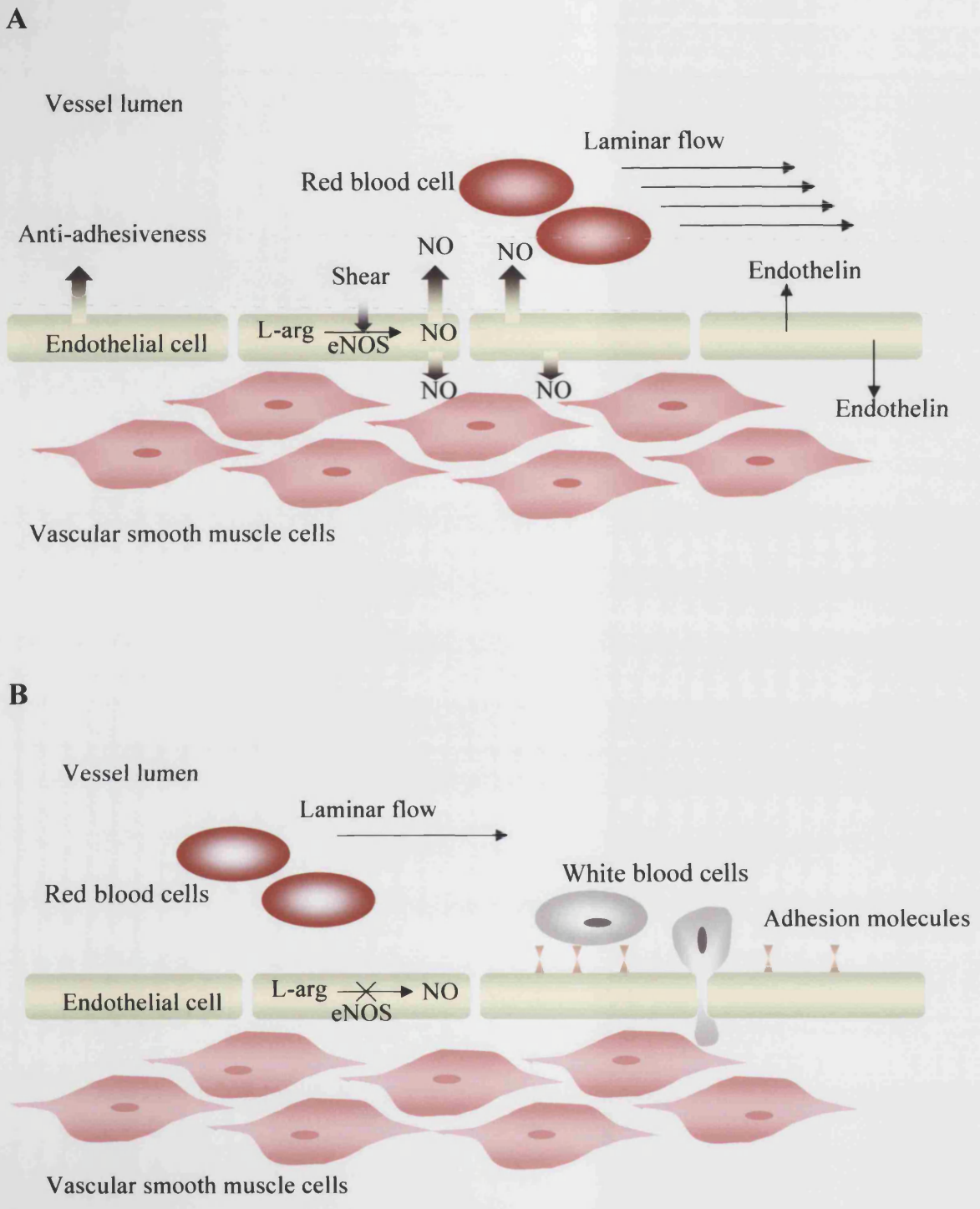

Figure 1.2. Diagrammatic representation of the vascular endothelium and underlying smooth muscle cells. A. The endothelium produces substances such as nitric oxide, which has anti-atherogenic and vasorelaxant properties essential for maintaining a healthy vasculature. **B.** In the presence of risk factors for CVD such as hypercholesterolaemia, hypertension and diabetes there is increased endothelial cell adhesiveness and permeability. Nitric oxide availability is decreased and consequently its anti-atherogenic and relaxant properties are attenuated.

1.1.3 Heritability of vascular disease

Common complex diseases such as atherosclerosis, hypertension, diabetes, and cancer are believed to be caused through the interaction of an individuals genes and the environment. Such diseases tend to be of late onset, have no clear pattern of inheritance and as a result the causative genes and risk factors have been difficult to identify. However, rare monogenic forms of these diseases such as autosomal dominant Familial hypercholesterolaemia (FH), autosomal dominant hypertension due to Liddle's syndrome, familial breast cancer and monogenic forms of type II diabetes have helped us to understand the pathophysiological basis of the complex disease state.

Table 1.1 gives three examples of monogenic diseases resulting in elevated LDL or blood pressure, which are risk factors for CVD development. FH is caused by mutations in the low-density lipoprotein receptor (LDLR) gene (Hobbs et al., 1992), and is one of the most common autosomal inherited disorders, with 1 out of every 500 individuals affected (Smilde et al., 2001). Individuals who carry the mutant gene are characterized by elevated LDL cholesterol, due to the fact that it cannot be removed from the circulation. To date more than 500 mutations have been reported in the LDL receptor gene, resulting in a decrease in the number of receptors (in the case of heterozygote individuals) or a complete absence of receptors (homozygote individuals) on the liver cell surface. This directly results in elevated circulating LDL leading to vascular disease.

Disease	Mutant Gene	Inheritance	Effect
Familial hypercholesterolaemia (FH)	LDLR	AD	↑ LDL
Liddle's syndrome	ENaC	AD	↑ blood pressure
Glucocorticoid-remedial aldosteronism (GRA)	Aldosterone synthase	AD	↑ blood pressure

Table 1.1 Monogenic diseases. Three examples of monogenic diseases, which result in the development of premature CVD, and their respective mutant genes are shown. The study of such disorders and the identification of the causative genes, has helped improve our understanding of the more complex cardiovascular diseases

Advances in molecular biology have also enabled the identification of a vast number of candidate genes implicated in the development of common forms of atherosclerosis. CVD is therefore thought to be polygenic (caused by several genes) with a major contribution coming from environmental factors e.g. smoking. The Apolipoprotein E gene (*ApoE*) is another gene known to be involved in the development of vascular disease (Eichner et al., 2002). This gene encodes a protein, which acts as a ligand expressed on the surface of LDL particles, via which, LDL particles are cleared from the circulation by binding to the LDL receptor. Three variants of this gene are known to exist-E2, E3 and E4. The E2 isoform has the lowest affinity for the LDL-receptor and E4 the highest affinity. Individuals homozygous for the E2 isoform are predisposed to develop elevated cholesterol and triglyceride levels leading to premature atherosclerosis but, unlike FH, disease progression is also influenced strongly by environmental factors such as diet, obesity and diabetes. *ApoE* genotype is therefore classed as a risk factor for CVD.

1.1.3.1 Evidence for a heritable basis for atherosclerosis

Studies of the offspring of patients with premature cardiovascular disease show that structural and functional changes are present in arteries even before the onset of disease and such individuals may be at increased risk of developing atherosclerosis (Gaeta et al., 2000). Impaired endothelium dependent flow mediated dilatation (FMD) has been reported in individuals with a positive family history of coronary artery disease (CAD), and was most pronounced in those individuals who both themselves and also their affected first degree relative were free from conventional risk factors such as smoking and diabetes (Clarkson et al., 1997; Gaeta et al., 2000). Some of the most convincing evidence for a genetic contribution to common forms of cardiovascular diseases comes from studies of twins. In a follow-up study of 21,000 twins Marenberg *et al* in 1994 and Zdravkovic *et al* in 2002 found that in twin pairs, the risk of a CHD event in the second twin of a monozygotic pair (who share 100% of their genes) was 2-fold higher than that for a second twin of a dizygotic pair, (who share only 50% of their genes). This evidence suggests that both atherosclerosis and the endothelial dysfunction that may underlie it are at least in part heritable disorders. Screening of populations at high risk of developing CVD is an important strategy for preventing disease onset and progression, and genetic association studies have been used extensively to try and locate and identify genes that could influence susceptibility to vascular diseases.

1.1.4 Candidate genes for CVD

The process of atherosclerosis development, plaque formation and eventual rupture involves many proteins and pathways. Each protein is encoded by its own gene, and variation in the coding sequence of these genes due to polymorphisms or mutation may result in individual differences in protein expression or function and predisposition to disease. Both polymorphisms and mutations refer to alteration in the nucleotide sequence of a gene such as base substitutions or insertion/deletion of a nucleotide. Rare mutations usually occurring in less than 1% of the population are well known causes of monogenic disorders such as cystic fibrosis or sickle cell disease. Conventionally, polymorphisms are classed as more common sequence changes occurring throughout the genome. Common polymorphisms may be silent but some may increase the risk of developing common disorders such as atherosclerosis. Additional polymorphisms or environmental factors may modulate this risk. Both polymorphisms and mutations may result in a change in the protein sequence with the consequence of altered protein function or, if the change lies within the promoter, a change in gene expression. Changes in protein function may be the result of nucleotide alterations such as missense mutations (causing a change in amino acid), nonsense mutations (resulting in a stop codon and therefore premature termination of translation) or frameshift mutations (causing a change in the reading frame). It has been reported that approximately 1.42 million single nucleotide polymorphisms (SNP) exist throughout the human genome, with on average one SNP every 1300bp (The International SNP Map Working Group, 2001). Single nucleotide polymorphisms may lie within the coding regions of genes (c-SNPs), within promoters (p-SNPs) or in introns. Although, many c-SNPs may be 'silent' (fail to alter the amino acid sequence of the protein), others alter amino acid

sequence and, consequently, protein activity. P-SNPs may influence protein function through regulation of protein expression. In each case, it is envisaged that carriage of the variant is entirely compatible with health, but in the presence of adverse environmental factors or additional risk alleles in other genes, disease develops.

Like all multi-factorial diseases, the identification of a causative gene (or genes) is proving to be a difficult task for CVD. Association analysis of polymorphisms in candidate genes has led to the study of hundreds of possible genes including those encoding cytokines, adhesion molecules, growth factors and coagulation-fibrinolysis mediators. In addition, genes encoding enzymes involved in the regulation of blood pressure such as the renin-angiotensin system, lipid metabolism and also the nitric oxide system have been included in this search. A few of these genes and their polymorphisms, which have been investigated for association with risk of CVD are shown in table 1.2. A recent study in which 4152 Japanese individuals were genotyped for 112 polymorphisms in 71 candidate genes for myocardial infarction (MI), identified the 1019C/T polymorphism in the connexin 37 gene and the p22phox 242C/T polymorphism to be associated with increased risk of MI in men, and the –688 4G/5G plasminogen activator inhibitor (PAI) polymorphism and –1171 5A/6A stromelysin 1 polymorphism to be associated with increased risk of MI in women (Yamada et al., 2002). The endothelial nitric oxide synthase gene (*NOS 3*) has also been the focus of several association studies for CVD. In particular, the –786T/C and Glu298Asp polymorphisms have been associated with increased risk of vascular disease (Nakayama et al., 1999; Hingorani et al., 1999; Miyamoto et al., 1998; Yoshimura et al., 1998). Such large-scale association studies between candidate genes and CVD have been aided by the completion of the first draft of the human genome sequence (International

Human Genome Sequencing Consortium, 2001) and subsequent generation of a comprehensive single nucleotide polymorphism (SNP) database. Improved high throughput genotyping techniques have also revolutionized the speed at which association studies can be performed with hundreds of individuals genotyped for multiple polymorphisms each day.

Gene	Gene symbol	Polymorphism	Amino acid change
Nitric oxide system			
Nitric oxide synthase 3	NOS 3	894G→T	Glu298Asp
		-786T→C	-
Renin-Angiotensin system			
Angiotensin	AGT	803T→C	Met235Thr
Angiotensin receptor 1	AGTR1	1166A→C	-
Lipid metabolism			
Apolipoprotein E	ApoE	388T→C	Cys112Arg
Low density lipoprotein Receptor	LDLR	IVS12+2T→C	-
Cytokines & adhesion molecules			
Interleukin 1-beta	IL1B	-581C→T	-
Tumor necrosis factor receptor superfamily	CD40L	420C→G	Trp140Cys
Intercellular adhesion molecule 1	ICAM1	167A→T	Lys29Met
Coagulation factors			
Plasminogen activator inhibitor 1	PAI 1 (SERPINE1)	-1965 del G	-
Fibrinogen	FGA	116T→A	Val20Asp

Table 1.2. Examples of some of the genes investigated for association with CVD. The corresponding gene symbols and polymorphisms are shown, and where appropriate the amino acid change.

1.2 The L-Arginine→NO system

1.2.1 Discovery of Nitric Oxide

In 1980 Furchgott and Zawadzki observed that the endothelium was necessary for vascular relaxation induced by acetylcholine (Furchgott and Zawadski, 1980). If the endothelium was removed this relaxation was abolished. They postulated that this endothelium-dependent relaxation was mediated by an unstable diffusible factor, with a biological half-life of only a few seconds. It was subsequently named endothelium-derived relaxant factor (EDRF). In 1986 it was proposed that EDRF was in fact nitric oxide (NO) (Ignarro et al., 1987). This hypothesis was later confirmed when several investigators showed that vascular endothelial cells synthesize NO, and that administration of exogenous NO reproduced the biological effects of EDRF (Palmer et al., 1987; Ignarro et al., 1987; Radomski et al., 1987a).

1.2.2 Different isoforms of NO exist

NO is synthesized by the enzyme nitric oxide synthase (NOS), of which three isoforms have been identified; neuronal nitric oxide synthase (nNOS), inducible nitric oxide synthase (iNOS) and endothelial nitric oxide synthase (eNOS), named after the tissues in which the genes were first cloned and characterized (Fostermann et al., 1994). All three isoforms have since been found in a variety of different tissues, and undergo complex regulation. The binding of calmodulin (CaM) was found to be pre-requisite for all isoforms of NOS activity, and is regulated by intracellular calcium (Ca^{2+}) levels. The requirement for Ca^{2+} differs between the three isoforms. nNOS and eNOS require

greater concentrations of intracellular Ca_2^+ for activity, whereas it has been suggested that CaM is very tightly bound to the iNOS enzyme and therefore only low levels of Ca^{2+} are needed for activation. nNOS and eNOS were formerly considered to be constitutive enzymes, but their expression is now known to be subject to up or down regulation for example during pregnancy and exercise (Dotsch, 2001; Tatchum-Talom et al., 2000). eNOS released by the endothelium induces vascular relaxation and inhibits many processes involved in atherosclerosis development, whereas nNOS is the major isoform found in the brain where it acts as a neurotransmitter (Dawson et al., 1996). iNOS is expressed in cells such as macrophages and vascular smooth muscle cells (VMSC) after exposure to cytokines and lipopolysaccharide (Chester, 1998), and through its potent cytotoxic actions is one mechanism by which macrophages kill invading pathogens (Bogdan et al., 2000).

The three nitric oxide synthases are similar in structure, each comprising a reductase and an oxygenase domain. The active enzyme is in the form of a dimer as illustrated for eNOS in figure 1.3. Each reductase domain has recognition sites for the cofactors nicotinamide adenine dinucleotide phosphate (NADPH), flavine adenine dinucleotide (FAD), flavine mononucleotide (FMN) and CaM. Electrons are shuttled form NADPH to FAD and then FMN and ultimately to the iron protoporphyrin IX (haem) within the oxygenase domain, which harbors the catalytic active site for the reaction L-arginine+O_2→NO+citrulline. The oxygenase domain also binds tetrahydrobiopterin (BH_4), which is thought to have multiple roles in NOS function (section 1.3.3).

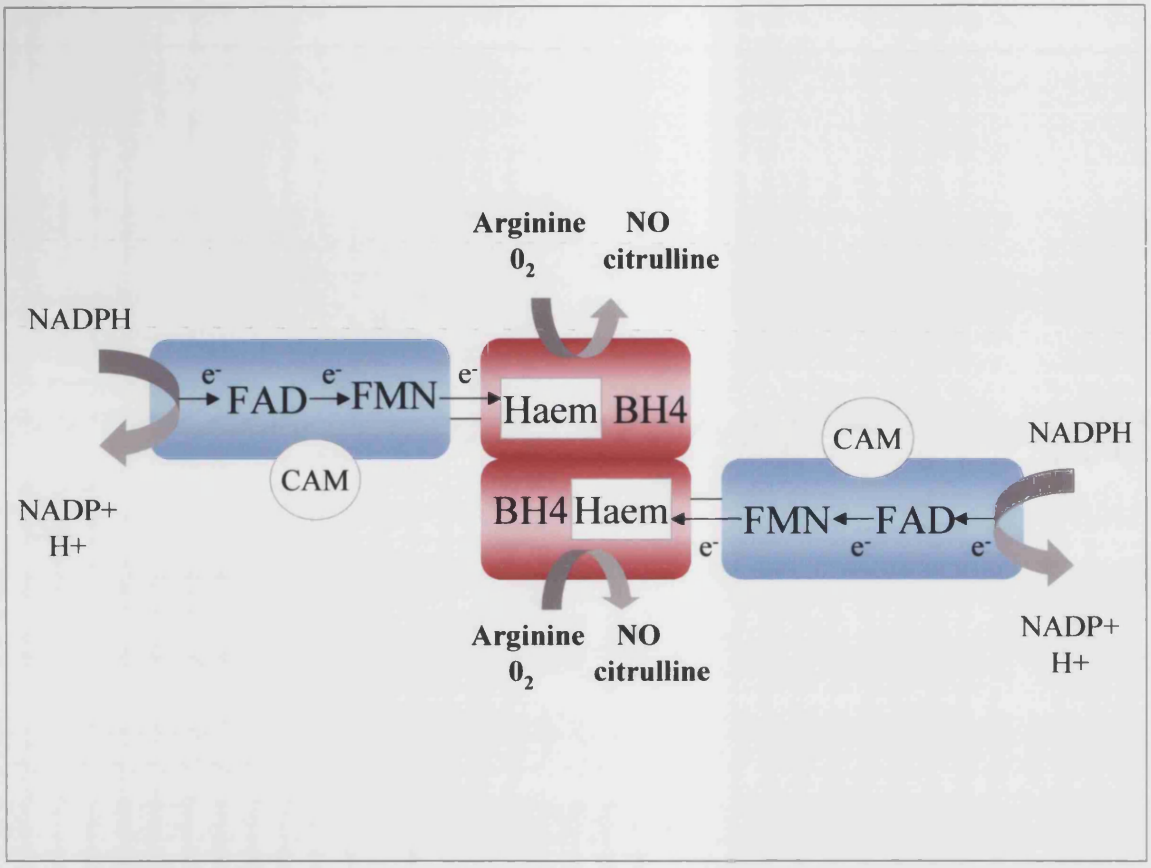

Figure 1.3. Diagrammatic representation of endothelial nitric oxide synthase (eNOS). The protein comprises a homodimer in its active state. Each monomer has an oxygenase domain (highlighted in red) and a reductase domain (highlighted in blue). Electrons are passed from NADPH to FAD and FMN within the reductase domain and then to haem within the oxygenase domain. The oxygenase domain binds BH_4, which could be involved in stabilization of the NOS dimer.

The corresponding three human NOS genes have each been characterized (Marsden et al., 1992; Charles et al., 1993; Hall et al., 1994). The genes encoding nNOS and eNOS (termed *NOS 1* and *NOS 3*) are located on chromosomes 12q24.2 and 7q35-36 respectively, and the gene encoding iNOS (*NOS 2*) is located on chromosome 17cen-q11.2. Each isoform exhibits an 80-90% homology between species, which is indicative of their high evolutionary conservation, and each isoform bears a 50-60% homology to each other within a species, suggesting a common ancestral NOS gene

(Alderton et al., 2001). The eNOS and iNOS genes are similar in structure, each composed of 26 exons. The iNOS gene is 37kb and encodes a protein of 1153 amino acids (131kDa), while the eNOS gene is smaller-21-22kb but encodes a protein 1203 amino acids (133kDa). In contrast the nNOS gene is much larger comprising 29 exons and has a complex structural organization over a distance of more than 200kb resulting in a protein of 1434 amino acids (161kDa). It is highly regulated by alternate splicing, which could be important for tissue specific NOS activity (Brenman et al., 1997). Splice variants have also been detected for iNOS, but not eNOS.

1.2.3 Physiological actions of eNOS

Endothelial NO is the most potent vasodilator known. It is synthesized from L-arginine and molecular oxygen with citrulline as the co-product (Moncada et al., 1993). Endothelial NO exerts its effects by diffusing into sub-adjacent vascular smooth muscle cells, where it activates soluble guanylate cyclase (sGC), which in turn stimulates the conversion of guanosine triphosphate to cyclic GMP (Rapoport et al., 1983). Increased levels of cyclic GMP lead to vascular smooth muscle cell relaxation and consequently vasodilation (Rapoport et al., 1983; Murad, 1986; Murad, 1990.). Other intrinsic properties of NO include: inhibition of platelet aggregation (Radomski et al., 1987b), inhibition of smooth muscle cell growth and migration (Nakiki et al., 1990; Sarkar et al., 1996) and anti-inflammatory properties such as inhibition of endothelial adhesion molecule expression and leukocyte adhesion (Bath et al., 1991; Bath et al., 1993). Thus physiological levels of NO are considered to confer atheroprotective and thromboresistant properties to the endothelium.

1.3 Decreased NO availability, endothelial dysfunction and cardiovascular disease

The onset of atherosclerosis is preceded by attenuation in functions of the endothelium, caused by environmental influences, genetic factors or both. The underlying causes of endothelial dysfunction are as yet not fully understood, however it is likely, given the key anti-atherogenic and anti-thrombotic properties of NO, that a reduction in its synthesis or action is an important part of this process. Studies of normal NO synthesis and regulation are providing a number of possible mechanisms to account for decreased availability of NO that underlies vascular disease. Some of the factors and pathways that might be involved are illustrated in figure 1.4. Decreased NO bioavailability that predates/predicts atherosclerotic events might result from reduced eNOS expression, increased ADMA (inhibitor of NOS), decreased BH_4 (co-factor for NOS) or increased inactivation of NO by reactive oxygen species. The evidence for these will be discussed in detail.

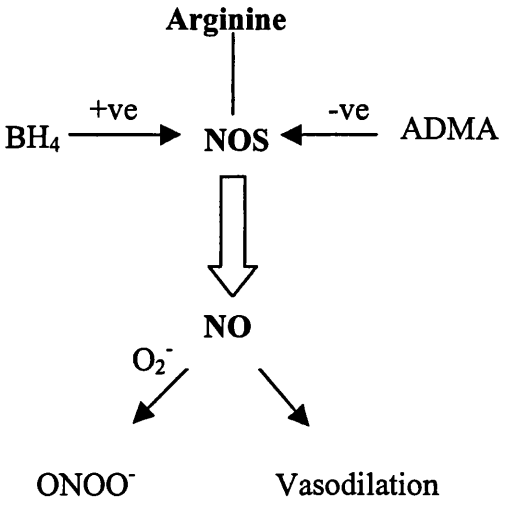

Figure 1.4 Regulation of NO synthesis. NO is synthesized by the enzyme NOS which requires BH_4 as a cofactor and is inhibited by asymmetric dimethylarginine (ADMA). NO has vasodilator and antiatherogenic properties but can be inactivated by oxidation to $ONOO^-$.

1.3.1 Decreased NOS expression or activity-studies of the eNOS gene (*NOS 3*)

The human eNOS gene, *NOS 3*, located on chromosome 7q35-36, comprises 26 exons and spans a distance of 21kb (Marsden et al., 1993). The 5' regulatory region exhibits a structure that is consistent with a constitutively expressed gene- it is TATA-less and harbours consensus sequences for transcription factors Sp1 and GATA. Decreased expression or activity of *NOS3* would be expected to result in decreased NO synthesis predisposing to endothelial dysfunction and vascular disease. It is not surprising therefore that the *NOS 3* gene has been the focus of intensive research to identify any polymorphisms or mutations, which could affect NO synthesis through differences in expression or activity. To date more than 100 polymorphisms have been identified in the *NOS 3* gene (NCBI SNP database, http//www.ncbi.nlm.nih.gov/SNP/), and at least four of these investigated as risk factors for atherosclerosis (Bonnardeaux et al., 1995; Wang et al., 1996; Yoshimura et al., 1998; Nakayama et al., 1999).

Decreased expression of *NOS 3* leading to reduced NO synthesis has been demonstrated in human atherosclerotic arteries (Oemar et al., 1998). To date more than 15 polymorphisms in the *NOS3* promoter have been described (NCBI SNP database, http//www.ncbi.nlm.nih.gov/SNP/) that might influence transcription. The –786T/C, -922A/G and –1468T/A polymorphisms were found to be associated with coronary spasm (Nakayama et al., 1999). In addition the –786T/C polymorphism has been associated with increased risk of CAD (Rossi et al., 2003) and influenced promoter activity in a luciferase/reporter assay system (Nakayama et al., 1999).

Polymorphisms within the coding region of the *NOS 3* gene could alter NOS enzymatic activity. One of the most studied eNOS polymorphisms (894G→T) within exon 7, is the only polymorphism identified that encodes an amino acid change- Glu298Asp (Glutamate to Aspartate at position 298). Individuals carrying the Asp variant have been reported as having an increased risk of developing IHD (Hingorani et al., 1999; Miyamoto et al., 1998; Yoshimura et al., 1998). These observations are supported by a recent meta-analysis in which data was available in 9867 cases and 13161 controls from 26 previous studies. The authors concluded that individuals homozygous for the 298Asp allele had a moderately increased risk of IHD (Casas et al, *unpublished data reproduced with permission of authors*). Expression studies have revealed that the Asp variant maybe more susceptible to proteolytic cleavage (Tesauro et al., 2000), and carriers of the Asp298 allele have been shown to have reduced endothelium-dependent vasodilation of the brachial artery during pregnancy (Savvidou et al., 2001).

1.3.2 Decreased L-arginine availability

Despite the fact that its concentration in cells/blood is greater than the K_m (1-4μM) of NOS for arginine (Charles et al., 1996; Bredt and Snyder, 1990), the availability of arginine may, in some circumstances become one of the rate limiting factors for the synthesis of NO. This observation has become known as the "arginine paradox". Several human *in vivo* studies have demonstrated that endothelial function can be improved by administration of arginine to both healthy (Bode-Boger et al., 1994; Mehta et al., 1996; Imaizumi et al., 1992) and atherosclerotic coronary arteries (Boger et al., 1998a; Tousoulis et al., 1998), but to date the reason for this phenomenon is still unexplained. Three possible theories have been put forward, the first suggests that

cellular arginine concentrations available to the NOS enzyme are somehow limited, for example if arginine is sequestered within storage pools inaccessible to NOS (McDonald et al., 1997). The second theory proposes that binding of arginine to the active site of NOS may be hindered by the presence of an inhibitor (Vallance et al., 1992), and the third that the transport of arginine into the cell via specific transporters may be down regulated (Kaye et al., 2002). The large oral dose of L-arginine that is required to improve endothelial function, has, however limited its use as a potential therapeutic agent.

1.3.3 Limited availability of BH_4 for NOS enzyme activity

It has been hypothesized that a deficiency in BH_4, either caused by a reduction in its synthesis or increased oxidative inactivation could lead to reduced NO availability and endothelial dysfunction. When BH_4 is limiting, NOS generates O_2^- rather than NO from oxygen and NADPH (Pou et al., 1992), but the reason why has continued to elude scientists possibly because the precise role of BH_4 in the synthesis of NO is still unclear (Vasquez-Vivar et al., 1999; Wever et al., 1997; Xia et al., 1998). Administration of low dose BH_4 to smokers, hypertensives, hypercholesterolemics and diabetics – all states in which endothelium-dependent vasodilation is attenuated can reinstate normal endothelial function, whereas BH_4 has no effect on healthy vessels at the same dose (Ueda et al., 2000; Stroes et al., 1997; Pieper, 1997). This observation is consistent with the theory that BH_4 availability may be limited in diseased vessels. Insufficient BH_4 availability maybe caused by reduced synthesis or oxidative inactivation. GTPcyclohydrolase 1 is the first and rate-limiting enzyme in the synthesis pathway of BH_4 (Duch and Smith, 1991). However, to date, no studies have investigated any

differences in expression of GTPCH-1 between atherosclerotic and non-atherosclerotic vessels. However, agents that improve endothelial function such as HMG-CoA reductase inhibitors (statins) also upregulate GTPCH-1 mRNA (Hattori et al., 2003). Oxidative inactivation of BH_4 is supported by studies in which endothelial function can be improved by vitamin C and folic acid supplementation and by the observation that in diseased tissues the BH_4/BH_2 ratio is reduced (Heller et al., 1999; Heitzer et al., 1996; Stroes et al., 2000). The beneficial effects of these anti-oxidants maybe due to direct scavenging of oxygen-derived free radicals. However it has also been proposed that vitamin C and folic acid may increase availability of BH_4, increase the affinity of BH_4 for eNOS or could facilitate the 1-electron oxidation of BH_4 to the BH_4 radical (Baker et al., 2001; Stroes et al., 2000).

1.3.3.1 Multiple functions of BH_4-essential NOS cofactor

The NOS enzymes depend on the cofactor BH_4, which binds to the haem-containing domain of the enzyme and forms part of the dimer interface. Its position within the NOS enzyme has led to the hypothesis that BH_4 is involved in stabilization of the NOS dimer (Klatt et al., 1995; Ghosh et al., 1996). However, the amount of BH_4 required for each isoform of NOS has been reported to differ, the iNOS isoform relying on more BH_4 for activity compared to eNOS and nNOS (reviewed in Stuehr et al., 1999). Other studies have proposed functions such as: promoting coupling of NADPH oxidation to NO synthesis (Vasques-Vivar et al., 1999), allosteric binding effects (Giovanelli et al., 1991; Klatt et al., 1994; Alderton et al., 1998) and modification of the haem environment (Wang et al., 1993; Wang et al., 1995). BH_4 is also an essential cofactor for the phenylalanine, tryptophan and tyrosine hydroxylases. These enzymes are

essential for the synthesis of hormones and neurotransmitters such as dopamine, noradrenaline, adrenaline and serotonin.

1.3.3.2 Synthesis of BH_4

Reduced synthesis of BH_4 could be one reason for decreased NOS activity leading to endothelial dysfunction, but this has not been systematically investigated. The pathway of synthesis of BH_4 is illustrated in figure 1.5. The initial step is the conversion of GTP to dihydroneopterin triphosphate by GTP cyclohydrolase 1 (GTPCH-1), which is the first and rate-limiting enzyme in this pathway (Duch and Smith, 1991). In man, but not rodents, a proportion of the dihydroneopterin triphosphate is converted to neopterin, which serves as a marker of pterin pathway activity. The majority of dihydroneopterin triphosphate is converted to 6-pyruvoyl tetrahydropterin by 6-pyruvoyl tetrahydropterin synthase (PTPS) and finally to BH_4 by sepiapterin reductase (SR). Mutations in GTPCH-1 and PTPS result in decreased BH_4 leading to hyperphenylalanaemia and a neurological disorder L-DOPA responsive dystonia (DRD) (Thony et al., 1997). However, the effects of polymorphisms or mutations in GTPCH-1 on endothelial function and risk of vascular disease have not yet been studied.

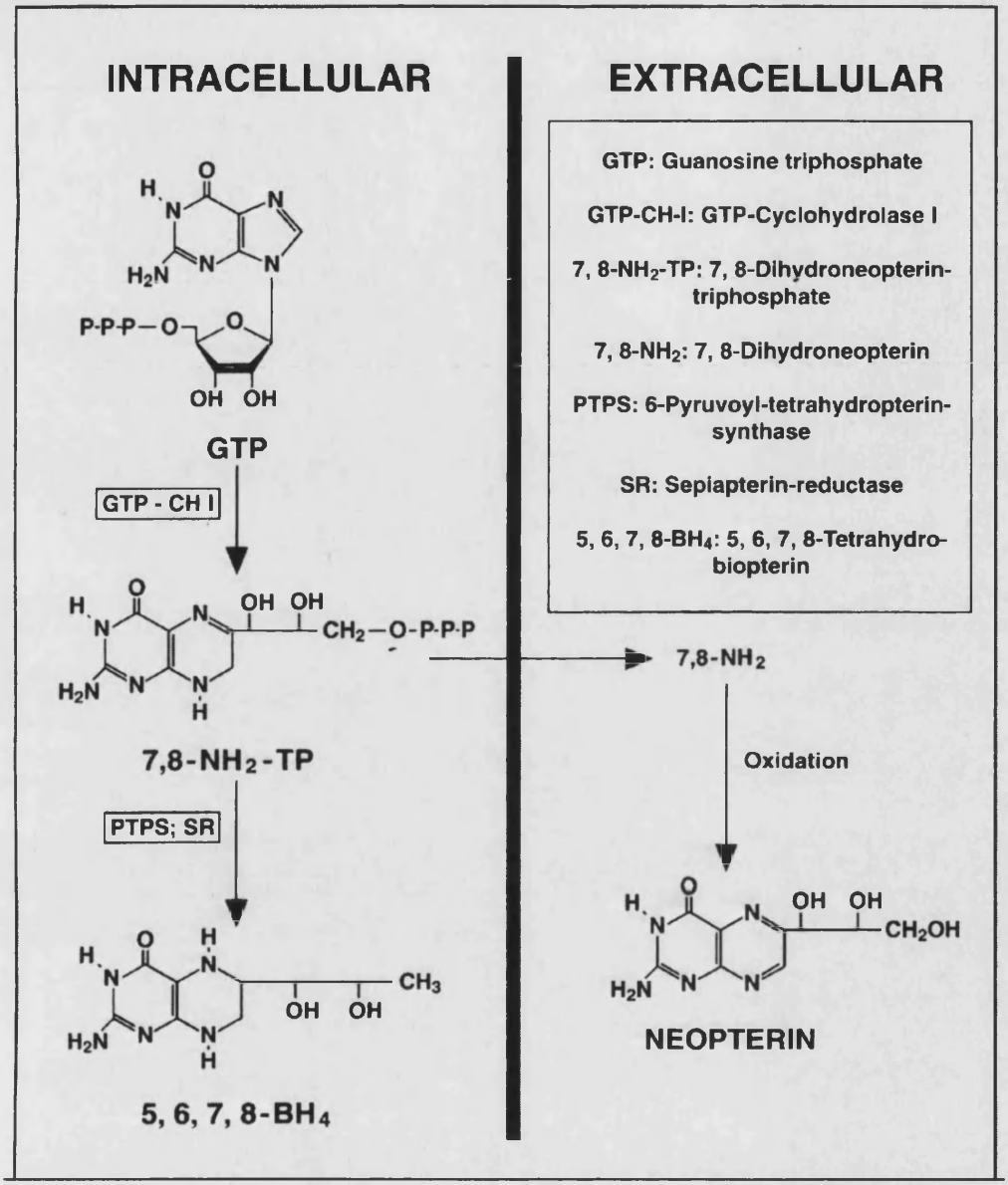

Figure 1.5. Synthesis of BH_4. BH_4 is synthesized from GTP via GTPCH-1 (the rate limiting enzyme), 6-pyruvoyl –tetrahydropterin- synthase and sepiapterin reductase. In man, but not rodents, a proportion of the dihydroneopterin triphosphate is converted to neopterin, which serves as a marker of pterin pathway activity.
Adapted from Brahms Diagnostica.

1.3.4 Inhibitors of nitric oxide synthase

Endogenous asymmetric methylarginines might have a profound effect on NO synthesis by inhibiting the NOS enzyme. Protein methylation occurs via a group of enzymes known as protein arginine methyltransferases (PRMT) and the breakdown of these proteins results in the release of free methylarginines including N^G-monomethyl-L-arginine (L-NMMA), asymmetric dimethyl-L-arginine (ADMA) and symmetric dimethylaginine (SDMA) (Kakimoto et al., 1970), which are cleared from the body via the kidneys. In addition L-NMMA and ADMA (but not SDMA) are also metabolized by dimethylaginine dimethylaminohydrolase (DDAH). It is interesting to note that SDMA, which is not metabolized by DDAH is also not capable of inhibiting the NOS enzyme (Figure 1.6). L-NMMA and ADMA are analogues of L-arginine and are elevated in various disease states in which vascular disease is a clinical manifestation such as hypertension (Goonasekera et al., 1997; Fujiwara et al., 2000), renal failure (Vallance et al., 1989; Vallance et al., 1992; Rees et al., 1989), preeclampsia (Pettersson et al., 1998) and peripheral arterial occlusive disease (Boger et al., 1997). Normalization of ADMA levels in renal failure patients by dialysis has been shown to associated with improved endothelium-dependent vasodilation (Cross et al., 2001). In a recent study, administration of ADMA to twelve healthy volunteers reduced heart rate and cardiac output, and increased blood pressure and systemic vascular resistance (Achan et al., 2003). Increased circulating levels of ADMA may therefore be a contributing factor of endothelial dysfunction. Sufficient concentrations of these methylarginines to "out compete" arginine for NOS has been put forward as an explanation for the arginine paradox (section 1.3.2).

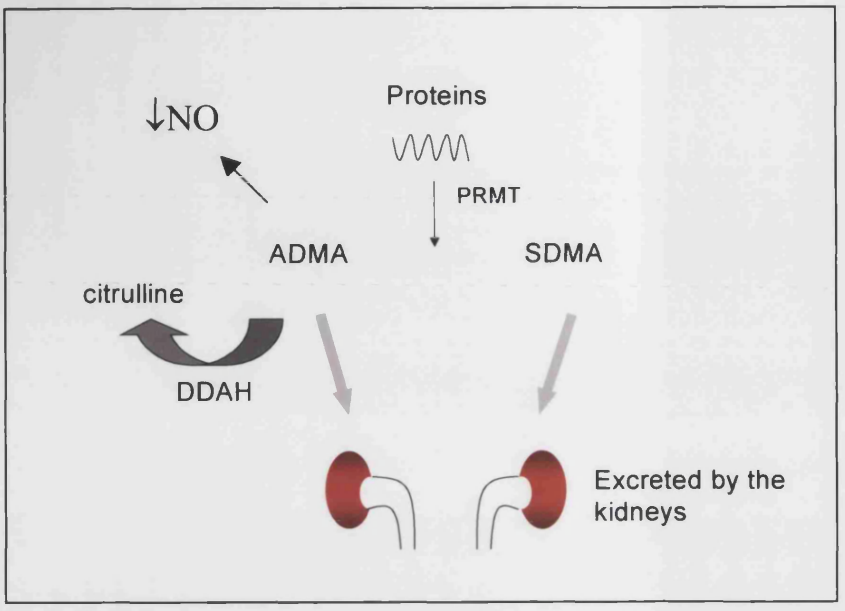

Figure 1.6 Synthesis and metabolism of ADMA. The methylarginines ADMA and SDMA are synthesized from the proteolysis of arginine methylated proteins, which involves protein arginine methyltransferases (PRMT). ADMA is a competitive inhibitor of NOS. Both ADMA and SDMA are eliminated from the body via the kidneys, however ADMA is also metabolized by DDAH.

L-NMMA has been utilized as a tool for research into the role of NO and endothelial relaxation for the past 10-15 years, however circulating concentrations of ADMA (0.5μm-1μM) are up to 10 times higher than L-NMMA in healthy individuals, and for this reason ADMA has attracted most interest as a possible endogenous inhibitor of NOS. The underlying cause of elevated ADMA in patients at risk of vascular disease development in unknown, but at present two potential mechanisms have been proposed:

(1) Upregulation of PRMTs resulting in increased protein methylation and subsequent breakdown would lead to elevated circulating methylarginines. Studies have shown that release of ADMA by endothelial cells is upregulated by

LDL cholesterol and this may be due to enhanced PRMT gene expression (Boger et al., 2000).

(2) Failure of ADMA to be cleared from the body. In addition to being excreted via the kidneys, ADMA is also metabolized by the enzymes dimethylarginine dimethylaminohydrolases (DDAH I + II). A decrease in metabolism or excretion would lead to an increase in circulating ADMA and inhibition of NO synthesis (MacAllister et al., 1996; Ito et al., 1999).

1.3.4.1 Reduced DDAH expression or activity could account for elevated ADMA

The observation that ADMA but not SDMA levels are elevated in patients at risk of developing CVD suggests that down-regulation or dysfunction of DDAH could be implicated in the pathogenesis of disease. DDAH has two isoforms named DDAH1 and DDAH2 (Leiper et al., 1999). Both enzymes are found in a variety of tissues, but the DDAH1 isoform is found predominantly in tissues expressing nNOS such as the brain, whereas DDAH2 is found in tissues expressing eNOS such as the heart and placenta (Tran et al., 2000). This may suggest isoform specific regulation of NOS enzymes, with DDAH2 possibly being the major functional variant within the vasculature.

The *DDAH2* gene is located on chromosome 6 within the major histocompatibility complex (MHC) class III region (Ribas et al., 1999). This region contains a number of genes, which are involved in autoimmune diseases such as insulin dependent diabetes mellitus, ankylosing spondylitis and celiac disease (Thomson et al., 1988; Benjamin et al., 1990; McManus et al., 1996). The *DDAH2* gene comprises 8 exons that span a

distance of 3kb and encodes a protein of 35kDa. To date a detailed analysis of the *DDAH2* gene has not been attempted, but it is possible that polymorphisms or mutations could alter expression or activity resulting in elevated ADMA.

1.3.5 Inactivation of NO by superoxide (O_2^-)

The production of reactive oxygen species (ROS) such as superoxide (O_2^-), hydrogen peroxide (H_2O_2), and peroxynitrite ($ONOO^-$) in the vasculature, have long been suspected as being implicated in the development of vascular disease. O_2^- levels are elevated in hypertension, heart failure, hypercholesterolemia, diabetes, preeclampsia and renal failure and could prove to be a common cause of endothelial dysfunction among these patients (Mehta et al., 1994; Keith et al., 1998; Ohara et al., 1993; Langenstroer et al., 1992; Sikkema et al., 2001; Canaud et al., 1999). The precise source of increased O_2^- in individuals at risk of CVD is unknown, but a number of enzymes expressed in the vasculature, are potential sources. These include xanthine oxidase, cyclooxygenase, NADH/NADPH oxidase (Griendling et al., 2000) and the mitochondrial electron transport chain. Decreased inactivation by antioxidant enzymes such as superoxide dismutases (SOD) of which there are three isoforms (Noor et al., 2002) may also contribute to increased O_2^- effects. It has been shown that endothelial function can be markedly improved after administration of anti-oxidants in individuals where endothelial function was previously impaired (Heller et al., 1999; Heitzer et al., 1996) and in cholesterol fed rabbits (Mugge et al., 1991), suggesting that O_2^- may inhibit the vasodilator properties of NO. Inactivation of NO may be caused by the rapid reaction of NO with O_2^- to produce $ONOO^-$ (Goldstein and Czapski, 1995), which can itself act as a potent oxidant (Beckman and Crow, 1993). In addition to oxidative

inactivation of NO, ROS species may also inactivate cofactors for NOS such as BH_4 (discussed in section 1.3.3). ROS species not only function as molecules able to inactivate many important proteins, but are known to be involved in many intracellular signaling pathways, which lead to regulation of gene transcription, smooth muscle cell proliferation and induction of adhesion molecule expression (Konishi et al., 1997; Fei et al., 2000; Weber et al., 1994). These diverse properties have made ROS, in particular O_2^-, prime suspects in the development of vascular disease.

1.3.5.1 NADPH oxidase is a major source of ROS in the vasculature

One of the main sources of ROS are the NADH/NADPH oxidases. Phagocytes use this enzyme system to produce bursts of O_2^- to kill invading pathogens, and it was subsequently found that endothelial cells and fibroblasts express their own NADH/NADPH oxidases, which are a major source of ROS in blood vessels. NADPH oxidase (in both phagocytic and non-phagocytic cells) is composed of five subunits: Gp91phox (the catalytic subunit), p22phox, p47phox, p67phox and p40phox (Figure 1.7), however the catalytic Gp91phox is both genetically and structurally different between phagocytic and non-phagocytic cells. Animal and human *in vitro* studies have demonstrated that production of ROS can be increased upon activation of NADPH oxidase (Gorlach et al., 2000; Heinloth et al., 2000). ROS generation is also enhanced through mechanical stress, inflammatory mediators such as TNF-α, angiotensin II and coagulation factors, possibly by induction of NADPH oxidase (Hishikawa et al., 1997; De Keulenaer et al., 1998; Bhunia et al., 1998; Griendling et al., 1994; Zhang et al., 1999; Patterson et al., 1999). The genes encoding each of the NADPH oxidase subunits are also attracting interest, as polymorphisms or mutations could have effects upon ROS

production and consequences for vascular disease. Currently eleven variants have been identified within the p22phox gene (*CYB A*) and most of these are associated with chronic granulomatous disease (Dinauer et al., 1990; Dinauer et al., 1991; de Boer et al., 1992; Yamada et al., 2000; Stasia et al., 2002). The C242T polymorphism which results in a histidine to tyrosine substitution at position 72 of the protein, has been the focus of most interest to date in relation to CVD (Parkos et al., 1988). This polymorphism has been associated with atherosclerosis, coronary artery disease (CAD) and cerebrovascular disease (Guzik et al., 2000a; Cahilly et al., 2000; Ito et al., 2000).

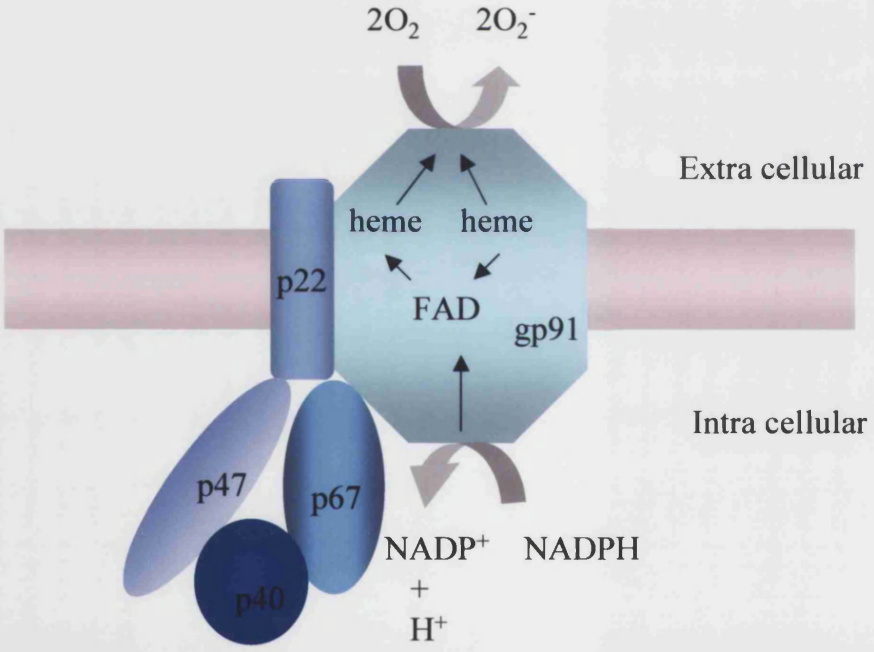

Figure 1.7 NADPH oxidase enzyme complex. The NADPH oxidase enzyme is composed of a membrane-spanning catalytic subunit called gp91phox, which is genetically and structurally different between phagocytic and non-phagocytic cell types. The gp91phox subunit interacts with p22phox to form the stable complex flavocytochrome b_{558}. Upon stimulation, the cytosolic components p47phox, p67phox and p40phox translocate to the flavocytochrome b_{558} complex to form the active enzyme.

1.4 Hypothesis

NO is a potent anti-atherogenic molecule produced in the endothelium by eNOS. A decrease in expression or activity of NO has been suggested as a causative agent in the development of vascular disease, which has a heritable basis. NOS requires the essential cofactor BH_4 which is synthesized from GTP via GTPCH-1 (which is the rate-limiting enzyme for this process). Reduced availability of BH_4 has been shown to result in increased production of O_2^- from eNOS, which can cause vascular damage. NOS can be inhibited by the endogenous L-arginine analogue ADMA. Plasma ADMA accumulates in hypercholesterolemics, hypertensives and in renal failure possibly resulting in endothelial dysfunction. The increase in ADMA may be attributed to a decrease in DDAH activity.

Based on the above, the central hypothesis explored in the studies of this thesis, is that common genetic variation (polymorphism) in the genes encoding enzymes regulating ADMA, BH_4 and O_2^- availability in the endothelium, influence NO availability and endothelial function and through this, might alter susceptibility to cardiovascular disease.

1.5 Aims

The aims of the work reported in this thesis were to:

1. identify common polymorphisms in the *GCH1* and *DDAH2* genes that might influence expression or activity.

2. relate any polymorphisms found to indices of gene expression or activity.

3. investigate associations between these polymorphisms and previously identified polymorphisms in the p22phox gene (*CYBA*) and NO synthesis and vascular function in healthy individuals and disease groups.

CHAPTER 2

MATERIALS AND METHODS

2.1 Materials

2.1.1 General reagents

All general purpose chemicals and reagents were supplied by Sigma Aldrich Company Ltd (Poole, Dorset, UK), BDH (Merck, Dorset, UK) or Invitrogen (Paisley, UK) unless otherwise stated.

2.1.2 Enzymes used for PCR and restriction digests

DNA polymerase was obtained from Invitrogen, (Paisley, UK). Restriction endonucleases were supplied by New England Biolabs (Hertfordshire, UK) and are listed in table 2.1.

Restriction enzyme	Recognition sequence
BsmF1	5' GGGAC(N)10↓ 3'
BsrD1	5' GCAATGNN↓ 3'
BstU1	5' CG↓CG 3'
Mwo1	5' GCNNNNN↓NNGC 3'
Rsa1	5' GT↓AC 3'

Table 2.1 Restriction endonucleases used for PCR-RFLP analysis. ↓ indicates the cutting site of each enzyme.

2.1.3 Oligonucleotides

Oligonucleotides were purchased from Sigma Aldrich Company Ltd (Poole, Dorset, UK). All oligonucleotides were synthesized at 0.2μM scale and desalted.

2.1.4 DNA ladders for agarose gel electrophoresis and genescan

100bp, 1kb and 1kb plus DNA ladders for sizing PCR products on agarose gels were obtained from Invitrogen (Paisley, UK). Genescan TAMRA-350 DNA ladder for sizing fluorescent-labeled PCR products was from Perkin Elmer, Applied Biosystems (Warrington, UK).

2.1.5 Gel loading buffers

Agarose gel loading buffer (6x concentrated) was purchased from Sigma Aldrich Company Ltd (Poole, Dorset, UK).

Polyacrylamide gel loading buffer (for SSCP) was made up as follows: 96% formamide, 2.5% bromophenol blue, 2.5% xylene cyanol, 0.5M EDTA.

Polyacrylamide gel loading buffer (for DNA sequencing) was made up as follows: 83% deionised formamide, 4.2mM EDTA (pH 8.0), 5% blue dextran.

TE buffer (for re-suspending DNA) was made up as follows: 0.01M Tris, 1mM EDTA (Ethylenediaminetetraacetic acid) adjusted to Ph 7.6 with concentrated hydrochloric acid (HCL).

2.1.6 Cell culture reagents

E.coli strain DH5α for cloning experiments was purchased from Invitrogen (Paisley, UK). Human umbilical vein endothelial cells (HUVEC) for transfection studies were from PromoCell (Heidelberg, Germany). HUVEC were cultured in EGM media (Biowhittaker, Cambrex Bioscience, Wokingham Ltd).

2.1.7 Kits

A list of kits (and their contents) used during this study are summarized below:

DNA miniprep kit (*Qiagen, Boundary Court, UK*):

Spin columns, 2ml collection tubes, buffers; P1, P2, N3, PB, PE, EB, RNaseA.

DNA midiprep kit (*Qiagen, Boundary Court, UK*):

Qiagen tips 100, QiaFilter cartridges, buffers; P1, P2, P3, QBT, QC,QF, RNaseA.

dRhodamine sequencing kit (*Perkin Elmer, Warrington, UK*):

Terminator ready reaction mix: A-Dye terminator labeled with dichloro[R6G], C-Dye terminator labeled with dichloro[TAMRA], G-Dye terminator labeled with dichloro[R110], T-Dye terminator labeled with dichloro[ROX], AmpliTaq FS, $MgCl_2$, Tris-HCL buffer.

Dual light luciferase reporter assay kit (*Promega, Madison, UK*):

Luciferase assay buffer II, Luciferase assay substrate, Stop and Glow® buffer, Stop and Glow substrate, Stop and Glow substrate solvent, 5x passive lysis buffer.

Neopterin ELItest® competitive enzyme immunoassay kit (*B.R.A.H.M.S diagnostica GMBH*):

96 well microtitre plate coated with anti-neopterin antibodies, uncoated plate, neopterin/alkaline phosphatase conjugate, enzyme conjugate buffer, substrate (4-nitrophenylphosphate), substrate buffer, stop solution (2M sodium hydroxide), wash solution, human serum neopterin standards, control sera.

Phastgel silverstain kit (*Amersham, UK*):

Formaldehyde 37%, fixing solution (0.7% benzene sulphonic acid, 24% ethanol), staining solution (0.2% silver nitrare, 0.7% benzene sulphonic acid), sodium carbonate 2.5%, stopper/preserver solution (1% acetic acid, 5% sodium acetate, 10% glycerol), sodium thiosulphate 2%.

QIAamp® DNA Blood mini kit (*Qiagen, Boundary Court, UK*):

Spin columns, 2ml collection tubes, Buffers; AL, AW1, AW2, AE, Proteinase K.

QIAquick gel extraction kit (*Qiagen, Boundary Court, UK*):

Spin columns, 2ml collection tubes, buffers: QC, PE, EB

QIAquick PCR purification kit (*Qiagen, Boundary Court, UK*):

Spin columns, 2ml collection tubes, buffers; PB, PE, EB.

TOPO TA cloning kit (*Invitrogen, UK*):

PCR®2.1-TOPO: 10ng/µl plasmid (in 50% glycerol, 50Mm Tris-HCL, 1Mm EDTA, 1Mm DTT, 0.1% Triton X-100, 100µg/ml BSA, phenol red), salt solution (1.2M NaCl), sterile water.

2.2 Methods

2.2.1 Extraction of DNA from whole blood samples

Two methods of DNA extraction were used during this study.

2.2.1.1 Salting out method

This method was originally described by Miller *et al*, 1988. Cell lysis was achieved by the addition of 10ml reagent A (109.54g sucrose dissolved in 10ml of 1M Tris pH7.5, 5ml of 1M $MgCl_2$ and 10ml Triton-X-100, made up to 1L with deionised water) followed by mixing and then centrifugation. The supernatant was discarded and the pellet re-suspended in a further 10ml of reagent A. This step was repeated to obtain a clean pellet. 2 ml of reagent B (2.34g NaCl and 1ml Tris-HCl (1M), 0.4ml Na-EDTA (0.5M), 90ml deionised water and 10ml of 10% SDS) was added to the pellet to complete nuclear lysis followed by 1ml of 5M sodium perchlorate for deproteinisation. Separation of protein was performed by the addition of 2ml chloroform and the samples mixed thoroughly. After centrifugation the upper aqueous phase containing the DNA was transferred to a fresh propylene tube and the lower phase containing protein discarded. 100ml of ice-cold ethanol was added to the samples for DNA precipitation. The DNA was removed by inserting and swirling a sterile pasteur pipette into the solution (the DNA adheres to the outside of the pipette) and washing the pipette in 70% ethanol to remove salt and organic molecules. DNA was re-suspended in TE buffer.

2.2.1.2 DNA purification kit method (*QiAmp blood minikit*)

Cell lysis was achieved by adding proteinase K to 200µl of whole blood. The lysate was then pipetted into a 1.5ml tube containing a silica-gel membrane. During centrifugation DNA adsorbs to the membrane whilst protein and other contaminants pass through. The membrane was then washed with a series of salt solutions to remove all traces of contaminants. The genomic DNA was eluted off the membrane with elution buffer (10mM Tris-Cl; 0.5Mm EDTA; pH9.0). An average of 6µg of DNA is purified using this protocol.

All DNA samples were stored at –20°C.

2.2.2 DNA amplification by PCR

All PCR reactions were performed in 30µl volumes containing, 2µl DNA, 10x buffer (500mM KCL, 100mM Tris (pH8.3), 0.01% Gelatin, 2mM each dNTP (dATP dGTP dTTP and dCTP), 10pmol of each oligonucleotide and 0.1U *Taq* DNA polymerase. The $MgCl_2$ concentration and annealing temperature were optimised for each oligonucleotide pair. Reactions were performed in 96-well microtitre plates (Abgene, Epsom, Surrey, UK). Cycling conditions were 95°C for 5min, followed by 35 cycles of 95°C for 30sec, annealing temperature for 30sec, 72°C for 1 minute and a final extension at 72°C for 10 mins on a (Techne-Genius, 96 well PCR machine). For each set of PCR reactions a negative control was carried out (by using sterile dH_2O in place of DNA) to test for DNA contamination.

2.2.3 Agarose gel electrophoresis

Molecular biology grade agarose (Invitrogen) was dissolved in 1xTBE (Invitrogen) to prepare gels of between 1 and 2% depending on the application. Ethidium bromide (0.5μg/ml) was added to the gel before allowing it to set. Samples were mixed 5:1 with 6x gel loading buffer to give a final concentration of 1x gel loading buffer. In addition a DNA ladder was loaded as a size marker. Samples were electrophoresed in 1xTBE running buffer at a constant voltage of 100V. After electrophoresis gels were visualized in a UV transilluminator (Syngene, UK).

2.2.4 Single-strand conformation polymorphism analysis (SSCP)

2.2.4.1 Radioactive SSCP

PCR was carried out in 30μl reaction volumes as described in section 2.2.2 with one modification- 90% dCTP was substituted with 0.2 mM α-^{32}P dCTP. 7.5% acrylamide gels were prepared by mixing 7.5ml 10xTBE, 11.25ml 49% acrylamide:Bis, 3ml 0.5M EDTA, 7.5ml glycerol and dH_2O up to a final volume of 75ml. 115μl of 25% APS and 115μl of TEMED were added prior to gel pouring into glass plates measuring 40cmx30cmx0.4mm. Gels were allowed to set at room temperature for a minimum of 2 hours. 3μl of radiolabelled PCR product was mixed with 6μl of loading buffer and denatured at 95°C for 3mins. Gels were run for 21 hours at 300 Volts. After electrophoresis gels were dried at 80°C for 30 minutes on a BioRad 583 gel dryer, and exposed to film (Hyperfilm MP,

Amersham, UK) for 1-2 days at –70°C. The films were developed by silver nitrate staining. Staining was stopped by acetic acid and background staining reduced with formaldehyde and sodium carbonate. Finally, films were washed with dH_2O.

2.2.4.2 Non-radioactive SSCP (*PhastSystem*)

Genomic DNA was amplified by PCR as described in section 2.2.2 with no radioactive label. PCR products were mixed with an equal volume of gel loading buffer, denatured at 95°C and immediately placed on ice to stabilize the structure of the single strands. The samples were loaded onto 12% or 20% ready prepared acrylamide gels and run at 4°C for approximately 700 average voltage hours (avh) on a PhastSystem electrophoresis apparatus (Amersham, UK) capable of running 2 gels simultaneously (total number of samples 16). The gels were visualised by silver staining with the PhastSystem silver stain kit as described by the manufacturers (Amersham, UK). Briefly the gels were fixed in a solution containing 0.7% benzene sulphonic acid and stained with 0.2% silver nitrate. The reaction was stopped with a stopper/preserver solution comprising 1% acetic acid, 5% sodium acetate and 10% glycerol. Sodium thiosulphate (2%) was used to reduce the background on the gels. Silver staining allows the detection of as little as 20-50pg/band of DNA.

2.2.5 DNA sequencing

2.2.5.1 Template preparation

The genomic region to be sequenced was amplified by PCR as described in section 2.2.2 and the PCR product used as a template. A total of 4 PCR reactions were carried out for each sample and combined to ensure adequate template was obtained after purification. All PCR products were purified using spin columns (Qiagen, UK) to remove excess primers and oligonucleotides. Briefly this process involved adding the PCR products to a tube containing a silica-membrane. The DNA adsorbs to the membrane under high salt concentrations, whilst contaminants pass through. The membrane was then washed with a low salt buffer to eliminate impurities such as unbound oligonucleotides (up to 40bp in length), and the DNA eluted with Tris buffer. This method allows the purification of up to 10μg of DNA.

2.2.5.2 Sequencing reaction

Sequencing was performed in 20μl reaction volumes containing 8μl dRhodamine dye terminator mix (Applied Biosystems,Warrington,UK), 3.2pmol of primer and 1μl of purified PCR product. Both forward and reverse reactions were performed on each PCR template to accurately verify sequencing in both directions. Cycling conditions used were: 25cycles of 95°C for 30sec, 55°C for 18sec, 60°C for 4mins on a (Techne-Genius, 96 well PCR machine). Sequencing products were precipitated with 95% ethanol and 3M sodium

acetate pH5.2 to remove any unincorporated nucleotides and primers and left to dry at room temperature. Samples were stored at –20°C until loading.

2.2.5.3 Gel loading and electrophoresis of sequencing products

5% polyacrylamide gels were prepared for DNA sequencing as follows: 18g urea, 27ml dH2O, 5.2ml 40% acrylamide (Anachem Ltd, Bedfordshire, UK) and 0.5g amberlite resin to de-ionise the solution were mixed thoroughly until all urea was dissolved and then filtered through 0.2μm sterile filter units. 5ml of 10xTBE was then filtered into the mix and the gel solution de-gassed for 5 minutes. 250μl of 10% ammonium persulphate and 35μl of TEMED were added immediately prior to gel pouring. The gels were cast in 36cm plates with 0.2mm thick spacers and left to set at room temperature for at least 2 hours. Four μl of loading buffer was added to each sequencing product and the samples denatured by heating at 95°C for approximately 3 minutes to separate the single strands. Denatured samples were placed immediately on ice and loaded without delay. Gels were run for 7 hours on an ABI377 DNA sequencer (Applied Biosystems, Warrington,UK) and data collected on an Apple Macintosh computer.

2.2.6 Genotyping

2.2.6.1 Genotyping by PCR-RFLP analysis

The genomic region of interest was amplified by PCR as described in section 2.2.2. Restriction sites either created or abolished by the presence of a polymorphism were identified by Webcutter software (http://www.firstmarket.com/cutter/cut2.html). Restriction digests were undertaken in 15μl reaction volumes comprising 10μl of PCR product, 2units of restriction enzyme, dH_2O and 1x appropriate buffer supplied by the manufacturers (final concentration). Digestion was carried out in 96 well plates by incubation for 16 hours at the optimum temperature for each particular enzyme on a Techne Genius 96 well PCR machine.

2.2.6.2 Genotyping by Genescan analysis

PCR was carried out as described in section 2.2.2. The forward reading oligonucleotide was labeled with the fluorescent dye 6-FAM (6-carboxyfluorescein). All PCR products were purified by spin column to remove any surplus oligonucleotides, which could interfere with the results. Samples were stored at –20°C until required.

4% polyacrylamide gels were prepared and cast in the same manner as for DNA sequencing (section 2.2.5.3), the gel mix comprising 18g urea, 25ml dH2O, 5ml 40% acrylamide (Anachem Ltd, Bedfordshire, UK) and 0.5g amberlite resin to de-ionise the solution. Prior

to gel loading the samples were diluted 1 in 20 with sterile dH_2O to reduce fluorescence produced by the labelled oligonucleotides. Four µl of loading buffer was added to 1µl of diluted sample and the samples denatured at 95°C for 3 minutes. Gels were electrophoresed in 1xTBE running buffer for 2.5 hours at on an ABI 377 DNA sequencer (Perkin Elmer, Warrington, UK). The data was collected on an Apple Macintosh computer using Genescan software.

2.2.7 Search of the National Center for Biotechnology Information (NCBI) SNP database for polymorphisms

The NCBI SNP database (http://www.ncbi.nlm.nih.gov/SNP/) was established in 1988 and is a resource of freely available molecular biology information compiled by genome sequencing consortiums worldwide. The database was searched by entering the genomic DNA accession number or gene symbol of interest and viewing the sequence in graphical format. All previously identified polymorphisms are listed and information regarding the flanking sequence, location, heterozygosity and identification numbers are shown. This information was used to compare polymorphisms in the database with polymorphisms identified by SSCP during this study.

2.2.8 Search of the MatInspector database for putative transcription factor binding sites

Genomatix software (http://www.genomatix.de/free_login.html) comprises tools and databases for the analysis of genomic sequences. The MatInspector database was used during this study to identify transcription factor binding sites within the promoter sequences of the *GCH1* and *DDAH2* genes. The software scans the sequence against a library of matrix descriptions for transcription factor binding sites to find sequence matches. All potential transcription factor binding sites are listed including the core binding sequence and its matrix similarity (a measure of how conserved each base in the core binding sequence is compared to the matrix).

2.2.9 Measurement of plasma nitrite and nitrate (*NOx*).

Plasma NOx was measured using a modification of the Griess reaction as described previously (Jeerooburkhan et al., 2001). All plasma samples were filtered through Ultrafree microcentrifuge filter units (Biomax-5, Millipore) prior to analysis to remove any proteins such as haemoglobin (Hb) which may interfere with the reaction. Plasma nitrate (NO_3^-) was reduced to nitrite (NO_2^-) by nitrate reductase and quantified by the addition of 1% sulphanilamide in 5% phosphoric acid and 0.1% N-(-naphthyl)ethylenediamine. All measurements were carried out in duplicate and the mean value of each sample taken as the reading. 40µl of plasma was added to 10µl of phosphate buffered saline (PBS) in a 96 well microtitre plate (Beckton Dickinson). To each sample well was added 1µM nicotinamide

adenine dinucleotide phosphate dehydrogenase (NADPH), followed by a master mix containing 500μM glucose-6-phosphate, 80U/L nitrate reductase and 160U/L glucose-6-phosphate dehydrogenase. The plates were then incubated in the dark for 1 hour at room temperature. 1% sulphanilamide in 5% phosphoric acid was then added to each well along with an equal volume of 0.1% N-(naphthyl)ethylenediamine and the plates incubated for 15 minutes at room temperature. To quantify NO_2^- produced, the absorbance was measured by UV visible spectroscopy on a Spectra Max 250, using SOFTmax Pro software (Molecular devices, Menlo Park, CA, USA).

2.2.10 Measurement of plasma neopterin

Neopterin was measured using the ELItest® competitive enzyme immunoassay kit (B.R.A.H.M.S diagnostica GMBH). Briefly, plasma samples were analysed in 96 well microtitre plates, which were coated with polyclonal sheep anti-neopterin antibody. Standards were made by adding 150μl of enzyme conjugate (consisting of neopterin-alkaline phosphatase conjugate) and 50μl neopterin standards (2-250nmol/L). Reactions were carried out by adding 50μl of patient plasma and 150μl enzyme conjugate to the pre-coated wells. The neopterin in the patient samples competes with the neopterin-enzyme conjugate for the active site of the sheep polyclonal antibodies. 100μl of 4-nitrophenylphosphate was added to the samples and standards which catalyses the removal of the phosphate from 4-nitrophenylphosphate resulting in a yellow colour (4-nitrophenole) forming in the reaction wells. Results were obtained by measuring the OD_{405nm} on a spectrophotometer using Softmax Pro software.

2.2.11 Luciferase reporter gene assay

2.2.11.1 Cell culture and transfection

HUVEC (Promocell, Germany) were cultured as monolayers in EGM media supplied by Biowhittaker at 37°C, 5% $C0_2$. Cells were seeded ~18hours prior to transfection at a density of $5x10^4$ cells/well into 12 well culture plates and were deemed suitable for transfection when approximately 70% confluent. Solution A containing Lipofectin (Invitrogen, Paisley, UK) (5.125µl for each well transfected) and Optimem 1 (Invitrogen, Paisley, UK) (82µl for each well to transfected) was mixed and left to warm to room temperature for 45 minutes. Solution B was made by mixing 0.6µg/well of plasmid construct, ~3ng/well *renilla* expression vector and 82µl/well optimem 1. A transfection mix was prepared by adding 87.125µl of solution A to solution B and left at room temperature for 15 minutes. Cells were washed with Optimem 1 to discard traces of growth media, which could interfere with transfection, and 330µl of Optimem 1 was added to each well. 168 µl of transfection mix was then added to each well and the cells incubated at 37°C, 5%CO_2 for four hours. After incubation the spent media/transfection mix was discarded and 1ml of EGM media added to each well. Cells were cultured for a further 48 hours.

2.2.11.2 Cell lysis and luciferase assay

Cell lysis and luciferase measurements were performed using the dual light luciferase reporter assay kit (Promega, Madison, USA). Cells were lysed by the passive lysis method. 250µl of passive lysis buffer was added to each well and mixed for 20 minutes to ensure complete lysis. Cell lysates were transferred to 1.5ml Eppendorf tubes and stored at –20°C until required, but for no longer than 48 hours. For luciferase measurement 20µl of cell lysate was transferred to a 96 well opti-plate (Packard Bioscience, Netherlands) and placed in a Tropix TR717 dual injection microplate luminometer (Applied Biosystems). The luminometer was programmed to inject 50µl of LAR1 followed by 50µl of Stop and Glow. For each experiment transfections were performed in triplicate for each construct and luciferase activity was normalised to *renilla* activity.

2.2.12 Populations collected for vascular phenotyping/disease studies

DNA from seven populations was collected for genotype/phenotype studies. Each of these cohorts had been developed with differing/complementary phenotypic measures.

2.2.12.1 Healthy Subjects

A) Prospective cohort study-NPHSII

Subjects were selected from the NPHSII cohort for analysis. This cohort comprises approximately 3000 healthy men recruited from 9 primary care practices in the UK (Table 2.2). The study was originally setup to test the hypothesis that prior to myocardial infarction there is a hypercoagulable state within the body (Meade et al., 1986). Demographic characteristics of the study cohort are summarized in table 2.3. The men were aged between 50 and 61 years and were healthy at the time of recruitment. All subjects were reviewed annually and asked to avoid heavy meals, refrain from smoking and vigorous exercise from the midnight before the examination. Smoking status, blood pressure, BMI, serum cholesterol, trigycerides, fibrinogen, factor VII coagulant activity (FVIIc % standard) and HDL cholesterol were measured at the time of recruitment and during follow-up visits over the following 9 years. Serum cholesterol and triglyceride levels were measured by automated enzymatic methods (Sigma, UK and Wako Chemicals, Alpha Laboratories, UK). Venous blood was taken at time of recruitment and the plasma

separated and stored at -80°C. All IHD events have been recorded over the time of the study.

Clinic	Number of men recruited
Aston Clinton	111
Camberley	416
Carnoustie	408
Chesterfield	261
Halesworth	435
Harefield	291
North Mymms	291
Parkstone	413
St. Andrews	386

Table 2.2. Number of men recruited from each of the 9 UK clinics for the NPHSII study cohort.

Characteristic	Mean (SD)
N	2965
Age (years)	56.1 (3.5)
BMI (kg/m^2)	26.5 (3.5)
SBP (mmHg)	138.1 (19.2)
DBP (mmHg)	84.5 (11.4)
Cholesterol (mmol/l)	5.7 (1.02)
Triglycerides (mmol/l)	1.79 (0.95)
FVIIc (% standard)	109.1 (28.9)
Fibrinogen (μmol/l)	0.08 (0.02)
ApoA1 (mmol/l)	1.63 (0.32)

Table 2.3 Demographic characteristics of the NPHSII study cohort.

B) German population screen

Blood was collected from 128 healthy German individuals by Professor Rainer Boger (Department of Clinical Pharmacology, University of Hamburg). ADMA and SDMA measurements were collected by HPLC. Measurements of age, height, weight, blood pressure, heart rate, triglycerides and cholesterol were recorded and entered into an excel database. Of the 128 individuals studied, 3 were hypercholesterolemic, 2 were hypertensive, and no individuals were recorded as diabetic. Demographic characteristics of this cohort are summarized in table 2.4

Characteristic	**Mean (SD)**
N	128
Age (years)	36.03 (11.16)
Height (cm)	177.0 (9.05)
Weight (kg)	75.85 (12.71)
SBP (mmHg)	127.9 (12.96)
DBP (mmHg)	79.30 (7.31)
Heart rate (bpm)	73.14 (8.10)
ADMA (μmol/l)	0.78 (0.40)
SDMA (μmol/l)	0.59 (0.29)

Table 2.4 Demographic characteristics of the German population screen cohort.

C) Cambridge Young Adults Study

This cohort was originally recruited by Dr. John Deanfield (University College London) to investigate associations between eNOS genotype and vascular function (Leeson et al., 2002). Healthy individuals born in the Cambridge Maternity Hospital between 1969 and 1975 (in whom early growth measures had been recorded) were invited to attend a clinic for cardiovascular risk profile evaluation. A total of 264 subjects aged 20-28 years were recruited. Blood was collected by venepuncture and personal and family medical history (including details of heart disease and risk factors) assessed by questionnaire. In each subject a fasting venous blood sample was analysed for insulin, glucose, total cholesterol, HDL, LDL and triglycerides. Individuals were classed as smokers if one of more cigarette was smoked per day for the previous six months. Blood pressure, weight (to +/-0.1kg) and height (+/-0.1mm) were also recorded. Measurement of endothelial dependent and independent vascular responses of the brachial artery were performed using high resolution ultrasound imaging (Acuson 128XP/10. 7MHz probe and automated vessel diameter measurement) as described in section 2.2.13.2. All FMD measurements were carried out by Dr. Paul Leeson. Phenotypic characteristics of this cohort are shown in table 2.5.

Characteristic	Mean (SD)
N	264
Age (years)	23.49 (1.837)
Height (cm)	168.4 (10.42)
Weight (kg)	68.42 (12.54)
SBP (mmHg)	127.3 (13.98)
DBP (mmHg)	70.34 (8.75)
Total cholesterol (mmol/l)	4.58 (1.01)
LDL cholesterol (mmol/l)	2.84 (0.91)
HDL cholesterol (mmol/l)	1.2 (0.3)

Table 2.5 Demographic characteristics of the Cambridge Young Adults Study.

2.2.12.2 Renal Failure patients

A) London renal failure patients

A cohort of individuals comprising 130 renal failure patients of different ethnicity, 53% males and 47% females, were recruited from the Middlesex Hospital, London by Dr. Jenny Cross. Endothelial function was assessed in vivo by the measurement of conduit artery in response to increased blood flow (flow mediated dilatation; FMD) (section 2.2.13.2). Systolic and diastolic blood pressure measurements were taken using a sphygmomanometer. ADMA and SDMA measurements were made by Miss Rachel Jackson (University College London), using reverse phase high-pressure liquid chromatography (HPLC) as described by Vallance et al., 1992. Demographic characteristics of the study cohort are summarised in table 2.6.

Characteristic	Mean (SD)
N	130
Age (years)	53.4 (17.59)
SBP (mmHg)	144.8 (32.02)
DBP (mmHg)	85.16 (52.83)
FMD (% change)	4.64 (4.45)
ADMA (μmol/l)	1.57 (1.16)
SDMA (μmol/l)	3.71 (2.05)

Table 2.6 Demographic characteristics of the London Renal Failure cohort.

B) Italian renal failure patients (CREED)

DNA from 277 renal failure patients was kindly donated by Dr Carmine Zoccali (IBIM-CNR, Italy). Subjects were originally recruited for the CREED (Cardiovascular Risk Extended Evaluation in Dialysis) study, in which a total of 278 dialysis patients were followed up over a 4 year period to determine risk markers for CVD among patients with advanced renal disease (Malatino et al., 1999). Demographic characteristics of the study cohort are summarised in table 2.7. Measures of cardiovascular risk factors such as ADMA, SDMA, fibrinogen, homocysteine, cholesterol, C-reactive protein and age were recorded as well as time of death (all cause and CVD related).

Characteristic	Mean (SD)
N	277
Age (years)	61.02 (15.38)
SBP (mmHg)	132.2 (22.64)
DBP (mmHg)	74.36 (12.16)
Total cholesterol (mmol/l)	5.39 (1.46)
HDL (mmol/l)	1.06 (0.3)
LDL (mmol/l)	3.41 (1.26)
Triglycerides (mmol/l)	2.0 (1.02)
BMI (kg/m^2)	24.89 (4.37)
Fibrinogen (μmol/l)	13.39 (6.16)
ADMA (μmol/l)	3.26 (2.04)
SDMA (μmol/l)	3.71 (2.18)

Table 2.7 Demographic characteristics of the Italian Renal Failure cohort (CREED).

2.2.12.3 Diabetic patients and controls (EBCT cohort)

A cohort of 385 individuals comprising 188 type I diabetic patients and 197 control subjects was collected by Dr. H Colhoun (University College London) initially to measure the effect of diabetes on coronary artery calcification (CAC) (Colhoun et al., 2000). Diabetic patients were recruited form five London hospitals and defined by age of onset ≤25years. Control subjects were drawn from two London general practices and were included regardless of heart disease. All participants gave informed written consent. The health status of all subjects was assessed by questionnaire, which noted alcohol consumption, smoking status and amount of exercise taken weekly. Blood pressure was

measured in triplicate and the mean of the second and third reading used. CAC was measured by electron beam computerised tomography (EBCT), using an Ultrafast CT scanner (IMATRON C-150XL). In vivo vascular function studies were performed by venous occlusion plethysmography as described previously (Chan et al., 2003) (section 2.2.13.1). Briefly, forearm blood flow was measured in response to intra-brachial artery infusion of acetylcholine (ACh) at doses 25, 50 and 100 nmol/min each dose for 3 minutes, bradykinin (BK) at doses 10, 30 and 100pmol/min each dose for 3 minutes, glyceryl trinitrate (GTN) at doses 4, 8 and 16 nmol/min each dose for 5 minutes, N^G-monomethyl-Larginine (LNMMA) at doses 1, 2 and 4μmol/min each dose for 5 minutes and noradrenaline (NA) at doses 60, 120 and 240pmol/min each dose for 5 minutes. Total cholesterol, HDL, LDL, triglycerides and C-reactive protein (CRP) were also recorded.

Characteristic	**Total cohort** Mean (SD)	**Diabetics** Mean (SD)	**Non-Diabetics** Mean (SD)
N	385	197	188
Age (years)	37.9 (3.9)	37.9(3.9)	37.9(3.9)
SBP (mmHg)	121.1 (14.24)	124.9 (13.47)	117.5 (14.1)
DBP (mmHg)	73.4 (9.2)	73.92 (8.6)	72.79 (9.75)
Cholesterol (mmol/l)	5.42 (1.16)	5.34 (1.09)	5.5 (1.22)
HDL (mmol/l)	1.77 (0.44)	1.84 (0.47)	1.7 (0.41)

Table 2.8 Demographic characteristics of the Diabetic patients and controls. The mean (SD) of CVD risk factors are shown for the total cohort, diabetics and non-diabetics.

2.2.12.4 Pregnant Females

139 unrelated Caucasian women with normal singleton pregnancies were previously recruited from the Harris Birthright Centre antenatal clinic by Dr Makrina Savvidou (Kings College London) to study the association of the Glu298Asp eNOS polymorphism with FMD during pregnancy (Savvidou et al., 2001). All were healthy and had no history of cardiovascular disease. Age, smoking status, blood pressure, FMD, gestational age, parity and heart rate were recorded. Demographic characteristics of this study cohort are summarised in table 2.9.

Characteristic	**Mean (SD)**
N	139
Age (years)	33 (30-35)
BMI (kg/m^2)	22.94 (21.11-25.21)
Smokers	24%
SBP (mmHg)	115.4 (10.17)
DBP (mmHg)	68.8 (10.33)
Cholesterol (mmol/l)	5.11 (0.80)
FMD (% max)	9.33 (3.29)
Gestational age (weeks)	12.4 (12.3-12.9)
Heart rate (bpm)	75 (9.0)

Table 2.9 Demographic characteristics of the pregnancy cohort.

2.2.13 Measures of vascular function

2.2.13.1 Venous occlusion plethysmography

Forearm blood flow was measured by venous occlusion plethysmography as described previously (Benjamin et al., 1995). All studies were carried out by the individual who recruited the patient cohort. Briefly, the subject lay supine in a quiet temperature controlled laboratory and the brachial artery of the non-dominant arm was cannulated with a 27-gauge needle inserted under local anaesthesia (2mL of 1% lidocaine). A strain-gauge (mercury in silastic) was placed around the forearm to measure the change in forearm circumference in millimetres per minute, which is proportional to arterial blood inflow. Resting blood flow was allowed to normalise for 30 minutes following needle insertion prior to the infusion of vasoactive drugs. Drugs (ACh, BK, LNMMA, NA and GTN) or normal saline (sodium chloride 0.9% wt/vol) were infused continuously at 0.5mL/min. During periods of recording, the hands were excluded from the circulation by inflating wrist cuffs to 200 mmHg. The needle was removed at the end of each study period.

2.2.13.2 Flow mediated dilatation (FMD)

Measurement of endothelial dependent and independent vascular responses of the brachial artery were performed using high resolution ultrasound imaging. All studies were carried out by the individual who recruited the patient cohort. Each subject lay supine in a quiet temperature controlled laboratory and, after ten minutes brachial artery diameter and blood

flow were recorded at baseline. A pneumatic cuff was then inflated to suprasystolic pressure on the forearm for four and a half minutes. Deflation of the cuff resulted in reactive hypereamia causing increased flow through the brachial artery stimulating endothelium dependent flow mediated dilation (FMD). The change in brachial artery diameter was measured one minute after cuff deflation (maximal response). Measurements were then repeated after a ten minute rest, and between three and four minutes after a single sublingual spray of glyceryl trinitrate (GTN) to measure endothelium-independent response.

2.2.14 Statistical analysis

All statistical analyses were carried out using Graphpad Prism software (version 3.0), or STATA. Phenotypic measures are described by the mean and standard deviation (SD). Observed numbers of each genotype were compared with those expected under the assumption of Hardy-Weinberg equilibrium by χ^2 analysis (see appendix I). Allele frequencies were deduced from genotype frequencies. Pairwise linkage disequilibrium coefficients between polymorphisms were estimated by log linear analysis (Chakravarti et al., 1984) (Appendix II). Allelic associations were tested by One-Way Analysis of Variance (ANOVA) or student t test where appropriate. A P value of <0.05 was taken to be statistically significant. The Bonferroni test was used where necessary to correct for multiple comparisons.

CHAPTER 3

ASSOCIATION STUDIES OF THE NADPH OXIDASE p22PHOX C242T POLYMORPHISM AND ENDOTHELIAL FUNCTION

3.1 Aim

To investigate the association between the p22phox (*CYBA*) C242T polymorphism and endothelial function in healthy subjects.

3.2 Background

The possible role of ROS in the development of vascular diseases such as atherosclerosis has attracted widespread interest over recent years. ROS mediate oxidation of LDL particles, which accumulate causing damage to the endothelium, and contribute to atherosclerotic plaque development (Witztum et al., 1991). In addition ROS have been implicated in the promotion of smooth muscle cell growth, migration and apoptosis (Griendling et al., 2000) all of which occur during the atherogenic process. The reactions between ROS and NO may also have implications for vascular disease development. For example, NO reacts rapidly with O_2^- to produce $ONOO^-$, which can lead to protein and DNA damage, but perhaps most importantly results in 'quenching' of the vasodilator and numerous athero-protective functions of NO, leading, potentially to endothelial dysfunction (Beckman et al., 1990). Several studies have indicated that O_2^- is indeed elevated in disease states such as hypertension, heart failure, hypercholesterolemia, diabetes, preeclampsia and renal failure, and could be contributing to the endothelial dysfunction seen in these disorders (Mehta et al., 1994; Keith et al., 1998; Ohara et al., 1993; Langenstroer et al., 1992; Sikkema et al., 2001; Canaud et al., 1999). Diverse sources for the increased O_2^- in the vessel wall have been proposed including enzymes such as the NADPH oxidases,

xanthine oxidase, cyclooxygenase or, under some circumstances, NOS. Decreased inactivation of O_2^- for example by SOD might also contribute (Kodja et al., 1999; Fukai et al., 2002). O_2^- production by the NADPH oxidase enzyme in the vasculature has attracted a vast amount of interest to date, and is the main focus of this chapter.

3.2.1 NADPH oxidase generates O_2^- in both phagocytic and non-phagocytic cells

Release of O_2^- by cells of the immune system (primarily macrophages) is part of an innate defense mechanism against bacterial pathogens. The production of O_2^- is mediated by the enzyme NADPH oxidase which utilizes either NADH or NADPH as an electron donor to reduce molecular oxygen (O_2) to O_2^- in the reaction: $NAD(P)H + 2O_2 \rightarrow NAD(P)^+ + 2O_2^-$. A functional NADPH oxidase in non-phagocytic cells was proposed when patients with the X-linked form of the immunodeficiency syndrome-chronic granulatomous disease (CGD, which is caused by a dysfunctional or absent gp91phox subunit of the NADPH oxidase), were found to have normal O_2^- production in fibroblasts (Meier et al., 1993). Subsequently mRNA and protein for NADPH oxidase subunits have been identified in a variety of cell types including human and animal endothelial cells and vascular smooth muscle cells (Van Heerebeek et al., 2002), leading to the theory that NADPH oxidase may represent a major source of O_2^- in the human vasculature. This theory is supported by evidence that the vascular wall is a site of O_2^- generation (Barbacanne et al., 2000), and the finding of an association between O_2^- generated from NADPH oxidase in the vascular wall and risk factors for atherosclerosis (Guzik et al., 2000a). In addition, a number of studies have recently demonstrated evidence for increased NADPH oxidase subunit expression in

diseased vessels. For example Morawietz et al., 2001 demonstrated a 10 fold increase in expression of gp91phox mRNA in aortic rings of spontaneously hypertensive rats which correlated with a 3 fold increase in production of O_2^- (although this might also reflect the recruitment of macrophages in diseased vessels). p22phox mRNA expression was shown to be elevated in aortic VSMC of hypertensive rats (Fukui et al., 1997), and also in human atherosclerotic coronary arteries compared to non-atherosclerotic arteries (Azumi et al., 1999). Also, studies of smooth muscle cells from genetically modified mice ($p47phox^{-/-}$) demonstrated reduced O_2^- production and proliferation compared to wild type mice. Smooth muscle cells from mice lacking the gp91phox subunit ($gp91phox^{-/-}$) however were indistinguishable from smooth muscle cells from wild type mice. Comparison of aortic atherosclerotic lesions of ApoE knockout mice ($ApoE^{-/-}$, a model of atherosclerosis) with ApoE and p47phox double knockout mice ($ApoE^{-/-}/p47phox^{-/-}$) demonstrated reduced lesion size in the $ApoE^{-/-}/p47phox^{-/-}$ mice, suggesting a role for NADPH oxidase in the development of atherosclerosis (Barry-Lane et al., 2001).

3.2.2 Vasculature NADPH oxidase is distinct from phagocytic NADPH oxidase

Both phagocytic and vascular NADPH oxidases are transmembrane proteins comprising five subunits-gp91phox, p22phox, p47phox, p67phox and p40phox (Chapter 1.3.5.1). The gp91phox and p22phox subunits associate with each other to form the active flavocytochrome b_{558}, whereas the three other phox proteins are cytosolic and associate with the flavocytochrome b_{558} to modulate its function. In contrast to the phagocytic NADPH oxidase, which releases O_2^- almost instantaneously, the vascular enzyme releases O_2^- more

slowly and it has been estimated that its capacity is one third that of the phagocytic enzyme (Griendling et al., 1998).

Recent research indicates that in non-phagocytic cells the gp91phox subunit of phagocytic NADPH oxidase is replaced by homologous proteins designated Nox1, Nox3, Nox4 and Nox5, depending on the cell type in which it is expressed. These differences account for the reduced enzyme activities in phagocytic versus non-phagocytic cells. Nox1 mRNA has been detected in colon, prostate, uterus and vascular smooth muscle cells (Suh et al., 1999; Kikuchi et al., 2000), Nox3 is expressed by fetal kidney tissue, and Nox4 and 5 by renal epithelial cells (Geiszt et al., 2000; Shiose et al., 2001). The phagocytic NADPH oxidase contains the prototype gp91phox (also termed Nox2). Differential expression of gp91phox isoforms was first demonstrated by Sorescu et al., 2002. They reported gp91phox (Nox2) expression predominantly in the adventitia and intima of non-atherosclerotic arteries and in the plaque core of atherosclerotic arteries where macrophages are most active. In contrast the expression of the Nox4 isoform was complementary to that of gp91phox (Nox2), being mainly expressed in the media of non-atherosclerotic arteries and again where gp91phox (Nox2) was absent in atherosclerotic arteries. Only one isoform of p22phox has been reported, and its expression correlates with regions of O_2^- production. Thus differences in the expression pattern of gp91phox (Nox2) isoforms maybe relevant in the progression of atherosclerosis. However, as yet no genetic analysis of the Nox subunits expressed in the vasculature has been reported other than gp91phox mutations causing the X-linked form of CGD (OMIM database, www.ncbi.nlm.nih.gov). In contrast the gene encoding p22phox (*CYBA*) has been studied in detail and, in addition to mutations causing an autosomal

recessive form of CGD, several polymorphisms have also been identified (Parkos et al., 1988; Dinauer et al., 1991; de Boer et al., 1992).

3.2.3 Common Genetic variation in p22phox

Conjugation of the p22phox subunit with any of the Nox isoform subunits is essential for NADPH oxidase enzyme activity, and p22phox expression has been shown to correlate primarily with regions of elevated O_2^- production (Sorescu et al., 2002). Polymorphisms in one or more of the NADPH oxidase subunits could either up or down regulate the generation of O_2^- and prove to be an important risk factor for vascular disease development. Several mutations in the p22phox gene (*CYBA*) are known to cause autosomal recessive CGD (Dinauer et al., 1991; de Boer et al., 1992), but vascular function has not been systematically investigated in these individuals. To date two polymorphisms (C242T and A640G) have been described in the *CYBA* gene and investigated for association with atherogenesis (Guzik et al., 2000a; Cahilly et al., 2000; Cai et al., 1999; Gardemann et al., 1999). The *CYBA* C242T polymorphism, which results in a His72→Tyr substitution that lies in a potential heme-binding site within exon 4 of the protein (Parkos et al., 1988), has been the main focus of study. Several conflicting reports have been published as to the significance of this variant for vascular O_2^- production. For example, Guzik et al., 2000 demonstrated that the 242T allele was associated with reduced NADPH oxidase activity in human blood vessels from patients with CAD. Carriage of the T allele was also associated with augmented FMD of the brachial artery in 93 patients, 30% of whom had evidence of CAD (Schachinger et al., 2001), suggesting that the 242T allele may exert a protective

effect upon the vasculature by down-regulating O_2^- production. This data is supported by a case-control study in which the 242T allele was present at higher frequency in control subjects than individuals with CAD in a Japanese population (Inoue et al., 1998). In contrast, Cahilly et al., 2000, reported the 242T allele was associated with increased progression of CAD and decreased regression of disease upon treatment compared to CC homozygotes in a study of 313 individuals from the Lipoprotein and Coronary Artery Study. The C242T polymorphism was not associated with the occurrence or severity of CAD in a cohort of 689 Australian Caucasians, however in a small subset of 44 males the T allele was found to be more common amongst those with CAD (Cai et al., 1999). However, functional genetic studies in patients might be confounded by the presence of disease and/or drug treatment. The aim of this study therefore, was to genotype two cohorts (one comprising healthy individuals and one comprising 199 diabetics and 201 controls) for the p22phox C242T polymorphism, and investigate the hypothesis that endothelium-dependent vaso-reactivity in healthy subjects would be dependent on genotype for the C242T polymorphism of p22phox.

3.3 Subjects and Methods

3.3.1 Subjects

Two subject groups were investigated for association between p22phox genotype and vascular function during this study:

Cambridge Young Adults Study:

Individuals from the Cambridge Young Adults Study were selected for association studies between genotype and endothelium dependent and independent vascular response (Chapter 2.2.12.1). Briefly, this cohort comprises 264 healthy individuals (127 males, 137 females) born in the Cambridge Maternity Hospital between 1969 and 1975. A fasting venous blood sample was obtained form each participant and measures of various CVD risk factors such as cholesterol, blood pressure and glucose were recorded (detailed in Chapter 2.2.12.1). Subjects were classed as smokers (if 1 or more cigarette was smoked per day for the past 6 months), previous smokers or non-smokers. Demographic characteristics of the study participants are outlined in table 2.5. Brachial artery diameter was measured in response to endothelium dependent (FMD) and independent (sublingual GTN) stimulus using high-resolution ultrasound imaging.

EBCT cohort:

Individuals from the EBCT cohort were investigated for associations between genotype and endothelial function. Briefly, this cohort consists of 385 individuals comprising 188 type 1

diabetic patients and 197 control subjects (Chapter 2.2.12.3). Blood samples were collected from participants after an overnight fast and measures of total cholesterol, HDL cholesterol and triglycerides were recorded. Vascular function was assessed *in vivo* by forearm venous occlusion plethysmography (Chapter 2.2.13.1), which involves measuring forearm blood flow in response to intrabrachial infusion of the endothelium-dependent dilators acetylcholine (ACh) at doses 25, 50 and 100 nmol/min and bradykinin (BK) at doses 10, 30 and 100 pmol/min, each dose for 3 min, and the endothelium-independent dilator glyceryl trinitrate (GTN) at doses 4, 8 and 16 nmol/min, each dose for 5 min. N^G-monomethyl-L-arginine (L-NMMA) at doses 1, 2 and 4 μmol/min, each dose for 5 min, and noradrenaline (NA) at doses 60, 120 and 240 pmol/min, each dose for 5 min, were infused as endothelium-dependent and independent constrictors respectively.

3.3.2 DNA extraction

DNA was extracted from whole blood samples using the salting-out method as described in Chapter 2.2.1.1.

3.3.3 Genotyping by PCR-RFLP analysis

Exon 4 of the p22phox (*CYBA*) gene was amplified by PCR as described in Chapter 2.2.2 with forward (5' TGCTTGTGGGTAAACCAAGGCCGGTG 3') and reverse (5' AACACTGAGGTAAGTGGGGGT 3') oligonucleotides described by Inoue et al., 1998. The optimum annealing temperature and $MgCl_2$ concentration for the reaction were 60°C

and 2mM respectively, and amplification resulted in a band of 348bp containing the p22phox C242T polymorphic site. The C→T base substitution of the p22phox C242T polymorphism resulted in the creation of an *Rsa1* restriction enzyme site. Genotyping was therefore carried out as described in Chapter 2.2.6.1 using restriction enzyme *Rsa1* to distinguish between allelic variants. Digests were carried out overnight at 37°C. Upon digestion the 348bp PCR product was cleaved into fragments of 188bp and 160bp in the presence of the T allele. Products were electrophoresed on 1.5% agarose gels stained with ethidium bromide.

3.3.4 Data analysis

Genotype frequencies were compared to those expected under Hardy-Weinberg equilibrium by χ^2 analysis. Allelic associations were tested by One-Way Analysis of Variance (ANOVA) or Student t-test where appropriate. Multiple logistic regression was applied to analyse the relationship between genotype and endothelial function, and a linear regression model was used to look at the effect of risk factors on endothelial function using absolute FMD with resting vessel size as an independent factor. A p value of <0.05 was taken to be statistically significant.

3.4 Results

3.4.1 Genotype and allele frequencies of the p22phox (*CYBA*) C242T polymorphism

Genotype and allele frequencies are summarized in table 3.1. A total of 249 out of 264 individuals were genotyped successfully from the Cambridge Young Adults Study, and 332 out of 385 from the EBCT study. PCR failed to amplify the remaining samples due to poor quality DNA. Genotype frequencies did not differ from those expected under Hardy-Weinberg equilibrium.

	p22phox C242T						
Cohort	**Genotype N (%)**			**Allele %**		χ^2	**P**
	CC	CT	TT	C	T		
Cambridge Young Adults	119 (48.0)	107 (43.0)	23 (9.0)	69.0	31.0	0.00	0.88
EBCT	151 (46.0)	149 (44.0)	32 (10.0)	68.0	32.0	0.30	0.58
(Diabetics)	76 (45.0)	75 (44.0)	19 (11.0)	67.0	33.0	0.00	0.94
(Controls)	75 (46.0)	74 (46.0)	13 (8.0)	69.0	31.0	0.80	0.37

Table 3.1 Genotype and allele frequencies of the p22phox C242T polymorphism. Genotype frequencies did not differ from those expected by the Hardy-Weinberg equation calculated by Chi-squared analysis.

3.4.2 p22phox genotype and CVD risk factors in the Cambridge Young Adults cohort

Conventional cardiovascular risk factors and other demographic details are shown in table 3.2 according to p22phox genotype. TT homozygotes had significantly higher HDL cholesterol compared to C allele carriers (*P=0.03, students t-test, table 3.2), but no significant association was observed between genotype and other cardiovascular risk factors.

	p22phox C242T		
	CC+CT Mean (SD) N=226	**TT** Mean (SD) N=23	**P**
Age (years)	23.4 (1.89)	23.83 (1.86)	P=0.32
Weight (kg)	68.7 (12.6)	67.9 (12.94)	P=0.98
SBP (mmHg)	127 (13.57)	126 (17.26)	P=0.70
DBP (mmHg)	70.5 (8.29)	68.43 (11.01)	P=0.29
Total cholesterol (mmol/l)	4.58 (1.01)	4.61 (0.81)	P=0.90
LDL cholesterol (mmol/l)	2.84 (0.89)	2.7 (0.82)	P=0.72
HDL cholesterol (mmol/l)	1.19 (0.29)	1.33 (0.28)	P=0.03*
Glucose (mmol/l)	5.01 (0.50)	5.1 (0.64)	P=0.24
Fasting Insulin (IU)	9.1 (6.04)	7.71 (4.39)	P=0.30
FMD (% change from baseline)	3.29 (2.6)	4.51 (2.78)	P=0.03*
GTN (% change from baseline)	21.65 (7.7)	24.31 (8.7)	P=0.13

Table 3.2 Phenotypic characteristics of the Cambridge Young Adults cohort according to p22phox C242T genotype. C allele carriers were analysed against TT homozygotes. C allele carriers had lower FMD compared to TT homozygotes. Data is represented as mean (SD). *P=<0.05 (statistically significant). All data was analysed by students t test.

3.4.3 Relationship between p22phox genotype and vascular function in the Cambridge Young Adults cohort.

A significant association was observed between genotype and endothelium dependent FMD (*P=0.03, One-way ANOVA). Mean (SD) FMD was 3.5±2.5 in CC homozygotes, 3.0±2.7 in CT individuals and 4.51±2.78 in TT homozygotes. Post hoc comparison of FMD between all three genotypes by Tukey's post-test, revealed the major significant difference in FMD was between CT and TT subjects ($p<0.05$). No significant difference in FMD was observed between CC and CT individuals ($p>0.05$). The data was therefore analysed according to a recessive genetic model where TT subjects were compared to C allele carriers. TT homozygotes had significantly increased FMD compared to C allele carriers (*P=0.03, figure 3.1 and table 3.2). No significant difference was observed for endothelium independent response (P=0.13, figure 3.2 and table 3.2). In a linear regression model the positive association between TT homozygosity and endothelial function was independent of classical risk factors - systolic blood pressure, smoking, fasting glucose, LDL and HDL (regression coefficient for C242T alone = 0.0378 mm (95%CI: 0.00 to 0.08), $p<0.05$, r=0.13, and in a model including risk factors = 0.0399 mm (95%CI: 0.00 to 0.08) $p<0.05$, r=0.26.

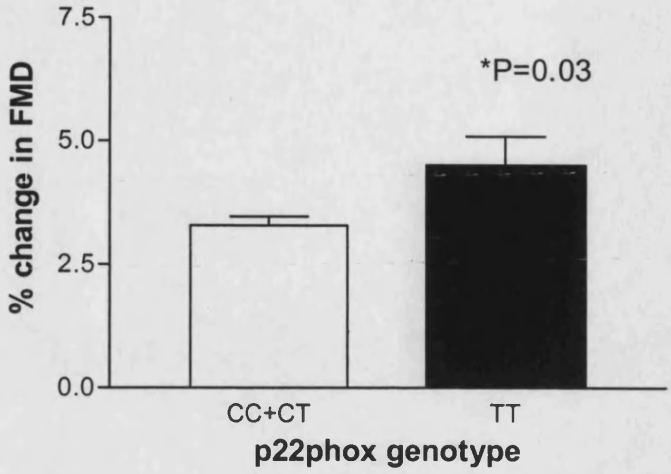

Figure 3.1 FMD according to p22phox genotype in the Cambridge Young Adults Study. Individuals homozygous for the T allele has significantly higher FMD compared to CC+CT individuals *P=0.03 (students t test).

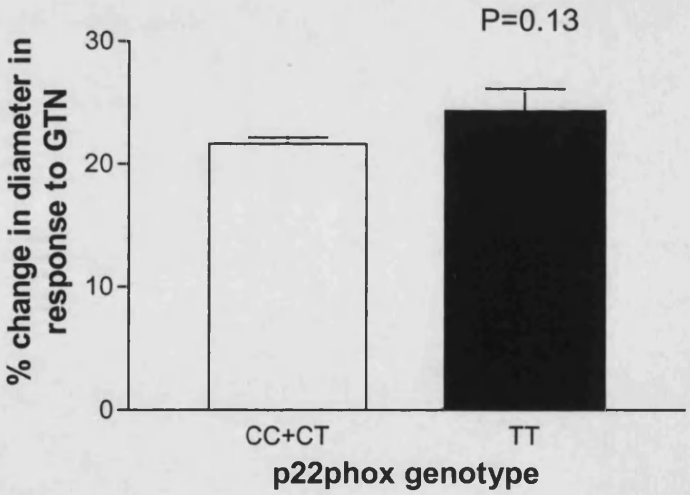

Figure 3.2 % change in brachial artery diameter in response to GTN (endothelium-independent response) according to p22phox genotype in the Cambridge Young Adults Study. No significant difference was observed between TT homozygotes and C allele carriers. P=0.13 (students t test).

3.4.4 p22phox genotype and cardiovascular risk factors in the EBCT cohort

Phenotypic characteristics according to p22phox C242T genotype are shown in table 3.3. C allele carriers were grouped and analysed against TT homozygotes. No significant association was observed between p22phox genotype and total cholesterol, HDL cholesterol, systolic blood pressure or diastolic blood pressure in the whole cohort.

	p22phox C242T		
	CC+CT Mean (SD) N=300	**TT** Mean (SD) N=32	**P**
Age (years)	38.1 (3.96)	36.7 (4.01)	0.07
SBP (mmHg)	121.5 (14.23)	117.5 (13.74)	0.13
DBP (mmHg)	73.4 (9.28)	72.0 (8.73)	0.43
Total cholesterol (mmol/l)	5.4 (1.17)	5.3 (1.16)	0.59
HDL cholesterol (mmol/l)	1.8 (0.44)	1.7 (0.52)	0.72

Table 3.3 Phenotypic characteristics of individuals from the EBCT study according to p22phox C242T genotype. C allele carriers were analysed against TT homozygotes. Data is represented as mean (SD). All data was analysed by students t test.

3.4.5 Relationship between p22phox genotype and vascular function in the EBCT cohort.

Endothelial function according to p22phox genotype is shown in figure 3.3. No significant association was observed between p22phox genotype (TT versus CC+CT individuals) and endothelial function in this cohort (Figure 3.3). This was also the case after analyzing diabetics, non-diabetics, smokers and non-smokers separately (table 3.4).

	Diabetics β (P)	**Non-diabetics** β (P)	**Smokers** β (P)	**Non-smokers** β (P)
Acetylcholine	0.03 (0.82)	0.16 (0.39)	0.04 (0.86)	0.04 (0.71)
Bradykinin	0.02 (0.85)	0.17 (0.17)	0.17 (0.19)	0.05 (0.58)
GTN	0.04 (0.60)	0.06 (0.64)	0.07 (0.60)	0.01 (0.91)
Noradrenaline	0.05 (0.26)	0.02 (0.83)	0.08 (0.46)	0.03 (0.44)
L-NMMA	0.004 (0.89)	-0.05 (0.25)	0.05 (0.36)	-0.03 (0.37)

Table 3.4 Results of multiple regression analysis of endothelial function according to p22phox genotype in diabetics, non-diabetics, smokers and non-smokers. Effect of genotype on vascular function in response to acetylcholine (doses 25, 50 and 100 nmol/l), bradykinin (doses 10, 30 and 100 pmol/min, each dose for 3 min), GTN (doses 4, 8 and 16 nmol/min, each dose for 5 min), noradrenaline (doses 60, 120 and 240 pmol/min, each dose for 5 min), L-NMMA (doses 1, 2 and 4 μmol/min, each dose for 5 min) was measured by venous occlusion plethysmography as described in chapter 2.2.13.1. Individuals were divided into diabetic/non-diabetic and smokers/non-smokers and analysed for a relationship between genotype (CC+CT versus TT) and endothelial function by multiple regression analysis. β coefficients and p value for the effect of genotype using a recessive model on forearm blood flow in response to drug infusion is reported.

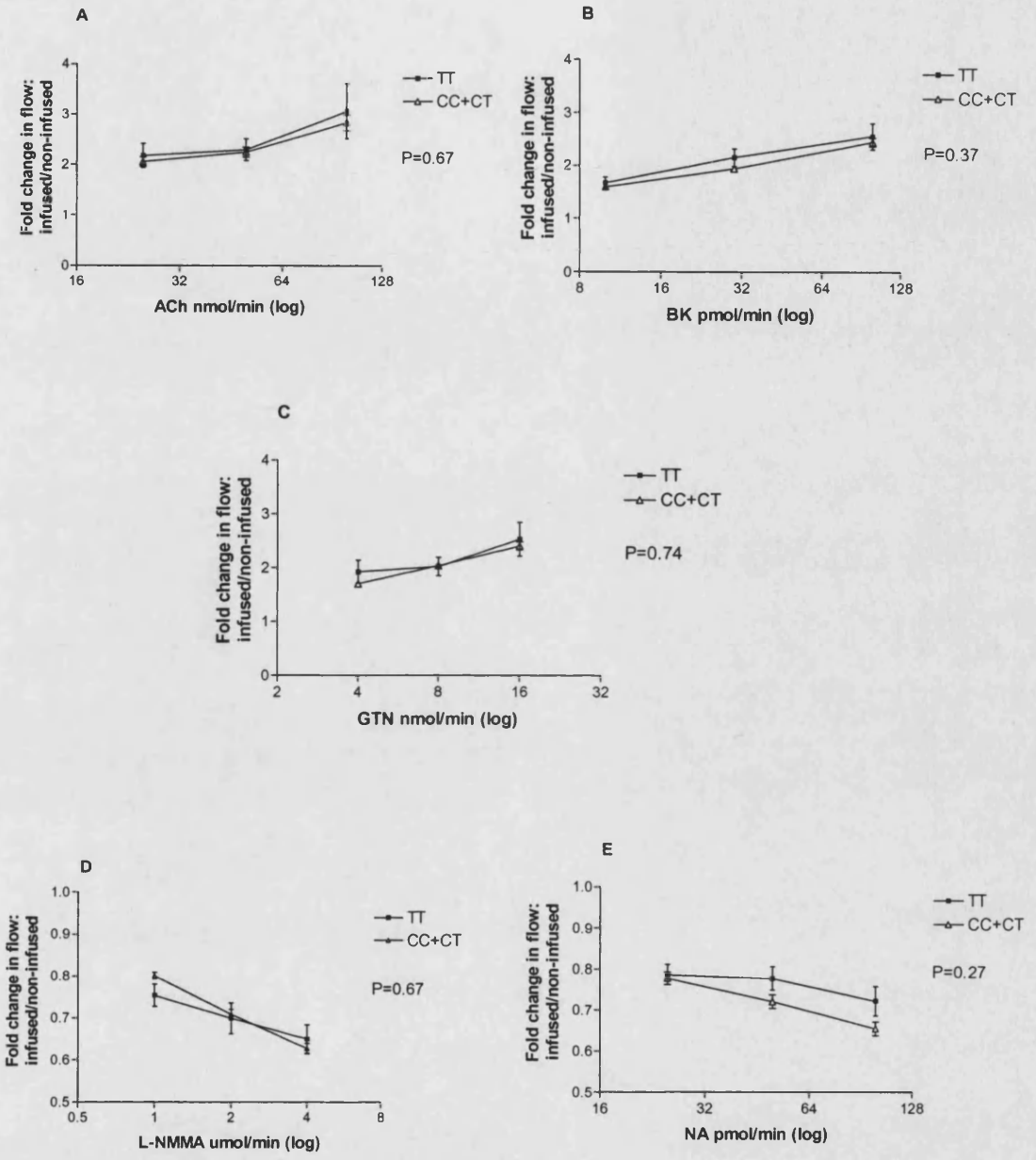

Figure 3.3 p22phox genotype and vascular function in the EBCT study cohort. Graphs A-E show the fold change in forearm blood flow according to genotype (TT versus CC+CT individuals) after infusion with **A**-acetylcholine (25, 50 and 100 nmol/l), **B**-bradykinin (10, 30 and 100 pmol/min), **C**-glyceryl trinitrate (4, 8 and 16 nmol/min), **D**- L-NMMA (1, 2 and 4 μmol/min) and **E**- noradrenaline (60, 120 and 240 pmol/min). No significant association was observed between genotype and forearm vascular reactivity.

3.5 Discussion

During this study an association between the p22phox C242T polymorphism and FMD of the brachial artery was observed in a cohort of healthy subjects recruited from the Cambridge area. When analysed under a recessive model, individuals homozygous for the rare T allele exhibited significantly greater FMD compared to those individuals carrying the C allele. This difference was not confounded by differences in other cardiovascular risk factors including smoking, blood pressure, total and HDL cholesterol, since after adjustment for these in a multiple regression model, the relationship was preserved. No difference was observed for endothelium independent response between the two groups. In contrast no association was seen between p22phox genotype and endothelial function in the forearm vasculature in a cohort of type I diabetics and controls.

Diminished FMD in healthy individuals is associated with a family history of IHD and, in patients with CVD, endothelial function is predictive of future events (Suwaidi et al., 2000; Schachinger et al., 2000). Down-regulation of NO synthesis or activity is a possible cause of such endothelial dysfunction (Gaeta et al., 2000). Endothelium-dependent vasodilation in response to flow is largely dependent on NO release (Joannides et al., 1995). The rapid reaction between ROS such as NO and O_2^- resulting in the formation of $ONOO^-$ is a plausible mechanism whereby the vasodilator actions of NO might be attenuated in this vessel. In addition, oxidative inactivation of the essential NOS cofactor BH_4 could also lead to sub-optimal NOS activity resulting in decreased NO production and more O_2^- (Figure 3.4). If subjects homozygous for the 242T allele of p22phox produce less O_2^-

basally as has been reported previously (Guzik et al., 2000), this might lead to increased NO availability and enhanced FMD. In contrast, no relationship was detected between endothelium-dependent dilatation in the forearm vessels of type 1 diabetics or controls and p22phox genotype. Endothelium-dependent vasodilation in the smaller forearm resistance vessels that are studied by plethysmography is dependent not only on the release of NO, but also on the release of EDHF (Garland et al., 1995). This might be a potential explanation for the failure to detect an effect of p22phox genotype on endothelial function in this vessel type.

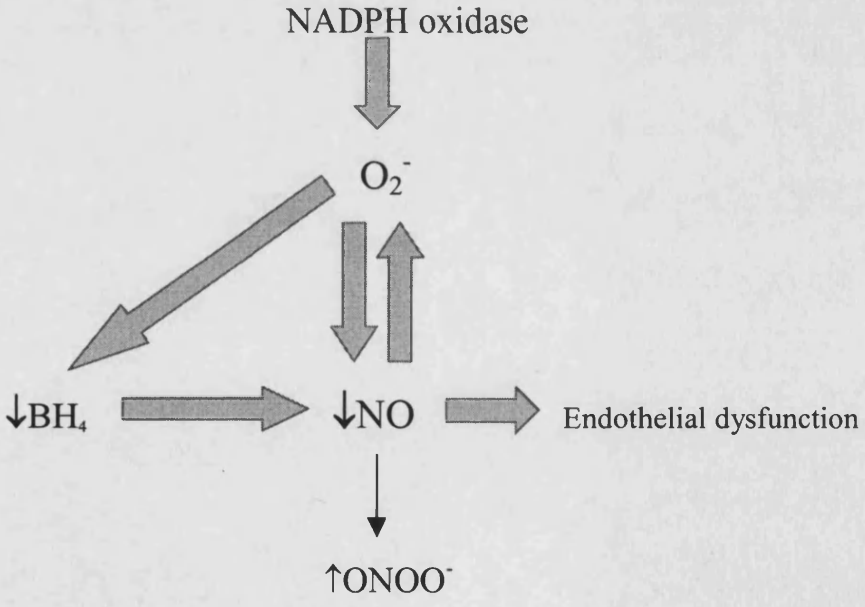

Figure 3.4 Endothelial dysfunction as a manifestation of depleted NO caused by ROS generation. O_2^- production by NADPH oxidase can lead to inactivation of NO either directly resulting in the generation of $ONOO^-$ or by causing oxidative inactivation of BH_4. At sub-optimum levels of BH_4 eNOS produces O_2^- instead of NO. Reduced NO is thought to implicated in endothelial dysfunction.

The discovery of NADPH oxidases in cells of the vascular system has led to renewed interest in this family of enzymes as a possible source of constitutive O_2^- release (Van Heerebeek et al., 2002). Recent research has focused on the expression pattern of various isoforms of the active subunit gp91phox and its associated subunit p22phox, and demonstrated that while the gp91phox subunits are differentially expressed depending on the cell type, p22phox is exclusively expressed in regions of most O_2^- production (Sorescu et al., 2002). Discovery of several polymorphisms in p22phox led to speculation that common genetic variation in the p22phox gene (*CYBA*) may have subtle influences on O_2^- generation, which could influence endothelial function and alter susceptibility to CVD. Consequently p22phox polymorphisms have become a focus of investigation for association with CVD risk. This study revealed that healthy subjects who carry two copies of the rare T allele for the p22phox C242T polymorphism exhibited greater FMD compared to subjects who carried at least one C allele. This finding fits with previous reports that the T allele may exert a protective effect upon the vasculature by down-regulating NADPH oxidase activity (Guzik et al, 2000a). The position of the polymorphism at nucleotide 242 gives a clue as to how enzyme activity may be modulated, as the resulting histidine to tyrosine substitution at position 72 of the protein lies in a heme binding domain which may be essential for optimal enzyme activity (Parkos et al., 1988). However, in vitro studies of isolated enzyme function will be needed to verify this hypothesis.

The risk of developing CVD such as atherosclerosis is greatly enhanced in the presence of diseases such as diabetes and renal failure (Bierman et al., 1992; Wheeler et al., 1996). Endothelial function in these individuals is reported to be attenuated by disruption of the L-

arginine→NO system, but the precise mechanisms remain unknown. The discovery that vascular O_2^- production is elevated in such disease states has led to the hypothesis that NO is inactivated by reaction with O_2^- thereby predisposing to vascular disease. In the light of the findings of an association between the p22phox C242T polymorphism and FMD, this study also investigated the effect of p22phox genotype on endothelial function assessed by venous occlusion plethysmography in a cohort of diabetic subjects. No association was seen between genotype and endothelial function in the resistance vasculature even when diabetics and non-diabetics and smokers and non-smokers were analysed separately. This data suggests that p22phox C242T genotype does not influence endothelial function in the resistance arteries of the forearm in either healthy subjects or in type 1 diabetics. The most likely explanation for this is that NO is a less important endothelium-dependent vasodilator in the small resistance arteries than it is in the larger conduit brachial artery. Alternatively, it is possible that the increased O_2^- reported in diabetic individuals originates from a different source other than NADPH oxidase, although the presence of other functional polymorphisms or mutations within the p22phox gene or indeed other NADPH oxidase subunits cannot be ruled out. During the time frame of the studies in this thesis, three new polymorphisms have been described within the coding region of *CYBA* resulting amino acid substitutions (NCBI SNP database, http//www.ncbi.nlm.nih.gov/SNP/). Two of these polymorphisms reside in exon 2 and confer a Thr→Ala substitution at amino acid 29 and a Phe→Ser at amino acid 38. The third is situated within exon 6 and results in a Val→Ala at amino acid 174. Further studies to investigate the role of these variants and endothelial function and indeed risk of vascular disease are now needed.

In summary, these data demonstrate a significant association between p22phox genotype and endothelial function in the brachial artery of healthy individuals. Subjects who carry the TT genotype showed increased FMD in comparison to C allele carriers. This finding supports the hypothesis that the presence of the T allele may down-regulate NADPH oxidase generation of O_2^- thereby preserving the vasodilator properties of NO. No association was observed between genotype and endothelial function in smaller forearm resistance vessels in a cohort of diabetic subjects, suggesting that O_2^- generation from NADPH oxidase and NO availability are less important mediators of vasoreactivity in these vessels.

CHAPTER 4

IDENTIFICATION OF POLYMORPHISMS IN THE HUMAN GTP-CYCLOHYDROLASE 1 GENE (*GCH1*)

4.1 Aim

To scan the human GTP cyclohydrolase 1 gene (*GCH1*) for novel genetic variants, with the intension of investigating the role of any polymorphisms discovered in the regulation of endothelial dilator function, plasma neopterin and the susceptibility to CVD.

4.2 Background

Limited availability of the essential NOS cofactor BH_4 has been proposed as one mechanism which may result in decreased NO production and susceptibility to CVD in some individuals. The amount of BH_4 available to the NOS enzyme depends upon two factors: its rate of synthesis and rate of inactivation/breakdown. While inactivation of BH_4 is most probably subject to the presence of ROS within the microenvironment of the enzyme, generated from a variety of sources in the vessel wall, the *de novo* production of BH_4 is reliant upon three enzymes – GTPcyclohydrolase 1, 6-pyruvoyl-tetrahydropterin synthase and sepiapterin reductase (Chapter 1.3.3.2). BH_4 is also regenerated via a 'salvage' pathway, which is a part of the aromatic amino acid hydroxylase system, but will not be discussed in this thesis (*for review see Thony et al, 2000).*

GTPCH1 catalyses the initial conversion of GTP to7,8-dihydroneopterin triphosphate and is considered the rate limiting step in BH_4 synthesis. Its expression can be up-regulated by various cytokines including tumour necrosis factor-α (TNF-α), interferon-γ (IFN-γ), interleukin-1β (IL-1) and also bacterial endotoxin – lipopolysaccharide (LPS). Increased

GCH1 transcription upon stimulation with cytokines is also associated with increased enzyme activity and elevation of intracellular BH_4 in endothelial cells (Werner-Felmayer et al., 1989; Werner-Felmayer et al., 1993; Hattori et al., 1993). In contrast PTPS and SR have been considered to be largely constitutive (Werner et al., 1990), though at least one group has demonstrated cytokine inducibility of PTPS (Linscheid et al., 1998). GTPCH1 enzyme activity is regulated via post-translational modification, which has been shown to occur by phosphorylation, and is associated with an increase in enzyme activity and elevated BH_4 production (Lapize et al., 1998). Phosphorylation can be mediated through protein kinase C, and amino acid sequence studies have revealed a possible target (Ser 167 in rat and mouse protein sequence) for protein kinase C phosphorylation that is conserved between several species including man. In addition several sites for potential phosphorylation by casein kinase II have also been reported (Hatakeyama et al., 1991). Enzyme activity is also regulated by the GTPCH1 feedback regulatory protein (GFRP), which in the presence of BH_4 and GTP forms an inhibitory complex with the GTPCH1 enzyme (Figure 4.1). This inhibition is non-competitive, and can be reversed by L-phenylalanine (Harada et al., 1993; Yoneyama et al., 1997).

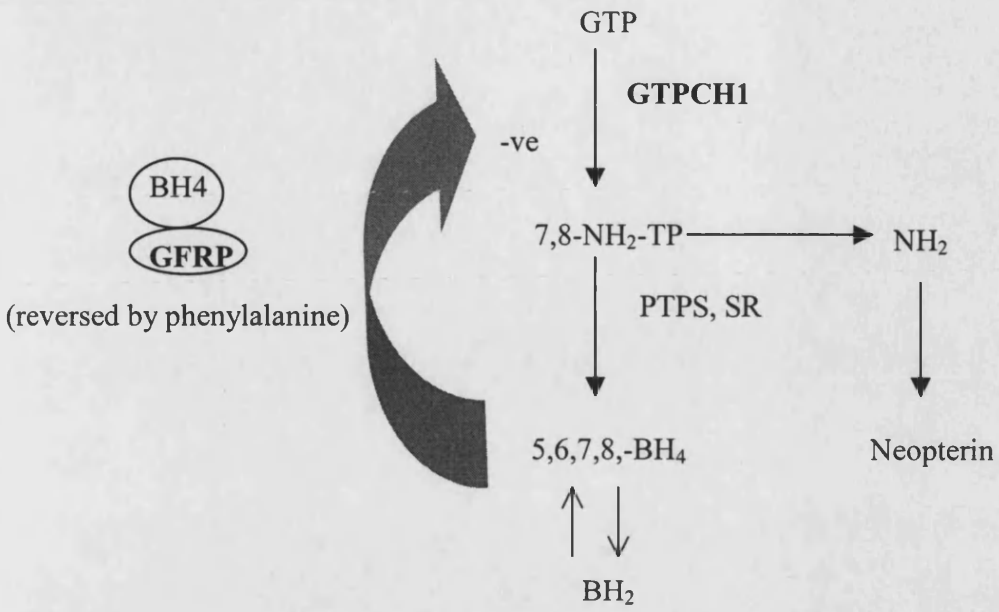

Figure 4.1 Synthesis of BH_4 and its regulation by GFRP
BH_4 synthesis is regulated by feedback inhibition by the product via GTPCH1 feedback regulatory protein (GFRP). In the presence of BH_4 and GTP, GFRP forms an inhibitory complex with GTPCH1. Inhibition can be reversed by L-phenylalanine.

GTPCH1 cDNA was first isolated from a rat library by Hatakeyama et al., 1991. In 1992, three different human GTPCH1 cDNA clones were isolated from a human liver cDNA library, each with identical 5' and central structures but differing 3' ends (Togari et al., 1992). Subsequently the human *GCH1* gene was mapped to chromosome 14q22.1-q22.2 by fluorescence *in situ* hybridisation (Ichinose et al., 1994), which led to a comprehensive characterization of human and mouse *GCH1* genes (Ichinose et al., 1995). Human *GCH1* is encoded by a single copy gene composed of 6 exons spanning a length of ~30kb, and alternate splicing at the sixth exon was discovered to generate the three cDNAs (type 1 - 1181bp, type 2 - 994bp and type 3 - 819bp) isolated by Togari *et al.* The presence of two

of these cDNAs (Type 1 + 2) in a human liver cDNA library was confirmed by Gutlich et al., 1994, and expression of all three cDNA types in *E.coli* demonstrated that only the full-length type 1 cDNA has GTPCH1 enzyme activity (Gutlich et al., 1994). In contrast 2 species of mRNA (3.6kb and 1.4kb) were identified in rat and mouse tissues corresponding to type 1 and type 2 cDNAs. The biological significance of multiple splice variants of GTPCH1 is unknown, but could be important in cell-specific regulation of BH_4 synthesis. GTPCH1 mRNA has been isolated from a variety of tissues including liver, brain, kidney, spleen, lymphocytes and vascular smooth muscle cells endothelial cells reflecting its function in the synthesis of catecholamines and NO (Gutlich et al., 1992; Hattori et al., 1993; Katusic et al., 1998).

The 5' region of the human *GCH1* gene, which incorporates the promoter is ~600bp in length upstream of the translation start site (Ichinose et al., 1995; Witter et al., 1996). No TATA sequence motif was observed in this region. Instead an AT-rich sequence and a CAAT box are present 21bp upstream and 68bp upstream of the transcription start site respectively, both of which are conserved between human and mouse *GCH1* promoters (Witter et al., 1996; Ichinose et al., 1995). In addition putative consensus sequences for transcription factors CCAAT-box/enhancer binding protein (C/EBP), hepatic nuclear factor 1 (HNF1), upstream stimulating factor (USF), activator protein 1 (AP-1), serum response factor (SRF), glucocorticoid response element (GRE), nuclear factor κB (NFκB) and several GC boxes (SP1 sites) have been identified in the promoter region (Witter et al., 1996). Interestingly no consensus sequences for IFN-γ signal tranduction such as the IFN-γ

activated site (GAS) or IFN-γ response region (GRR) have been identified. This is particularly surprising since GTPCH 1 expression is upregulated by interferon-γ.

To date 80 mutations have been reported in the human *GCH1* gene (BH_4 database, http://www.bh4.org accessed Jan 2003), but these are rare, and many are now known to be the cause of monogenic diseases such as dopa-responsive dystonia (DRD) and atypical hyperphenylalaninaemia (Bandmann et al., 2002; Niederwieser et al., 1984). The effect that these and indeed any undiscovered polymorphisms may have on BH_4 production in the vasculature is unknown, but could have implications for NO synthesis. Common sequence variation within the *GCH1* gene between individuals could result in subtle differences in the amount of BH_4 available to the eNOS enzyme and act as a predisposing factor for CVD development.

The aim of this study was therefore to screen the *GCH1* gene for novel common polymorphisms using a technique called single strand conformation polymorphism analysis (SSCP). This is a relatively quick and easy way to detect inter-individual differences in the DNA sequence in any given region of the genome. Disadvantages of this technique however are its limited sensitivity. The principle relies on the fact that single stranded DNA will take on a particular conformation dependent on its base sequence. Sequences of different conformation will migrate differently when electrophoresed on acrylamide gels, thereby allowing the detection of polymorphisms without the need for large-scale sequencing efforts.

4.3 Subjects and Methods

4.3.1 Subjects

Anonymised DNA samples from 32 healthy unrelated individuals, were used to screen the *GCH1* gene for polymorphisms. Written informed consent was obtained from each volunteer and medical status ascertained by questionnaire. Blood was collected into EDTA tubes and DNA extracted by Qiagen DNA purification kit method (Chapter 2.2.1.2).

4.3.2 Oligonucleotide design and amplification of genomic DNA

Oligonucleotides were designed to cover the promoter and exons of the *GCH1* gene. All oligonucleotides were designed to be approximately 50% GC rich with minimum secondary structure formation. Each oligonucleotide pair was designed to have similar annealing temperatures, non-complementary sequence (which could result in 'primer-dimer' production) and produce a PCR product 200-400bp in length (optimum length for SSCP analysis). Promoter oligonucleotides were designed using the Genbank/EMBL database sequence (accession number NT_026437). Five pairs of oligonucleotides were designed to produce five PCR products, which overlapped one another to cover the region spanning +48 to –1080 relative to the transcription start site. This incorporates the 600bp sequence depicted to be the *GCH1* promoter by Ichinose *et al.*, 1995. Oligonucleotides used to amplify exons 2-6 have been reported previously (Bandmann et al., 1998). Exon 1 was divided into two overlapping PCR products because of its relatively large size (506bp),

and oligonucleotides designed from the Genbank/EMBL database. Tables 4.1 and 4.2 list all oligonucleotide sequences, positions relative to the transcription start site and PCR conditions.

Amplification was carried out by PCR as described in Chapter 2.2.2. All PCR products were electrophoresed on 1% agarose gels with 100bp ladder to ensure a single-band product of the correct size was achieved.

4.3.3 Screening for polymorphisms by SSCP analysis

Two SSCP methods were used to scan the *GCH1* gene for polymorphisms. The promoter region was screened in collaboration with Dr. Noor Jeerooburkhan (UCL) using the radioactive method as described in Chapter 2.2.4.1. The non-radioactive PhastSystem was used to scan the six exons as described in Chapter 2.2.4.2.

4.3.4 DNA sequencing to define the nature of variants detected by SSCP

Genomic regions exhibiting different banding patterns on gel electrophoresis were chosen for sequence analysis. Samples were selected so that each different banding pattern produced by SSCP was represented at least twice and the region re-amplified from genomic DNA. The PCR product was used as a template and both forward and reverse sequencing reactions set up using the same oligonucleotides as for PCR. Sequencing was carried out as described in Chapter 2.2.5.

Position of oligonucleotides relative to transcription start site	$MgCl_2$ (mM)	Annealing Temp (°C)	Sequence
Promoter 1 (-258 → +48)	1.5	56	F – 5' ttt tcg ggt tcg gct cat tcc
			R – 5' gtg atc taa gca ggt cgc gta
Promoter 2 (-379 → -163)	2.0	64	F – 5' ttt cac agg gcg agg gga ccg g
			R – 5' ctc cct gcg ctt gcg aac ccc
Promoter 3 (-552 → -342)	1.5	60	F – 5' gtg aca ctt gcc ccg aca gcg
			R – 5' acc gga gcc ctt caa tgc agc
Promoter 4 (-768 → -421)	1.5	62	F- 5' tat gtt ttc cag gct ggt ctc g
			R – 5' gtt ggt tcc taa tcg gtg gct t
Promoter 5 (-1080 → -707)	1.5	62	F – 5' acc cag gag gcg gag gat gaa g
			R – 5' tcc tcc cgc ctc ggt ctc cc

Table 4.1. Oligonucleotides designed to amplify the *GCH1* promoter. A set of five overlapping oligonucleotides were designed to amplify the *GCH1* promoter by PCR. The region amplified by each oligonucleotide pair is shown with the corresponding $MgCl_2$ concentration and annealing temperature.

Exon amplified and position of oligonucleotides	$MgCl_2$ (mM)	Annealing Temp (°C)	Sequence
Exon 1a (-64 →226)	2.0mM	64°C	F - 5' gtt tag ccg cag acc tcg aag cg 3'
			R - 5'acg agt agg cgg ctg cca ggt ta 3'
Exon 1b (178 →431)	1.5mM	68°C	F - 5'agg agg ata acg agc tgaa cct c 3'
			R - 5'gag gca act ccg gaa act tcc tg 3'
Exon 2 (37441 →37127)	1.5 mM	64° C	F - 5'acc tga gat atc agc aat tgg cag c 3'
			R - 5'gta acg ctc gct tat gtt gac tgt c 3'
Exon 3 (42789 →43048)	2.5 mM	64° C	F - 5'tag att ctc agc aga tga ggg cag 3'
			R - 5'aga tgt ttt caa ggt aat aca ttg tcg 3'
Exon 4 (55449 →55739)	1.5 mM	60° C	F - 5'gtc ctt ttt gtt tta tga gga agg c 3'
			R - 5'ggt gtg cac tct tat aat ctc agc 3'
Exon 5 (56768 →56943)	1.5 mM	64° C	F - 5'gtg tca gac tct caa act gag ctc 3'
			R - 5'tca ctt cta gtg cac cat tat gac g 3'
Exon 6 (58695 →58462)	1.5 mM	68° C	F - 5'acc aaa cca gca gct gtc tac tcc 3'
			R - 5'aat gct act ggc agt acg atc gg 3'

Table 4.2. Oligonucleotides designed to amplify *GCH1* exons. Oligonucleotides were designed to cover exons 1-6 of the *GCH1* gene. A set of 2 overlapping oligonucleotide pairs were designed to cover exon 1. Oligonucleotide sequences, annealing temperatures, $MgCl_2$, concentrations and the region amplified by each oligonucleotide pair are shown.

4.3.5 Search of the National Center for Biotechnology Information (NCBI) SNP database for *GCH1* polymorphisms

The NCBI SNP database (http://www.ncbi.nlm.nih.gov/SNP/) was also searched for all polymorphisms identified to date within the *GCH1* gene as described in Chapter 2.2.7. The database was established in 1988 and is a resource of freely available molecular biology information compiled by genome sequencing consortiums worldwide.

4.3.6 Search of the MatInspector promoter database for putative *GCH1* transcription factor binding sites

A search of the MatInspector database (http://www.genomatix.de/free_login.html) with the *GCH1* promoter sequence was undertaken to identify transcription factor binding sites as described in Chapter 2.2.8.

4.4 Results

4.4.1 Polymorphisms identified in *GCH1*

Four novel polymorphisms were identified within the *GCH1* gene (Figure 4.2). SSCP analysis revealed a difference in banding pattern for PCR products generated with the oligonucleotides promoter 4, promoter 5 and exon 1b (Tables 4.1 and 4.2), suggesting the presence of genetic variation within these regions. This was confirmed by DNA sequencing, which revealed a total of four single base substitutions. Three of these variants were found to be located in the promoter (one within PCR product promoter 4 and two within PCR product promoter 5) at positions –796 (G→A), -741 (T→C) and –577 (G→A) (Figures 4.3-4.5). The fourth variant (observed within PCR product exon 1b) was identified as a C→G substitution at position +559, which lies within intron 1 (Figure 4.6).

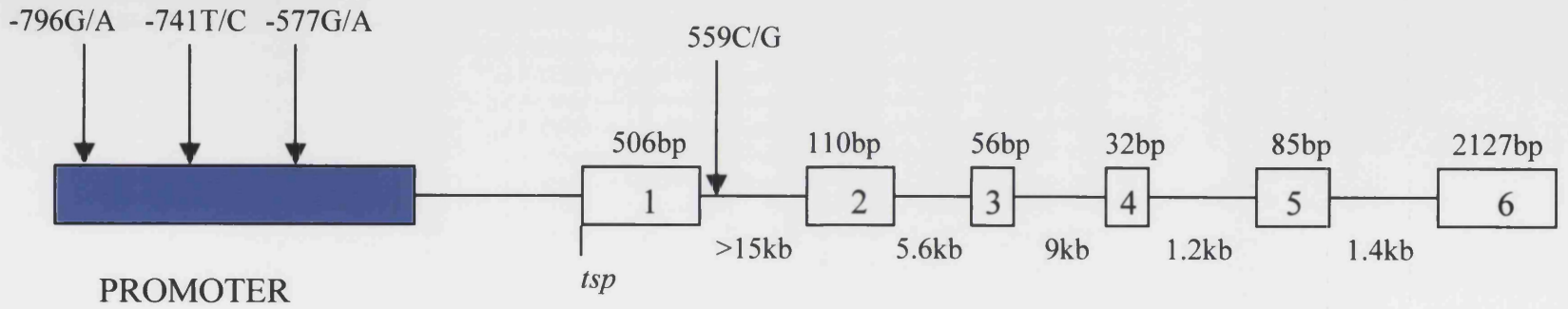

Figure 4.2 *GCH1* gene structure.
The human GCH1 gene is encoded by a single copy gene on chromosome 14. The promoter is highlighted in blue, and spans a distance of at least 600bp upstream of the *tsp*. Exons are numbered 1-6 and the size of each exon and intron indicated (kb). The position of polymorphisms identified by SSCP analysis are indicated by ↓ .

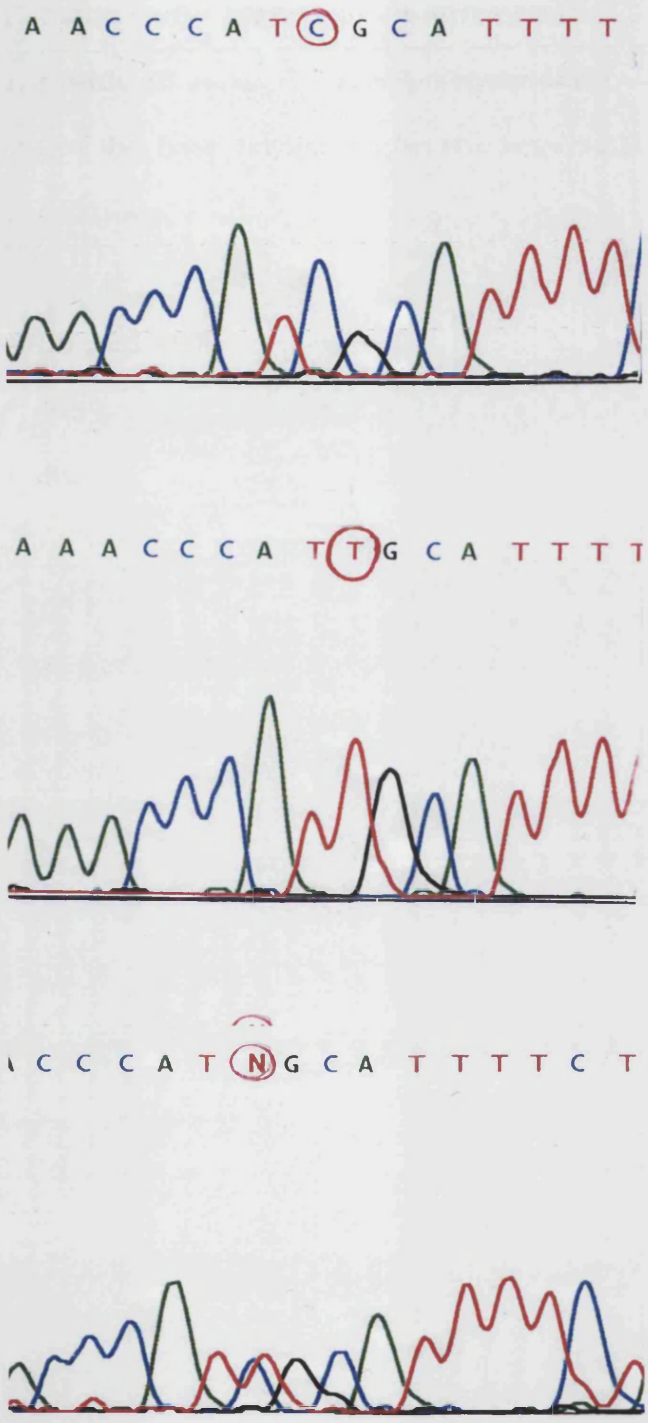

Figure 4.3. DNA sequence (of the reverse strand) confirming a G→A substitution at position –796 in the *GCH1* promoter. The top sequence shows a homozygote for the C (G on forward strand) allele, the middle sequence a homozygote for the T (A on forward strand) allele and the bottom sequence a heterozygote showing both the C and T alleles.

Figure 4.4 DNA sequence (of the reverse strand) confirming a T→C substitution at position –741 in the *GCH1* promoter. The top sequence shows a homozygote for the A (T on forward strand) allele, the middle sequence a homozygote for the G allele (C on forward strand) and the bottom sequence a heterozygote showing both the A and G alleles.

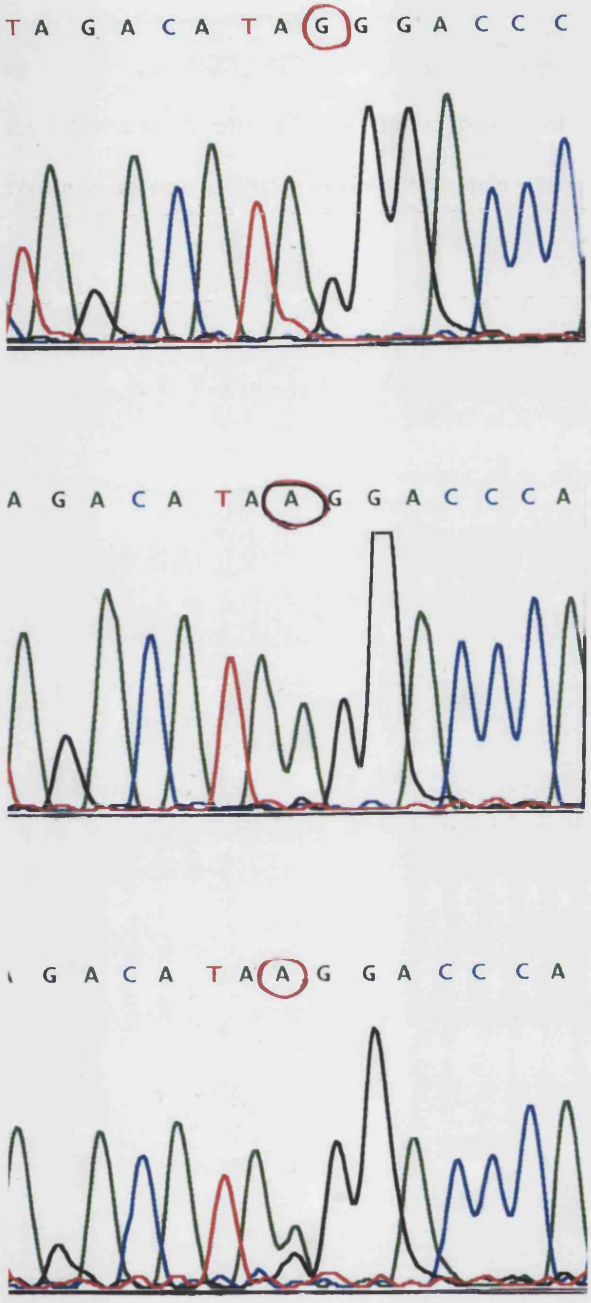

Figure 4.5 DNA sequence electropherogram confirming a G→A substitution at position –577 in the *GCH1* promoter. The top sequence shows a homozygote for the G allele, the middle sequence a homozygote for the A allele and the bottom sequence a heterozygote showing both the G and A alleles.

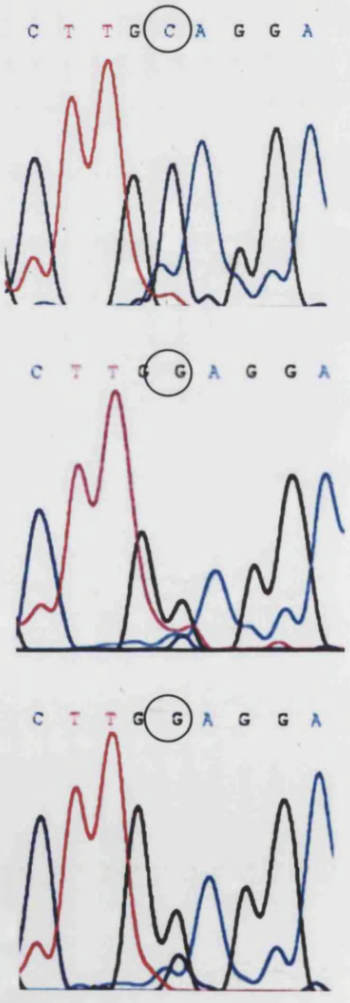

Figure 4.6 SSCP gel image (*Phastsystem*) and DNA sequence of *GCH1* Exon 1b PCR. Samples 2 and 4 have a different banding pattern (4 visible bands) on the SSCP gel, suggesting the presence of a polymorphism in this PCR fragment. The DNA sequence electropherogram confirms a C→G substitution at position 559 in intron 1. The top sequence shows a homozygote for the C allele, the middle sequence a homozygote for the G allele and the bottom sequence a heterozygote showing both the C and G alleles.

4.4.2 Analysis of the *GCH1* promoter and comparison of polymorphisms in the NCBI SNP database and those identified by SSCP.

The NCBI SNP database (http//www.ncbi.nlm.nih.gov/SNP/) revealed the presence of 5 previously identified polymorphisms in the 3kb upstream of the *GCH1* transcription start site (*tsp*). The nature of each SNP, identification number and position are shown in table 4.3. The three promoter polymorphisms (-796, -741 and –577) identified by SSCP during this study were not represented on the NCBI SNP database. One polymorphism was found in the database 44bp downstream of the *tsp,* and lies in the sequence of the reverse oligonucleotide promoter 1 (Figure 4.7). The location of this polymorphism within an oligonucleotide makes it difficult to identify by SSCP. The +559C/G variant was represented in the NCBI database (Table 4.3), but no further information regarding heterozygosity was available at the time of writing this thesis.

MatInspector analysis (http//www.genomatix.de) of the 1.2kb immediately upstream of the *GCH1* transcription start site indicated that none of the polymorphisms identified by SSCP were situated in transcription factor binding sites or other known regulatory regions (Figure 4.7). However the -741 T/C lies just downstream of a shear stress element (SSRE) encoded by the sequence GAGACC and 1bp upstream of a nuclear factor 1 site (NF1). The -796G/A polymorphism is situated 10bp from the core binding domain of a signal transducer and activator of transcription site (STAT3) and the –577 G/A lies 5bp upstream of a serum response factor site (SRF).

NCBI SNP ID	Base change	Position relative to *tsp*
rs2183080	C/G	+559
rs3759660	C/T	-1042
rs3759661	C/T	-1044
rs3759664	C/T	-2034
rs3759665	C/T	-2059
rs3074168	CT/-	-2811

Table 4.3 Human *GCH1* promoter polymorphisms identified in the NCBI SNP database. The three promoter polymorphisms identified by SSCP during this study were not represented on the NCBI SNP database.

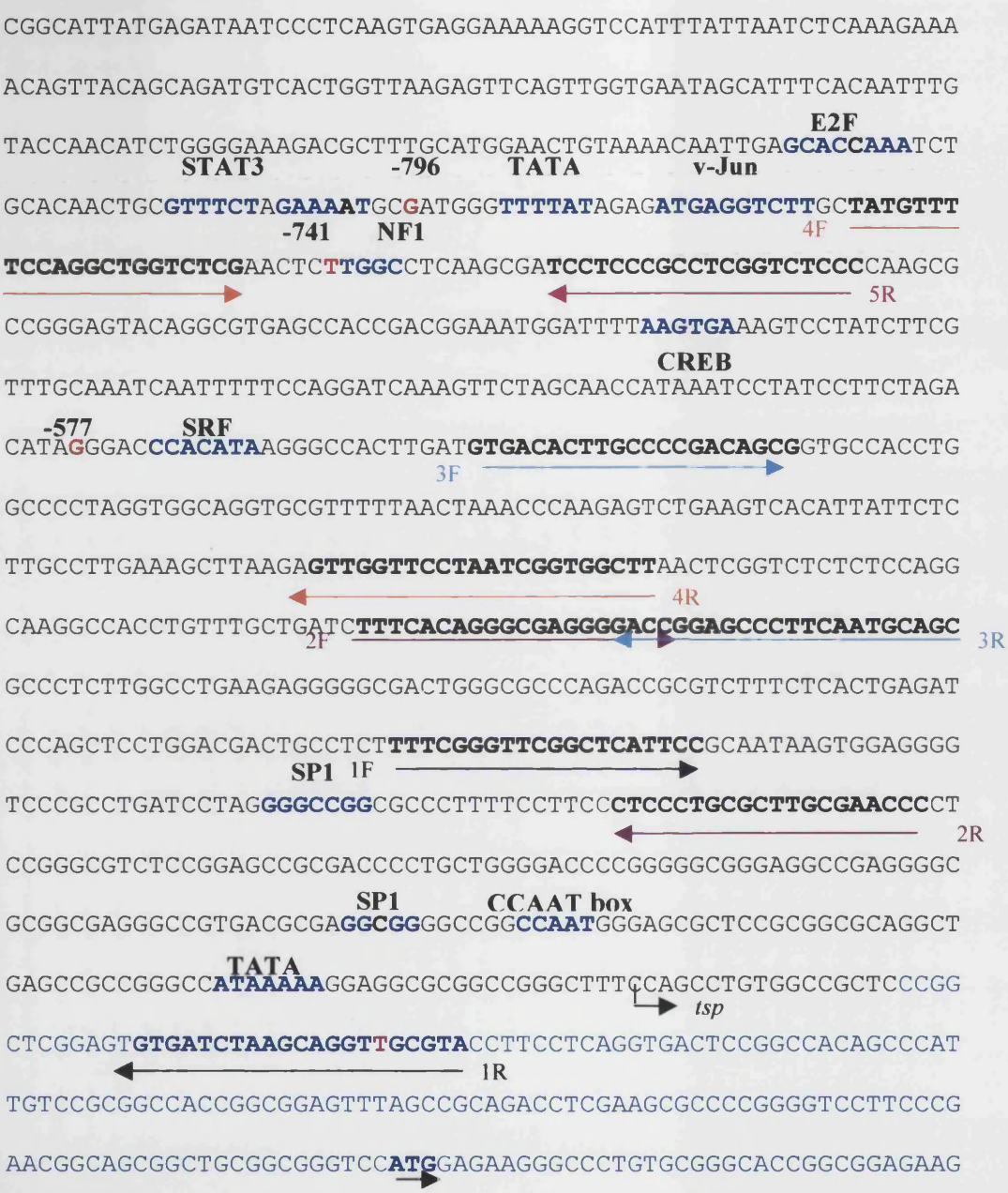

Figure 4.7. Nucleotide sequence of the human *GCH1* promoter region. The transcription start site is indicated by *tsp* and exon 1 is highlighted in blue. Oligonucleotide sequences are in bold and underlined by arrows. Transcription factor binding sites identified by MatInspector software are highlighted in bold blue. Polymorphisms at positions –796, -741 and –577 are indicated in red type, and the SNP at position +44 identified from the NCBI SNP database is highlighted in pink type.

4.5 Discussion

4.5.1 *GCH1* promoter polymorphisms

Three new polymorphisms were identified in the promoter of *GCH1* during this study. Two of these polymorphisms lie further upstream than the predicted ~600bp core promoter sequence reported by Ichinose et al., 1995 and Witter et al., 1996, but are situated just downstream of putative transcription factor binding sites. The –741 T/C polymorphism lies 6bp from a shear stress response element (SSRE), and the –796 G/A lies 3bp from a CCAAT box/enhancer binding protein element (C/EBP). Although these polymorphisms are outside the core sequence binding motifs for these transcription factors, it is possible the protein-DNA interaction extends to the upstream and downstream flanking sequences. It is therefore conceivable that variation within these regions could influence transcription factor binding or stability of the protein-DNA complex. CCAAT enhancer elements play a role in determining promoter efficiency, therefore disruption of this site could result in a weaker promoter and decreased gene expression. SSRE sites convey responsiveness to laminar shear stress (LSS), which is generated by blood flow over the endothelium. It is not surprising therefore that a number of endothelial genes contain SSRE consensus sequences and exhibit markedly elevated gene expression under experimentally induced shear stress (Gimbrone et al., 2000). Areas of high LSS are known to be less susceptible to atherosclerotic lesion formation (Cornhill et al., 1976; Zarins et al., 1983), and it has been proposed that coordinated up-regulation of so-called atheroprotective genes such as *eNOS* via SSRE sites could account for this phenomenon (Topper et al., 1996). Further studies

are required to deduce if *GCH1* is also upregulated by LSS in endothelial cells, but logic suggests that if *eNOS* expression and activity is increased then an increase in BH_4 production may also be required to support NO production.

4.5.2 Polymorphisms within *GCH1* exons

Only one polymorphism (559 C/G) was identified by SSCP analysis of the *GCH1* coding regions. This variant was found to lie just downstream of exon 1 (made possible due to the fact that each oligonucleotide for PCR was designed within an intronic region, resulting in a small amount of intron being amplified as well as the exon itself). Disappointingly, as well as not residing within the coding sequence, this polymorphism did not lie within any obvious consensus sequence involved in splicing. In addition, a search of the NCBI SNP database indicated that no polymorphisms have as yet been identified in the *GCH1* coding region, however the NCBI database only compares sequences from a small number of chromosomes. It is therefore possible that as more sequences are analysed, polymorphisms will be identified.

This study indicates that very little genetic variation is present within the *GCH1* coding regions, which may be indicative of an essential role of GTPCH 1 for survival, which in turn has ensured the *GCH1* gene has remained highly conserved throughout evolution (McLean et al., 1993). However, it is also possible that in this instance SSCP failed to reveal the presence of additional polymorphisms due to the limited (80-90%) sensitivity of detection of this technique. Advances in high-throughput sequencing technology have now

made it possible to accurately sequence and compare genes from hundreds of individuals relatively quickly without the need for SSCP. These large-scale sequencing efforts have led to the generation of SNP databases, which can provide an easily accessible source of information about potentially functional polymorphisms.

A search of the NCBI SNP database revealed the +559G/A polymorphism identified by SSCP during this study has already been described. The NCBI SNP database also highlighted a single polymorphism in the 5' untranslated region that was not detected by SSCP. This polymorphism at position +44bp lies within the reverse oligonucleotide sequence used to amplify the promoter 1 fragment.

4.5.3 Future work

The 3' untranslated sequence of the *GCH1* gene was omitted from SSCP analysis, but it is now recognized that this region could be involved in the regulation of translation through the interaction of specific 3'UTR binding proteins (Mazumder et al., 2003). One polymorphism has recently been described in the *GCH1* 3'UTR (NCBI accession number NT_026437). SSCP analysis of the *GCH1* 3'UTR is therefore needed to complete a full scan of the gene. Promoter-reporter gene assays are required in order to elucidate the importance of the promoter variants with respect to regulation of gene expression, and band-shift experiments to determine if either the –796G/A or –741T/C polymorphisms influence the binding of transcription factors to consensus sequences in close proximity.

However, the potential for the *GCH1* promoter variants described to influence GTPCH1 activity and endothelial function is further discussed in Chapter 5.

CHAPTER 5

GCH 1 POLYMORPHISMS AND THEIR FUNCTIONAL IMPACT ON PTERIN METABOLISM AND ENDOTHELIAL FUNCTION

5.1 Aim

To investigate the relationship between *GCH1* promoter polymorphisms (–577G/A and -796G/A) pterin metabolism and endothelial function in healthy individuals.

5.2 Background

Endothelial dysfunction and reduced NO availability are thought to be important in the initiation, progression and complications of atherosclerosis. Decreased synthesis or increased inactivation of the vasodilator NO is thought to play a vital part in this process. The mechanisms by which biologically active NO levels are reduced are not fully understood, but one important process might be depletion of the essential NOS cofactor BH_4, resulting in the preferential generation of O_2^- instead of NO by eNOS (Vasquez-Vivar et al., 1999; Wever et al., 1997; Xia et al., 1998). Generation of O_2^- can itself result in excessive oxidation of BH_4 leading to its inactivation (Laursen et al., 2000). Endothelium dependent vasodilation is attenuated in smokers, hypertensives, hypercholesterolemics and diabetics, and administration of low dose BH_4 to these individuals can improve endothelial function possibly by restoring NO/O_2^- balance (Ueda et al., 2000; Stroes et al., 1997; Pieper et al., 1997). Improved endothelial function upon supplementation with BH_4, suggests this essential cofactor could be limited in patients at risk of vascular disease.

Administration of anti-oxidants such as vitamin C and folic acid has also been shown to improve endothelial function in patients with coronary artery disease (CAD), hypertension,

diabetes, hypercholesterolemia and smokers, and low plasma levels of ascorbic acid have been correlated with atherosclerosis (Levine et al., 1996; Solzbach et al., 1997; Ting et al., 1996; Ting et al., 1997; Hornig et al., 1998; Heitzer et al., 1996). The protective mechanism behind administration of such anti-oxidants however is now thought to be more complex than just the scavenging of ROS. Baker et al., 2001 reported increased eNOS activity and BH_4 levels in cultured human umbilical vein endothelial cells (HUVEC) upon administration of vitamin C. However no such effect was observed upon treatment with the ROS scavenger Mn(III) tetrakis (4-benzoic acid) porphyrin chloride (MnTBAP), suggesting that the ability of vitamin C to restore endothelial function may be through increased intracellular BH_4 levels rather than ROS scavenging alone. This theory is supported by a recent publication that demonstrated $ONOO^-$ (generated by the reaction of NO and O_2^-) is a potent oxidizer of BH_4. The authors also showed that the reaction between $ONOO^-$ and BH_4 results in the production of the intermediate BH_3 radical, and that BH_3 can be recycled back to BH_4 by ascorbate reinstating NO synthesis from eNOS (Kuzkaya et al., 2003).

The consequence of depleted BH_4 is the generation of ROS such as O_2^- and H_2O_2 by eNOS itself which, in turn, might mediate oxidative inactivation of BH_4. The cause of the initial depletion of BH_4 in the presence of atherosclerotic risk factors is unclear. Many theories have been proposed including the up-regulation of ROS by systems such as NADPH oxidase (discussed in chapter 3) by oxLDL, ATII or high glucose and down-regulation of SOD (Fukai et al., 1998; Landmesser et al., 2000). Another possibility is that some individuals have reduced pterin pathway activity due to common polymorphisms in pterin synthesizing enzymes. The synthesis of BH_4 begins with the conversion of GTP to

dihydroneopterin triphosphate by GTPCH1. The majority of dihydroneopterin triphosphate is converted to 6-pyruvoyl tetrahydropterin by 6- pyruvoyl tetrahydropterin synthase (PTPS) and finally to BH_4 by sepiapterin reductase (SR). In human cells the low activity of PTPS results in a proportion of dihydroneopterin triphosphate being converted to neopterin, an inert molecule excreted by the kidneys which serves as a marker of pterin pathway activity and which has been used to assess the activation state of the cellular immune system (Murr et al., 2002; Berdowska et al., 2001). The circulating pool of neopterin probably reflects that generated by neuronal cells, immune cells and endothelial cells, but the relative contributions of these cell types to the overall pool is not known.

Genetic variation within genes encoding the enzymes involved in the synthesis of BH_4 could result in differences in local cellular as well as circulating BH_4 or neopterin levels thereby predisposing to endothelial dysfunction and vascular disease. GTPCH1 is the first and rate-limiting enzyme in the synthesis pathway of BH_4 (Duch and Smith, 1991). A number of rare mutations within the gene encoding GTPCH1 (*GCH1*) are known to cause DRD and hyperphenylalanemia but, as yet, no mutations or polymorphisms influencing endothelial function or risk of CVD development have been described. The detection of BH_4 requires HPLC-based techniques that are time consuming and consequently difficult to apply at the population level. Enzyme linked immunoassays (ELISA) for neopterin are commercially available in which multiple samples can be analysed in parallel in 96-well plate format.

This study has investigated whether novel polymorphisms in the *GCH1* gene are related to variation in plasma neopterin level in a subset of healthy subjects from the NPHSII cohort. We then investigated whether these polymorphisms were also associated with functional differences in endothelial function, in a cohort of young adults for whom non-invasive high-resolution ultrasound measurements of endothelial dependent flow mediated dilatation were available.

5.3 Subjects and Methods

Two subject groups were analysed for association between *GCH1* polymorphisms, serum noepterin, and endothelial function during this study.

5.3.1 Subjects investigated for association between *GCH1* genotype and neopterin

Northwick Park Heart Study II (NPHSII)

Subjects were selected from the NPHSII prospective cohort for analysis (section 2.2.12.1). Briefly this cohort comprises approximately 3000 men recruited from 9 primary care practices in the UK. All subjects selected for the study were healthy at the time of recruitment. The men were aged between 50 and 61 years and medical history was assessed by questionnaire. All subjects were reviewed annually. Smoking status, blood pressure (mmHg), BMI (kg/m^2), serum cholesterol (mmol/L), trigycerides (mmol/L), fibrinogen (μmol/L), factor VII coagulant activity (FVIIc % standard) and HDL cholesterol

(mmol/L) were measured at the time of recruitment and during follow-up visits over the following 9 years. Venous blood was taken at time of recruitment and the plasma separated and stored at -80°C. DNA was extracted by the salting-out method described in section 2.2.1.1 and also stored at -80°C. All IHD events have been recorded over the time of the study and the mean follow up is 5 years. A total of 2390 out of 3000 subjects were genotyped for *GCH1* polymorphisms and plasma neopterin measured in a subset of 939 individuals during this study.

5.3.2 Subjects investigated for association between *GCH1* genotype and endothelial function

Cambridge Young Adults Study cohort

248 subjects aged 20 to 28 years for whom blood had been stored for genotyping were studied from the Cambridge Young Adults Study (section 2.2.12.1). The study group comprised a sample of individuals born in Cambridge Maternity Hospital between 1969 and 1975 as described previously (Leeson et al., 2002). They were invited to attend a clinic for cardiovascular risk profile evaluation by questionnaire followed by venepuncture, physical measurements and vascular studies. In each subject, a fasting venous blood sample was analysed for insulin, glucose, total cholesterol, HDL and triglycerides, and LDL. Personal and family medical history (including details of heart disease and risk factors) was gathered by questionnaire at interview. Current or past smoking was recorded. Blood pressure was measured as the average of the last two of three seated readings using an automated oscillometric device (Critikon Inc, USA). Weight was recorded (to +/- 0.1

kg) using scales (Soenhle Ltd) and height (to +/- 0.1 mm) with a portable stadiometer. Every subject underwent measurement of endothelial dependent and independent vascular responses of the brachial artery, using high-resolution ultrasound imaging as described in section 2.2.13.2.

5.3.3 Measurement of plasma neopterin in the NPHSII cohort

Neopterin measurements were taken from a total of 939 individuals from the NPHSII cohort, using the ELItest® competitive enzyme immunoassay kit (B.R.A.H.M.S diagnostica GMBH) as described in section 2.2.10. All measurement were carried out in collaboration with Dr Noor Jeerooburkhan (University College London). 243 and 288 neopterin samples were collected from the Chesterfield and North Mymms primary care practices respectively and a further 513 neopterin measurements collected from a random data set. The three data sets were pooled to give a total data set of 939 subjects. Plasma samples were collected and stored at –80°C until required. Neopterin has been shown to be stable in this state. The lower limit of detection for this assay was 2nmol/L, with an intra-assay variation of 3.5% and an inter-assay variation of 6.5%.

5.3.4 Genotyping studies

PCR-RFLP analysis was used for genotyping studies as described in section 2.2.6. Two out of the four *GCH1* polymorphisms identified by SSCP (-577G/A and -796G/A) were chosen for genotyping analysis. Genomic DNA was amplified by PCR as described in

chapter 4 (section 4.3.2). The restriction enzyme *BsmF1* (which cuts in the presence of the G allele) was used for genotyping the –577G/A polymorphism to produce bands of 206 and 142bp. The restriction enzyme *BsrD1* (which cuts in the presence of the A allele) was used for genotyping the –796G/A polymorphism to produce bands of 290 and 84bp. Digested products were electrophoresed on 2.5% agarose gels and visualised by ethidium bromide staining.

5.3.5 Statistical Analysis

Observed numbers of each genotype were compared with those expected under the assumption of Hardy-Weinberg equilibrium by χ^2 analysis. Allele frequencies were deduced from genotype frequencies. Pairwise linkage disequilibrium coefficients between polymorphisms were estimated by log linear analysis (Chakravarti et al., 1984). Data are presented as arithmetic mean (±SD) except for neopterin for which geometric mean (approximate SD) is presented due to the skewed nature of the distribution. Allelic associations were carried out by One-Way Analysis of Variance (ANOVA) and the significance of differences between genotype groups by Students t-test. Standard regression and interaction models were used to determine whether the association between endothelial function and genotype was influenced by classical risk factors. The primary hypothesis was that polymorphisms in the *GCH1* gene would be associated with differences in neopterin and/or endothelial function. Sixty subjects were required to detect a 0.25 standard deviation difference in log neopterin between rare allele carriers and non-carriers at 80% power, 2P=0.05. With a sample size of 248 individuals from the Cambridge Young

Adults cohort, the study had 80% power at 2P=0.05 to identify a 0.02 mm or 0.6% difference in FMD between groups. A secondary hypothesis, that *GCH1* polymorphisms would be associated with cardiovascular events was also tested. With 188 events in the genotyped NPHSII cohort the study had an 80% power to detect an odds ratio of 1.4 among rare allele carriers at 2P=0.05.

5.4 Results

5.4.1 Genotype and allele frequency of *GCH1* polymorphisms

Genotype and allele frequencies for the –577G/A and -796G/A *GCH1* polymorphisms are shown in table 5.1. The –796G/A variant did not conform to the Hardy Weinberg rule in either the NPHSII cohort (χ^2=275.3, P=<0.0001) or the Cambridge Young Adults Study cohort (χ^2=20.8, P=<0.05). Repeat genotyping and DNA sequencing confirmed that this was not the result of mis-genotyping. As there were no related individuals within the NPHSII cohort this was also ruled out as an explanation for the difference in observed and expected genotypes. The –796G/A and –577G/A polymorphisms were in tight linkage disequilibrium in both cohorts (NPHSII Δ0.79, P=<0.0001; Cambridge Young Adults cohort Δ0.66, P=<0.0001).

NPHSII cohort

Polymorphism	Genotype N (%)			Allele %		χ^2	P
	GG	GA	AA	G	A		
-577G/A	1897 (79.0)	453 (19.0)	40(2.0)	88.0	12.0	3.96	0.05
-796G/A	1770 (74.0)	437 (18.0)	179 (8.0)	83.0	17.0	275.3	<0.0001

Cambridge Young Adults cohort

Polymorphism	Genotype N (%)			Allele %		χ^2	P
	GG	GA	AA	G	A		
-577G/A	185 (82.0)	37 (16.0)	4 (2.0)	90.0	10.0	1.7	0.19
-796G/A	171 (77.0)	38 (17.0)	13 (6.0)	86.0	14.0	20.8	<0.05

Table 5.1 Genotype and allele frequencies of *GCH1* polymorphisms in the NPHSII cohort (top panel) and the Cambridge Young Adults Study cohort (bottom panel). The –796G/A polymorphism did not conform to the Hardy-Weinberg equilibrium in either cohort.

5.4.2 Baseline demographics of NPHSII study participants

Baseline characteristics of the NPHSII cohort according to *GCH1* genotype are shown in tables 5.2a and 5.2b. Orthodox cardiovascular risk factors such as blood pressure, pulse pressure, cholesterol, fibrinogen, BMI or age did not differ among groups of different genotype.

	Genotype –577G/A		
	GG Mean (SD) N=1789	**GA+AA** Mean (SD) N=485	**P**
Age (Years)	56.1 (3.4)	56.0 (3.4)	0.77
Diastolic BP (mmHg)	84.6 (11.4)	84.8 (11.1)	0.64
Systolic BP (mmHg)	138.7 (19.2)	138.5 (19.4)	0.84
Pulse Pressure	54.1 (14.5)	53.6 (14.7)	0.53
Cholesterol (mmol/L)	5.72 (1.02)	5.72 (0.98)	0.98
Fibrinogen (μmol/L)	0.08 (0.02)	0.08 (0.02)	0.33
BMI (kg/m^2)	26.5 (3.5)	26.2 (3.3)	0.11

Table 5.2a Demographic details of subjects in the NPHSII cohort according to *GCH1* –577G/A genotype. GA+AA individuals were grouped and analysed together. No significant difference was found in age, blood pressure, cholesterol, fibrinogen or BMI between genotypes.

	Genotype –796G/A		
	GG Mean (SD) N=1666	**GA+AA** Mean (SD) N=572	**P**
Age (Years)	56.0 (3.4)	56.2 (3.4)	0.44
Diastolic BP (mmHg)	84.4 (11.3)	84.2 (11.1)	0.67
Systolic BP (mmHg)	138.3 (19.1)	137.5 (19.2)	0.38
Pulse Pressure	53.9 (14.4)	53.3 (14.3)	0.41
Cholesterol (mmol/L)	5.72 (1.01)	5.75 (1.00)	0.52
Fibrinogen (μmol/L)	0.08 (0.02)	0.08 (0.02)	0.29
BMI (kg/m²)	26.5 (3.5)	26.5 (3.4)	0.86

Table 5.2b Demographic details of subjects in the NPHSII cohort according to *GCH1* –796G/A genotype. GA+AA individuals were grouped and analysed together. No significant difference was found in age, blood pressure, cholesterol, fibrinogen or BMI between genotypes.

5.4.3 Distribution and determinants of plasma neopterin

Among the 939 healthy men from the NPHSII cohort, the distribution of neopterin values were skewed with a geometric mean neopterin value of 6.0nmol/L (range: 2.16 nmol/L to 33.5 nmol/L), similar to that reported previously (Diamondstone et al., 1994). Univariate analysis revealed a significant positive correlation between plasma neopterin and fibrinogen (r=0.11, p=0.0006), and negative correlations with cholesterol (r= -0.12, p=0.0002) and apoA1 (r= -0.16, p=0.0001) (Table 5.3). Plasma neopterin was not significantly different between smokers (n=228) and non-smokers (n=711) (mean neopterin 6.11±1.42nmol/L vs 5.95±1.46nmol/L, p=0.16). No significant correlation was observed between levels of neopterin and systolic or diastolic pressure. Cardiovascular events were recorded in 41 individuals out of the 939 with neopterin measurements. No evidence of an association

between neopterin levels and cardiovascular outcome was observed, mean (SD) neopterin values for subjects in whom an event was recorded and those without an event was 6.10 (1.00) nmol/L and 6.25 (1.56) nmol/L respectively (P=0.38).

Characteristic	R	P
Diastolic BP	0.01	0.75
Systolic BP*	-0.04	0.23
Triglycerides	-0.03	0.4
ApoA1*	-0.16	<0.0001
ApoB	-0.007	0.84
Cholesterol*	-0.12	0.0002
Fibrinogen$^{\Psi}$	0.11	0.0006
BMI	-0.008	0.81
Age	0.05	0.10

Table 5.3. Correlation of neopterin with risk factors for cardiovascular disease in the NPHSII cohort by stepwise multiple regression. An inverse relationship was observed between neopterin and cholesterol and ApoA1*. A positive relationship was observed between neopterin and fibrinogen$^{\Psi}$.

5.4.4 Relationship between *GCH1* genotype and plasma neopterin in the NPHSII cohort

Full genotype and neopterin data were available for 696 individuals out of the 939 selected. Both the –577G/A and -796G/A polymorphisms showed significant association with neopterin levels both before and after adjustment for fibrinogen, cholesterol, apoA1 and primary care practice (Table 5.4). The associations also persisted after correction for renal

function (p=0.001 for both variants, table 5.4) with A-allele carriers having lower neopterin/creatinine ratio. In a stepwise multiple regression analysis fibrinogen (r=0.13, p=0.001), cholesterol (r=-0.09, p=0.02), ApoA1 (r=-0.15, p=<0.0001) and genotype (r=-0.11, p=0.004) were independently associated with plasma neopterin, accounting for 6.9% of variation.

Genotype –577G/A

	GG Mean (SD) N=565	**GA+AA** Mean (SD) N=131	**P**	**P***
Neopterin	6.30 (1.69)	5.87 (1.35)	0.006	0.004
Neopterin/Creatinine	0.067 (0.019)	0.061 (0.014)	0.0008	0.001

Genotype –796G/A

	GG Mean (SD) N=565	**GA+AA** Mean (SD) N=131	**P**	**P***
Neopterin	6.29 (1.61)	5.95 (1.52)	0.02	0.01
Neopterin/Creatinine	0.066 (0.018)	0.061 (0.016)	0.0006	0.001

Table 5.4. Neopterin and neopterin/creatinine according to *GCH1* –577G/A (top panel) and –796G/A genotype (bottom panel). Individuals homozygous for the *GCH1* –577 and –796 G allele (GG) had significantly higher neopterin and neopterin/creatinine compared to A allele carriers (GA+AA). Data has been adjusted for practice. *Also adjusted for fibrinogen, cholesterol and apoA1.

5.4.5 *GCH1* polymorphism, and CVD risk

A secondary hypothesis explored in the NPHSII cohort was that *GCH1* genotype influenced CHD risk. The total number of CHD events for the whole NPHSII cohort was 188. No evidence was found of an association between genotype and risk of IHD overall (Table 5.5). However, a significant interaction was observed between –796 genotype and smoking (p=0.02). Individuals homozygous for the –796 A allele who smoked had a hazard ratio for CHD of 7.78 (95%CI: 2.12-29.14), compared to a hazard ratio for CHD of 1.51 (95%CI: 1.11-2.06) for smokers overall. No evidence was found for an interaction between –577 genotype and smoking (p=0.92).

Polymorphism	Genotype	Hazard Ratio (95% CI)	P value
-577 G/A	GG	1.00	
	GA/AA	0.76(0.46-1.24)	P=0.27
-796 G/A	GG	1.00	
	GA/AA	1.11(0.58-2.12)	P=0.76

Table 5.5. *GCH1* genotype and IHD risk in the NPHSII cohort. A allele carriers were grouped and analysed against GG homozygotes. No association was found between *GCH1* genotype and IHD risk.

5.4.6 Baseline demographics of Cambridge Young Adults Study participants

The characteristics of the study sample according to *GCH1* genotype are summarised in tables 5.6a and 5.6b. There were no significant differences between genotype groups in levels of cholesterol, LDL, HDL, blood pressure, BMI, age, height, weight or smoking status within the whole group, males or females.

As previously reported (Leeson et al., 2002), there were no associations between cardiovascular risk factors and resting vessel size or brachial artery blood flow in this cohort. There was no difference in mean FMD or GTND between sexes. Smokers had lower mean FMD than non-smokers (0.090 ± 0.080 mm v 0.109 ± 0.081 mm respectively, $p<0.05$), with no difference in GTND (0.677 ± 0.225 mm v 0.674 ± 0.184 mm, $p=0.90$).

	Genotype –577G/A		
	GG Mean (SD) N=175	**GA+AA** Mean (SD) N=38	**P**
Age (range, years)	23.0 (20-27)	23.0 (20-27)	ns
SBP (mmHg)	128.0 (14.0)	128.0 (14.0)	ns
DBP (mmHg)	71.0 (9.0)	71.0 (8.0)	ns
Cholesterol (mmol/L)	4.54 (0.94)	4.69 (1.11)	ns
LDL (mmol/L)	2.81 (0.83)	2.89 (0.96)	ns
HDL (mmol/L)	1.19 (0.3)	1.18 (0.33)	ns
BMI (kg/m²)	2.4 (0.4)	2.5 (0.4)	ns

Table 5.6a. Demographic characteristics of the Cambridge Young Adults Study cohort according to *GCH1* –577G/A genotype. No significant difference was observed in age, blood pressure, cholesterol or BMI between genotypes (ns=not significant, P>0.05).

	Genotype –796G/A		
	GG Mean (SD) N=161	**GA+AA** Mean (SD) N=47	**P**
Age (range, years)	23.0 (20-27)	23.0 (20-27)	ns
SBP (mmHg)	128.0 (14.0)	129.0 (14.0)	ns
DBP (mmHg)	71.0 (8.0)	71.0 (7.0)	ns
Cholesterol (mmol/L)	4.52 (0.91)	4.67 (0.97)	ns
LDL (mmol/L)	2.78 (0.80)	2.92 (0.87)	ns
HDL (mmol/L)	1.20 (0.29)	1.17 (0.36)	ns
BMI (kg/m^2)	2.4 (0.3)	2.4 (0.4)	ns

Table 5.6b. Demographic characteristics of the Cambridge Young Adults Study cohort according to *GCH1* –796G/A genotype. No significant difference was observed in age, blood pressure, cholesterol or BMI between genotypes (ns=not significant, P>0.05).

5.4.7 Relationship between *GCH1* genotype and endothelial function.

The association between genotype and FMD is shown in table 5.7. Only subjects from whom scans of adequate quality for endothelial function together with successful genotyping data were chosen for analysis, leaving full details of genotype and vascular function available for 213 individuals for the –577G/A variant and 208 individuals for the –796G/A variant. FMD was lower in A-allele carriers for the –796G/A variant (p=0.03) and a similar but non-significant trend was observed between groups for the –577G/A variant (p=0.27). There were no differences in GTND between genotype groups.

Genotype –577G/A

	GG Mean (SD) N=175	GA+AA Mean (SD) N=38	P
Resting vessel size (mm)	3.30 (0.61)	3.27 (0.52)	0.76
FMD (mm)	0.115 (0.09)	0.095 (0.06)	0.18
FMD (%)	3.55 (2.64)	3.05 (2.18)	0.27
GTND (mm)	0.688 (0.20)	0.674 (0.15)	0.54
GTND (%)	21.75 (7.79)	21.22 (6.72)	0.69

Genotype –796G/A

	GG Mean (SD) N=161	GA+AA Mean (SD) N=47	P
Resting vessel size (mm)	3.31 (0.62)	3.27 (0.48)	0.64
FMD (mm)	0.118 (0.09)	0.087 (0.06)	0.02*
FMD (%)	3.62 (2.64)	2.78 (1.92)	0.03*
GTND (mm)	0.692 (0.20)	0.663 (0.14)	0.26
GTND (%)	21.88 (7.98)	20.77 (5.80)	0.37

Table 5.7. Endothelial function according to *GCH1* –577G/A (top panel) and –796G/A (bottom panel) genotype in the Cambridge Young Adults Study cohort. A significant difference in FMD was observed between GG homozygotes and A allele carriers of the –796G/A polymorphism. A allele carriers had lower FMD than GG individuals (% FMD, *P=0.03). A similar but non-significant trend was observed for the –577G/A polymorphism (P=0.27)

5.5 Discussion

This study has identified two common novel variants in the *GCH1* gene and examined their phenotypic consequences in two large population-based studies of healthy individuals. Carriage of an A-allele for the –796G>A and –577G>A variants for the *GCH1* gene was associated with lower levels of plasma neopterin in the NPHSII cohort. Carriage of an A-allele for the –796G>A variant was associated with reduced endothelial-dependent vasodilation in the Cambridge Young Adults cohort, with a similar, though non-significant trend in endothelial function noted for the –577G>A variant.

We hypothesised that common genetic variation of the *GCH1* gene could influence expression or activity of the GTPCH-1 enzyme in the general population and that this in turn could affect BH_4 availability. This study has demonstrated an association between two variants within the *GCH1* promoter and levels of plasma neopterin, a surrogate marker of BH_4 synthesis. These variants might themselves influence *GCH1* mRNA expression, or might be in linkage disequilibrium with regulatory variants elsewhere in the gene. The –796 G>A polymorphism lies 3bp from a CCAAT box/enhancer binding protein element (C/EBP) and could alter transcription factor binding and therefore gene expression. However, further *in vitro* analysis is needed to clarify the molecular mechanism of the observed associations.

GCH1 variants associated with changes in neopterin concentration were also associated with corresponding changes in endothelium-dependent vasodilation of the brachial artery, a

systemic *in vivo* bioassay of endothelial NO availability. This association was independent of any effect of classical cardiovascular risk factors on vascular responses. Impaired flow mediated dilatation has been shown to relate to the presence of cardiovascular risk factors and disease in the general population (Celermajer et al., 1992), to be predictive of future vascular events (Gokce et al., 2003), and to be largely mediated by endothelium-derived NO (Palmer et al., 1987). Impaired endothelium-dependent dilatation and NO availability may be due to reduced NO synthesis, increased inactivation by rapid chemical reaction with reactive oxygen species including O_2^-, or both. The restoration of endothelial function by local intra-arterial BH_4 infusion demonstrated in previous studies might therefore reflect augmentation of NO synthesis or an antioxidant effect of this molecule (Fukuda et al., 2002; Maier et al., 2000; Heitzer et al., 2000). Some studies suggest that functional BH_4 deficiency in cardiovascular disease is itself the result of increased oxidative inactivation of BH_4 (Heller et al., 2001). Our data suggest that changes in pterin synthesis, regulated by *GCH1* expression might also play a role.

Despite associations between *GCH1* polymorphisms, neopterin concentration and endothelial function, the NPHSII study of 2390 males did not provide evidence that *GCH1* genotype altered future risk of CHD events. However, the NPHSII study is only powered to detect a genotype relative risk of >1.4 with 80% power at 2p=0.05 and thus relative risks of 1.2-1.3, such have now been demonstrated in combined data sets for variants in other candidate genes such as ACE or MTHFR, could not be excluded (Keavney et al., 2000; Wald et al., 2002). There was statistical evidence that the –796 genotype, but not the –577 genotype, interacted with smoking to increase coronary disease risk. A significant

association was only demonstrated between the –796 genotype and flow mediated dilatation. However, differences in neopterin were seen with both genotypes and there was a trend to an association between flow mediated dilatation and the –577 genotype. Due to the small numbers involved these data must be interpreted with caution.

In summary we have identified novel variants in the *GCH1* gene. Those situated within the promoter region are associated with plasma neopterin levels in a large prospective cohort of healthy men, which suggests neopterin and therefore BH_4 synthesis is influenced by *GCH1* genotype. Furthermore, in a cohort of young adults the –796 G>A variant is associated with significant differences in NO-dependent endothelial function, which is known to be a key early pathophysiological stage in the development of atherosclerosis. Variants relevant to BH_4 synthesis appear to have an independent impact on endothelial function in healthy individuals from early in life.

CHAPTER 6

IDENTIFICATION OF POLYMORPHISMS IN THE HUMAN DIMETHYLARGININE DIMETHYLAMINOHYDROLASE GENE (*DDAH2*)

6.1 Aim

To scan the human dimethylarginine dimethylaminohydrolase gene (*DDAH2*) for novel genetic variants, with the intention of investigating the role of any polymorphisms in the regulation of ADMA metabolism, in the modulation of endothelial function and the susceptibility to CVD.

6.2 Background

Asymmetric dimethylarginine (ADMA) is a naturally occurring methylated arginine that inhibits the synthesis of nitric oxide (NO) from L-arginine. It impairs endothelium-dependent vasodilation, is found in elevated concentrations in plasma from patients with risk factors for vascular disease and its levels predict future vascular events (Vallance et al., 1992; Boger et al., 1998; Pettersson et al., 1998; Usui et al., 1998). Although ADMA levels vary between individuals little is known about the mechanism of such variation.

ADMA and symmetric dimethylarginine (SDMA) are generated by methylation of proteins by protein arginine methyltransferases (PRMTs) (Clarke, 1993). Unlike ADMA, SDMA has no inhibitory activity on the NOS enzyme. Whilst both ADMA and SDMA are excreted by the kidneys, and so accumulate when the kidneys fail, ADMA is also actively metabolised by the dimethylarginine dimethylaminohydrolase enzymes -DDAH1 and DDAH2 (Ogawa et al., 1987; Ogawa et al., 1989; Leiper et al., 1999).

The DDAH1 enzyme was first identified in rat kidney by Ogawa and colleagues in 1989. Ten years later Leiper *et al* reported the cloning and deduced amino acid sequence of human DDAH1 and the discovery of a novel DDAH isoform termed DDAH2. The DDAH2 isoform was shown to share approximately 62% homology with the DDAH1 amino acid sequence, and the DDAH2 cDNA and protein sequences exhibit 98% homology between human and mouse species. Northern blot experiments revealed distinct tissue distributions for DDAH1 and DDAH2, which showed some similarities with the tissue distribution of NOS isoforms. DDAH1 is highly expressed in brain, kidney, pancreas and liver, tissues in which the neuronal isoform of NOS is predominant. In contrast DDAH2 is highly expressed in the heart, kidney and placenta correlating with expression of eNOS (Leiper et al., 1999). A more in depth analysis of the tissue distributions of DDAH1 and DDAH2 also revealed that DDAH2 is highly expressed in foetal tissue and may have a role to play in cellular differentiation and cell cycle control (Tran et al., 2000). Thus tissue specific regulation of ADMA concentrations by distinct DDAH isoforms could be an important process regulating NO bioavailability. The expression of DDAH2 in highly vascularised tissues has also led to interest in this enzyme as a potential candidate for the predisposition to CVD.

Ribas et al, 1999, were the first to report the chromosomal localisation of a human gene thought to be homologous to rat *DDAH*. This gene (which they termed G6A) is located within the class three region of the major histocompatibility complex (MHC class III) on chromosome 6p21.3. The identity of this gene was confirmed as being *DDAH2* by Tran et al., 2000 who also verified its location by radiation hybrid mapping and fluorescent *in-situ*

hybridisation (FISH). This region of human chromosome six contains a number of genes that are thought to be involved in autoimmune diseases such as insulin dependent diabetes mellitus, ankylosing spondylitis and coeliac disease (Bertrams, 1984; Brown et al., 1998; McManus et al., 1996). Localisation of *DDAH2* to the MHC class III region and the observation that DDAH2 is expressed in many types of immune cell, suggests that regulation of ADMA may also be important for iNOS activity which is known to contribute to many autoimmune pathophysiologies (Weinberg et al., 1994).

The *DDAH2* gene comprises 8 exons that span a distance of 3kb. The 5' untranslated region of the mRNA is encoded by exons 1, 2 and part of exon 3. Three transcription initiation sites have been identified at the beginning of exons 1, 2 and 3, and alternate splicing results in transcripts originating from all three as identified by EST database searches (Ribas et al., 1999; Tran et al., 2000). In comparison the *DDAH1* gene has 6 exons spread over a distance of more than 65kb. The translation start site of *DDAH1* lies within exon 1, but no splice variants have been identified. The highly conserved exon/intron boundaries between *DDAH1* and *DDAH2* have led to the theory that these two genes arose through block duplication (Tran et al., 2000).

Publication of the crystal structure of a bacterial DDAH by Murray-Rust et al., 2001, revealed the nature of the enzyme active site and opened the way for research into the regulation of DDAH activity. They reported a catalytic triad (Cys-His-Glu), which is conserved in all known DDAH enzymes including human DDAH1 and DDAH2. Further work by Leiper et al., 2002 demonstrated that S-nitrosylation of the active site cysteine

(Cys) residue reversibly inhibits enzyme activity, and these authors proposed that *in-vivo* S-nitosylation in the presence of high concentrations of NO for example seen after induction of iNOS, could lead to elevated ADMA levels. The authors also suggested that the elevated ADMA would lead to inhibition of all three NOS isoforms, explaining the observation that very high levels of NO from iNOS can suppress endothelium-dependent vasodilation due to NO release from eNOS (Kessler et al., 1997). Nitrosylation of DDAH could also account for the observations of Ito et al., 1999, who showed DDAH activity but not expression is reduced in ECV304 cells treated with oxLDL or cytokines and also in rabbits fed a high cholesterol diet. Initial up-regulation of iNOS by oxLDL and cytokines is now a plausible explanation for these findings.

Regulation of DDAH at the level of enzyme expression is also attracting interest as a mechanism of regulating circulating ADMA. To date the only publication demonstrating direct regulation of DDAH expression has highlighted *all-trans* retinoic acid (*at*-RA) as a transcription factor capable of increasing DDAH2 expression. Treatment of sEnd1 cells (a murine cell line) with *at*-RA not only increased DDAH2 expression, but also decreased ADMA and increased NO production without increasing NOS expression (Achan et al., 2002). *At*-RA is a powerful morphogen and has important effects on the developing cardiovascular system (Lansink et al., 1998), and these findings re-enforce the theory that DDAH2 may be involved in cell cycle control in the cardiovascular system.

Up to the writing of this thesis, no mutations or polymorphisms had been identified in either *DDAH1* or *DDAH2* by other groups. However, *DDAH2* is a potential candidate gene

for vascular disease because of its likely importance in regulating ADMA levels, and through this NO availability and vascular function. The aim of this study was to screen the *DDAH2* gene for common polymorphisms or mutations by SSCP analysis.

6.3 Subjects and Methods

6.3.1 Subjects

Anonymised DNA samples from 32 healthy unrelated individuals, was used to screen the *DDAH2* gene for polymorphisms. Blood was collected into EDTA tubes and DNA extracted by the Qiagen DNA purification kit method (section 2.2.1.2).

6.3.2 Oligonucleotide design and amplification of genomic DNA

Oligonucleotides were designed to cover the promoter and exons of the *DDAH2* gene. All oligonucleotides were designed to be approximately 50% GC rich with minimum secondary structure formation. Each oligonucleotide pair was designed to have similar annealing temperatures, non-complementary sequence (which could result in 'primer-dimer' production) and produce a PCR product 200-400bp in length (the optimum for SSCP analysis). Oligonucleotides were designed using the Genbank/EMBL database sequence (accession number AJ012008). Table 6.1 lists all oligonucleotide sequences, positions relative to the translation start site, and PCR conditions. Three pairs of

oligonucleotides were designed to produce three PCR products, which overlapped one another to cover the promoter region spanning -1078 to –1881 relative to the translation start site. Because of the small size of exon 4, intron 4 and exon 5 (100bp, 122bp and 73bp respectively), oligonucleotides were designed to amplify both exons in one PCR reaction.

Amplification was carried out by PCR as described in section 2.2.2. All PCR products were electrophoresed on 1% agarose gels with 100bp ladder to ensure a single-band product of the correct size was achieved.

Position of oligonucleotides relative to translation start site	$MgCl_2$ (mM)	Annealing Temp (°C)	Sequence
Promoter 1			F - *5'*ggt cta aca tgt tgg tcc ctc*3'*
-1536→ -1881	1.5	64	R - *5'*ctc ttc cac cac acc atc ccg*3'*
Promoter 2			F - *5'*tgc tac cca atg gac aca ctc*3'*
-1315→ -1617	1.5	64	R - *5'*agc agc ccc acc aca aac att*3'*
Promoter 3			F - *5'*agg ggt ggg tca gtg atc ttg*3'*
-1078→ -1389	1.5	64	R - *5'*cgg ctc cgg ggc att gtc taa*3'*
Exon 1			F - *5'*cga aga agc ccc gcc ccg tcc*3'*
-869→ -1221	1.5	68	R - *5'*ggc ccc ccc acg caa gac tca*3'*
Exon 2			F - *5'*ctt cgg gac tcg gtc tgg ttt*3'*
-403→ -652	1.5	62	R - *5'*tta acc ctc agc tgc tcg cta*3'*
Exon 3			F - *5'*aac gcc ctt gtc tgc atg tct*3'*
-121→ +297	1.5	62	R - *5'*tct gcc ttt ccc cat acc aca*3'*
Exon 4 +5			F - *5'*cct gca ccc cct ccc tcc cta*3'*
389→ 751	1.5	68	R - *5'*gct ccg tgc cct ctt ctc cta*3'*
Exon 6			F - *5'*ata ccc cat cac ccc tcc cgc*3'*
818→ 1273	2.0	68	R - *5'*ttt caa ccc cct acc ttc ccc*3'*
Exon 7			F - *5'*tta gtg gtg gtt gag cag gca3'
1398→ 1795	1.5	64	R- *5'*aca tgg agt ggg gag agg gga*3'*
Exon 8			F - *5'*tct cac tcc cct ctc ccc act*3'*
1769→2164	2.0	67	R - *5'*cct atc cct ttg ccc ctg taa*3'*

Table 6.1. Oligonucleotides used for PCR amplification of the human *DDAH2* gene. A set of three overlapping oligonucleotide pairs were designed to amplify the promoter region from position –1078 to –1881 relative to the translation start site. The region amplified by each oligonucleotide pair is shown with corresponding $MgCl_2$ concentration and annealing temperatures for PCR.

6.3.3 Screening for polymorphisms by SSCP analysis

The non-radioactive PhastSystem SSCP technique was used to scan the *DDAH2* gene as described in section 2.2.4.2.

6.3.4 DNA sequencing to define the nature of variants detected by SSCP

Genomic regions exhibiting different banding patterns on SSCP gel electrophoresis were chosen for sequence analysis. Samples were selected so that each different banding pattern produced by SSCP was represented at least twice and the region re-amplified from genomic DNA. The PCR product was used as a template and both forward and reverse sequencing reactions set up using the same oligonucleotides as for PCR. Sequencing was carried out as described in section 2.2.5.

6.3.5 Search of the National Center for Biotechnology Information (NCBI) SNP database for *DDAH2* polymorphisms

The NCBI SNP database (http://www.ncbi.nlm.nih.gov/SNP/) was searched for all polymorphisms identified to date within the *DDAH2* gene as described in chapter 2.2.7. The database was established in 1988 and is a resource of freely available molecular biology information compiled by genome sequencing consortiums worldwide.

6.3.6 Search of the MatInspector promoter database for putative *DDAH2* transcription factor binding sites

A search of the MatInspector database (http://www.genomatix.de/free_login.html) with the *DDAH2* promoter sequence was undertaken to identify transcription factor binding sites as described in chapter 2.2.8.

6.3.7 Identification of restriction enzyme sequences and genotyping of *DDAH2* polymorphisms

Restriction enzyme sites created or abolished by the presence of a polymorphism were identified using Webcutter software (http://www.firstmarket.com/cutter/cut2.html). Two cohorts of healthy subjects were used for initial genotyping analysis to ascertain genotype and allele frequencies of polymorphisms identified by SSCP. Individuals from the NPHSII cohort (North Mymms and Chesterfield clinics, n=498) described in section 2.2.12.1, were genotyped for the –449G/C, -1151A/C and –1020C/G polymorphisms, and 128 individuals from the German population screen (section 2.2.12.1) were genotyped for the –1151A/C, -1020C/G and –871 6G/7G polymorphisms.

Genotyping of the –1151A/C, -1020C/G and –449G/C polymorphisms was carried out by PCR-RFLP analysis as described in chapter 2.2.6.1, using restriction enzymes *BstUI*, *MwoI* and *BstUI* respectively (table 6.2). The –871 6G/7G bi-allelic length variation polymorphism was genotyped by Genescan analysis as described in section 2.2.6.2, using

the fluorescent labelled forward reading oligonucleotide – 5' **6-FAM-**TCTCCACCAACTCTGTCCTC3' and reverse oligonucleotide 5'TAGCTCCGCGCCCAAATACCC3' to amplify a 191bp fragment containing the 6G variant or a 192bp fragment containing the 7G.

DDAH2* Polymorphism	**Restriction enzyme**	**Recognition sequence**	**Digest products (size bp)**
-1151 C/A	*BstUI*	5' CG↓CG 3'	238+73
-1020C/G	*MwoI*	5' GCNNNNN↓NNGC 3'	144+109
-449C/G	*BstUI*	5' CG↓CG 3'	204+46

Table 6.2 *DDAH2* polymorphisms – restriction enzymes and digestion products. Characters in bold type indicate polymorphic bases recognized and cut by the restriction enzyme. ↓ =cutting site. * numbering with respect to the translation start site.

6.4 Results

6.4.1 Polymorphisms in *DDAH2*

Six polymorphisms were identified within the *DDAH2* gene (Figure 6.1). The position of each polymorphism is numbered relative to the translation start site (ATG). SSCP analysis revealed a difference in banding pattern for PCR products generated with the oligonucleotides promoter 2, promoter 3, exon 1, exon 2 and exon 4+5 (tables 6.1), suggesting the presence of genetic variation within these regions. Figures 6.2a-6.2d show the SSCP gel images and the variation in banding pattern between individuals for the promoter 3, exon 1, exon 2 and exon 4+5 PCR products. Genetic variation in these regions was confirmed by DNA sequencing, which revealed a total of five single base substitutions at positions –1415G→A, -1151C→A, -1020C→G, -449C→G and +618C→T and a 6G/7G bi-allelic length variation at position –871 (Figures 6.3a-6.3f). Two of the polymorphisms reside upstream of exon 1 (-1415G/A and -1151C/A), one within exon 1 (-1020C/G), one within intron 1 (-871 6G/7G), one within intron 2 (-449C/G) and one within intron 4 (618C/T).

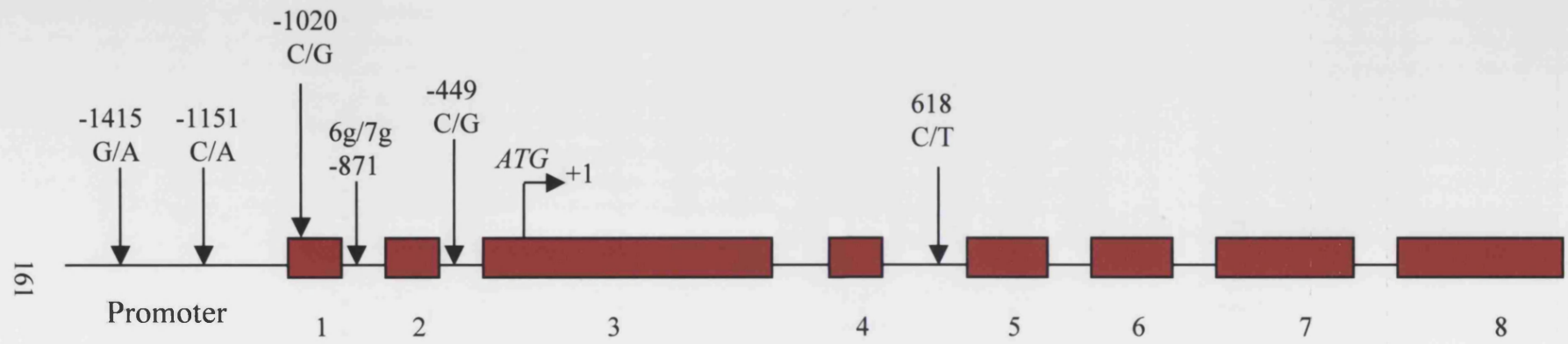

Figure 6.1 ***DDAH2*** **gene structure and polymorphisms identified by SSCP.**
Polymorphisms identified by SSCP during this study are indicated by vertical arrows ↓. The position of each variant is numbered relative to the translation start site located in exon 3 (ATG). Exons 1-8 are numbered and filled in red. Five polymorphisms were identified upstream of the translation start site, one of these residing in the non-coding exon 1(-1020C/G). Only one polymorphism was found downstream of the translation start site within intron 4 (618C/T).

A

Figure 6.2a. SSCP gel of *DDAH2* promoter 3 PCR. An extra band can be seen in samples 2, 3, 6 and 7 (indicated by an arrow). DNA sequencing identified this polymorphism as a C→A substitution at position –1151 (figure 6.3b).

B

Figure 6.2b. SSCP gel of *DDAH2* exon 1 PCR. An extra band is observed in lanes 2, 4 and 5 (indicated by an arrow). DNA sequencing identified this polymorphism as a C→G substitution at position –1020 (figure 6.3c). DNA sequencing also revealed an insertion/deletion (6g/7g) polymorphism at position –871(figure 6.3d).

C

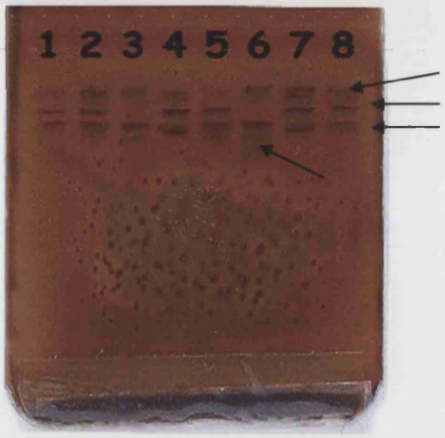

Figure 6.2c. SSCP gel of *DDAH2* Exon 2 PCR Lanes 3 and 6 have two bands that have migrated to different positions compared to three bands observed in all other lanes. DNA sequencing identified this polymorphism as a C→G substitution at position –449 (figure 6.3e).

D

Figure 6.2d. SSCP gel of *DDAH2* Exon 4+5 PCR. Extra bands in samples 3 and 6 indicate the presence of sequence variation in these PCR products. DNA sequencing identified this polymorphism as a C→T substitution at position 618 (figure 6.3f).

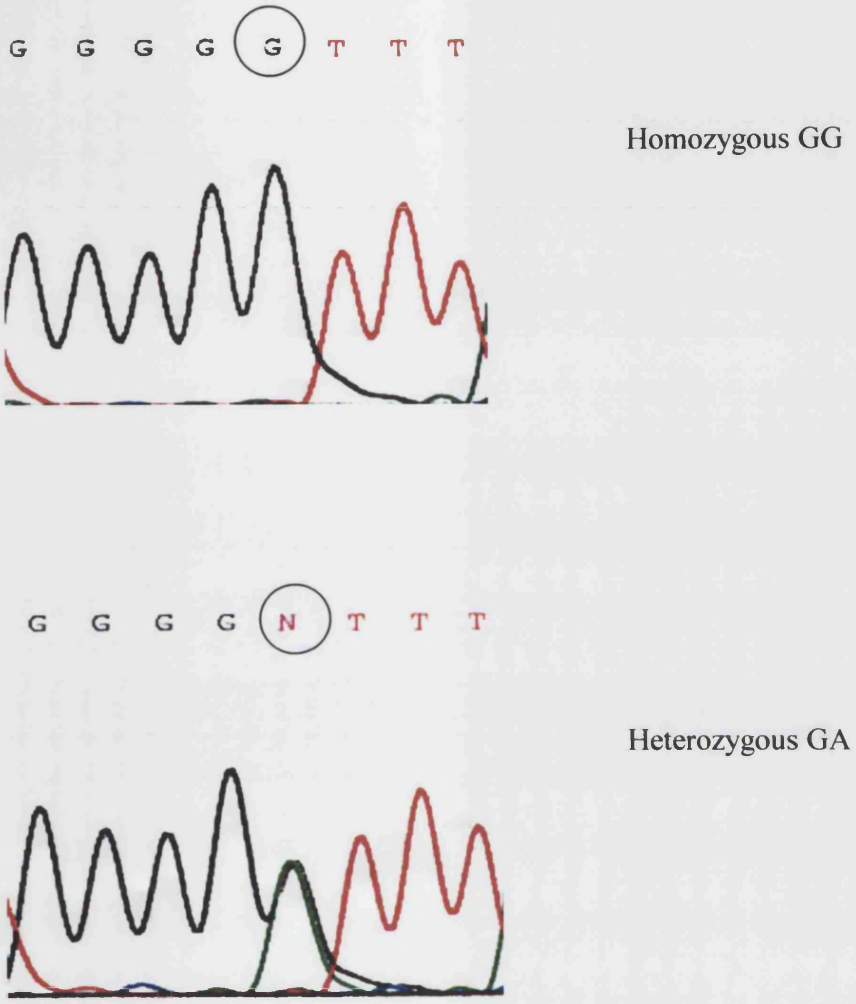

Figure 6.3a. DNA sequence confirming a G→A substitution at position –1415 in *DDAH2* promoter 2 PCR. Each peak is generated by the fluorescence emitted by the dye-terminator nucleotides. Each termination nucleotide is labeled with a different fluorescent dye, which emits light of different wavelengths (A=green. G=black, C=blue, T=red). The upper sequence shows a homozygote for the G allele, the lower sequence a heterozygote for both G and A alleles.

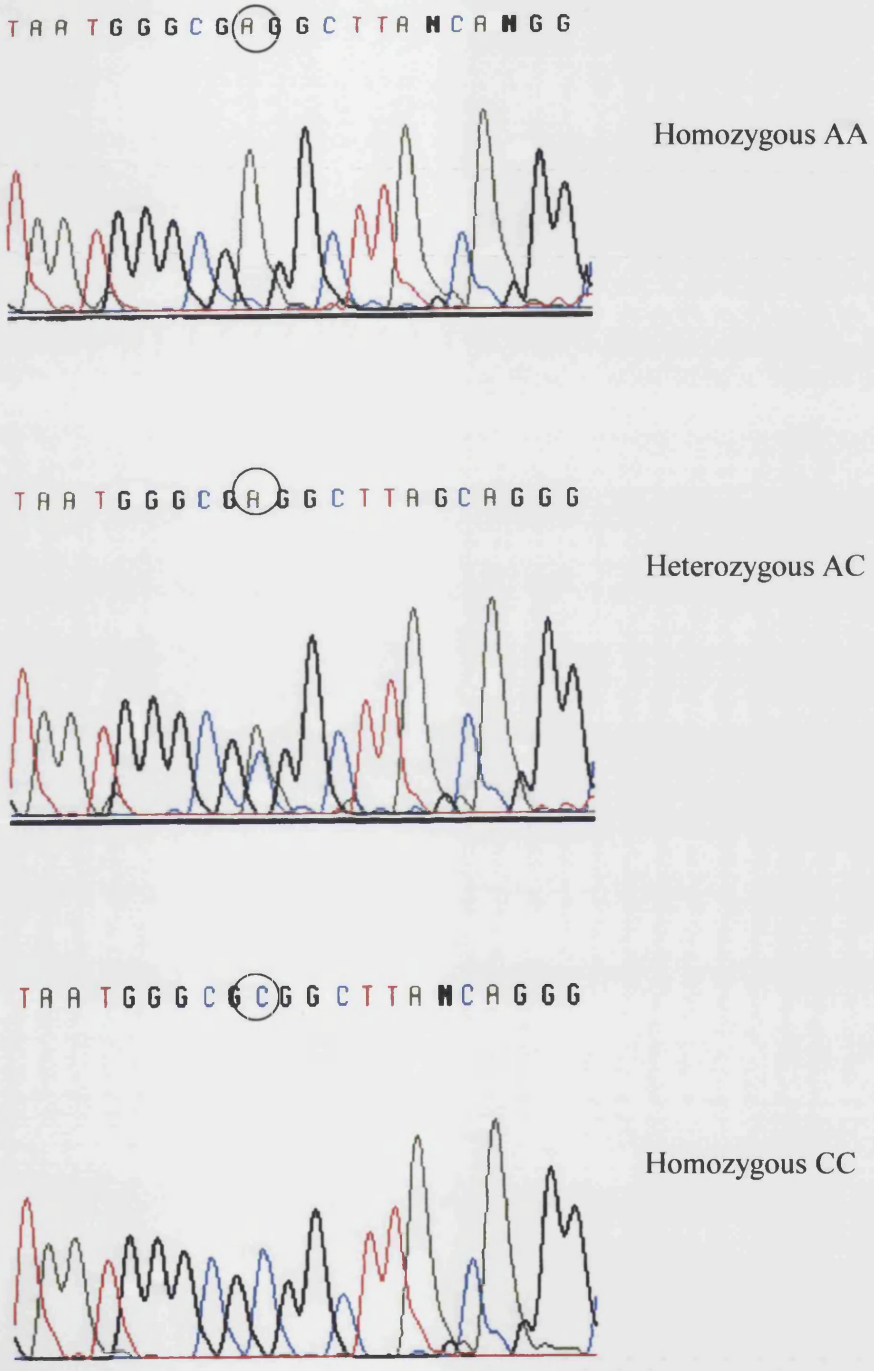

Figure 6.3b. DNA sequence confirming a C→A substitution a position –1151 in the *DDAH2* promoter 3 PCR. The upper sequence shows a homozygote for the A allele, the middle sequence a heterozygote for both A and C alleles, and the lower sequence a homozygote for the C allele. The numbers represent the position of each nucleotide in the PCR product. This sequence variation confirms the presence of a polymorphism as was indicated by SSCP (Figure 6.2a).

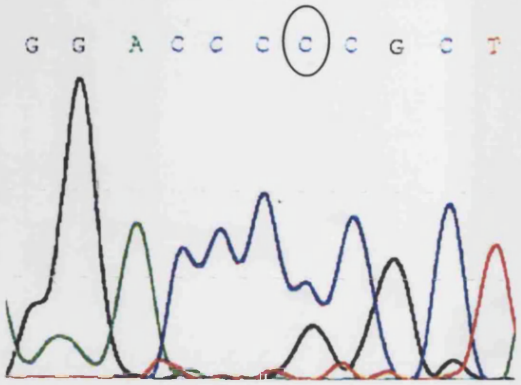

Heterozygous CG

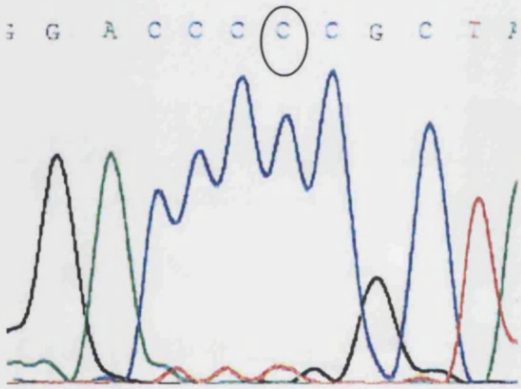

Homozygous CC

Figure 6.3c. DNA sequence confirming a C→G substitution at position –1020 in *DDAH2* exon1. The upper sequence shows a heterozygote for both the C and G alleles, the lower sequence a homozygote for the C allele. No sequence electropherogram was available to illustrate a GG homozygote. This sequence variation confirms the presence of a polymorphism as was indicated by SSCP (Figure 6.2b).

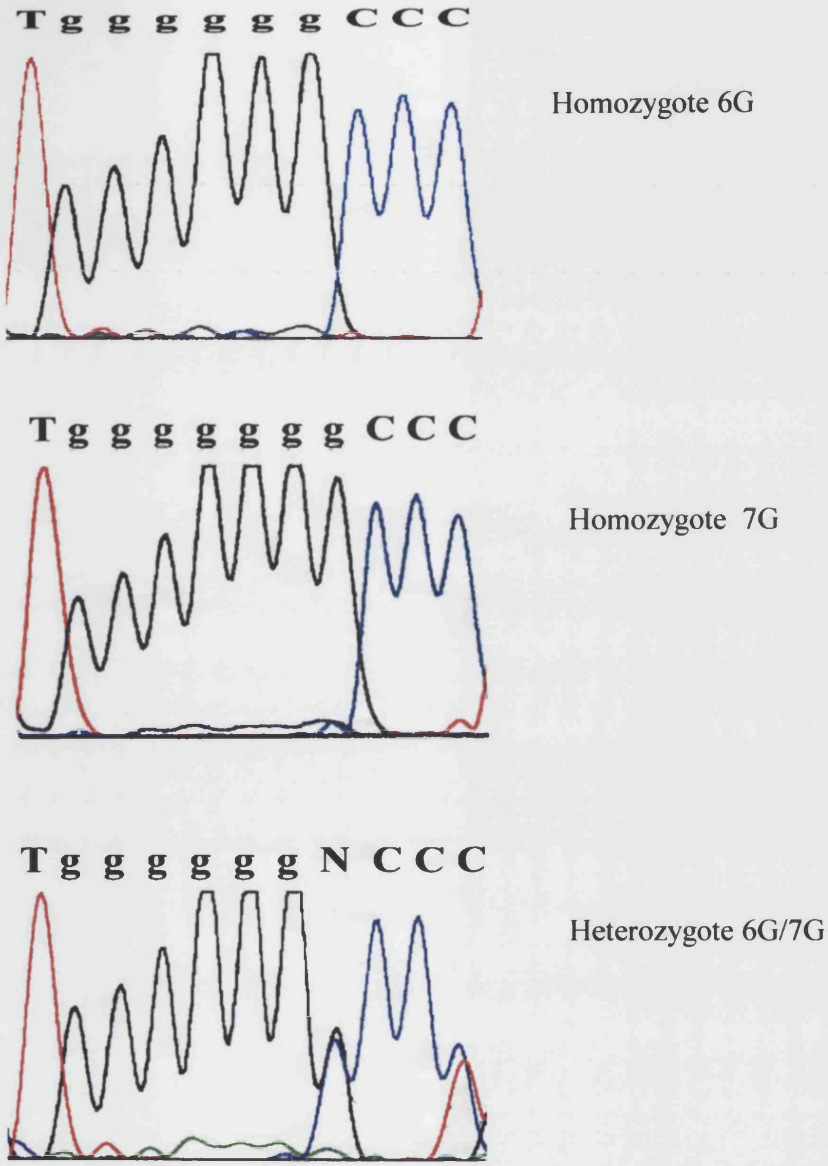

Figure 6.3d. DNA sequence electropherogram confirming the presence of an extra G at position –871 in the *DDAH2* promoter. The upper sequence illustrates a homozygote carrying 6G nucleotides at position –871, the middle sequence shows a homozygote carrying 7G nucleotides, and the lower panel identifies a heterozygote who has both 6G and 7G alleles.

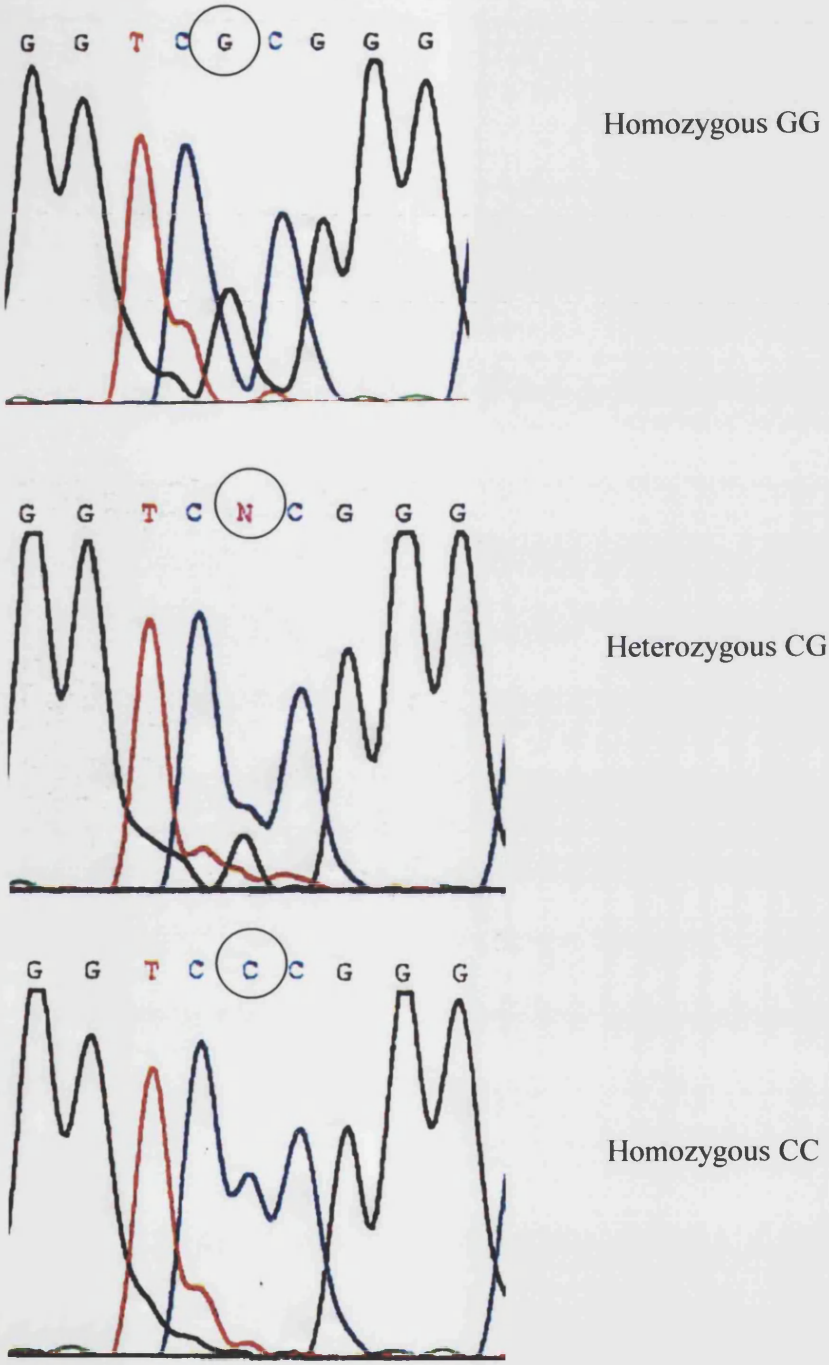

Figure 6.3e. DNA sequence electropherogram confiming the presence of a C→G polymorphism within the *DDAH2* exon2 PCR. The upper sequence shows a homozygote GG, the middle sequence a heterozygote G/C and the lower sequence a homozygote CC. This sequence variation confirms the presence of a polymorphism as was indicated by SSCP (Figure 6.2c).

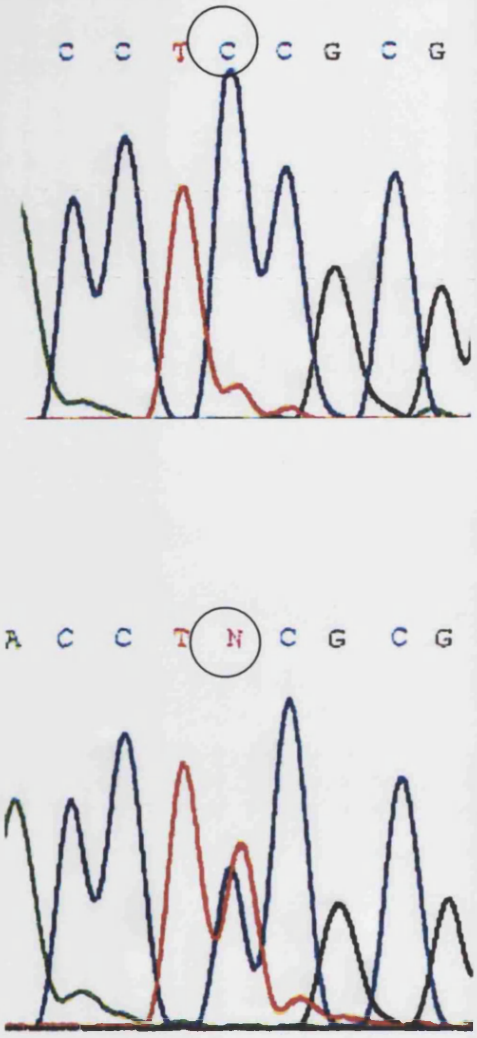

Figure 6.3f. DNA sequence eletropherogram confirming the presence of a C→T polymorphism within the exon 4+5 PCR product. The upper sequence shows illustrates a homozygote for the C allele and the lower sequence a heterozygote for both T and C alleles. No sequence electropherogram was available for a TT homozygote. This sequence variation confirms the presence of a polymorphism as was indicated by SSCP (Figure 6.2d).

6.4.2 Analysis of the *DDAH2* promoter and comparison of polymorphisms in the National Center for Biotechnology Information (NCBI) SNP database with those identified by SSCP.

At the time of writing the NCBI SNP database contained information on 6 polymorphisms in the *DDAH2* gene. The nature of each SNP, identification number and position are shown in table 6.3. All polymorphisms in the SNP database lie upstream of the translation start site and, in line with the current study no polymorphisms were identified in the coding exons or in the 3' region of the gene. The –1415 C/T, -1151 C/A and the –449G/C polymorphisms identified by SSCP during this study were represented in the NCBI SNP database. The average allele frequencies reported for these variants are; -1415 G=90%, A=8%, -1151 A=64%, C=36%. Allele frequency was unavailable for the –449 variant.

NCBI SNP ID	Base change	Position relative to *tsp*
rs2272592	G/A	-1415
rs805304	C/A	-1151
rs453560	G/C	-738
rs3763297	G/C	-728
rs707916	T/C	-620
rs805305	G/C	-449

Table 6.3. Human *DDAH2* promoter polymorphisms identified in the NCBI SNP database. The –1415 C/T, -1151A/C and the –449C/G polymorphisms were also identified by SSCP during this study. No polymorphisms have been identified in the coding exons.

MatInspector analysis of the 1.6kb immediately upstream of the *DDAH2* translation start site revealed two of the polymorphisms identified by SSCP were situated in potential transcription factor binding sites (Figure 6.4). The –1020C/G polymorphism lies with a putative E2F transcription factor binding site (TTTCGCGC), and the –871 6G/7G bi-allelic length variation lies in a region encoding a nerve growth factor induced protein C/ early growth response (NGFIC/Egr-3) binding sequence GCGTGGGGGG and a MYC-associated zinc finger protein related transcription factor site (MAZF).

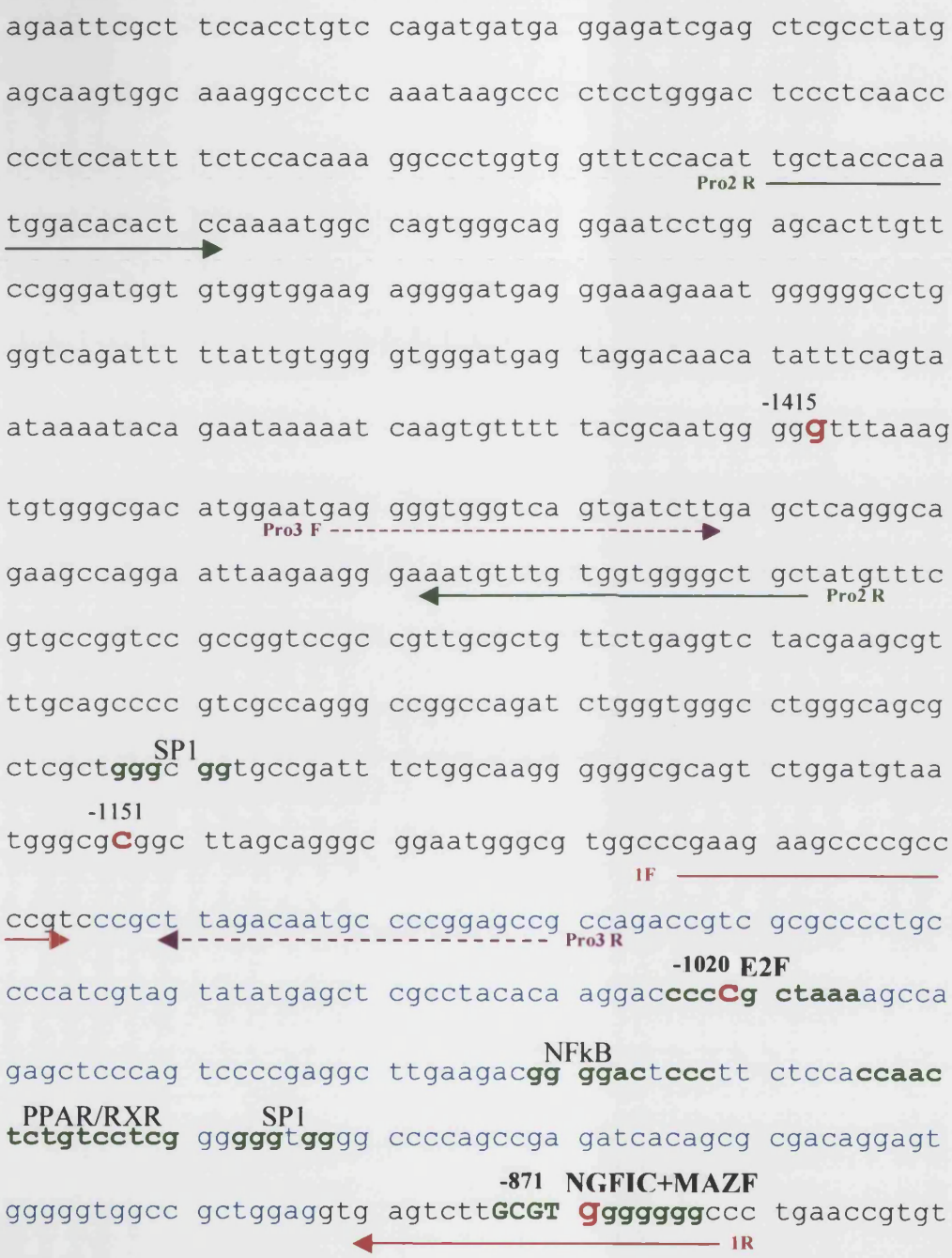

Figure 6.4 continued →

Figure 6.4 DNA sequence of the *DDAH2* 5' untranslated region. Exon sequences are indicated in blue. Oligonucleotide sequences are underlined by arrows. The position of transcription factor binding sites identified by MatInspector are shown in green and polymorphisms are shown in red type and numbered by position relative to the translation start site. The –1020C/G polymorphism lies in an E2F transcription factor binding site and the –871 6G/7G polymorphism lies within a NGFIC/MAZF binding sequence.

6.4.3 Genotype and allele frequencies of *DDAH2* polymorphisms

Gel images representing common homozygotes, heterozygotes and rare homozygotes for the single nucleotide polymorphisms –1151A/C, -1020C/G and –449G/C polymorphisms are shown in figure 6.5. Figure 6.6 shows the electropherogram trace produced by Genescan analysis of the –871 6G/7G insertion/deletion polymorphism. The peaks correspond to PCR products 191bp (6G/6G), 191+192bp (6G/7G) and 192bp (7G/7G).

The genotype and allele frequencies of each polymorphism are shown in table 6.4. Rare allele frequency for the -1151A/C, –1020C/G and –449G/C, polymorphisms in the NPHSII cohort were 0.31, 0.12 and 0.34 respectively. Rare allele frequencies for the –1151A/C, -1020C/G and –871 6G/7G polymorphisms in the German population screen were 0.31, 0.16 and 0.01 respectively. All polymorphisms were in Hardy-Weinberg equilibrium except for the –1020C/G polymorphism in the German population screen (χ^2 =8.6, P=0.003). Table 6.5 shows the linkage disequilibrium coefficients for each polymorphism. The –1151A/C, -1020C/G and –449G/C polymorphisms were in very tight linkage disequilibrium in the NPHSII cohort (P=<0.0001). In the German population screen the –1151A/C and –1020C/G were in tight linkage disequilibrium (*Δ=-0.3, P=0.0008).

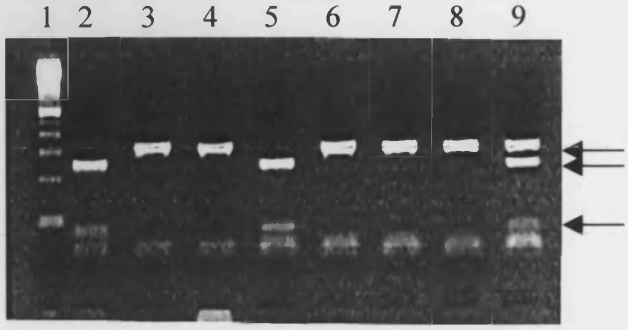

***BstU1* restriction digest of the –1151A/C polymorphism.**
Lane 1 – 100bp ladder.
Lanes 2+5 – CC individuals (283bp and 73bp).
Lane 9 – heterozygote A/C (356bp+283bp+73bp).
Lanes 3,4,6,7,8 – AA individuals (356bp).

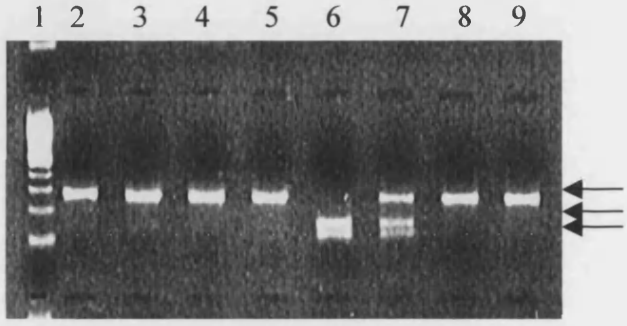

***Mwo1* restriction digest of the –1020C/G polymorphism.**
Lane 1 – 100bp ladder.
Lanes 2-5+8-9 CC individuals (253bp).
Lane 6 – GG individual (144bp+109bp).
Lane 7 – Heterozygote C/G (253bp+144bp+109bp)

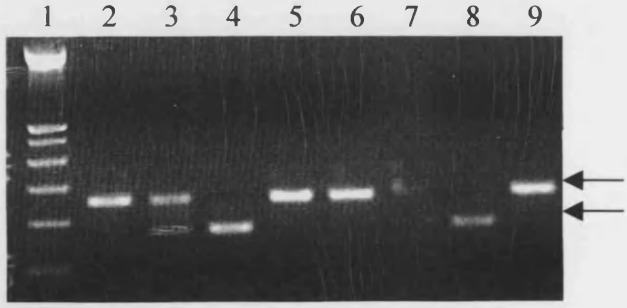

***BstU1* restriction digest of the –449C/G polymorphism.**
Lane 1 – 100bp ladder
Lanes 2, 5, 6+9 CC homozygotes (250bp)
Lane 3 – C/G heterozygote individuals (250bp+204bp+46bp)
Lanes 4+8 – GG homozygous individuals (204bp)

Figure 6.5 Restriction digest gel images. The top panel shows the digest products after restriction of the –1151A/C polymorphisms with the enzyme *BstU1*. The middle panel shows the digest products after restriction of the –1020C/G polymorphism with *Mwo1* and the bottom panel shows the digest products after restriction of the –449G/C polymorphism with *BstU1*. All three genotypes for each polymorphism are represented.

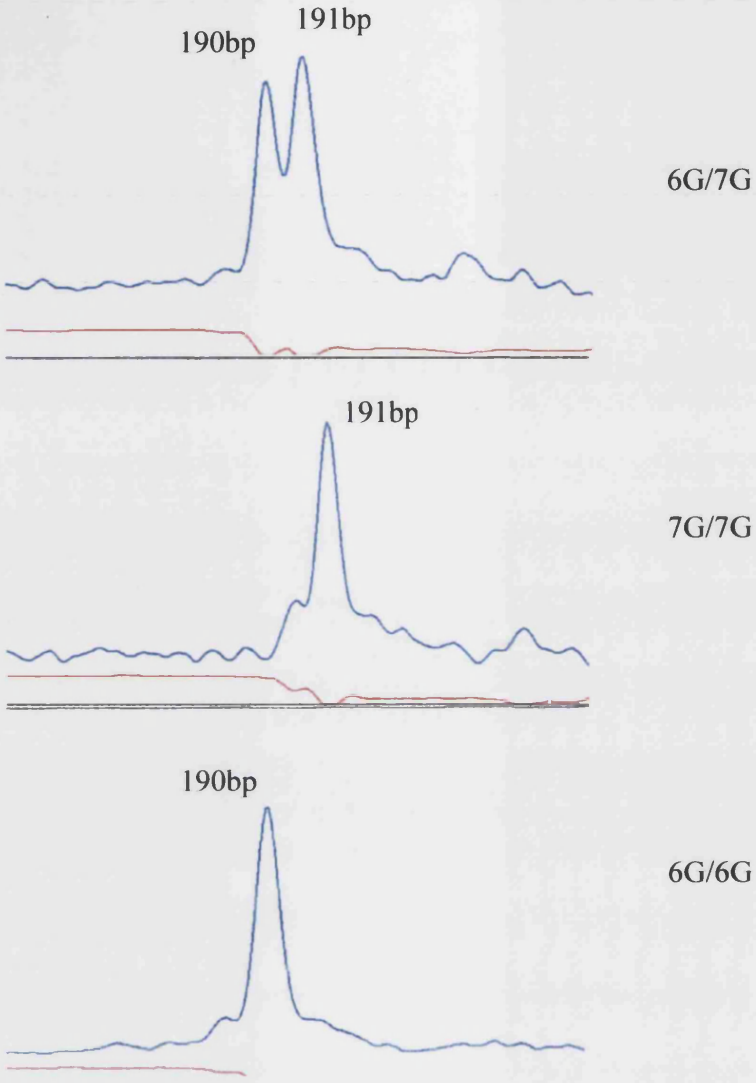

Figure 6.6 Genescan trace produced upon genotyping the *DDAH2* –871 6G/7G bi-allelic length variation. The region encompassing the polymorphism was amplified by PCR using a fluorescent labelled forward oligonucleotide and electrophoresed on an ABI 377 DNA sequencer. Data from 3 individuals is shown. The top trace shows two peaks (190bp+191bp) corresponding to a heterozygous 6G/7G individual. The middle trace shows 1 peak (191bp) corresponding to a homozygous 7G/7G individual and the bottom trace shows 1 peak (190bp) corresponding to a homozygous 6G/6G individual. Peaks were automatically sized by Genotyper software.

NPHSII cohort

Polymorphism	Genotype N	Allele %	χ^2	P
-1151A/C	AA=216 AC=184 CC=44	A=69.0 C=31.0	0.3	0.6
-1020C/G	CC=342 CG=94 GG=7	C=88.0 G=12.0	0.0	0.89
-449G/C	GG=186 GC=184 CC=54	G=66.0 C=34.0	0.6	0.42

German Population Screen

Polymorphism	Genotype N	Allele %	χ^2	P
-1151A/C	AA=64 AC=45 CC=16	A=69.0 C=31.0	3.0	0.08
-1020C/G	CC=94 CG=26 GG=8	C=84.0 G=16.0	8.6	0.003*
-871 6G/7G	6G6G=123 6G7G=3 7G7G=0	G=99.0 C=1.0	0.0	0.89

Table 6.4. Genotype and allele frequencies of *DDAH2* polymorphisms in the NPHSII cohort (top panel) and the German Population Screen cohort (bottom panel). All polymorphisms conformed to the Hardy-Weinberg equilibrium except the –1020C/G polymorphism in the German Population Screen (χ^2=8.6, *P=0.003).

	-1020C/G Δ (P)	-1151A/C Δ (P)
-449G/C	-0.24 (<0.0001)$^{\Psi}$	-0.45 (<0.0001)$^{\Psi}$
-871 6G/7G	-0.05 (0.58)*	0.17 (0.06)*
-1020C/G		-0.30 (0.0008)* -0.54 (<0.0001)$^{\Psi}$

Table 6.5. Pairwise linkage disequilibrium coefficients (Δ) for *DDAH2* polymorphisms. The –1020C/G and –1151A/C polymorphisms were in tight linkage disequilibrium in both the German population screen (*Δ=-0.30, P=0.0008) and NPHSII cohort ($^{\Psi}$Δ=-0.54, P=<0.0001). The –449G/C polymorphism was in tight linkage with both the –1020C/G and the –1151A/C polymorphisms in the NPHSII cohort ($^{\Psi}$P=<0.0001). The –871 6G/7G polymorphism was not in linkage disequilibrium with either the –1020C/G or –1151A/C polymorphisms in the German population screen.

6.5 Discussion

6.5.1 *DDAH2* promoter polymorphisms

Five polymorphisms were identified upstream of the *DDAH2* translation start site during this study in the putative promoter region. The *DDAH2* translation start site is located within exon 3, and therefore the promoter incorporates the non-coding exons 1 and 2. Alternate splicing between exons 1, 2 and 3 generates three transcripts, which have been identified in the EST database. The -1020C/G polymorphism is situated within exon 1. Although this exon is non-coding in terms of protein synthesis, it may act as a promoter for

transcription starting at exons 2 and 3. Alternatively, as the –1020C/G polymorphism changes a nucleotide that will reside in the 5' untranslated region (5'UTR) of the mRNA, it could effect gene expression through mRNA stability and translation efficiency. MatInspector analysis revealed the presence of putative transcription factor binding sites within this region, and the position of the –1020G/C variant falls within an E2F consensus sequence. E2F transcription factor sequences are a common feature within the promoter regions of genes involved in control of the cell cycle. Interaction of the E2F protein with the retinoblastoma (RB) family of proteins (pRb/105, 107, and pRb/p130) determines transcription of E2F regulated genes. VSMCs from atherosclerotic plaques have a higher ratio of the active form of RB compared to the inactive form and show lower level of E2F regulated gene transcription and cell proliferation compared to normal VSMCs. This fits with the observation that plaque VSMCs exhibit slow proliferation, senescence and undergo apoptosis in culture (Gordon et al., 1990; Bennett et al., 1995). E2F regulation of *DDAH2* transcription during VSMC proliferation could be involved in the process of atherosclerotic plaque formation and restenosis (Black et al., 1999; Bennett et al., 1998). Further work is needed to determine if this polymorphism is functional via interaction with E2F.

The four remaining upstream polymorphisms do not lie within exon sequences. The –1415G/A and –1151C/A are situated farthest upstream and are not known to reside within any important regulatory regions. The –871 6G/7G bi-allelic length variant and the –449C/G are located in introns 1 and 2 respectively. Neither polymorphism disrupts an exon/intron boundary sequence, but the –871 6G/7G lies within a nerve growth factor

induced protein C/early growth response (NGFIC/Egr-3) consensus site which overlaps with a MYC-associated zinc finger protein related transcription factor site (MAZF). Genotyping of 128 healthy German subjects revealed a 7G allele frequency of just 1%. Previous investigators have shown that length variations in runs of bases such as Gs may alter the rate of gene transcription. Such genes include the stromelysin and plasminogen activator inhibitor (PAI) genes among others (Terashima et al., 1999; Gardemann et al., 1999). Stromelysin (*MMP3*) is a member of the matrix metalloproteinase enzyme family, which regulates the accumulation of extracellular matrix (Sellers and Murphy, 1981) and has been implicated in connective tissue remodeling during atherogenesis (Ye et al., 1996). A common polymorphism at position –1171 in the *MMP3* promoter, which results in one allele containing a run of 5A nucleotides and the other allele 6A nucleotides, has been shown to alter gene transcription in a promoter/reporter assay (Ye et al., 1996). A common polymorphism in the *PAI1* gene promoter, which results in ether 4 or 5G nucleotides has also been shown to influence gene expression. The 5G allele demonstrated reduced promoter activity, and an additional protein binding site not present in the 4G allele (Dawson et al., 1993). It was subsequently shown that the 4G allele binds only to an activator, whereas the 5G allele binds an activator and an inhibitor protein. The 4G allele has been associated with higher levels of PAI1 and increased risk of vascular disease (Dawson et al., 1993; Rossaak et al., 2000).

The position of the –871 6G/7G polymorphism within a NGFIC/MAZF transcription factor site may have implications for *DDAH2* expression. Nerve growth factor (NGF) mediates a whole host of responses including cell differentiation, cell survival and gene expression.

Recently, studies have shown that NGF activates PRMT1 activity in PC12 cells, consequently leading to the asymmetric methylation of arginine residues in target proteins, which upon metabolism release free ADMA (Cimato et al., 2002). NGF has also been shown to induce *GCH1* and *NOS* expression leading to elevated BH_4 and NO respectively (Anastasiadis et al., 1996; Hirayama et al., 1995; Peunova et al., 1995; Kalisch et al., 2002). Evidence of a role for NGF in the development of atherosclerosis has been put forward by a number of investigators who have observed reduced NGF expression in atherosclerotic coronary arteries and reduced levels of plasma NGF in individuals with congestive heart failure compared to healthy controls (Chaldakov et al., 2001; Kaye et al., 2000). Taken together these observations suggest that NGF might provide co-ordinate regulation of NO synthesis in target cells by concerted modulation of multiple relevant target genes in the NO pathway. Disruption of the NGFIC binding site in the *DDAH2* gene promoter by the –871 6G/7G polymorphism could alter *DDAH2* expression and the breakdown of ADMA in the body, but further research will be needed to test this hypothesis. The transcription factor MAZF has been identified as an important regulator of TATA-less promoters (Parks et al., 1996). In addition to binding its consensus DNA sequence, MAZF also interacts with SP1 to modulate gene transcription (Parks et al., 1996). Genes identified as being regulated by MAZF include *eNOS*, *serotonin 1a receptor*, *c-myc* and *CD4* (Karantzoulis-Fegaras et al., 1999; Parks et al., 1996; Bossone et al., 1992; Duncan et al., 1995). The observation that *eNOS* expression is regulated by MAZF raises the possiblility that this transcription factor is also involved in the control of genes that regulate cell differentiation, survival and in particular NO availability.

6.5.2 Polymorphisms within *DDAH2* coding exons

Only one polymorphism was identified downstream of the translation start site. This variant encodes a C→T substitution at position +618 within intron 4. No obvious consensus sequences for splicing are situated in this region. The absence of any polymorphisms in the coding exons, either suggests this region has remained highly conserved throughout evolution or that SSCP failed to detect all variants present in the samples analysed.

A search of the NCBI SNP database revealed six polymorphisms in the *DDAH2* 5' untranslated region, three of which (–1415 G/A, -1151A/C and the –449C/G) were identified by SSCP during this study. Of the remaining three (rs453560, rs3763297 and rs707916) none are located in consensus sequences for any transcription factor binding sites or other important regulatory sequences. The NCBI SNP database did not contain any polymorphisms downstream of the translation start site, indicating that this region is highly conserved.

In summary, six polymorphisms were identified by SSCP in the *DDAH2* gene. Three of these variants have been described on the NCBI SNP database. Two polymorphisms upstream of the translation start site reside with transcription factor binding sites and may influence *DDAH2* promoter activity. A luciferase promoter/reporter gene assay has been used to investigate the effect of the –1151A/C and –871 6G/7G polymorphisms on *DDAH2* expression, and the results are described in chapter 7.

CHAPTER 7

INFLUENCE OF *DDAH2* POLYMORPHISMS ON PROMOTER FUNCTION

7.1 Aims

To assess the influence of *DDAH2* polymorphisms on *DDAH2* gene expression *in vitro* using a luciferase reporter assay.

7.2 Background

Common genetic variation within the promoters of many genes has been demonstrated to alter gene expression. A polymorphism that resides in the consensus sequence for a transcription factor may modulate the affinity of that factor for its binding site, thereby either enhancing or repressing gene transcription. The identification of several polymorphisms within the *DDAH2* gene promoter (Chapter 6) raises the hypothesis that *DDAH2* expression maybe influenced by common genetic variation at these sites. If so, variation in DDAH2 expression between individuals could have consequences for local or systemic concentrations of ADMA and rates of NO synthesis. Therefore, in theory, individuals with a lower DDAH2 expression would be expected to have elevated levels of ADMA, which would compete with L-arginine for the active site of the NOS enzyme, leading to decreased NO synthesis and, potentially, an increased risk of cardiovascular disease.

The analysis of gene expression by commercially available genetic reporter systems is now a widely used technique. In essence, a promoter of interest is cloned into a vector containing a gene whose protein product can be readily assayed, the construct is transfected into a target cell, and protein expression or activity quantified. Expression or activity of the reporter protein serves as an indirect semi-quantitative index of

promoter function. Basal reporter activity, as well as activity following exposure of cells to chemical or physical signals can be assayed. Several different vector systems are available to clone and study virtually any eukaryotic gene promoter. Examples include plasmids, which can accommodate relatively small pieces of DNA sequence (typically up to ~8kb), cosmids (hybrids between a phage DNA molecule and a bacterial plasmid), which can hold more than 40kb of sequence and yeast expression vectors such as yeast artificial chromosomes (YAC), which are capable of accommodating much larger DNA sequences. Commercial vectors contain a range of genetic elements to facilitate cloning and expression. For example, polylinkers which contain many restriction enzyme sites into which DNA can be inserted, an origin of replication, enhancer and promoter sequences. The critical component of a reporter vector is the presence of genes such as luciferase or chloramphenicol acetyltransferase (CAT) whose expression can be readily quantified by standard techniques. Reporter gene vectors also contain selectable genes such as antibiotic resistance genes. During this study, the plasmid vector pGL3basic (manufactured by Promega) was used to clone the *DDAH2* promoter. This vector comprises 4818bp of circular DNA and harbours a polylinker upstream of the firefly (*Photinus pyralis*) luciferase reporter gene, and the ampicillin resistance gene for easy selection (Figure 7.1).

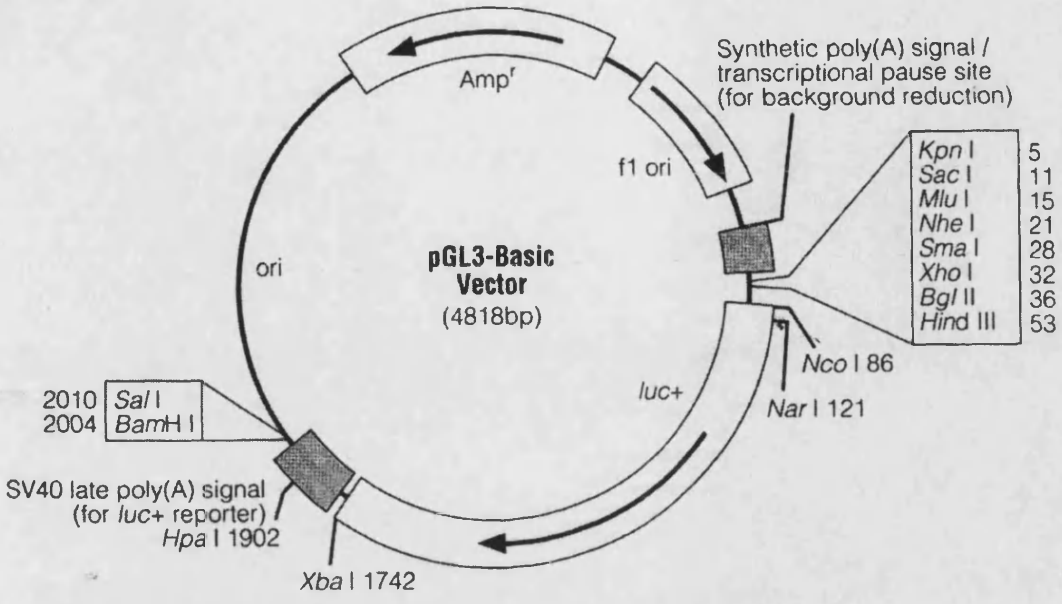

Figure 7.1 Diagrammatic representation of the vector pGL3basic. The circular vector comprises 4818bp of DNA and incorporates the luciferase gene (luc$^+$), ampicillin resistance gene (Amp^r) and a polylinker site into which a promoter sequence can be inserted. *Adapted from Promega-Protocols and Applications Guide, 1996.*

The luciferase reporter assay involves inserting the DNA of interest (in this case the *DDAH2* promoter) into a vector (pGL3basic), upstream of the firefly luciferase reporter gene. The reporter construct is then transfected into a relevant target cell maintained in cell culture. The construct will then be replicated along with the host cell genome, and the luciferase enzyme expressed in proportion to the activity of the promoter of interest. Upon addition of the luciferase substrate (beetle luciferin) the product oxyluciferin is generated together with AMP, PPi, CO_2 and a flash of light (in proportion to the amount of luciferase expressed), which can be quantified in a luminometer (Figure 7.2).

To assess the influence of polymorphisms on *DDAH2* promoter activity, constructs representing all four possible permutations of the –871 6G/7G and –1151A/C variants

(6G/A, 6G/C, 7G/A, 7G/C) were made and expressed in HUVEC. These variants were chosen because the –871 6G/7G polymorphism lies in a transcription factor binding site for NGFIC/MAZF and preliminary genotyping analysis of the –1151A/C variant suggested a possible association with ADMA/SDMA ratio. Primary HUVEC were chosen because DDAH2 is highly expressed in this cell type (Tran et al., 2000) and therefore all the necessary components for transcription of the *DDAH2* gene are available. HUVEC were simultaneously co-transfected with the pRL-SV40 vector (Promoga, Dual-Luciferase Reporter Assay System), which contains the *Renilla* (*Renilla reniformis*) luciferase gene under control of the SV40 promoter. Co-transfection of HUVEC with the *Renilla* luciferase allows correction for variability in transfection efficiency. Due to the different evolutionary origins of the firefly and *Renilla* luciferases, they have dissimilar enzyme structures and substrate requirement, making it possible to discriminate between the bioluminescence reactions (Figure 7.2).

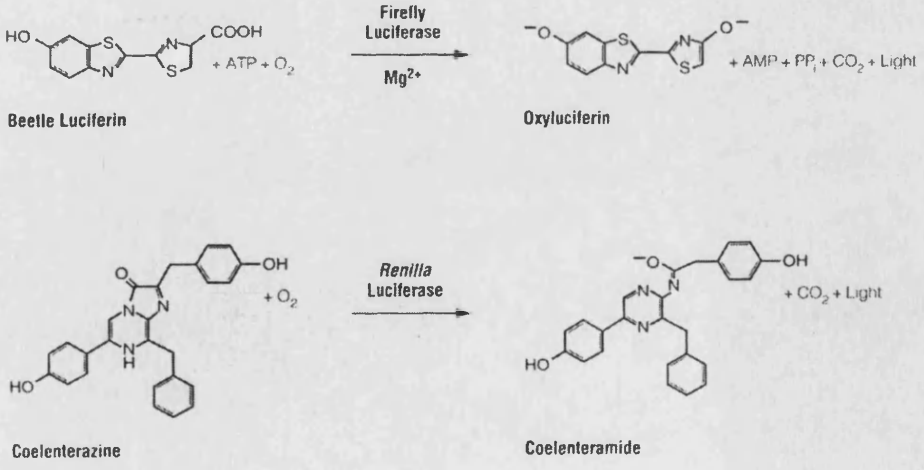

Figure 7.2. Bioluminescent reactions of the firefly and *Renilla* luciferases. The firefly and *renilla* luciferase enzymes have different evolutionary origins and therefore different enzyme structures and substrate requirements. Firefly luciferase catalyses the oxidation of beetle luciferin and renilla luciferase the oxidation of coelenterazine to produce light and CO_2. *Adapted from Promega Technical Manual No. 040.*

A restriction fragment spanning nucleotides –1755 to –216 and incorporating the *DDAH2* promoter has already been shown to direct gene expression in an ECV304 cell line (Achan et al., 2002). Several *at*-RA acid transcription factor-binding sequences (PPAR/RXR) are present within the *DDAH2* promoter, and treatment of transfected ECV304 cells with *at*-RA was shown to enhance *DDAH2* promoter activity by 47% during this study. During the same study treatment of murine endothelioma cells (sEnd.1) with at-RA was shown to increase NO_2^- production without increasing eNOS expression. The authors concluded that increased generation of NO by *at*-RA treatment might be mediated through changes in DDAH2 expression and modulation of ADMA concentrations and eNOS activity.

The *DDAH2* gene has three transcription initiation sites at exons 1, 2 and 3. Alternate splicing between the 3' ends of exons 1 and 2 and an internal site within exon 3 results in 3 possible *DDAH2* transcripts (Tran et al., 2000). The aim of this study therefore, was to identify which splice variants of the *DDAH2* gene are expressed in HUVEC and therefore which sequences might be acting as a promoter in these cells. This study also investigated whether the –871 6G/7G (which lies within a NGFIC and a MAZF consensus sequence) and –1151A/C polymorphisms affect *DDAH2* promoter activity in primary HUVEC. As a positive control, promoter activity in the presence of *at*-RA was also assessed.

7.3 Materials and Methods

7.3.1 Identification of *DDAH2* transcripts in HUVEC

mRNA was isolated form HUVEC and cDNA generated by Dr. Juan Pablo Casas Romero (University College London). mRNA was isolated using the Microfast Track kit (Invitrogen). mRNA was reverse transcribed by RT-PCR in a 20µl reaction volume containing 2µl of mRNA, 150ng of random primers (hexamers), 0.5mM each of dATP, dCTP, dGTP and dTTP, 5x first strand buffer (250mM Tris-HCl [pH8.3], 375mM KCl, 15mM $MgCl_2$), 0.1M dithiothreitol (DTT), 9µl of DEPC H_2O and 200units of superscriptII RNAse H^- (Life Technologies). The reactions were incubated at 42°C for 55 minutes followed by 72°C for 10 minutes.

PCR to amplify exons 1, 2 and 3 was carried out as described in Chapter 2.2.2 using the following oligonucleotides; Exon 1 forward (-1097 to -1076) 5'TTAGACAATGCCCCGGAGCCGC3', Exon 1 reverse (-929 to -908) 5'ATCCTGTCGCGCTGTGATCTC3' (product 190bp), Exon 2 forward (-588 to -568) 5' GAGAGGATGCTTAACTCCTTA3', Exon 2 reverse (-544 to -524) 5'GAACGAGAAGGGAGAGAGGTG3' (product 66bp), Exon 3 forward (-148 to -127) 5'AGACCTGGGCGCTCTTAACCAC3' and Exon 3 reverse (59-80) 5'TCCCCCGACGCGAGGCTCTCTG3' (product 230bp). The annealing temperature for each PCR reaction was 60°C. PCR amplification of the glyceraldehyde-3 phosphate dehydrogenase (GAPDH) housekeeping gene was used as a positive control (forward oligo 5'AAGGTGAAGGTCGGAGTCAACG3', reverse oligo

5'GGCAGAGATGATGACCCTTTTGGC3'). PCR products were electrophoresed on 1% agarose gels and visualised by ethidium bromide staining.

7.3.2 Cloning of human *DDAH2* promoter/reporter constructs containing allelic variants

Promoter/reporter constructs containing allelic variants identified by SSCP at position –871(6G/7G) and –1151(A/C) were generated as shown in figure 7.3. A 1.6kb fragment containing the *DDAH2* promoter was cloned into the vector - pGL3basic by Miss Lucy Tran, University College London (Achan et al., 2002). The region containing the –871 6G/7G and –1151A/C variants was sequenced to identify the genotype of the primary construct. This construct was used as a template for generating allelic variants by site-directed mutagenesis, so that all four possible permutations were represented: - 6G/A, 7G/A, 6G/C and 7G/C. All variants were verified by DNA sequencing.

7.3.2.1 Site-directed mutagenesis

DNA sequencing revealed the *DDAH2* promoter cloned into the vector pGL3basic, contained the 6G variant at position –871 and an A allele at position –1151. Both forward and reverse allele-specific oligonucleotides for site-directed mutagenesis were designed to cover the regions incorporating the –871 7G allele and –1151 C allele (Table 7.1). Two PCR reactions for each variant were carried out using the allele-specific oligonucleotides and the forward and reverse reading vector oligonucleotides RV3 and GL2 (Table 7.1). PCR reactions were carried out in 50µl volumes containing 1µl of pGL3basic vector containing the *DDAH2* promoter, 5µl 10x buffer, dNTPs,

50pmol of each oligonucleotide, 1.5mM $MgCl_2$ and 2 units of Taq Expand (Roche Expand High Fidelity PCR kit). Cycling conditions were 95°C for 5mins followed by 10 cycles of 95°C for 30sec, 60°C for 30sec and 72°C for 2mins and a final extension at 72°C for 10mins. PCR products were electrophoresed on a 1% agarose gel to check products were the expected size and gel extracted using the QIAquick gel extraction kit (Qiagen).

The two PCR products were annealed to give the full *DDAH2* promoter containing the desired allelic variant by 5 cycles of PCR in which oligonucleotides were omitted from the reaction. After 5 cycles 50pmol of the forward and reverse vector oligonucleotides – RV3 and GL2 were added and the reaction continued for a further 20 cycles. PCR products were electrophoresed on a 1% agarose gel to check the expected band size (1.6kb), and sequenced to confirm the desired allele had been incorporated.

Oligonucleotide	**Sequence**
DDAH2 –871 7G	F 5' ttg cgt ggg ggg **g**cc ctg aac 3'
	R 5' gtt cag gg**c** ccc ccc acg caa 5'
DDAH2 –1151 C	F 5' taa tgg gcg **c**gg ctt agc agg 3'
	R 5' cct gct aag cc**g** cgc cca tta 3'
pGL3 basic vector RV3	F 5' cta gca aaa tag gct gtc cc 3'
pGL3 basic vector GL2	R 5' ctt tat gtt ttt ggc gtc ttc c 3'

Table 7.1 Allele-specific and vector oligonucleotides used for site directed mutagenesis to generate *DDAH2* promoter constructs. Mismatched bases are highlighted in bold.

7.3.2.2 TOPO TA cloning of allele-specific PCR products

Allele-specific PCR products were initially TA cloned using the TOPO TA cloning kit. (Invitrogen). 2μl of PCR product was TA cloned into TOPO vector by incubating at room temperature for 5 minutes. 2μl of the cloning reaction was then added to a vial of One Shot chemically competent *E.coli* cells and incubated on ice for 30 minutes. Cells were then heat-shocked for 30 seconds at 42°C to facilitate uptake of DNA. 250μl of SOC medium (containing 2% tryptone, 0.5% yeast extract, $NaCl_2$, KCl_2, $MgCl_2$, $MgSO_4$, and glucose) was added to the reaction and the cells incubated at 37°C for 1 hour. 100μl of cells was then spread onto agar plates containing the β-galactosidase substrate-X-gal (5-bromo-4-chloro-indolyl-β-D-galactosidase) and incubated overnight at 37°C. Insertion of the PCR product into the TOPO cloning vector disrupts the β-galactosidase (*lacZ*) gene and renders the cell unable to metabolise X-gal resulting in white colonies on agar/xgal plates. Non-transformed cells produce blue colonies on agar/X-gal plates. White colonies were picked and grown overnight in 3ml of LB media containing 0.1mg/ml Ampicillin. The plasmid DNA was isolated using the Qiagen DNA miniprep kit.

7.3.2.3 Cloning allele-specific constructs into pGL3basic vector

The TOPO vector containing the *DDAH2* promoter allele-specific PCR was digested with *HindIII* to excise the *DDAH2* promoter sequence and electrophoresed on a 1% agarose gel. The 1.6kb product was then gel purified using the QIAquick gel extraction kit (Qiagen). The purified 1.6kb product was ligated into *HindIII* digested pGL3basic vector in a 10μl reaction containing 1μl *HindIII* digested pGL3basic vector, 2μl of the

1.6kb product, 2µl T4 DNA ligase buffer (Gibco) and 1µl T4 DNA ligase (Gibco). The reaction was incubated at 4°C overnight.

7.3.2.4 Transformation of DH5α competent cells

Subcloning efficiency DH5α competent cells were purchase form Invitrogen, UK. 10µl of ligation reaction was added to 100µl of cells and incubated on ice for 30 minutes. The cells were then heat-shocked at 37°C for 45 seconds and placed immediately on ice for 2 minutes. 950µl of SOC media was added to the cells and incubated while shaking at 37°C for 1 hour. The cells were pelleted by centrifugation and 900µl of spent media removed. The cells were re-suspended in the remaining media and 100µl spread onto agar/X-gal plates. Plates were incubated overnight at 37°C. White colonies were picked, grown in 3ml of LB media and the plasmid isolated using the Qiagen DNA miniprep kit. To identify colonies containing the *DDAH2* promoter and the orientation of the insert, samples were digested with restriction enzymes *HindIII* and *NarI* respectively.

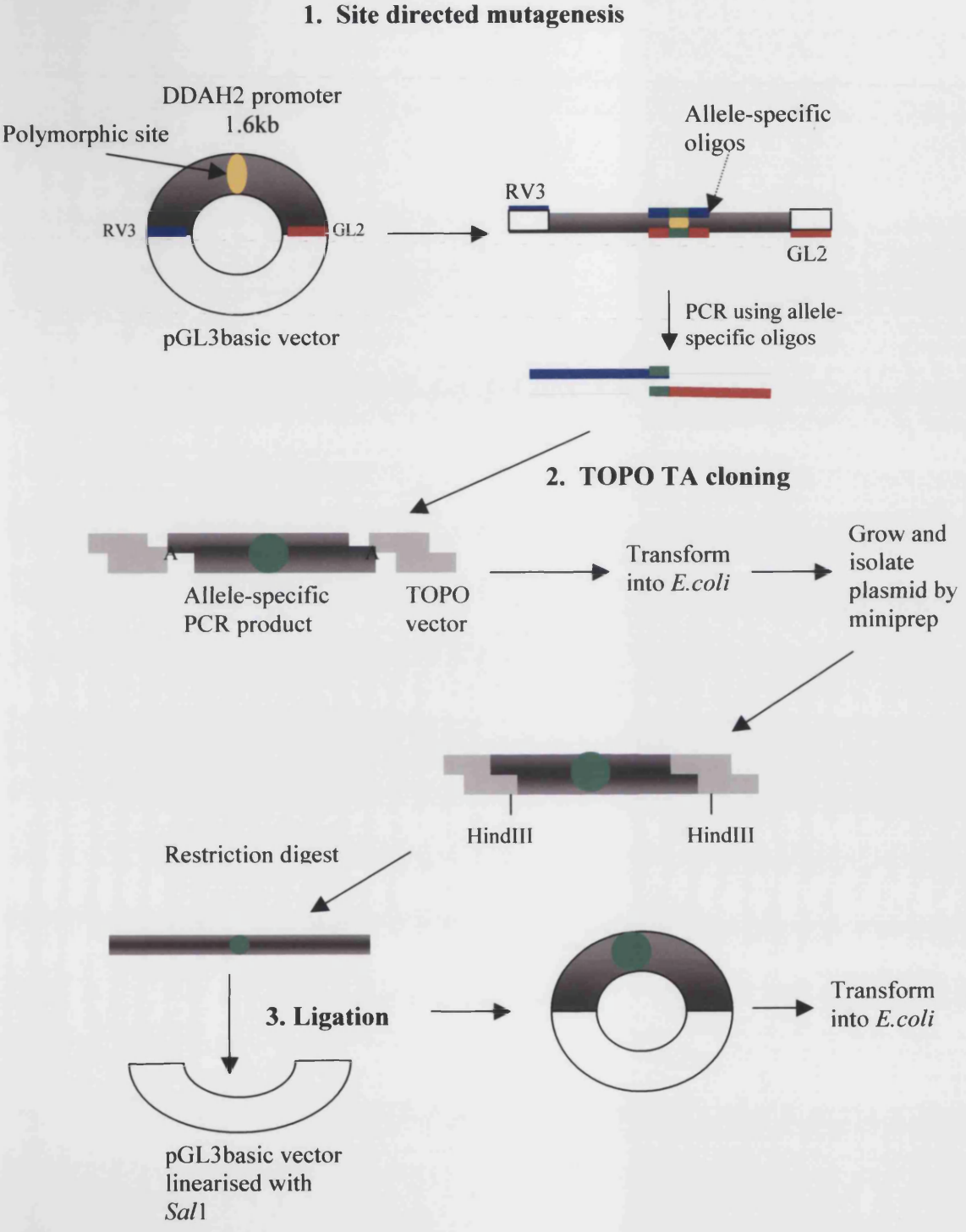

Figure 7.3. A diagramatic representation of the steps involved in cloning *DDAH2* promoter/reporter constructs containing allelic variants. Step 1. Incorporation of the desired allele (represented in green) into the *DDAH2* promoter sequence (shown in grey) by two rounds of PCR (site-directed mutagenesis). Step 2. Cloning the allele-specific PCR product into the TOPO vector, transformation of *E.coli* and harvesting the recombinant plasmid. Step 3. Ligation of the new *DDAH2* promoter into pGL3basic vector for luciferase assay.

7.3.3 Luciferase reporter gene assay

7.3.3.1 Cell culture and transfection

HUVEC were purchased form Promocell (Germany) and cultured prior to transfection as described in Chapter 2. Transfection of HUVEC with the promoter/reporter constructs and *renilla* expression vector (to control for transfection efficiency) was carried out in 12 well culture plates as described in Chapter 2. Briefly, transfection of HUVEC was mediated by incubating the cells with lipofectin reagent (Invitrogen) in serum free media (Optimem 1) for four hours, after which the transfection reagent was removed and replace with endothelial cell growth media (EGM). For each experiment transfections were performed in triplicate for each construct and luciferase activity was normalised to *renilla* activity. A total of 7 independent experiments were conducted for each construct. To test the effect of *at*-RA on promoter activity, HUVEC were treated for 24 hours with 10μmol/L atRA 24 hours after transfection.

7.3.3.2 Cell lysis and luciferase assay

Cell lysis and luciferase measurements were performed using the dual light luciferase reporter assay kit (Promega, Madison, USA) as described in Chapter 2.2.11.2.

7.3.3.3 Statistical analysis

Transformations were performed in triplicate and the average reading taken after correction for transfection efficiency. Promoter activity between constructs was

analysed by One-way ANOVA and Students t-test where appropriate. Results are presented as relative activity measured by the amount of light generated by activation of luciferase, which is proportional to promoter activity.

7.4 Results

7.4.1 Identification of *DDAH2* transcripts in HUVEC

PCR bands corresponding to exons 2 and 3 were amplified from HUVEC cDNA (Figure 7.4). No PCR band was observed corresponding to exon 1. This data indicates that transcription of the *DDAH2* gene in HUVEC begins at exon 2 and the sequence residing upstream of exon 2 could potentially function as a promoter. This region incorporates four of the polymorphisms identified by SSCP (Chapter 6) including the –871 6G/7G and the –1151A/C polymorphisms.

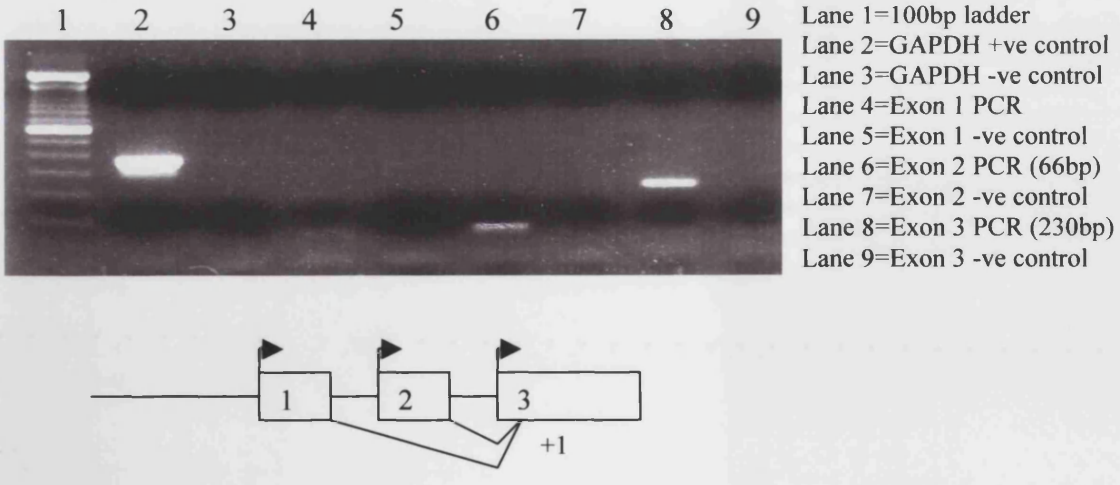

Figure 7.4 *DDAH2* transcripts identified in HUVEC. PCR bands corresponding to exons 2 and 3 were amplified from HUVEC cDNA by PCR, indicating that transcription starts at exon 2. No band was amplified corresponding to exon 1 (top panel). The bottom panel illustrates alternate slicing between the 3' ends of exons 1 and 2 and an internal site in exon 3 of the *DDAH2* gene. Three transcription start sites are indicated by arrows.

7.4.2 Effect of *DDAH2* polymorphisms on promoter activity

Reporter gene constructs representing the four possible permutations for the –1151A/C and –871 6G/7G polymorphisms were transfected into HUVEC and assayed for luciferase activity. A significant difference in promoter activity was observed between the four DDAH2 constructs with the highest activity being seen with the 7G/C construct and the lowest activity with the 6G/A construct (*P=0.01 one-way ANOVA, Figure 7.5). Both constructs containing the 7G variant had greater activity than their 6G counterparts (*P=0.001, figure 7.6). The 7G allele enhanced promoter activity to a greater degree in the presence of a –1151C allele (mean difference between 6G/A and 7G/A was 0.63, and between 6G/C and 7G/C was 1.42, P=0.33). Treatment with *at*-RA increased promoter activity in all constructs by at least 48% (Figure 7.7). The largest increase was seen for the 6G/C variant (179%). Increased activity of the 7G/C construct in response to *at*-RA indicates that the higher basal expression demonstrated by this construct can be increased still further by transcriptional regulators.

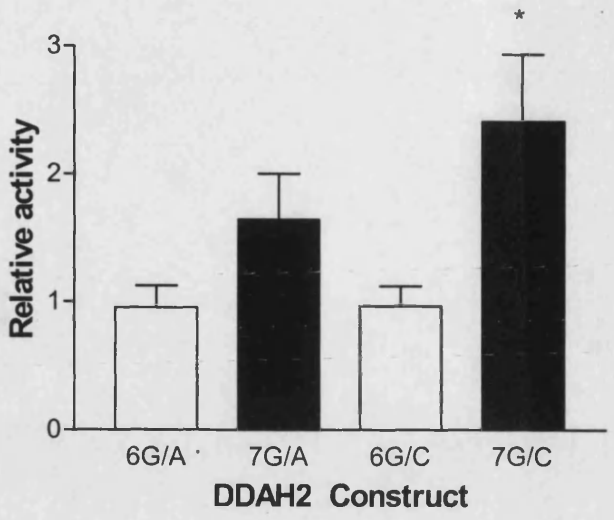

Figure 7.5 Effect of different promoter variants on DDAH2 expression. Mean luciferase activity generated by the 4 DDAH2 constructs representing the –1151A/C and –871 6G/7G polymorphisms transfected into HUVEC cells. The construct representing 7G at position –871 and C at position –1151 of the *DDAH2* promoter demonstrated the greatest promoter activity (*P=0.01 for 7G/C compared to 6G/A by One-Way ANOVA). n=7

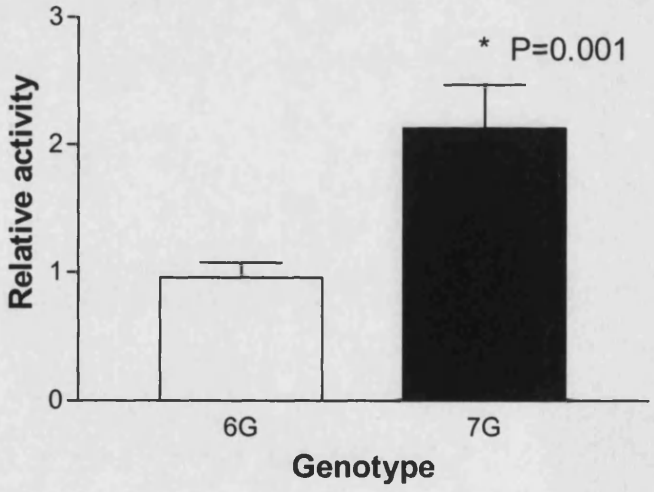

Figure 7.6 Promoter activity of 6G constructs compared to 7G constructs. Mean luciferase activity was combined for the two 6G constructs and compared with luciferase activity for the combined 7G constructs transfected into HUVEC. Mean luciferase activity for the 7G constructs was significantly greater than the 6G constructs (*P=0.001 by Students t-test).

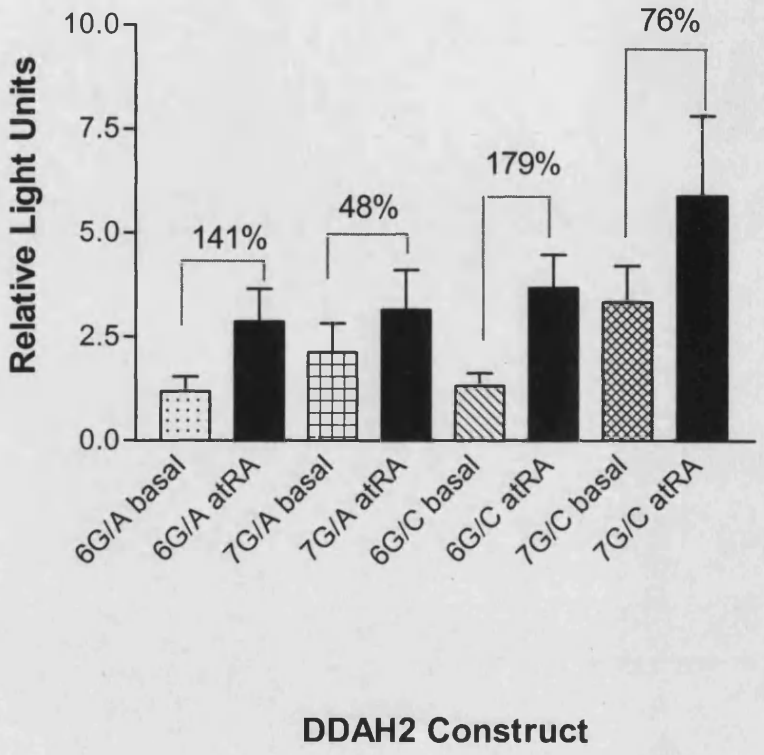

Figure 7.7 Effect of *at*-RA treatment on *DDAH2* promoter activity. To test if *at*-RA had any effect on *DDAH2* promoter activity and to ascertain if this was influenced by promoter genotype, HUVEC were treated 24 hours post transfection with 10μmol/L *at*-RA for 24 hours. *at*-RA increased *DDAH2* promoter activity of all constructs by at least 48% (P=>0.05 for each construct).

7.5 Discussion

SSCP analysis of the *DDAH2* promoter identified several polymorphisms of potential interest (Chapter 6). RT-PCR of mRNA isolated from HUVEC revealed that exons 2 and 3, but not exon 1 were expressed in this cell type and therefore the sequence upstream of exon 2 could act as a promoter. Two polymorphisms situated upstream of exon 2 were chosen for further investigation for potential effect on promoter activity using a luciferase promoter/reporter assay in HUVEC. The –871 6G/7G variant was chosen because of its location within a putative NGFIC/MAZF transcription factor binding sequence and because it is located in the core promoter sequence identified by site specific deletion analysis (Jones et al., 2003). The –1151A/C variant was chosen because the results of preliminary genotyping analysis indicated this variant might be associated with plasma ADMA/SDMA concentration (see Chapter 8). To determine if either of these variants influenced promoter activity, promoter/reporter constructs representing all four possible permutations of the –1151A/C and –871 6G/7G polymorphisms in the *DDAH2* promoter (linked to the luciferase reporter gene) were made and expressed in HUVEC.

Based on the promoter/reporter gene assay, at least one of these polymorphisms was identified as being of potential interest as a functional variant. A genotype specific difference was observed in promoter activity between the four constructs, with the construct containing 7G at position –871 showing highest promoter activity. Indeed, in HUVEC, constructs carrying the 7G variant showed a 2-fold increase in activity compared to constructs with the 6G variant at this position. Although the 7G variant appeared to increase promoter activity, in all constructs, the size of the effect was

contingent on the allele at the –1151 locus. The 7G allele enhanced promoter activity to a greater degree in the presence of a C allele at position –1151. This observation suggests that –1151 genotype might modulate the effect of the –871 genotype. Furthermore, the 6G/7G polymorphism lies in a region defined as a basal promoter element on the basis that the region from –927 to –216 (relative to the translation start site) supports transcription at the same level as the full length promoter in ECV304 cells. It is possible that binding of the transcription factor NGFIC or MAZF may be either up or down regulated due to the presence of an extra G allele at position –871, resulting in variation of DDAH2 expression. NGF has been shown to influence the expression or activity of several genes involved in the regulation NO synthesis such as *PRMT*, *GCH1* and *eNOS* (Cimato et al., 2002; Anastasiadis et al., 1996; Hirayama et al., 1995; Peunova et al., 1995; Kalisch et al., 2002). NGF exerts its effects by binding two distinct receptors on the cell surface, the high affinity $trkA^{NGFR}$ receptor and the low affinity $p75^{NTR}$ receptor. It is thought that the $trkA^{NGFR}$ receptor mediates cell proliferation and differentiation while the $p75^{NTR}$ receptor is thought to mediate apoptosis in some cell types (Barker, 1998; Lopez-Sanchez et al., 2002). Binding of NGF to the $trkA^{NGFR}$ receptor causes activation of the receptor tyrosine kinase and downstream signalling cascades, resulting in mobilisation of transcription factors such as NGFIC/Egr-3. Recent research has shown that HUVEC express both the $trkA^{NGFR}$ and $p75^{NTR}$ receptors, and also significant levels of NGF protein and mRNA under standard culture conditions that are up-regulated during serum starvation (Cantarella et al., 2002). NGF promotes HUVEC proliferation and exerts a potent angiogenic effect *in-vivo* possibly through regulation of NO synthesis (Cantarella et al., 2002). The transcription factor MAZF has been shown to interact with the human *eNOS* promoter and exhibits a negative effect on *eNOS* promoter activity in Drosophila Schneider cells

(Karantzoulis-Fegaras et al., 1999). Further studies to investigate the possible role of these transcription factors on DDAH2 expression are now required.

At-RA was capable of inducing the *DDAH2* promoter activity of all four constructs in HUVEC including the 7G variants, indicating that although the 7G increased basal expression, these constructs retained the ability to increase activity in response to *at*-RA. Upregulation of expression in response to *at*-RA in HUVEC is in agreement with the findings in the ECV304 cell line reported by Achan et al., 2002, and served as a useful positive control for the integrity of the assay system. *At*-RA is known to be an important mediator in the development of the cardiovascular system and may exert its effects by upregulating genes involved in maintaining sufficient NO production. Although it is likely that this regulation is likely to operate through transcription factor binding distinct from the –1151A/C and –871 6G/7G sites studied here, the observation that the magnitude of the *at*-RA response differed by –1151 and –871 genotype suggests that these sites may modulate transcription regulated primarily through the PPAR/RXR sites, in particular the PPAR/RXR site at position –927.

In summary, the presence of an extra G allele at position –871 within the *DDAH2* promoter is associated with increased basal DDAH2 expression and might be expected to confer protection against the harmful effects of elevated ADMA generation. Further analysis to determine if the increased *DDAH2* promoter activity of the 7G variant at position -871 is relevant to *in vivo* concentrations of ADMA is needed. Genotyping cohorts of individuals and comparing their circulating ADMA and SDMA levels is one possible way to achieve this, and the results of such investigation are presented in Chapter 8.

CHAPTER 8

DDAH2 POLYMORPHISMS AND CIRCULATING METHYLARGININE CONCENTRATION

8.1 Aims

To investigate the association between *DDAH2* polymorphisms and plasma concentrations of ADMA, SDMA and the ADMA/SDMA ratio.

8.2 Background

Synthesis of NO can be inhibited by the endogenous methylarginine ADMA. Vallance et al., 1992, were the first to describe elevated plasma ADMA concentrations in patients with renal failure, and proposed that impaired renal excretory function would result in accumulation of ADMA which, in sufficient concentrations, would inhibit the synthesis of NO and lead to endothelial dysfunction. They proposed that this might account for the increased susceptibility to CVD among such patients (Vallance et al., 1992). Recent studies have shown that ADMA concentration in patients with renal failure is predictive of future CVD (Zoccali et al., 2001), and that dialysis, which significantly reduces serum ADMA levels, is associated with improved endothelial function (Cross et al., 2001). One potential explanation for higher ADMA concentrations in renal failure is reduced excretion of ADMA by the kidneys. However, in contrast to SDMA, which is exclusively eliminated by renal excretion, ADMA is also metabolised by the enzymes DDAH1 and DDAH2. Indeed, increases in SDMA concentration in renal failure are greater than the increase in ADMA concentration suggesting that metabolism of ADMA persists. However, since DDAH2 is expressed in the kidney (Tran et al., 2000), it is conceivable that the elevated ADMA concentration seen in patients with renal failure reflects both decreased elimination and reduced metabolism. It is possible that inter-individual differences in the expression or activity of the DDAH enzymes (DDAH1 and

DDAH2) could influence ADMA levels not only in renal failure but also in patients with disorders such as diabetes, preeclampsia, hypertension and hypercholesterolemia where ADMA levels are high but renal function is normal (Stuhlinger et al., 2002; Pettersson et al., 1998; Boger et al., 1997; Surdacki et al., 1999; Boger et al., 1998b). Both ADMA and SDMA are generated upon metabolism of methylated proteins, and both are excreted via the kidneys. However, ADMA but not SDMA is additionally metabolised by the DDAH enzymes and therefore the ADMA/SDMA ratio may be used as an index of DDAH activity.

The DDAH2 isoform is highly expressed in endothelium and is thought to play an important role in regulating ADMA levels and endothelium-derived NO synthesis in the vasculature. Thus variation in DDAH2 expression or activity maybe an important mechanism underlying variation in ADMA concentrations, either locally within endothelial cells or systemically. The aim of the studies in the present chapter was to determine whether the novel common polymorphisms in the *DDAH2* gene identified as part of this thesis (Chapter 6), and which were associated with differences in promoter activity relate to differences in ADMA concentration or ADMA/SDMA ratio in healthy subjects and in individuals with renal failure.

8.3 Subjects and Methods

8.3.1 Subjects investigated for association between *DDAH2* polymorphisms and ADMA, SDMA and ADMA/SDMA ratio.

Three subject groups with differing and complementary phenotypic measurements were analysed for association between *DDAH2* polymorphisms and plasma ADMA and SDMA concentration and ADMA/SDMA ratio as well as other relevant cardiovascular disease phenotypes or risk factors. Table 8.1 summarises the cohorts and their phenotypic characteristics. Full demographic characteristics of each study cohort are outlined in Chapter 2.

Healthy subjects (German population screen)

Blood was collected from a cohort of 128 healthy individuals from a German population screen (Chapter 2.2.12.1) and genotyped for the –1020C/G, -1151A/C and the –871 6G/7G *DDAH2* polymorphisms. ADMA and SDMA measurements were made using HPLC by Professor Rainer Boger (Department of Clinical Pharmacology, University of Hamburg). Measurements of age, height, weight, blood pressure, heart rate, triglycerides and cholesterol were recorded and entered into an Excel database.

Renal failure patients (London Renal Failure cohort)

A cohort of individuals comprising 126 patients with renal failure (London Renal Failure cohort) of varying ethnicity (recruited from the Middlesex Hospital, London by Dr. Jenny Cross) were also genotyped for the –1020C/G, -1151A/C and the –871 6G/7G *DDAH2* polymorphisms (Chapter 2.2.12.2). Endothelial function was assessed *in vivo*

by FMD measurement of the conduit artery in a subset of these patients, and ADMA and SDMA measurements were made by HPLC.

Renal failure patients (CREED)

DNA from 277 renal failure patients was kindly donated by Dr Carmine Zoccali (IBIM-CNR, Italy) for association studies between *DDAH2* genotype and plasma ADMA and SDMA concentrations and ADMA/SDMA ratio (Chapter 2.2.12.2). Subjects were originally recruited for the CREED (Cardiovascular Risk Extended Evaluation in Dialysis) study, in which a total of 278 dialysis patients were followed up over a four year period and in whom baseline ADMA concentrations have been found to be predictive of later CVD (Malatino et al., 1999).

		Phenotypes		Genotypes		
Cohort	**Description of Cohort**	**Conventional CV risk factors**	**ADMA/SDMA**	**Polymorphism**		
				-1020 C/G	**-1151 C/A**	**-871 6G/7G**
HEALTHY						
Healthy subjects (German)	128 healthy subjects	+	+	+	+	+
DISEASE						
Renal failure (London)	126 renal failure patients	+	+	+	+	+
Renal failure (CREED)	277 renal failure patients	+	+		+	+

Table 8.1 Summary of cohorts genotyped for association between *DDAH2* polymorphisms and various risk factors for CVD. Risk factors and polymorphisms analysed for each cohort are indicated by +.

8.3.2 Genotyping *DDAH2* polymorphisms

Three out of the six *DDAH2* polymorphisms identified by SSCP in chapter 6 were chosen for genotyping studies. The -1020C/G and -1151A/C were genotyped by PCR-RFLP analysis (Chapter 6.3.7). The –871 6G/7G bi-allelic length variation polymorphism was genotyped by Genescan analysis (Chapter 6.3.7).

8.3.3 Measurement of plasma ADMA and SDMA by HPLC analysis

Plasma concentrations of ADMA and SDMA were measured by HPLC. ADMA and SDMA concentrations in the London renal failure subjects were measured in our laboratory by Miss Rachel Jackson using the method described by Vallance et al., 1992. Briefly, venous blood samples were centrifuged at 3000rpm for 15 minutes at 4°C to separate plasma. 1ml of plasma was loaded onto a 2ml Bondelut SCX column (Anachem) previously washed with ddH_2O and HPLC grade methanol. Methylarginines were serially eluted in 25% ammonia/methanol and the 50% ammonia/methanol eluate evaporated at 100°C. The dried extract was resuspended in 2ml ddH_2O and applied to a washed Bondelut CBA column. Methylarginines were again eluted using 10% ammonia/methanol and the eluate dried at 100°C and then resuspended in 100µl ddH_2O. Each sample was spiked with a known quantity of L-NMMA, which acted as an internal standard and allowed calculation of extraction efficiency. The extracted samples were applied to a C18 HPLC column (BDH). 40µl of the 100µl sample was injected into the column and the absorbance read at 200nm.

8.3.4 Statistical Analysis

Observed numbers of each genotype were compared with those expected under the assumption of Hardy-Weinberg equilibrium by χ^2analysis. Allele frequencies were deduced from genotype frequencies. Values are represented as median (inter-quartile range) for skewed distributions and mean (standard deviation) for normally distributed data. Allelic associations were assessed using parametric (One-Way Analysis of Variance or Students t test) and non-parametric (Kruskal-Wallis test or Mann-Whitney test) where appropriate.

8.4 Results

8.4.1 Genotype and allele frequencies of *DDAH2* polymorphisms in study cohorts.

The allele frequencies for the -1020C/G, -1151A/C and the –871 6G/7G polymorphisms for each cohort are shown in table 8.2. Genotype frequencies did not differ from those expected under Hardy-Weinberg equilibrium except for the –1020C/G polymorphism in the German population screen (*P=0.003, table 8.2) and the –1151A/C polymorphism in the renal failure cohort (*P=0.04, table 8.2). The –1151A/C polymorphism was in Hardy-Weinberg equilibrium in the London renal failure cohort only after adjustment for race.

	-1020C/G C (%) G (%) χ^2 (P)	**-1151A/C** A (%) C (%) χ^2 (P)	**-871 6G/7G** 6G (%) 7G (%) χ^2 (P)
German Population screen	84.0 16.0 **8.6 (0.003)***	69.0 31.0 **3.0 (0.08)**	99.0 1.00 **0.0 (0.89)**
Renal Failure (London)	96.0 4.00 **3.5 (0.06)**	51.0 49.0 **4.1 (0.04)***	95.0 5.00 **0.4 (0.5)**
Renal Failure (CREED)	-	69.0 31.0 **0.0 (0.9)**	95.0 5.00 **0.7 (0.4)**

Table 8.2. Allele frequencies, χ^2 and P values of each *DDAH2* polymorphism. All polymorphisms were in Hardy Weinberg equilibrium except the –1020C/G in the German population screen (*P=0.003) and –1151A/C in the London renal failure cohort (*P=0.04). The London Renal Failure cohort was in Hardy Weinberg equilibrium after adjusting for race. The –1020C/G polymorphism was omitted from genotyping analysis in the CREED cohort due to limited availability of genomic DNA.

8.4.2. Relationship between *DDAH2* genotype, ADMA and SDMA concentration and ADMA/SDMA ratio in the German population screen.

Demographic characteristics of the cohort are shown according to –1020C/G, -1151A/C and –871 6G/7G genotype in tables 8.3a-c. A significant difference in systolic and diastolic blood pressure was observed between homozygous 6G individuals and 7G allele carriers for the –871 6G/7G polymorphism (*P=0.01 and *P=0.005 respectively, table 8.3c). Blood pressure was 14% lower in the 7G allele carriers compared to 6G/6G individuals.

	Genotype –1020C/G			
	CC Mean (SD) N=93	**CG** Mean (SD) N=26	**GG** Mean (SD) N=8	**P**
Systolic BP (mmHg)	128.4 (12.44)	125.6 (11.55)	121.9 (8.43)	0.24
Diastolic BP (mmHg)	78.45 (6.92)	76.40 (7.0)	75.63 (8.21)	0.30
Cholesterol (mmol/l)	4.60 (0.82)	4.37 (1.22)	4.38 (0.71)	0.44
LDL (mmol/l)	2.77 (0.72)	2.72 (1.19)	2.53 (0.65)	0.72
HDL (mmol/l)	1.12 (0.33)	1.04 (0.25)	1.29 (0.73)	0.23
Triglycerides (mmol/l)	1.59 (1.04)	1.29 (0.69)	1.30 (0.89)	0.32
Age (Years)	36.25 (10.51)	35.21 (11.55)	40.83 (8.47)	0.51
Weight (Kg)	76.22 (14.02)	77.64 (13.08)	80.13 (20.45)	0.72

Table 8.3a Demographic characteristics of the German Population Screen cohort according to –1020C/G genotype. No significant association was found between genotype and any of the conventional cardiovascular risk factors measured (by One-Way ANOVA).

	Genotype –1151A/C			
	AA Mean (SD) N=64	**AC** Mean (SD) N=45	**CC** Mean (SD) N=16	**P**
Systolic BP (mmHg)	128.8 (11.19)	125.9 (13.44)	127.5 (13.12)	0.50
Diastolic BP (mmHg)	78.31 (6.71)	77.20 (7.42)	77.86 (8.02)	0.74
Cholesterol (mmol/l)	4.47 (0.87)	4.58 (0.99)	4.81 (0.78)	0.38
LDL (mmol/l)	2.71 (0.80)	2.74 (0.93)	3.01 (0.67)	0.44
HDL (mmol/l)	1.10 (0.37)	1.12 (0.29)	1.04 (0.40)	0.77
Triglycerides (mmol/l)	1.43 (0.83)	1.60 (1.18)	1.73 (0.89)	0.46
Age (Years)	37.67 (10.82)	34.42 (9.95)	38.31 (11.83)	0.25
Weight (Kg)	78.10 (14.93)	74.88 (14.05)	77.36 (13.08)	0.53

Table 8.3b Demographic characteristics of the German Population Screen cohort according to –1151A/C genotype. No significant association was found between genotype and any of the conventional cardiovascular risk factors measured (by One-Way ANOVA).

	Genotype –871 6G/7G		
	6G/6G Mean (SD) N=123	**6G/7G** Mean (SD) N=3	**P**
Systolic BP (mmHg)	127.9 (11.88)	110.0 (10.00)	0.01*
Diastolic BP (mmHg)	78.09 (6.77)	66.67 (11.55)	0.005*
Cholesterol (mmol/l)	4.55 (0.91)	4.20 (0.82)	0.51
LDL (mmol/l)	2.75 (0.83)	2.53 (0.81)	0.65
HDL (mmol/l)	1.11 (0.36)	1.10 (0.36)	0.96
Triglycerides (mmol/l)	1.53 (0.99)	1.23 (0.55)	0.61
Age (Years)	36.29 (10.36)	31.67 (11.02)	0.45
Weight (Kg)	77.03 (14.41)	66.67 (6.11)	0.22

Table 8.3c Demographic characteristics of the German Population Screen cohort according to –871 6G/7G genotype. No 7G/7G homozygotes were observed in this cohort. A significant association was found between genotype and blood pressure (* Students t-test).

ADMA and SDMA measures were successful in 126 and 127 individuals respectively out of 128 subjects recruited. Both ADMA and SDMA exhibited skewed (to the right) distributions with median (IQR) values of 0.85μmol/l (0.63-1.21) and 0.55μmol/l (0.38-0.79) respectively. The median ADMA/SDMA ratio for the whole cohort was 1.44 (1.05-2.56)

DNA from 128 healthy individuals was genotyped for the *DDAH2* –1020C/G, -1151A/C and –871 6G/7G polymorphisms and analysed for association between genotype and plasma ADMA, SDMA and ADMA/SDMA ratio (Figures 8.1a-c.). No association was detected between –1020 genotype and either ADMA, SDMA or ADMA/SDMA ratio (P≥0.05, figure 8.1a). A trend towards a lower ADMA/SDMA ratio was observed for -1151CC homozygous individuals (P=0.04, figure 8.1b). This approached statistical significance when A allele carriers were grouped and analysed against CC homozygotes (1.62 [1.05-2.67] versus 1.16 [1.05-1.36], P=0.05 Mann-Whitney test). No significant association was detected between –871 6G/7G genotype and ADMA, SDMA or ADMA/SDMA ratio (P≥0.05, figure 8.1c). The three individuals carrying the –871 7G allele had a lower median ADMA/SDMA ratio (1.08 [1.00-1.11]) compared to 6G homozygotes (1.48 [1.05-2.57]).

A

	Genotype –1020C/G			
	CC Median (IQR) N=93	**CG** Median (IQR) N=25	**GG** Median (IQR) N=8	**P**
ADMA (μmol/l)	0.83 (0.63-1.25)	0.90 (0.65-1.15)	0.78 (0.62-1.02)	0.62*
SDMA (μmol/l)	0.55 (0.38-0.79)	0.54 (0.35-0.77)	0.64 (0.37-0.77)	0.86*
ADMA/SDMA	1.40 (1.08-2.37)	1.68 (0.97-2.71)	1.02 (0.90-2.49)	0.41*

B

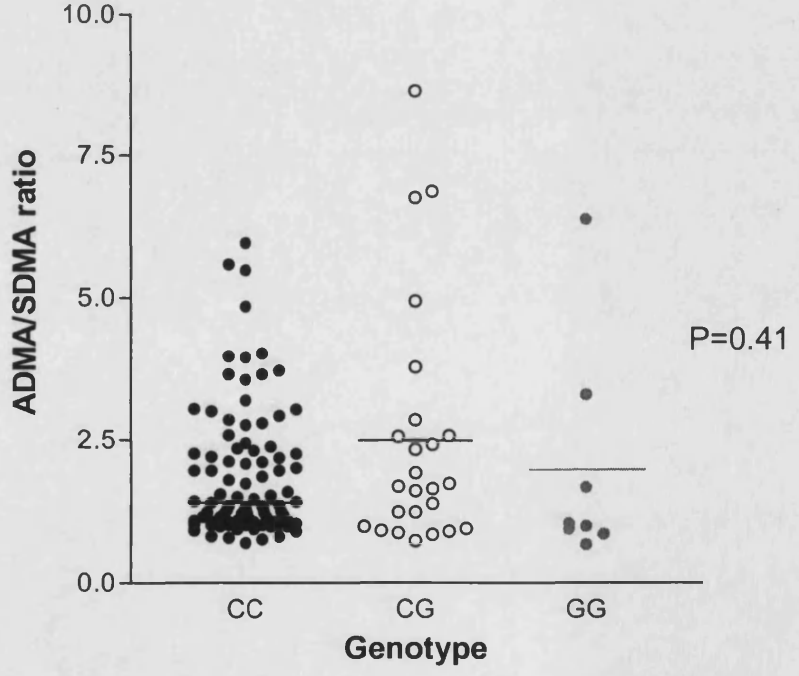

Figure 8.1a. ADMA and SDMA concentrations and ADMA/SDMA ratio according to –1020C/G genotype in the German Population Screen. **A.** Table showing the median (IQR) ADMA, SDMA and ADMA/SDMA ratio. No significant difference was observed for ADMA, SDMA or ADMA/SDMA ratio between genotypes (*Kruskal-Wallis test). **B.** Scatter plot of ADMA/SDMA ratio according to genotype. The median value is marked with a horizontal bar.

A

	Genotype –1151A/C			
	AA Median (IQR) N=62	**AC** Median (IQR) N=44	**CC** Median (IQR) N=16	**P**
ADMA (μmol/l)	0.83 (0.62-1.15)	0.92 (0.67-1.26)	0.77 (0.59-1.06)	0.40*
SDMA (μmol/l)	0.55 (0.38-0.81)	0.49 (0.32-0.70)	0.66 (0.48-0.81)	0.14*
ADMA/SDMA	1.43 (0.99-2.50)	1.91 (1.17-3.02)	1.16 (1.05-1.36)	0.04*

B

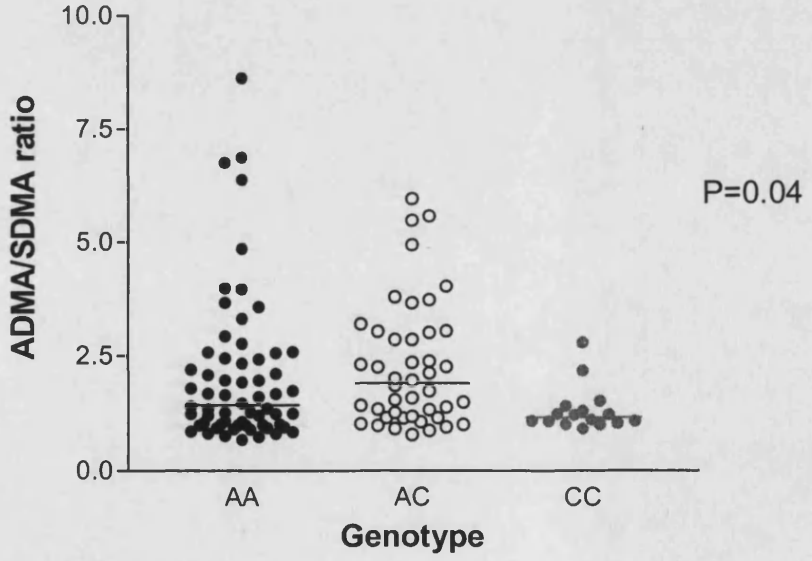

Figure 8.1b. ADMA and SDMA concentration, and ADMA/SDMA ratio according to –1151A/C genotype in the German Population Screen. **A.** Table showing the median (IQR) ADMA and SDMA concentration and ADMA/SDMA ratio. A significant difference was observed for ADMA/SDMA ratio between genotypes *Kruskal-Wallis test. B. Scatter plot of ADMA/SDMA according to genotype. The median value is indicated by a horizontal bar.

A

	Genotype –871 6G/7G		
	6G/6G Median (IQR) N=119	**6G/7G** Median (IQR) N=3	**P**
ADMA (μmol/l)	0.90 (0.64-1.23)	0.59 (0.54-0.83)	0.15*
SDMA (μmol/l)	0.55 (0.37-0.79)	0.53 (0.50-0.83)	0.79†
ADMA/SDMA	1.48 (1.05-2.57)	1.08 (1.00-1.11)	0.16*

B

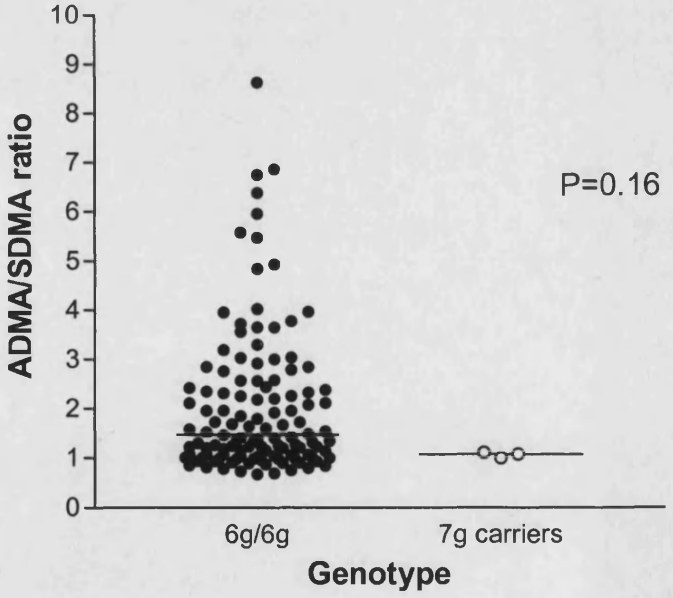

Figure 8.1c. ADMA and SDMA concentration, and ADMA/SDMA ratio according to –871 6G/7G genotype in the German Population Screen. **A.** Table showing the median (IQR) ADMA and SDMA concentration and ADMA/SDMA ratio. The SDMA concentration in this cohort exhibited a normal distribution. No 7G/7G homozygotes were observed in this cohort. No significant difference was observed in ADMA, SDMA or ADMA/SDMA ratio between genotypes (* Mann-Whitney test, †Students t-test). **B.** Scatter plot showing ADMA/SDMA ratio for 6G/6G individuals versus 7G carriers. The median value is indicated by a horizontal bar.

8.4.3. Relationship between *DDAH2* genotype, ADMA and SDMA concentration and ADMA/SDMA ratio in the London Renal Failure Cohort.

Demographic characteristics according to *DDAH2* genotype are shown in table 8.4a-c. Systolic and diastolic blood pressure measurements were available for 96 individuals and age was known for 116 individuals. No association was detected between *DDAH2* genotype and either blood pressure or age.

	Genotype –1020C/G		
	CC+CG Mean (SD) N	**CG** Mean (SD) N	**P**
Systolic BP (mmHg)	144.2 (32.07) 88	152.5 (34.60) 8	0.49
Diastolic BP (mmHg)	80.15 (17.09) 87	80.00 (20.16) 8	0.98
Age (years)	53.68 (17.38) 107	49.78 (17.98) 9	0.52

Table 8.4a. Demographic characteristics of the London Renal Failure Cohort according to –1020C/G genotype. No association was detected between genotype and either systolic BP, diastolic BP or age ($P \geq 0.05$, Students t-test).

	Genotype –1151A/C			
	AA Mean (SD) N	**AC** Mean (SD) N	**CC** Mean (SD) N	**P**
Systolic BP (mmHg)	136.1 (31.73) 23	146.8 (29.44) 41	148.7 (35.55) 32	0.32
Diastolic BP (mmHg)	77.22 (17.45) 23	77.29 (12.94) 41	86.06 (20.76) 31	0.06
Age (years)	50.24 (20.16) 34	57.43 (16.05) 47	51.00 (15.49) 35	0.12

Table 8.4b. Demographic characteristics of the London Renal Failure Cohort according to –1151A/C genotype. No association was detected between genotype and either systolic BP, diastolic BP or age (P≥0.05, One-Way ANOVA).

	Genotype –871 6G/7G		
	6G/6G Mean (SD) N	**6G/7G** Mean (SD) N	**P**
Systolic BP (mmHg)	143.0 (32.09) 82	157.8 (32.00) 13	0.12
Diastolic BP (mmHg)	79.46 (17.21) 82	84.38 (17.51) 13	0.34
Age (years)	53.29 (17.67) 103	52.08 (14.33) 12	0.82

Table 8.4c. Demographic characteristics of the London Renal Failure Cohort according to –871 6G/7G genotype. No association was detected between genotype and either systolic BP, diastolic BP or age (P≥0.05, Students t-test).

ADMA and SDMA measures were successful in all 126 subjects. Both ADMA and SDMA exhibited skewed (to the right) distributions with a median (IQR) of 1.28μmol/l (0.89-1.9) and 3.46μmol/l (2.35-4.41) respectively. The median ADMA/SDMA ratio for the whole cohort was 0.40 (0.25-0.62).

126 renal failure patients were genotyped for the *DDAH2* –1020C/G and –1151A/C polymorphisms, and 125 for the –871 6G/7G polymorphism and analysed for association with plasma ADMA, SDMA and ADMA/SDMA ratio (Figure 8.2a-c). No association was detected between *DDAH2* genotype and ADMA, SDMA or ADMA/SDMA ratio in this cohort.

A

	Genotype –1020C/G		
	CC Median (IQR) N=117	**CG+GG** Median (IQR) N=9	**P**
ADMA (μmol/l)	1.26 (0.92-1.87)	1.48 (0.78-2.16)	0.82*
SDMA (μmol/l)	3.50 (2.34-4.42)	3.16 (2.46-3.70)	0.54*
ADMA/SDMA	0.40 (0.24-0.62)	0.45 (0.27-0.68)	0.67*

B

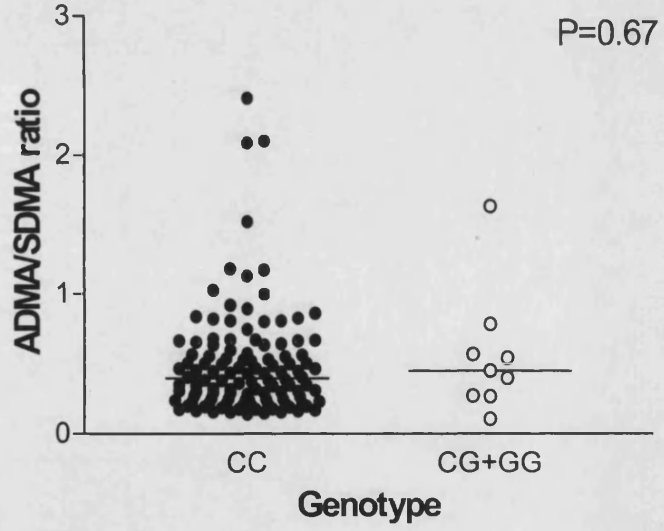

Figure 8.2a. ADMA and SDMA concentration, and ADMA/SDMA ratio according to –1020C/G genotype in the London Renal Failure cohort. A. Table showing the median (IQR) for ADMA and SDMA concentration and ADMA/SDMA ratio. Data for CG and GG individuals was combined due to the small number of GG (n=1) individuals identified. No significant difference was observed for ADMA, SDMA or ADMA/SDMA ratio between genotypes (* Mann-Whitney test). **B.** Scatter plot of ADMA/SDMA ratio according to genotype. The median value is marked with a horizontal bar.

A

	Genotype –1151A/C			
	AA Median (IQR) N=39	**AC** Median (IQR) N=51	**CC** Median (IQR) N=36	**P**
ADMA (μmol/l)	1.30 (0.87- 1.87)	1.35 (0.85- 2.06)	1.22 (1.00-1.76)	0.97*
SDMA (μmol/l)	3.47 (2.49- 4.42)	3.25 (2.47- 4.29)	3.54 (2.01-5.63)	0.93*
ADMA/SDMA	0.43 (0.29- 0.57)	0.43 (0.25- 0.70)	0.38 (0.23- 0.67)	0.79*

B

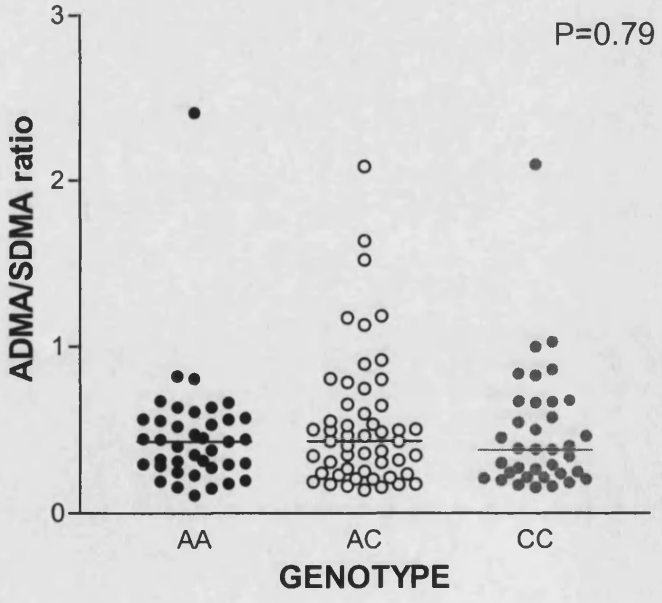

Figure 8.2b. ADMA and SDMA concentration, and ADMA/SDMA ratio according to –1151A/C genotype in the London Renal Failure cohort. A. Table showing the median (IQR) for ADMA and SDMA concentration and ADMA/SDMA ratio. No significant difference was observed for ADMA, SDMA or ADMA/SDMA ratio between genotypes (*Kruskal-Wallis test). **B.** Scatter plot of ADMA/SDMA ratio according to genotype. The median value is marked with a horizontal bar.

A

	Genotype –871 6G/7G		
	6G/6G Median (IQR) N=112	**6G/7G** Median (IQR) N=13	**P**
ADMA (μmol/l)	1.30 (0.91-1.87)	1.18 (0.86-1.62)	0.37*
SDMA (μmol/l)	3.46 (2.41-4.41)	3.26 (1.80-5.50)	0.94*
ADMA/SDMA	0.42 (0.27-0.60)	0.24 (0.21-0.65)	0.26*

B

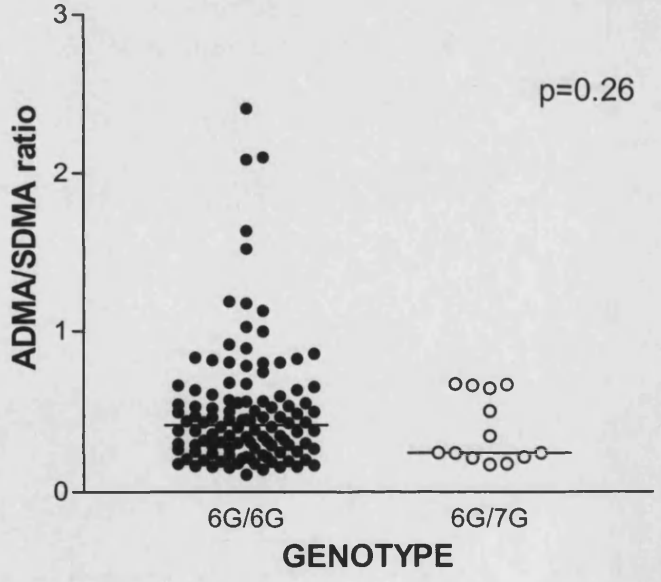

Figure 8.2c. ADMA and SDMA concentration, and ADMA/SDMA ratio according to –871 6G/7G genotype in the London Renal Failure cohort. A. Table showing the median (IQR) for ADMA and SDMA concentration and ADMA/SDMA ratio. No significant difference was observed for ADMA, SDMA or ADMA/SDMA ratio between genotypes (*Mann-Whitney test). **B.** Scatter plot of ADMA/SDMA according to genotype. The median value is marked with a horizontal bar. Only 13 individuals carrying the 7G allele were identified during this study. No 7G homozygotes were identified.

8.4.4 Relationship between *DDAH2* genotype and ADMA, SDMA and ADMA/SDMA ratio in the CREED cohort.

Demographic characteristics according to *DDAH2* genotype are shown in tables 8.5a-b. No significant correlation was observed between –1151A/C genotype and risk factors for CVD (Table 8.5a). A significant association was observed between –871 6G/7G genotype and levels of triglycerides (*P=0.02, table 8.5b). Carriers of the 7G allele for this variant had higher circulating levels of triglycerides (mean=2.48 mmol/l) compared with 6G homozygous individuals (mean=1.98 mmol/l). 7G allele carriers also had lower HDL cholesterol levels, but this did not reach significance (P=0.05, table 8.5b). No 7G homozygous individuals were identified in this cohort.

	Genotype –1151A/C			
	AA Mean (SD) N=125	**AC** Mean (SD) N=112	**CC** Mean (SD) N=26	**P**
Systolic BP (mmHg)	133.1 (21.87)	130.9 (24.18)	133.5 (21.11)	P=0.72
Diastolic BP (mmHg)	74.97 (12.10)	73.80 (12.90)	73.96 (10.27)	P=0.76
Cholesterol (mmol/l)	5.43 (1.56)	5.44 (1.44)	4.87 (1.21)	P=0.19
LDL (mmol/l)	3.43 (1.29)	3.46 (1.28)	2.87 (1.1)	P=0.09
HDL (mmol/l)	1.05 (0.27)	1.09 (0.32)	1.00 (0.31)	P=0.30
Triglycerides (mmol/l)	2.06 (1.06)	1.94 (1.03)	2.19 (0.94)	P=0.46
Age (years)	62.01 (15.68)	59.54 (14.45)	63.81 (15.01)	P=0.29
BMI (kg/m^2)	25.18 (4.64)	24.50 (4.14)	25.25 (4.57)	P=0.46
Fibrinogen (μmol/l)	13.31 (6.02)	13.34 (6.07)	15.42 (7.33)	P=0.27

Table 8.5a Demographic characteristics of the CREED cohort according to –1151A/C genotype. No significant association was found between genotype and any of the conventional cardiovascular risk factors measured (P≥0.05, One-Way ANOVA).

	Genotype –871 6G/7G		
	6G/6G Mean (SD) N=230	**6G/7G** Mean (SD) N=25	**P**
Systolic BP (mmHg)	132.6 (23.13)	127.7 (21.52)	P=0.31
Diastolic BP (mmHg)	74.26 (12.61)	75.20 (10.10)	P=0.72
Cholesterol (mmol/l)	5.37 (1.52)	5.40 (1.25)	P=0.89
LDL (mmol/l)	3.40 (1.30)	3.33 (1.12)	P=0.80
HDL (mmol/l)	1.07 (0.29)	0.95 (0.29)	P=0.05
Triglycerides (mmol/l)	1.98 (1.03)	2.48 (1.12)	P=0.02*
Age (years)	61.35 (15.09)	62.84 (16.71)	P=0.64
BMI (kg/m^2)	24.76 (4.39)	25.65 (4.06)	P=0.34
Fibrinogen (μmol/l)	13.55 (6.24)	12.94 (6.51)	P=0.65

Table 8.5b. Demographic characteristics of the CREED cohort according to –871 6G/7G genotype. No 7G/7G homozygotes were observed in this cohort. A significant association was found between genotype and triglyceride levels (*Students t-test).

ADMA and SDMA measurements were available for 259 individuals out of 277 recruited. Both ADMA and SDMA exhibited skewed (to the right) distributions with median (IQR) values of 3.02μmol/l (1.72-4.26) and 2.94μmol/l (2.30-4.41) respectively. The median (IQR) ADMA/SDMA for the whole cohort was 0.96 (0.36-1.82).

259 renal failure patients from the CREED study were genotyped for association between the –1151A/C and –871 6G/7G *DDAH2* polymorphisms and plasma ADMA, SDMA and ADMA/SDMA ratio (Figures 8.3a-c). The –1020C/G polymorphism was omitted from the genotyping study because of limited availability of DNA. No association was detected between –1151A/C genotype and either ADMA, SDMA or ADMA/SDMA ratio (Figure 8.3a). This was also true after grouping A allele carriers and analysing against CC homozygotes (ADMA 3.00μmol/l [1.71-4.16] versus 3.50μmol/l [1.64-5.24], SDMA 2.91μmol/l [2.24-4.45] versus 3.58μmol/l [2.55-4.28], ADMA/SDMA ratio 0.96 [0.36-1.79] versus 1.06 [0.31-2.12] $P \geq 0.05$, Mann-Whitney test). No association was detected between –871 6G/7G genotype and ADMA, SDMA or ADMA/SDMA ratio (Figure 8.3b).

A

	Genotype –1151A/C			
	AA Median (IQR) N=122	**AC** Median (IQR) N=111	**CC** Median (IQR) N=26	**P**
ADMA (μmol/l)	2.95 (1.77-4.31)	3.00 (1.67-4.15)	3.50 (1.64-5.24)	0.67*
SDMA (μmol/l)	2.99 (2.21-4.55)	2.81 (2.28-4.27)	3.58 (2.55-4.28)	0.62*
ADMA/SDMA	0.94 (0.40-1.82)	1.01 (0.34-1.78)	1.06 (0.31-2.12)	0.94*

B

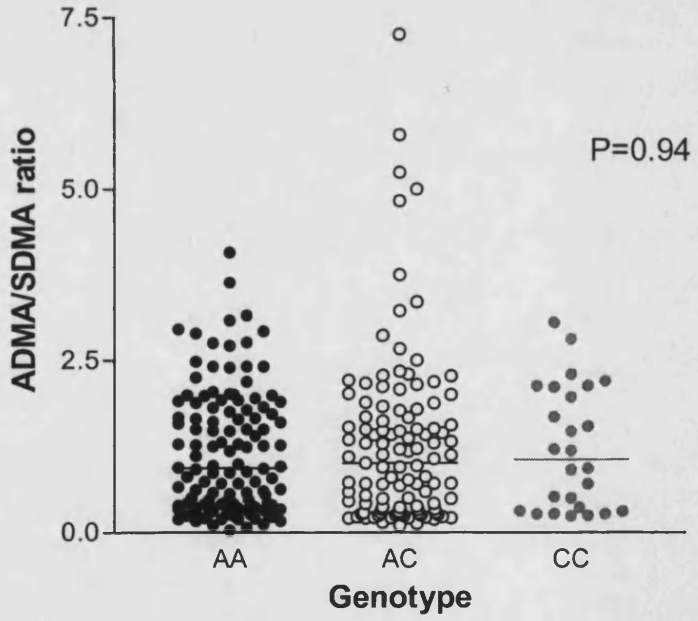

Figure 8.3a. ADMA and SDMA concentration, and ADMA/SDMA ratio according to –1151A/C genotype in the CREED cohort. A. Table showing the median (IQR) for ADMA and SDMA concentration and ADMA/SDMA ratio. No significant difference was observed for ADMA, SDMA or ADMA/SDMA between genotypes (*Kruskal-Wallis test). **B.** Scatter plot of ADMA/SDMA according to genotype. The median value is marked with a horizontal bar.

A

	Genotype –871 6G/7G		
	6G/6G Median (IQR) N=227	**6G/7G** Median (IQR) N=24	**P**
ADMA (μmol/l)	2.89 (1.71-4.13)	2.79 (1.51-4.77)	0.76*
SDMA (μmol/l)	2.86 (2.26-4.18)	3.60 (2.50-6.15)	0.11*
ADMA/SDMA	0.940 (0.36-1.89)	0.89 (0.29-1.65)	0.50*

B

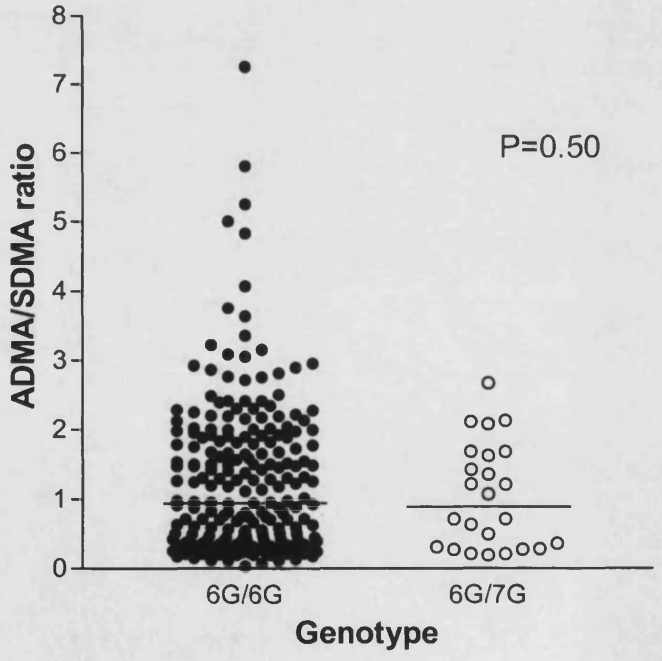

Figure 8.3b. ADMA and SDMA concentrations, and ADMA/SDMA ratio according to –871 6G/7G genotype in the CREED cohort. A. Table showing the median (IQR) for ADMA and SDMA concentration and ADMA/SDMA ratio. No significant difference was observed for ADMA, SDMA or ADMA/SDMA ratio between genotypes (*Mann-Whitney test). **B.** Scatter plot of ADMA/SDMA according to genotype. The median value is marked with a horizontal bar. No 7G homozygous individuals were identified in this study.

8.5 Discussion

During this study the association between three polymorphisms in the *DDAH2* promoter (identified by SSCP in Chapter 6) and plasma ADMA and SDMA concentrations and the ADMA/SDMA ratio as well as other relevant risk factors for the development of CVD has been explored. Three different cohorts were investigated including a group of healthy individuals and two groups of renal failure patients in whom susceptibility to CVD is greatly enhanced.

ADMA is an endogenous inhibitor of nitric oxide synthase (Vallance et al., 1992). It is synthesised during protein turnover (Najbauer et al., 1993) and is eliminated from the body via renal excretion (Kakimoto et al., 1970) and through metabolism by DDAH enzymes (Ogawa et al., 1987). In healthy individuals plasma levels of ADMA and SDMA are found in a ratio of approximately 1:1. However, in patients with renal failure, elevations in the circulating concentration of SDMA are higher than those of ADMA with the consequence that the ADMA/SDMA ratio falls to approximately 0.3 (MacAllister et al., 1996). The plasma levels of ADMA and SDMA reported during this study are comparable to those reported previously (Fleck et al., 2001; Kielstein et al., 2002; MacAllister et al., 1996; Wahbi et al., 2001). ADMA and SDMA concentrations were higher in both the renal failure cohorts compared to the healthy cohort, consistent with the renal impairment in these subjects. Consistent with previous findings, the ADMA concentration was lower than the SDMA concentration in the London Renal Failure cohort, which is explained by the fact that ADMA but not SDMA is a metabolised by DDAH enzymes (Ogawa et al., 1987). The observed similarity in ADMA and SDMA levels in the CREED cohort (ADMA/SDMA ratio = 1) may suggest

down-regulation of DDAH enzymes in these subjects, however no association was found between *DDAH2* polymorphisms and either the ADMA, SDMA or the ADMA/SDMA ratio during this study.

On the basis of the promoter/reporter assay results obtained in Chapter 7 (which identified the –871 7G allele as having a greater promoter activity), it might be expected that carriage of the –871 7G allele would be associated with lower ADMA concentrations and/or ADMA/SDMA ratio. This was seen in the German sample of healthy individuals, with 7G allele carriers exhibiting a lower ADMA/SDMA ratio and interestingly significantly lower systolic and diastolic blood pressure. These data must be interpreted with caution, however, as they are based on only three 7G carriers. No association was observed between *DDAH2* genotype and either circulating ADMA or SDMA concentration or the ADMA/SDMA ratio in either of the renal failure subjects during this study. There are several potential explanations for this including the relatively small size of the cohorts studied. The observation that the frequency of the 7G allele for the –871 6G/7G polymorphism is very low (and no 7G/7G individuals were detected) limits further the statistical power to detect any association in cohorts of the size studied. Also, in patients with renal failure the decreased excretory function may outweigh any small genetic differences in metabolism and make genotype dependent changes in ADMA concentration difficult to detect. Alternatively, local changes in ADMA concentration may occur without changing the systemic ADMA concentration.

In summary, *DDAH2* genotype was not associated with ADMA or SDMA concentration or ADMA/SDMA ratio in healthy subjects or renal failure patients during

this study. Also *DDAH2* genotype was not associated with conventional cardiovascular risk factors in the renal failure cohorts. Further work to compare *DDAH2* genotype and expression in patient groups where ADMA concentration is elevated would be useful in determining the role of DDAH2 in diseases such as hypertension and hypercholesterolaemia.

CHAPTER 9

DDAH2 POLYMORPHISMS, ENDOTHELIAL FUNCTION AND PLASMA NITROGEN OXIDES (NO_X)

9.1 Aims

To investigate the association between *DDAH2* polymorphisms and plasma concentration of nitrate/nitrite (NO_X) and endothelial function.

9.2 Background

The risk of developing CVD is significantly enhanced in many disease states. For example, diabetic patients are 3-8 times more likely to develop premature cardiovascular disease compared to healthy individuals (Bierman et al., 1992), and patients with renal failure have a 10-20 fold increased risk of developing cardiovascular disease compared to the general population (Wheeler et al., 1996). In addition, elevated cholesterol levels and increased blood pressure are also recognised as risk factors for the development of CVD (Danesh et al., 2000). Preeclampsia, which is characterised by hypertension and proteinuria during pregnancy has also been shown to be an independent risk factor for cardiovascular disease later in life. In a retrospective study of 129,290 births, women with a history of preeclampsia were shown to have a 1.5-2.0 fold increased risk of IHD (Smith et al., 2003). Also, in a case control study (in which 1199 women diagnosed with preeclampsia were compared to 1197 without preeclampsia/eclampsia and 1197 with gestational hypertension) women with preeclamsia/eclampsia had a 1.4-4.0 fold increased risk of hypertension and a 4 fold risk of stroke (Wilson et al., 2003).

The mechanism underlying increased risk of vascular disease in these patients is incompletely understood. However, individuals who have risk factors for CVD or

established CVD also exhibit endothelial dysfunction, which predates and predicts CVD onset (Gaeta et al., 2000). Endothelial dysfunction is thought to be due in part to deficient NO synthesis or action (Vallance and Chan et al., 2001). Elevated circulating levels of the NOS inhibitor ADMA have been demonstrated in all of the disorders mentioned above (Vallance et al., 1992; Pettersson et al., 1998; Usui et al., 1998; Swurdaki et al., 1999; Stuhlinger et al., 2002), and correlate with endothelial dysfunction providing a possible mechanism for limited NO availability. It is not surprising therefore that a large amount of interest has been generated in evaluating the role of ADMA in endothelial dysfunction in patients at risk of CVD.

In vivo NO has a half-life of approximately 30 seconds (Ignarro et al., 1987) and is readily oxidised to NO_2^- making it difficult to measure NO directly in biological samples. NO_2^- can undergo further oxidation by oxyhaemoglobin (O_2Hb) forming NO_3^-. NO_2^- and NO_3^- are stable in biological samples stored at –20°C (Moshage et al., 1995), existing in approximate proportions of 1:20. It has therefore been suggested that plasma levels of NO_2^- and NO_3^- (NOx) can be used as an indirect measure of NO production. NO_2^- can be measured by quantifying the coloured diazonium product formed after the reaction between NO_2^-, sulfonilamide and N-(1-naphthyl)ethylenediamine (also known as the Greiss reaction) and the concentration of NO_3^- can be ascertained by first converting NO_3^- to NO_2^- using the enzyme nitrate reductase. However, since NO_3^- is also a dietary constituent (present mainly in vegetables such as lettuce, celery, cauliflower, spinach and broccoli) (White, 1975), such measurement is potentially complicated by NO_3^- intake. Nevertheless, plasma concentrations of NOx have been reported to be a reliable marker of NO synthesis via the L-arginine-NOS pathway in fasted humans (Rhodes et al., 1995), although, since there are three enzymatic sources

of NO (iNOS, nNOS and eNOS) this technique cannot distinguish isoform specific NO formation. Several studies have reported lower plasma NOx levels in human and animal subjects with risk factors for CVD such as hypertension, renal failure, diabetes and LDL cholesterol (Node et al., 1997; Schmidt and Baylis, 2000; Kurioka et al., 2000; Tanaka et al., 1997). Plasma concentrations of NOx have also been reported to be lower in smokers compared to non-smokers and show a positive correlation with the percentage change in FMD (Jeerooburkhan et al., 2001; Hori et al., 2001).

Despite the evidence to support the theory that lower circulating NO levels are associated with risk factors for CVD, the cause of lower NO levels in individuals at risk of CVD is still unclear. Conflicting evidence has been put forward with regards to the influence of an individuals genetic 'makeup' on ability to synthesise NO. Two studies have reported an association between a 27bp repeat polymorphism within intron 4 of the *eNOS* gene and plasma concentration of NO (Wang et al., 1997; Tsukada et al., 1998). However, no such association was observed between several *eNOS* polymorphisms and NO in the large NPHSII study (Jeerooburkhan et al., 2001). These conflicting results may be the consequence of the difficulty in controlling for dietary NOx intake and/or the relative insensitivity of the assays. The most reliable measure of NO *in vivo* has proved to be an indirect bioassay of its action, namely endothelium-dependent vasodilation. Several genes involved in the regulation of NO synthesis have been investigated in this tissue for association with endothelial dysfunction. For example, polymorphisms in the *GCH1* gene were found to be associated with plasma neopterin levels (a marker of BH_4 synthesis) and FMD in healthy individuals, supporting the theory that genetic regulation of the *GCH1* gene can influence circulating BH_4 which in turn would be expected to affect NO synthesis resulting in endothelial dysfunction

(Chapter 5). The p22phox 242TT genotype was also associated with significantly greater FMD in healthy subjects, possibly due to reduced NADPH oxidase activity and therefore production of less O_2^- which could potentially react with NO (Chapter 3). In addition, variants in the eNOS, MTHFR, ACE and glutamate-cysteine ligase catalytic subunit (GCLC) genes, to name a few, have also been associated with differences in endothelial function (Savvidou et al., 2001; Leeson et al., 2002; Pullin et al., 2002; Mulder et al., 2003; Koide et al., 2003).

The aim of this study therefore was to investigate the hypothesis that *DDAH2* polymorphisms influence endothelial function and biochemical indices of NO synthesis. Although *DDAH2* polymorphisms were not associated with plasma concentrations of ADMA (Chapter 8), given the *in vitro* data obtained by promoter/reporter analysis (Chapter 7), it was considered possible that *DDAH2* polymorphisms might influence local endothelial cell ADMA and therefore endothelial function and NO availability, in the absence of detectable changes in circulating ADMA concentration.

9.3 Subjects and Methods

Four subject groups with differing and complementary phenotypic measurements were analysed for association between *DDAH2* genotype and either plasma NOx or endothelial function, as well as other relevant cardiovascular disease phenotypes or risk factors. Unfortunately, due to time constraints not all the polymorphisms identified by SSCP (Chapter 6) could be genotyped in every cohort. Where possible priority was given to the –1151A/C and –871 6G/7G polymorphisms in view of the results obtained in chapter 7. Table 9.1 summarises the cohorts and their phenotypic characteristics. Full demographic characteristics of each study cohort are outlined in Chapter 2.

9.3.1 Subjects investigated for association between *DDAH2* polymorphisms, plasma NO_X and blood pressure.

Healthy subjects (NPHSII cohort)

Briefly, subjects from the prospective NPHSII cohort (Chapter 2.2.12.1) were analysed for association between *DDAH2* polymorphisms, plasma NOx and blood pressure. This cohort comprises healthy men aged 50-61 years. Individuals from the Chesterfield (n=260) and North Mymms (n=290) clinics for whom plasma samples were available were selected. The –449G/C, -1020C/G and –1151A/C polymorphisms were genotyped in these subjects as these were the first variants identified by SSCP.

9.3.2 Subjects investigated for association between *DDAH2* polymorphisms and endothelial function

Healthy subjects (Cambridge Young Adults Study cohort)

Blood was collected from 264 healthy subjects from the Cambridge Young Adults Study recruited by Dr. Paul Leeson and Professor J. Deanfield (Chapter 2.2.12.1). DNA was extracted using the Qiagen DNA purification kit method described in Chapter 2.2.1.2 and genotyped for the –1151A/C and the –871 6G/7G polymorphisms. Measures of endothelium dependent and independent (mediated by GTN) vascular responses were performed using high-resolution ultrasound imaging (Leeson et al., 2002). In each subject a fasting venous blood sample was analysed for total cholesterol, HDL, LDL and triglycerides. Blood pressure and weight were also recorded.

Healthy subjects (Pregnancy cohort)

A cohort of women with normal singleton pregnancies was investigated for association between *DDAH2* genotype and endothelial function (Chapter 2.2.12.4). Common genetic variation in the eNOS gene had previously been associated with endothelial function in this cohort (Savvidou et al., 2001). Briefly, 139 unrelated Caucasian women with normal singleton pregnancies were recruited from the Harris Birthright Centre antenatal clinic by Dr. M Savvidou (Savvidou et al., 2001). All were healthy and had no history of cardiovascular disease. Age, smoking status, blood pressure (average of three seated readings), FMD, gestational age, parity and heart rate were recorded (Savvidou et al., 2001). DNA was extracted from whole blood using the Qiagen DNA purification kit method (Chapter 2.2.1.2) and genotyped for the –1020C/G, -1151A/C and the –871 6G/7G polymorphisms.

Disease subjects (EBCT cohort)

DNA from the EBCT cohort of 385 individuals, comprising 188 type I diabetic patients and 197 control subjects recruited by Dr. H Colhoun (Chapter 2.2.12.3) was analysed for association between the -1020C/G and -1151A/C *DDAH2* polymorphisms and endothelial function (assessed by venous occlusion plethysmography) as well as for other relevant cardiovascular disease phenotypes or risk factors (Chapter 2.2.12.3). The EBCT cohort was recruited with the primary aim of examining the effect of type I diabetes on coronary artery calcification (CAC) assessed by electron beam computerised tomography (EBCT), a surrogate marker of coronary artery atherosclerosis (Colhoun et al., 2000). Type I diabetic subjects with age of onset ≤25 years were recruited from five London hospitals. Control subjects were drawn from two London general practices and were included regardless of heart disease.

Cohort	Description of Cohort	Blood pressure	Endothelial function	NOx	Polymorphism -449 C/G	-1020 C/G	-1151 C/A	-871 6G/7G
HEALTHY								
Middle Age:								
NPHSII (Northwick Park Heart Study II)	Subjects selected from the Chesterfield (n=260) + N.Mymms (n=290) clinics	+		+	+	+	+	
Young:								
Cambridge Young Adults Study	264 healthy subjects	+	+*				+	+
Pregnancy Cohort	139 caucasian women with normal pregnancies	+	+*			+	+	+
DISEASE								
EBCT (Diabetics+ Controls)	188 type 1 diabetics+ 197 controls	+	+Ψ			+	+	+

Table 9.1 Summary of cohorts genotyped for association between DDAH2 polymorphisms and various risk factors for CVD. Risk factors and polymorphisms analysed for each cohort are indicated by +. *Measured by FMD Ψ Measured by venous occlusion plethysmography.

9.3.3 Genotyping *DDAH2* polymorphisms

Subjects were genotyped for the –449G/C, -1151A/C and –1020C/G polymorphisms by PCR-RFLP analysis as described in Chapter 6.3.7. The –871 6G/7G polymorphism was genotyped by Genescan analysis as described in Chapter 6.3.7.

9.3.4 Measurement of plasma nitrite and nitrate (NOx)

Plasma NOx concentrations were measured in collaboration with Dr. Noor Jeerooburkhan (UCL) by the Griess reaction, in individuals from the Chesterfield (n=260) and North Mymms (n=290) clinics of the NPHSII cohort as described in Chapter 2.2.9. Briefly, plasma samples were filtered using Ultrafree microcentrifuge filter units (Biomax-5, Millipore) to remove proteins such as Hb, which could interfere with the reaction. NO_3^- was reduced to NO_2^- by the addition of nitrate reductase in the presence of NADPH, glucose-6-phosphate and glucose-6-phosphate dehydrogenase. Upon addition of sulphanilic acid the NO_2^- formed a diazonium salt, which when coupled with NED produced a purple chromophore. The absorbance measured at 540nm is proportional to the amount of NO_2^- in the plasma sample. The lower limit of detection for this assay was 0.5μM, with an inter-assay variation of 4% and intra-assay variation of 3.4%.

9.3.5 Statistical Analysis

Observed numbers of each genotype were compared with those expected under the assumption of Hardy-Weinberg equilibrium by χ^2analysis. Allele frequencies were

deduced from genotype frequencies. Plasma NOx concentrations and cardiovascular risk factors are represented as mean (SD) or mean (SEM) and allelic associations were examined by parametric or non-parametric tests where appropriate. Endothelial function measured by FMD was expressed as the mean (SD) % change in diameter. Endothelial function measured by venous occlusion plethysmography was represented as mean (SEM) % change in flow in response to intra-brachial infusion of acetylcholine (ACh) at doses 25, 50 and 100 nmol/min each dose for 3 minutes, bradykinin (BK) at doses 10, 30 and 100pmol/min each dose for 3 minutes, glyceryl trinitrate (GTN) at doses 4, 8 and 16 nmol/min each dose for 5 minutes, N^G-monomethyl-Larginine (LNMMA) at doses 1, 2 and 4μmol/min each dose for 5 minutes and noradrenaline (NA) at doses 60, 120 and 240pmol/min each dose for 5 minute as described previously by Chan et al., 2003. The mean blood flow for each drug dose was assessed in each genotype group. From this, the difference in response between genotypes is expressed as the percentage difference in absolute flow in the presence of the drug, adjusted for baseline flow and averaged across three drug doses using the repeated-measures analysis of covariance model (XTREG procedure in STATA 6) with the data log transformed as appropriate (Statistical analysis was carried out by Miss Shona Livingstone, UCL).

9.4 Results

9.4.1 Genotype and allele frequencies of *DDAH2* polymorphisms in each study cohort.

The allele frequencies for the –449G/C, -1020C/G, -1151A/C and –871 6G/7G polymorphisms for each cohort are shown in table 9.2. Genotype frequencies did not differ from those expected under Hardy-Weinberg equilibrium except for the –871 6G/7G polymorphism in the Cambridge Young Adults cohort (χ^2 =183.3, P=<0.05, table 9.2). Repeat genotyping and DNA sequencing ruled out mis-typing as the cause of deviation from the Hardy-Weinberg equilibrium in this cohort.

	Polymorphism			
	-449G/C G(%) C(%) χ^2 (P)	**-1020C/G** C(%) G(%) χ^2 (P)	**-1151A/C** A(%) C(%) χ^2 (P)	**-871 6G/7G** 6G(%) 7G(%) χ^2 (P)
NPHSII	66.0 34.0 **0.6 (0.42)**	88.0 12.0 **0.0 (0.89)**	69.0 31.0 **0.3 (0.60)**	-
Cambridge Young Adults	-	86.0 14.0 **0.4 (0.52)**	71.0 29.0 **3.0 (0.08)**	90.0 10.0 **183.3 (<0.05)***
Pregnancy	-	87.0 13.0 **0.3 (0.60)**	67.0 33.0 **0.8 (0.37)**	99.0 1.00 **0.0 (0.86)**
EBCT	-	92.0 8.00 **3.7 (0.06)**	56.0 44.0 **2.5 (0.12)**	-

Table 9.2. Tests for Hardy-Weinberg equilibrium in four cohorts in which NOx or endothelial function was assessed. All polymorphisms were in Hardy-Weinberg equilibrium except the –871 6G/7G in the Cambridge Young Adults Study cohort (*P<0.05).

9.4.2 Relationship between *DDAH2* genotype and plasma NOx in the NPHSII cohort.

Patients from two clinics of the prospective NPHSII study cohort were analysed for association between *DDAH2* genotype and plasma nitrite and nitrate (NOx) concentrations. Plasma NOx measurements were successful in 235 individuals out of 260 from the Chesterfield cohort and 287 individuals out of 290 from the North Mymms cohort. Plasma NOx exhibited a skewed (to the right) distribution with median (IQR) of 9.21μmol/l (7.26-12.66) for the Chesterfield and 11.22μmol (9.10-14.65) for the North Mymms clinics respectively.

Subjects were genotyped for the –449G/C, -1020C/G and –1151A/C *DDAH2* polymorphisms and analysed for association between genotype and plasma NOx (Tables 9.3a-c). Due to the small number of rare homozygotes (GG) for the –1020C/G polymorphism, heterozygotes and rare homozygotes were grouped and analysed together. A significant association was observed between –1020C/G genotype and plasma NOx in the Chesterfield clinic only (*P=0.01, table 9.3b). Individuals carrying the G allele had higher average plasma NOx than CC homozygotes. No association was observed between *DDAH2* genotype and plasma NOx after combining the Chesterfield and North Mymms clinics ($^{\Psi}$P=0.59, table 9.3d).

9.4.2.1 *DDAH2* genotype and blood pressure in the NPHSII cohort

No statistically significant association was observed between genotype and blood pressure in either the North Mymms or Chesterfield subjects (Tables 9.3a-c, P≥0.05) or when both clinics were combined (Table 9.3d, P≥0.05).

	Genotype –449G/C			
	GG Mean (SD)	**GC** Mean (SD)	**CC** Mean (SD)	**P**
Chesterfield	N=69	N=73	N=19	
NOx (μmol/l)	10.08 (4.82)	10.47 (6.02)	9.98 (4.27)	0.95*
Systolic BP (mmHg)	141.3 (15.23)	139.3 (15.78)	143.2 (20.05)	0.57
Diastolic BP (mmHg)	87.51 (11.40)	86.68 (10.52)	89.93 (11.51)	0.52
Cholesterol (mmol/l)	5.78 (1.06)	5.82 (1.14)	5.74 (1.14)	0.96
North Mymms	N=117	N=111	N=35	
NOx (μmol/l)	12.23 (4.97)	13.10 (9.59)	12.63 (4.90)	0.38*
Systolic BP (mmHg)	138.7 (20.74)	135.5 (19.78)	133.3 (20.02)	0.28
Diastolic BP (mmHg)	85.82 (11.09)	84.90 (10.44)	81.36 (11.90)	0.12
Cholesterol (mmol/l)	5.88 (1.91)	5.70 (0.92)	5.90 (0.85)	0.27

Table 9.3a. Plasma NOx, systolic blood pressure (SBP), diastolic blood pressure (DBP) and cholesterol according to –449 G/C genotype for the Chesterfield (top) and North Mymms (bottom) NPHSII clinics. Genotyping was successful in 161 subjects out of 235 with NOx measurements in the Chesterfield clinic and 263 subjects out of 287 in the North Mymms clinic. No statistical significant association was observed between genotype and NOx (*by Kruskal-Wallis test), blood pressure or cholesterol (by One-way ANOVA).

	Genotype –1020C/G		
	CC Mean (SD)	**CG+GG** Mean (SD)	**P**
Chesterfield	N=128	N=40	
NOx (μmol/l)	9.69 (5.33)	11.51 (4.8)	0.01*
Systolic BP (mmHg)	139.5 (16.88)	143.5 (14.10)	0.18
Diastolic BP (mmHg)	86.55 (11.28)	88.82 (9.81)	0.26
Cholesterol (mmol/l)	5.76 (1.15)	5.82 (0.87)	0.77
North Mymms	N=214	N=62	
NOx (μmol/l)	12.94 (7.56)	11.74 (5.5)	0.21*
Systolic BP (mmHg)	137.1 (20.87)	133.9 (18.30)	0.27
Diastolic BP (mmHg)	84.68 (11.56)	85.18 (9.91)	0.76
Cholesterol (mmol/l)	5.82 (0.88)	5.70 (0.93)	0.36

Table 9.3b. Plasma NOx, systolic blood pressure (SBP), diastolic blood pressure (DBP) and cholesterol according to –1020 C/G genotype for the Chesterfield (top) and North Mymms (bottom) NPHSII clinics. Genotyping was successful in 168 subjects out of 235 with NOx measurements in the Chesterfield clinic and 276 subjects out of 287 in the North Mymms clinic. CG and GG individuals were analysed together because of the small number of GG homozygotes identified (n=3 Chesterfield, n=4 North Mymms). No statistically significant association was observed between genotype and blood pressure or cholesterol in the Chesterfield or North Mymms clinics ($P \geq 0.05$, Students t test). A significant association was observed between genotype and plasma NOx in the Chesterfield cohort only (*by Mann-Whitney test).

	Genotype –1151A/C			
	AA Mean (SD)	**AC** Mean (SD)	**CC** Mean (SD)	**P**
Chesterfield	N=82	N=72	N=14	
NOx (μmol/l)	10.00 (4.78)	10.26 (6.06)	9.65 (3.47)	0.98*
Systolic BP (mmHg)	140.4 (15.66)	140.3 (16.78)	140.9 (19.38)	0.99
Diastolic BP (mmHg)	86.94 (11.27)	86.38 (10.41)	90.41 (11.93)	0.45
Cholesterol (mmol/l)	5.81 (1.07)	5.77 (1.13)	5.81 (1.29)	0.97
North Mymms	N=134	N=112	N=30	
NOx (μmol/l)	12.35 (5.02)	13.25 (9.65)	11.76 (4.11)	0.71*
Systolic BP (mmHg)	138.3 (21.80)	135.3 (19.46)	134.9 (18.54)	0.47
Diastolic BP (mmHg)	85.69 (12.23)	84.52 (9.71)	83.50 (11.52)	0.54
Cholesterol (mmol/l)	5.84 (0.87)	5.76 (0.97)	5.72 (0.74)	0.68

Table 9.3c. Plasma NOx, systolic blood pressure (SBP), diastolic blood pressure (DBP) and cholesterol according to –1151 A/C genotype for the Chesterfield (top) and North Mymms (bottom) NPHSII clinics. Genotyping was successful in 140 subjects out of 235 with NOx measurements in the Chesterfield clinic and 276 subjects out of 287 in the North Mymms clinic. No statistically significant association was observed between genotype and NOx (*by Kruskal-Wallis test), blood pressure or cholesterol (by One-way ANOVA).

	Genotype –449G/C			
	GG Mean (SD)	**GC** Mean (SD)	**CC** Mean (SD)	**P**
Combined clinics	N=186	N=184	N=54	
NOx (μmol/l)	11.52 (5.01)	12.10 (8.50)	11.68 (4.82)	0.48*
Systolic BP (mmHg)	139.7 (18.88)	137.0 (18.34)	136.8 (20.41)	0.33
Diastolic BP (mmHg)	86.45 (11.20)	85.61 (10.48)	84.37 (12.37)	0.45
Cholesterol (mmol/l)	5.85 (0.97)	5.75 (1.01)	5.84 (0.95)	0.61

	Genotype –1020C/G		
	CC Mean (SD)	**CG+GG** Mean (SD)	**P**
Combined clinics	N=342	N=102	
NOx (μmol/l)	11.79 (7.02)	11.66 (5.25)	0.59$^{\Psi}$
Systolic BP (mmHg)	138.0 (19.48)	137.6 (17.35)	0.86
Diastolic BP (mmHg)	86.38 (11.47)	86.60 (9.98)	0.33
Cholesterol (mmol/l)	5.79 (0.99)	5.75 (0.90)	0.65

	Genotype –1151A/C			
	AA Mean (SD)	**AC** Mean (SD)	**CC** Mean (SD)	**P**
Combined clinics	N=216	N=184	N=44	
NOx (μmol/l)	11.54 (5.05)	12.12 (8.57)	11.07 (4.00)	0.76*
Systolic BP (mmHg)	139.1 (19.68)	137.3 (18.57)	136.8 (18.80)	0.58
Diastolic BP (mmHg)	86.16 (11.86)	85.25 (10.00)	85.70 (11.97)	0.71
Cholesterol (mmol/l)	5.83 (0.95)	5.76 (1.03)	5.75 (0.94)	0.75

Table 9.3d. Plasma NOx, systolic blood pressure (SBP), diastolic blood pressure (DBP) and cholesterol according to –449G/C (top), -1020C/G (middle) and –1151 A/C (bottom) genotype for the combined Chesterfield and North Mymms NPHSII clinics. No statistically significant association was observed between genotype and NOx, blood pressure or cholesterol by One-way ANOVA or Student t-test unless otherwise stated. *Kruskal-Wallis test, $^{\Psi}$Mann-Whitney test.

9.4.3 Relationship between *DDAH2* genotype and endothelial function in the Cambridge Young Adults Study

9.4.3.1 Baseline demographic details the Cambridge Young Adults Study

Characteristics of the study cohort according to *DDAH2* genotype are shown in tables 9.4a-c. No statistically significant association was observed between genotype and blood pressure, total cholesterol, HDL or LDL ($P \geq 0.05$).

9.4.3.2 *DDAH2* genotype and endothelial function

Subjects from the Cambridge Young Adults Study cohort comprising 264 healthy individuals were analysed for association between genotype and endothelial function. A total of 258 out of 264 individuals recruited were genotyped for the *DDAH2* –1020C/G and -1151A/C polymorphisms, and 261 individuals genotyped for the –871 6G/7G polymorphism and analysed for association with endothelium-dependent and independent (GTN mediated) FMD of the brachial artery. No association was observed between *DDAH2* genotype and either endothelium-dependent FMD or endothelium-independent (GTN mediated) dilation (Table 9.4a-c, $P \geq 0.05$). Furthermore, no association was observed between genotype and endothelial function after heterozygotes and rare homozygotes were grouped together for both the –1151A/C and –871 6G/7G polymorphisms ($P \geq 0.05$, Students t test).

	Genotype -1020C/G		
	CC Mean (SD) N=188	**CG+GG** Mean (SD) N=70	**P**
Age-years	23.44 (1.87)	23.7 (1.90)	0.33
Systolic BP-mmHg	125.4 (14.44)	125.7 (13.18)	0.86
Diastolic BP-mmHg	70.39 (10.09)	70.55 (8.88)	0.91
Cholesterol-mmol/l	4.62 (1.06)	4.55 (0.87)	0.65
LDL cholesterol-mmol/l	2.88 (0.96)	2.78 (0.75)	0.43
HDL cholesterol -mmol/l	1.19 (0.29)	1.21 (0.31)	0.77
FMD-% change	3.41 (2.69)	3.41 (3.37)	0.99
GTN -% change	21.20 (7.86)	22.35 (7.53)	0.31

Table 9.4a Endothelium-dependent and independent FMD and other CVD risk factors according to –1020C/G genotype in the Cambridge Young Adults Study cohort. Due to the small number of GG individuals (N=4) CG+GG individuals were grouped together. No significant difference was observed between genotype and either blood pressure, cholesterol or endothelium-dependent or independent dilation (by Students t test).

	Genotype -1151A/C			
	AA Mean (SD) N=136	**AC** Mean (SD) N=95	**CC** Mean (SD) N=27	**P**
Age-years	23.67 (1.95)	23.30 (1.86)	23.29(1.49)	0.29
Systolic BP-mmHg	125.5 (15.29)	126.7 (15.00)	125.1(14.83)	0.80
Diastolic BP-mmHg	69.85 (8.66)	70.50 (10.38)	72.50(12.56)	0.43
Cholesterol- mmol/l	4.62 (0.93)	4.47 (0.98)	4.88 (1.44)	0.15
LDL cholesterol-mmol/l	2.88 (0.85)	2.73 (0.88)	3.06 (1.24)	0.20
HDL cholesterol-mmol/l	1.18 (0.29)	1.22 (0.29)	1.22 (0.35)	0.56
FMD-% change	3.56 (3.19)	3.22 (2.59)	2.94 (2.30)	0.49
GTN-% change	22.40 (7.64)	20.99 (8.02)	18.62 (6.56)	0.05

Table 9.4b Endothelium-dependent and independent FMD and other CVD risk factors according to –1151A/C genotype in the Cambridge Young Adults Study cohort. No significant difference was observed between genotype and either blood pressure, cholesterol or endothelium-dependent or independent dilation (by One-Way ANOVA).

	Genotype -871 6G/7G			
	6G/6G Mean (SD) N=230	**6G/7G** Mean (SD) N=8	**7G/7G** Mean (SD) N=23	**P**
Age-years	23.43 (1.84)	24.75 (2.12)	23.68 (2.08)	0.13
Systolic BP-mmHg	125.7 (15.08)	130.5 (15.91)	123.0 (13.37)	0.48
Diastolic BP-mmHg	70.33 (9.57)	74.50 (14.74)	68.00 (9.12)	0.27
Cholesterol- mmol/l	4.59 (1.02)	4.85 (0.45)	4.46 (1.16	0.64
LDL cholesterol-mmol/l	2.82 (0.91)	3.28 (0.36)	2.85 (0.98)	0.37
HDL cholesterol-mmol/l	1.21 (0.29)	1.11 (0.22)	1.06 (0.26)	0.06
FMD-% change	3.31 (2.92)	3.72 (2.1)	4.11 (2.83)	0.46
GTN-% change	21.33 (7.67)	22.57 (7.27)	23.18(9.282)	0.55

Table 9.4c Endothelium-dependent and independent FMD and other CVD risk factors according to –871 6G/7G genotype in the Cambridge Young Adults Study cohort. No significant difference was observed between genotype and either blood pressure, cholesterol or endothelium-dependent or independent dilation (by One-Way ANOVA).

9.4.4 Relationship between *DDAH2* genotype and endothelial function in women with normal pregnancies

9.4.4.1 Baseline demographics of the pregnancy cohort

The characteristics of the study cohort according to *DDAH2* genotype are shown in tables 9.5a-c. No significant association was observed between genotype and age, blood pressure, cholesterol, gestational age or parity in this cohort (Tables 9.5a-c, $P \geq 0.05$).

9.4.4.2 *DDAH2* genotype and endothelial function

139 women with normal singleton pregnancies were genotyped for the *DDAH2* –1020C/G, -1151A/C and the –871 6G/7G polymorphisms and analysed for association between genotype and endothelial-dependent FMD. The results show both FMD 1 minute after cuff deflation and the maximum FMD recorded. Genotyping was successful in 137 individuals for the –1020C/G polymorphism and 136 individuals for the –1151A/C and –871 6G/7G polymorphism. No association was observed between *DDAH2* genotype and endothelium-dependent FMD in this cohort (Table 9.5a-c, $P \geq 0.05$).

	Genotype –1020C/G		
	CC Mean (SD) N=105	**CG+GG** Mean (SD) N=32	**P**
Age (Years)	32.02 (4.83)	33.16 (4.36)	0.24
Systolic BP (mmHg)	115.0 (9.87)	117.0 (11.40)	0.32
Diastolic BP (mmHg)	69.48 (6.54)	78.5 (14.20)	0.87
Cholesterol (mmol/l)	5.11 (0.78)	5.12 (0.88)	0.94
Gestational age (weeks)	20.76 (11.66)	21.38 (12.45)	0.79
Parity (N)	0.72 (0.82)	0.78 (1.16)	0.73
FMD at 1 minute (% change)	3.55 (0.56)	3.46 (0.45)	0.43
FMD max (% change)	9.36 (3.50)	9.31 (2.63)	0.94

Table 9.5a Endothelium-dependent FMD and other CVD risk factors according to –1020C/G genotype in the Pregnancy cohort. Due to the small number of GG individuals (N=3), CG+GG individuals were grouped together. No significant association was found between genotype and age, blood pressure, cholesterol, gestational age, parity or FMD (by Students t test).

	Genotype –1151A/C			
	AA Mean (SD) N=58	**AC** Mean (SD) N=65	**CC** Mean (SD) N=13	**P**
Age (Years)	32.66 (4.82)	32.12 (4.41)	31.31 (6.36)	0.62
Systolic BP (mmHg)	115.0 (8.5)	116.2 (11.81)	113.9 (9.723)	0.69
Diastolic BP (mmHg)	68.43 (13.7)	69.31 (7.30)	66.92 (5.88)	0.72
Cholesterol (mmol/l)	5.15 (0.81)	5.15 (0.81)	4.60 (0.65)	0.06
Gestational age (weeks)	19.87 (12.27)	21.17 (11.17)	21.44 (14.68)	0.80
Parity (N)	0.91 (1.08)	0.64 (0.78)	0.38 (0.51)	0.09
FMD at 1 minute (% change)	3.59 (0.66)	3.43 (0.43)	3.69 (0.35)	0.14
FMD max (% change)	9.25 (3.37)	9.64 (3.30)	8.63 (3.07)	0.56

Table 9.5b Endothelium-dependent FMD and other CVD risk factors according to –1151A/C genotype in the Pregnancy cohort. No significant association was found between genotype and age, blood pressure, cholesterol, gestational age, parity or FMD (by One-Way ANOVA).

	Genotype –871 6G/7G		
	6G/6G Mean (SD) N=132	**6G/7G** Mean (SD) N=4	**P**
Age (Years)	32.41 (4.56)	27.75 (8.22)	0.05
Systolic BP (mmHg)	115.5 (10.23)	113.9 (13.49)	0.75
Diastolic BP (mmHg)	68.80 (10.51)	68.75 (9.07)	0.99
Cholesterol (mmol/l)	5.10 (0.81)	5.38 (0.63)	0.49
Gestational age (weeks)	20.75 (11.77)	23.13 (14.81)	0.69
Parity (N)	0.75 (0.92)	0.25 (0.50)	0.28
FMD at 1 minute (% change)	3.52 (0.54)	3.84 (0.20)	0.32
FMD max (% change)	9.38 (3.33)	8.03 (2.71)	0.43

Table 9.5c Endothelium-dependent FMD and other CVD risk factors according to –871 6G/7G genotype in the Pregnancy cohort. No 7G/7G homozygotes were identified in this cohort. No significant association was found between genotype and age, blood pressure, cholesterol, gestational age, parity or FMD (by Students t test).

9.4.5 Relationship between *DDAH2* genotype and endothelial function in the EBCT cohort.

9.4.5.1 Baseline demographics of the EBCT cohort.

Demographic characteristics according to *DDAH2* genotype of the EBCT cohort are shown in tables 9.6a and 9.6b. No significant association was found between *DDAH2* genotype and risk factors for cardiovascular disease including age, sex, smoking status, total cholesterol, HDL and blood pressure ($P \geq 0.05$, tables 9.6a and 9.6b). However, a significant difference in allele distribution was observed between type I diabetics and non-diabetics for both the –1020C/G and –1151A/C polymorphisms (Table 9.7). The rare allele G for the –1020 polymorphism was less frequent amongst diabetics (*P=0.0001), and the rare allele C for the –1151 polymorphism was found to be less frequent amongst non-diabetics (*P=0.0001).

	Genotype –1151A/C			
	AA Mean (SEM) N=112	**AC** Mean (SEM) N=205	**CC** Mean (SEM) N=68	**P**
Age (Years)	38.0 (0.36)	37.8 (0.28)	37.9 (0.5)	0.83
Sex- Number (%)				0.30
Men	63 (55.3)	99 (48.3)	30 (44.12)	
Women	51 (44.74)	106 (51.7)	38 (55.9)	
Smoking status - Number (%)				0.40
Current	32 (28.1)	52 (25.4)	13 (19.12)	
Past	23 (20.3)	52 (25.4)	22 (32.4)	
Never	59 (51.8)	101 (49.3)	33 (48.53)	
Cholesterol (mmol/l)	5.5 (0.1)	5.5 (0.9)	5.3 (0.13)	0.46
HDL (mmol/l)	1.7 (0.04)	1.8 (0.03)	1.8 (0.06)	0.17
Systolic BP (mmHg)	118.5 (1.36)	122.2 (0.96)	122.1 (1.81)	0.07
Diastolic BP (mmHg)	72.4 (0.89)	74.0 (0.62)	72.7 (1.16)	0.27
Calcification	48 (42.86)	89 (44.28)	29 (42.65)	0.96

Table 9.6a Demographic characteristics of the EBCT cohort according to – 1151A/C genotype. Data are presented as mean (SEM). No significant association was found between genotype and age, sex, smoking status, cholesterol, blood pressure or coronary artery calcification (by One-Way ANOVA).

	Genotype –1020C/G			
	CC Mean (SEM) N=327	**CG** Mean (SEM) N=53	**GG** Mean (SEM) N=5	**p**
Age- Years	37.8 (0.22)	38.6 (0.6)	38.2 (1.42)	0.31
Sex- Number (%)				0.65
Men	159 (48.6)	29 (54.7)	2 (40.0)	
Women	168 (51.4)	24 (45.3)	3 (60.0)	
Smoking status - Number (%)				0.17
Current	79 (24.2)	18 (34.0)	0 (0.00)	
Past	83 (25.4)	10 (19.0)	3 (60.0)	
Never	165 (50.5)	25 (47.2)	2 (40.0)	
Cholesterol -mmol/l	5.4 (0.07)	5.5 (0.15)	5.3 (0.39)	0.73
HDL -mmol/l	1.8 (0.03)	1.9 (0.05)	1.5 (0.11)	0.16
Systolic BP-mmHg	121.6 (0.79)	118.9 (2.0)	117.2 (6.03)	0.36
Diastolic BP-mmHg	73.2 (0.5)	74.3 (1.33)	70.9 (4.12)	0.60
Calcification	143 (43.7)	22 (41.5)	2 (40.0)	0.97

Table 9.6b Demographic characteristics of the EBCT cohort according to – 1020C/G genotype. Data are presented as mean (SEM). No significant association was observed between genotype and age, sex, smoking status, cholesterol, blood pressure or coronary artery calcification (by One-Way ANOVA).

	-1151A/C			-1020C/G		
	AA n (%)	**AC** n (%)	**CC** n (%)	**CC** n (%)	**CG** n (%)	**GG** n (%)
Diabetic	33 (17.37)	114 (60.0)	43 (22.63)	175 (93.09)	12 (6.38)	1 (0.53)
Non-diabetic	81 (41.12)	91 (46.19)	25 (12.69)	152 (77.16)	41 (20.81)	4 (2.03)
Significance		*P=0.0001			*P=0.0001	

Table 9.7 Distribution of –1151A/C and –1020C/G alleles according to diabetic status. The rare allele G for the –1020 polymorphism was less frequent amongst diabetics compared to non-diabetics (*P=0.0001), and the rare allele C for the –1151 polymorphism was found to be less frequent amongst non-diabetics (*P=0.0001).

9.4.5.2 *DDAH2* genotype and endothelial function

385 individuals (188 type 1 diabetics, 197 controls) were genotyped for the *DDAH2* –1151A/C and –1020C/G polymorphisms and investigated for association between genotype and endothelium-dependent and independent vascular response as measured by venous occlusion plethysmography. Genotyping was successful in all 385 subjects for the –1020C/G polymorphism and the –1151A/C polymorphism. Flow responses to incremental doses of ACh, BK (endothelium-dependent dilators), GTN (endothelium-independent dilator), LNMMA (endothelium-dependent constrictor) and NA (endothelium-independent constrictor) are shown in figures 9.1a and 9.1b according to *DDAH2* –1020C/G and –1151A/C genotype. Overall, no difference was observed in endothelium-dependent dilator responses between genotypes either before or after adjustment for age and sex ($P \geq 0.05$, figures 9.1a and 9.1b). Neither was any significant difference in vascular function detected when subjects were divided by diabetic or smoking status (appendix 3, tables 1-4). A weak but statistically significant difference in endothelium-independent response (GTN mediated) was observed between –1151AA and –1151CC genotypes (*P=0.02, figure 9.1a). This was also observed when diabetics and non-smokers were analysed separately (P=0.02 and P=0.03 respectively, appendix 3; table 1 and 3). A small but significant difference between genotypes was observed for LNMMA response between –1020 CC and GG diabetic subjects (*P=0.04, appendix 3; table 2).

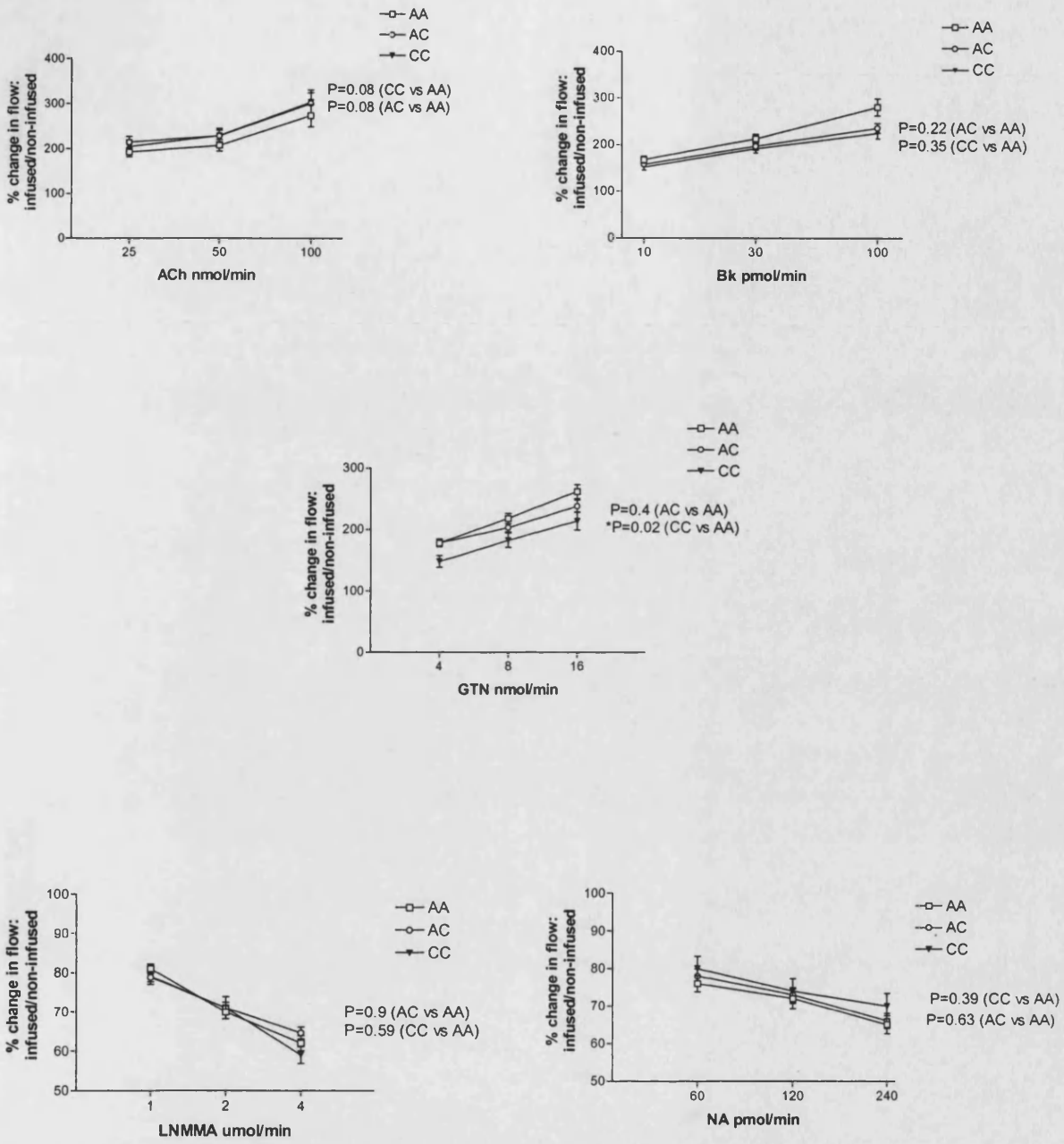

Figure 9.1a Endothelium-dependent and independent vascular responses according to –1151A/C genotype in the EBCT cohort. Data are presented as mean (SEM) % change in flow of infused/non-infused arm during drug treatment after adjustment for baseline flow. Genotypes AC and CC are compared to AA by multiple logistic regression and data are adjusted for age and sex. No significant difference in endothelium-dependent vascular response was observed between genotypes after infusion with acetylcholine (ACh) and bradykinin (BK) (P≥0.05). A significant difference was observed between genotypes AA and CC for endothelium- independent response after infusion of glyceryltrinitrate (GTN) (*P=0.02). No difference was observed in response to LNMMA or noradrenaline (NA) (P≥0.05).

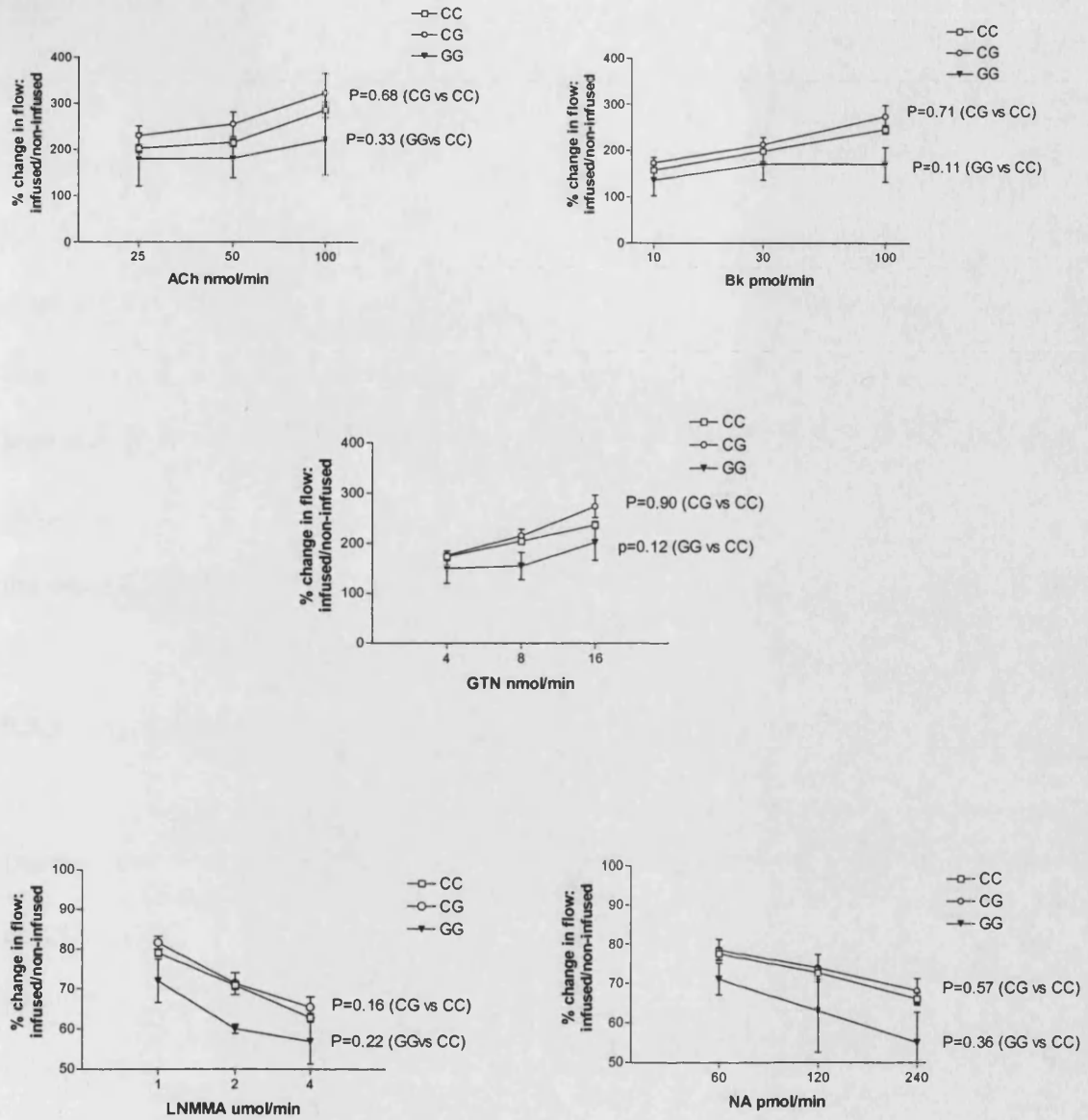

Figure 9.1b Endothelium-dependent and independent vascular responses according to –1020C/G genotype in the EBCT cohort. Data are presented as mean (SEM) % change in flow of infused/non-infused arm in response to drug dosage. Genotypes CG and GG are compared to CC by multiple logistic regression and data are adjusted for age and sex. No significant difference in vascular response was observed between genotypes after infusion with acetylcholine (ACh), bradykinin (BK), glyceryltrinitrate (GTN), LNMMA or noradrenaline (NA) (P≥0.05).

9.5 Discussion

During this study the association between *DDAH2* genotype and plasma NOx was investigated in a subset of healthy individuals selected form the NPHSII cohort. The relationship between *DDAH2* genotype and endothelial function was also explored in a cohort of 264 healthy individuals from the Cambridge Young Adults Study, 139 women with normal pregnancies and a cohort comprising 188 type I diabetics and 197 control subjects. The relationship between *DDAH2* genotype and other relevant risk factors for the development of CVD was also investigated in each cohort.

9.5.1 *DDAH2* genotype and plasma concentrations of NOx in the NPHSII cohort

During this study an association was observed between the *DDAH2* –1020C/G polymorphism and plasma NOx in subjects recruited from the Chesterfield clinic of the NPHSII cohort. However, failure to detect any association between genotype and NOx in the North Mymms clinic or when both clinics were combined indicates that this data needs to be interpreted with caution. These conflicting results could be due a lack of statistical power, differences in dietary NOx intake or undetected inflammatory processes, which would obscure any associations due to production of NO from other NOS isoforms. Alternatively, genetic variation within other genes that influence circulating NO may mask any association between *DDAH2* genotype and plasma NOx. DDAH2 enzyme activity would be expected to affect NO synthesis indirectly via ADMA, therefore any influence of DDAH2 on NO levels may be masked by other factors that affect circulating ADMA such as PRMT activity and LDL cholesterol or renal function. Due to time constraints, the NPHSII cohort was not genotyped for the –

871 6G/7G polymorphism, which in a lucuiferase promoter/reporter system demonstrated functionality when transfected into HUVEC (Chapter 7). Further studies to investigate the association between this variant (and differential DDAH2 expression) and plasma NOx in the NPHSII cohort are planned.

9.5.2 *DDAH2* genotype and endothelial function

The second part of this study investigated the association between *DDAH2* genotype and endothelial function. Endothelial dysfunction is an early marker of CVD and is thought to be a manifestation of deficient NO availability (Clarkson et al., 1997; Gaeta et al., 2000). Although no association was detected between *DDAH2* genotype and ADMA concentration (Chapter 8), the hypothesis explored in this chapter was that *DDAH2* polymorphisms effect local ADMA concentrations and through this, local NO availability and NO-dependent vasodilation. Three cohorts in whom endothelial function had been assessed previously were investigated. Firstly, no association was observed between *DDAH2* genotype and NO-mediated endothelial function in a group of young healthy subjects from the Cambridge Young Adults Study cohort. This same cohort has previously been investigated for association between endothelial function and the eNOS Glu298Asp polymorphism. Overall, no association was observed between this variant and FMD (Leeson et al., 2002), however, FMD was lower in male smokers carrying the Asp allele, suggesting a potential eNOS genotype-environment interaction in this population, and supporting the potential for detecting gene effects on endothelial function in this group. In the present study, with a sample size of 264 individuals, we had 80% power at 2P=0.05 to identify a 28% difference in FMD between groups.

The second cohort studied were women with normal pregnancies. During normal pregnancy there is an increase in circulating blood volume and cardiac output and a decrease in blood pressure due to systemic vasodilation. Some evidence suggests that this vasodilation is due to an increase in NO availability (Nelson et al., 2000), and it has also been shown that the circulating levels of ADMA are significantly lower in pregnant women compared with non pregnant women, suggesting that systemic vasodilation during pregnancy maybe regulated by ADMA (Maeda et al., 2003). In keeping with this, ADMA levels are elevated in preeclampsia (Holden et al., 1998) and in women in early pregnancy prior to the development of preeclampsia (Savvidou et al., 2003). Also, ADMA concentrations in these women correlate with endothelial dysfunction (Savvidou et al., 2003). Therefore we tested the hypothesis that genetic variation in the *DDAH2* gene, that alters DDAH2 transcription *in vitro*, may lead to differences in circulating ADMA levels, which, during pregnancy, might have an impact on maternal vascular endothelial function. However, during this study, no association was observed between *DDAH2* genotype and endothelial function, which suggests genotype does not influence endothelial function in women with normal pregnancies. In addition genotype did not correlate with other parameters (such as cholesterol or blood pressure) that might influence FMD. The cause of elevated ADMA in these individuals is unknown but, as SDMA levels are unchanged, variation in DDAH2 expression or activity is a likely candidate. DDAH2 is highly expressed in the placenta and common genetic variation in the *DDAH2* gene in this tissue may be important for differences in circulating levels of ADMA. Further work to characterise the expression of placental DDAH2 in women with preeclampsia and to determine the effects of DDAH2 variants in the susceptibility to preeclampsia is necessary.

The final part of this study investigated the association between *DDAH2* genotype and endothelial function in a cohort of diabetic patients and controls. A previous study in this cohort demonstrated dysfunction of endothelium-dependent vasodilation in diabetic subjects (Chan et al., 2003). However, the precise mechanisms behind endothelial dysfunction and increased risk of CVD seen in diabetics is still unknown. In this cohort, only ~13% of the variation in endothelial function could be explained by the presence of conventional CVD risk factors (Chan et al., 2001) suggesting, perhaps, that genetic and other influences may be important. However, during this study no association was observed between *DDAH2* genotype and endothelium-dependent function either when the whole cohort was analysed or when diabetics and non-diabetics and smokers and non-smokers were analysed separately, suggesting that *DDAH2* genotype does not play a significant role in regulation of endothelial function in this cohort.

One interesting observation to emerge from this study was the difference in allele distribution between diabetics and non-diabetics for both the –1020C/G and –1151A/C polymorphisms. However, this may be explained by the location of the *DDAH2* gene within the MHC class III region on chromosome 6, a region that has been strongly linked with type1 diabetes in previous studies (Field, 2002). Therefore it is possible that these *DDAH2* polymorphisms maybe acting as a marker for the presence of type1 diabetes in this cohort.

In summary, no association was observed between *DDAH2* genotype and endothelial function in young healthy subjects, in women with normal pregnancies or in a cohort of diabetic patients and controls. These data are in keeping with the findings of chapter 8

in which no association was detected between *DDAH2* genotype and ADMA concentration or ADMA/SDMA ratio. They are at odds however, with the findings of chapter 7 where in an *in vitro* reporter system, *DDAH2* promoter genotype was found to alter promoter activity. Taken together, these observations indicate that, in the healthy state *in vivo*, and despite the potential for *DDAH2* genotype to modulate DDAH2 transcription *in vitro*, it does not have a significant impact upon endothelial function. The reasons for this discrepancy between *in vitro* and *in vivo* observations are worthy of further investigation. Further research is also needed to ascertain whether *DDAH2* genotype is an important modulator of DDAH2 expression in the presence of other disorders or risk factors known to result in elevated circulating ADMA.

CHAPTER 10

GENERAL CONCLUSIONS

Despite numerous scientific breakthroughs in the understanding of the complex nature of the cardiovascular system and its disorders, cardiovascular disease remains the UK's biggest cause of mortality (BHF, 2003). It is fully recognized that environmental risk factors such as a diet rich in cholesterol, smoking and the presence of diseases such as diabetes and renal failure are major players in the cause of vascular disease. However a vast amount of evidence now implicates an individual's genotype as a relevant determinant of disease development. Research into some rare monogenic disorders such as familial hypercholesterolaemia has helped to gain an insight into genes, which may be influential in the more complex multi-factorial vascular disease process. It is envisaged that each individual carries a complement of such common susceptibility alleles ('a genetic load') and that the interaction between susceptibility genes and the environment determines the development of cardiovascular disease.

A plethora of genes have been associated with carrying an increased risk of developing cardiovascular disease such as those involved in lipid metabolism, blood pressure regulation and coagulation (Nakai et al., 2002; Yamada et al., 2002). The essential role of the endothelium for the maintenance of a healthy vasculature has focused one area of the search on genes that are expressed by the endothelial cell. The discovery that one product of the endothelium, the simple gaseous molecule NO which, has many atheroprotective functions (Ignarro et al., 1987), has led to an explosion of research into the regulation of NO synthesis and degradation.

During this study, genes encoding proteins in three different pathways implicated in the regulation of NO activity have been investigated. Firstly, inactivation of NO by O_2^- is thought to be one explanation for diminished endothelial function in some individuals (Kodja et al., 1999), and has prompted investigations into the enzymes responsible for O_2^- production such as NADPH oxidase. This study investigated the hypothesis that endothelium-dependent vaso-reactivity in healthy subjects would be dependent on genotype for the C242T polymorphism of the NADPH oxidase subunit - *p22phox*. The results demonstrated that a significant difference in endothelium-dependent vasodilation of the brachial artery does indeed exist between individuals of different genotype. Subjects who carried two copies of the 242T allele demonstrated augmented FMD of the brachial artery (an NO-dependent response) compared to subjects carrying the C allele. This implies that these individuals may have a preserved NO response due to decreased NADPH oxidase activity. A second study using venous occlusion plethysmography to assess endothelial function in the resistance arteries of the forearm, failed to reproduce this association in a case-control study of type 1 diabetic subjects. One potential explanation for this discrepancy is that endothelium-dependent vasodilation in resistance vessels is dependent more on the dilator substance EDHF than on NO.

The synthesis of NO from L-arginine requires BH_4, an essential cofactor for the NOS enzymes. In a second study, the hypothesis that common genetic polymorphisms within the human *GCH1* gene (the rate-limiting enzyme in the BH_4 synthesis reaction) could influence pterin synthesis and endothelial function was explored. Three bi-allelic variants within the *GCH1* promoter were identified, two of which correlated with plasma neopterin

(an index of pterin pathway activity) in healthy subjects, suggesting the synthesis of the NOS cofactor BH_4 is genetically determined. In addition, the finding that *GCH1* genotype was associated with NO-mediated, endothelium-dependent vasodilation of the brachial artery supports further the hypothesis that *GCH1* genotype can influence NO synthesis through the availability of BH_4. Future studies to investigate whether these *GCH1* promoter polymorphisms influence gene transcription, and therefore could account for the difference in neopterin seen in this study are needed. A system such as the luciferase reporter gene assay described in Chapter 7 will be used in this study.

Finally, the third series of investigations examined a pathway known to be involved in the regulation of NO synthesis through inhibition of NOS. The main objectives of this series of studies was to identify common polymorphisms in the *DDAH2* gene and investigate the relationship between *DDAH2* genotype and circulating levels of the NOS inhibitor ADMA. The relationship between *DDAH2* genotype and conventional CVD risk factors including endothelial function was also explored. Elevated ADMA levels are a common feature in patients with vascular disease including diabetics, subjects with renal failure and preeclampsia. The identification of several polymorphisms within the *DDAH2* promoter region, two of which are situated in transcription factor binding sequences, suggests that *DDAH2* transcription could be genetically regulated. This hypothesis was explored by a promoter/reporter assay, which confirmed different promoter activities for the variant alleles at position –871. Disappointingly, the present study failed to identify any association between *DDAH2* genotype and ADMA, ADMA/SDMA ratio or endothelial function, but given the rarity of the –871 variant among Caucasian subjects future large

scale genotyping studies including a wide range of disease phenotypes may be required to fully test the hypothesis that this DDAH2 variant is an important determinant of vascular disease development.

To conclude, the findings of this study indicate that some, but not all, common genetic variation within genes involved in NO synthesis and inactivation are associated with differences in endothelial function that predates and predisposes to atherosclerosis. It is likely that a combination of polymorphisms in a wide variety of genes interact to compose the genetic element of CVD and these polymorphisms in turn are modulated by the environment. During this study the completion of the human genome project was announced, which together with advances in large-scale genotyping efforts makes the prospect of defining multiple gene-gene interactions and their impact on complex diseases a potentially realisable goal in the not too distant future.

Appendix I

Hardy-Weinberg Principle

The relationship between the genotypic frequency and allelic frequency of a population was described by Godfrey Hardy and Wilhelm Heinberg in 1908, and became know as the Hardy-Weinberg principle. *The principle states that after one generation of random mating single locus genotypic frequencies can be represented as a function of the allelic frequencies (Hardy, 1908).* If a gene has two alleles designated *A* and *a*, then the frequency of these alleles in a population is *p* and *q* respectively where p+q=1. If random mating occurs (i.e. random union of male and female gametes) then the frequency of the offspring will be as follows:

		Male gametes	
		A (*p*)	a (*q*)
Female gametes	A (*p*)	AA (p^2)	Aa (*pq*)
	A (*q*)	Aa (*pq*)	Aa (q^2)

$$p^2+2pq+q^2=1$$

To determine whether the observed number of genotypes differs from those expected under the Hardy-Weinberg rule the Chi –square test (χ^2) is applied:

$$\chi^2 = \sum \frac{(O-E)^2}{E}$$

Appendix II

Linkage disequilibrium

Two genes (or in the context of this thesis-polymorphisms) in relative close proximity on the same chromosome are said to be linked. The closer the polymorphisms are to one-another, the less likely genetic recombination between them during gamete formation.

Linkage disequilibrium (non-random association) between alleles of two polymorphisms was calculated by Chakravarti et al, 1984.

Two loci A and B each with two allelic variants A1A2 and B1B2 will result in the production of gametes: A1B1, A1B2, A2B1, A2B2. The corresponding frequency of each gamete will be; $P_{11}=p1q1+\Delta$ for A1B1

$P_{12}=p1q2-\Delta$ for A1B2

$P_{21}=p2q1-\Delta$ for A2B1

$P_{22}=p2q2+\Delta$ for A2B2

Δ measures the non-random association or linkage disequilibrium between alleles.

$$\Delta = \frac{P_{11}P_{22}-P_{12}P_{21}}{\sqrt{(P_{11}+P_{12})(P_{21}+P_{22})(P_{11}+P_{21})(P_{12}+P_{22})}}$$

Δ values range between 0 and 1. The closer the Δ value is to 1 the more tightly linked the two loci. A negative Δ value indicates the rare allele at one loci is in complete linkage with the common allele at the second loci.

Appendix III

The difference in vascular responses between genotypes for Diabetics and non-diabetics and smokers and non-smokers.

Genotype –1151A/C

	Diabetics		Non-Diabetics	
	AA versus AC β coef (P)	**AA versus CC** β coef (P)	**AA versus AC** β coef (P)	**AA versus CC** β coef (P)
Ach	0.08 (0.40)	0.12 (0.29)	0.17 (0.13)	0.15 (0.40)
BK	-0.05 (0.45)	-0.04 (0.60)	-0.08 (0.36)	-0.07 (0.61)
GTN	-0.06 (0.29)	-0.18 (0.02)*	-0.01 (0.91)	-0.13 (0.30)
NA	0.01 (0.78)	-0.01 (0.8)	0.01 (0.80)	0.09 (0.18)
LNMMA	0.03 (0.34)	-0.004 (0.91)	-0.02 (0.48)	-0.02 (0.70)

Table 1. Vascular response of Diabetic and Non-diabetic subjects according to –1151 A/C genotype. Vascular response in AA genotypes were compare with AC and CC genotypes. A significant difference in endothelium independent response was observed between individuals genotyped as AA compared to CC individuals in the diabetic patients only (*P=0.02). Data are adjusted for age and sex.

Genotype –1020C/G

	Diabetics		Non-Diabetics	
	CC versus GC β coef (P)	**CC versus GG** β coef (P)	**CC versus GC** β coef (P)	**CC versus GG** β coef (P)
Ach	-0.07 (0.63)	-0.22 (0.52)	0.07 (0.56)	-0.18 (0.58)
BK	-0.06 (0.57)	-0.08 (0.75)	0.06 (0.48)	-0.37 (0.12)
GTN	-0.04 (0.67)	0.22 (0.35)	-0.00 (0.98)	-0.47 (0.02)*
NA	0.06 (0.35)	-0.10 (0.54)	0.00 (0.99)	-0.07 (0.56)
LNMMA	0.03 (0.46)	-0.19 (0.04)*	0.04 (0.18)	-0.01 (0.87)

Table 2. Vascular response of Diabetic and Non-diabetic subjects according to –1020 C/G genotype. Vascular response in CC genotypes were compare with GC and GG genotypes. A significant difference in endothelium independent response was observed between individuals genotyped as CC compared to GG individuals in the Non-diabetic patients only (*P=0.02). A weak significance was also observed for LNMMA response between CC and GG diabetic subjects (*P=0.04). Data are adjusted for age and sex.

Genotype –1151A/C

	Smokers		Non-Smokers	
	AA versus AC β coef (P)	**AA versus CC** β coef (P)	**AA versus AC** β coef (P)	**AA versus CC** β coef (P)
Ach	0.20 (0.19)	0.27 (0.23)	0.08 (0.29)	0.14 (0.22)
BK	0.09 (0.36)	0.16 (0.28)	-0.12 (0.06)	-0.14 (0.12)
GTN	0.06 (0.59)	-0.15 (0.32)	-0.06 (0.25)	-0.16 (0.03)*
NA	0.08 (0.33)	0.13 (0.27)	-0.002 (0.95)	0.01 (0.76)
LNMMA	0.01 (0.69)	-0.02 (0.68)	-0.01 (0.53)	-0.001 (0.96)

Table 3. Vascular response of Smokers and Non-smokers according to –1151 A/C genotype. Vascular response in AA genotypes were compare with AC and CC genotypes. A significant difference in endothelium independent response was observed between individuals genotyped as AA compared to CC individuals insmokers only (*P=0.03). Data are adjusted for age and sex.

	Genotype –1020C/G			
	Smokers		**Non-Smokers**	
	CC versus CG β coef (P)	**CC versus GG** β coef (P)	**CC versus CG** β coef (P)	**CC versus GG** β coef (P)
Ach	0.24 (0.08)	-	-0.04 (0.69)	-0.26 (0.24)
BK	-0.05 (0.56)	-	0.11 (0.22)	-0.28 (0.12)
GTN	-0.11 (0.23)	-	0.06 (0.42)	-0.22 (0.15)
NA	0.007 (0.92)	-	0.03 (0.47)	-0.09 (0.29)
LNMMA	-0.01 (0.88)	-	0.04 (0.15)	-0.05 (0.38)

Table 4. Vascular response of Smokers and Non-smokers according to –1020 C/G genotype. Vascular response in CC genotypes was compared with both GC and GG genotypes for Non-smokers. Vascular response of CC genotypes was compared to CG genotypes in smokers, no GG subjects were found among the smoking group. No difference in vascular response was observed between genotypes in either smokers or non-smokers. Data are adjusted for age and sex.

References

Achan V, Tran CT, Arrigoni F, Whitley GS, Leiper JM, Vallance P. all-trans-Retinoic acid increases nitric oxide synthesis by endothelial cells: a role for the induction of dimethylarginine dimethylaminohydrolase. *Circulation Res* 2002 Apr 19; 90(7): 764-9

Achan V, Broadhead M, Malaki M, Whitley GS, Leiper J, MacAllister R, Vallance P. Asymmetric Dimethylarginine Causes Hypertension and Cardiac Dysfunction in Humans and Is Actively Metabolized by Dimethylarginine Dimethylaminohydrolase. *Arterioscler Thromb Vasc Biol.* 2003 Jun 12

Alderton WK, Boyhan A, Lowe PN. Nitroarginine and tetrahydrobiopterin binding to the haem domain of neuronal nitric oxide synthase using a scintillation proximity assay. *Biochem J* 1998 332: 195-201

Alderton WK, Cooper CE, Knowles RG. Nitric oxide synthases: structure, function and inhibition. *Biochem J* 2001 Aug 1; 357(Pt 3): 593-615

Anastasiadis PZ, Kuhn DM, Blitz J, Imerman BA, Louie MC, Levine RA. Regulation of tyrosine hydroxylase and tetrahydrobiopterin biosynthetic enzymes in PC12 cells by NGF, EGF and IFN-gamma. *Brain Res* 1996 Mar 25; 713(1-2): 125-33

Azumi H, Inoue N, Takeshita S, Rikitake Y, Kawashima S, Hayashi Y, Itoh H, Yokoyama M. Expression of NADH/NADPH oxidase p22phox in human coronary arteries. *Circulation* 1999 Oct 5; 100(14): 1494-8

Baker TA, Milstien S, Katusic ZS. Effect of vitamin C on the availability of tetrahydrobiopterin in human endothelial cells. *J Cardiovasc Pharmacol* 2001 Mar; 37 (3): 333-8

Bandmann O, Valente EM, Holmans P, Surtees RA, Walters JH, Wevers RA, Marsden CD, Wood NW. Dopa-responsive dystonia: a clinical and molecular genetic study. *Ann Neurology* 1998 Oct; 44(4): 649-56

Bandmann O, Wood NW. Dopa-responsive dystonia-the story so far. *Neuropediatrics* 2002 Feb; 33(1): 1-5

Barbacanne MA, Souchard JP, Darblade B, Iliou JP, Nepveu F, Pipy B, Bayard F, Arnal JF. Detection of superoxide anion released extracellularly by endothelial cells using cytochrome c reduction, ESR, fluorescence and lucigenin-enhanced chemiluminescence techniques. *Free Radical Biol Med* 2000 Sep 1; 29(5): 388-96

Barker PA. p75NTR: A study in contrasts. *Cell Death Differ* 1998 May; 5(5): 346-56

Barry-Lane PA, Patterson C, van der Merwe M, Hu Z, Holland SM, Yeh ET, Runge MS. p47phox is required for atherosclerotic lesion progression in ApoE(-/-) mice. *J Clin Invest.* 2001 Nov;108(10):1513-22

Bath PMW, Hassall DG, Gladwin AM *et al.* Nitric oxide and Protacyclin. *Arterioscler Thromb.* 1991 11: 54-260

Bath PMW. The effect of nitric oxide–donating vasodilators on monocyte chemotaxis and intracellular cGMP concentrations in vitro. *Eur J Clin. Pharmacol.* 1993 45: 53-58

Beckman JS, Beckman TW, Chen J, Marshall PA, Freeman BA. Apparent hydroxyl radical production by peroxynitrite: implications for endothelial injury from nitric oxide and superoxide. *Proc Natl Acad Sci U S A.* 1990 Feb; 87(4): 1620-4

Beckman JS, Crow JP. Pathological implications of nitric oxide, superoxide and peroxynitrite formation. *Biochem Soc Trans* 1993 May; 21(2): 330-4

Benjamin R, Parham P. Guilt by association: HLA-B27 and ankylosing spondylitis. *Immunol Today* 1990 Apr; 11(4): 137-42

Benjamin N, Calver A, Collier J, Robinson B, Vallance P, Webb D. Measuring forearm blood flow and interpreting the responses to drugs and mediators. *Hypertension.* 1995 May;25(5):918-23.

Bennett MR, Evan GI, Schwartz SM. Apoptosis of human vascular smooth muscle cells derived from normal vessels and coronary atherosclerotic plaques. *J Clin Invest* 1995 May; 95(5): 2266-74

Bennett MR, Macdonald K, Chan SW, Boyle JJ, Weissberg PL. Cooperative interactions between RB and p53 regulate cell proliferation, cell senescence, and apoptosis in human vascular smooth muscle cells from atherosclerotic plaques. *Circulation Res* 1998 Apr 6; 82(6): 704-12

Berdowska A, Zwirska-Korczala K. Neopterin measurement in clinical diagnosis. *J Clin Pharm Ther* 2001 Oct; 26(5): 319-29

Bertrams J. The HLA association of insulin-dependent (type I) diabetes mellitus. *Behring Inst Mitt* 1984 Jul; (75): 89-99

Bhunia AK, Arai T, Bulkley G, Chatterjee S. Lactosylceramide mediates tumor necrosis factor-alpha-induced intercellular adhesion molecule-1 (ICAM-1) expression and the adhesion of neutrophil in human umbilical vein endothelial cells. *J Biol Chem* 1998 Dec 18; 273(51): 34349-57

Bierman EL. George Lyman Duff Memorial Lecture. Atherogenesis in diabetes. *Arterioscler Thromb* 1992 Jun; 12(6): 647-56

Black AR, Azizkhan –Clifford J. Regulation of E2F: a family of transcription factors involved in proliferation control. *Gene* 1999 237: 281-302

Bode-Boger SM, Boger RH, Creutzig A, Tsikas D, Gutzki FM, Alexander K, Frolich JC. L-arginine infusion decreases peripheral arterial resistance and inhibits platelet aggregation in healthy subjects. *Clin Sci (Lond).* 1994 Sep; 87(3): 303-10

Boerwinkle E. A contemporary research paradigm for the genetic analysis of a common chronic disease. *Ann Med* 1996 Oct; 28(5): 451-7

Bogdan C, Rollinghoff M, Diefenbach A. The role of nitric oxide in innate immunity. *Immunol Rev* 2000 Feb; 173: 17-26

Boger RH, Bode-Boger SM, Thiele W, Junker W, Alexander K, Frolich JC. Biochemical evidence for impaired nitric oxide synthesis in patients with peripheral arerial occlusive disease. *Circulation* 1997 95: 2068-2074

Boger RH, Bode-Boger SM, Thiele W, Creutzig A, Alexander K, Frolich J. Restoring Vascular Nitric Oxide Formation by L-Arginine Improves the Symptoms of Intermittent Claudication in Patients With Peripheral Arterial Occlusive Disease. *J Am Coll Cardio.* 1998a 32: 1336-44

Boger RH, Bode-Boger SM, Szuba A, Tsao PS, Chan JR, Tangphao O, Blaschke TF, Cooke JP. Asymmetric dimethylarginine (ADMA): A novel risk factor for endothelial function. *Cirulation* 1998b; 98: 1842-1847.

Boger RH, Sydow K, Borlak J, Thum T, Lenzen H, Schubert B, Tsikas D, Bode-Boger SM. LDL cholesterol upregulates synthesis of asymmetrical dimethylarginine in human endothelial cells: involvement of S-adenosylmethionine-dependent methyltransferases. *Circulation Res.* 2000 Jul 21; 87(2): 99-105

Bonnardeaux A, Nadaud S, Charru A, Jeunemaitre X, Corvol P, Soubrier F. Lack of evidence for linkage of the endothelial cell nitric oxide synthase gene to essential hypertension. *Circulation* 1995 Jan 1; 91(1): 96-102

Bossone SA, Asselin C, Patel AJ, Marcu KB. MAZ, a zinc finger protein, binds to c-MYC and C2 gene sequences regulating transcriptional initiation and termination. *Proc Natl Acad Sci U S A* 1992 Aug 15; 89(16): 7452-6

Bredt D S, Snyder S H. Isolation of nitric oxide synthetase, a calmodulin-requiring enzyme. *Proc. Natl. Acad. Sci USA* 1990; Vol 87: 682-685.

Brenman JE, Xia H, Chao DS, Black SM, Bredt DS. Regulation of neuronal nitric oxide synthase through alternative transcripts. *Dev Neurosci* 1997; 19(3): 224-31

Brown MA, Pile KD, Kennedy LG, Campbell D, Andrew L, March R, Shatford JL, Weeks DE, Calin A, Wordsworth BP. A genome-wide screen for susceptibility loci in ankylosing spondylitis. *Arthritis Rheum* 1998 Apr; 41(4): 588-95

Cahilly C, Ballantyne C, Lim D, Gotto A, Marian AJ. A variant of p22phox, Involved in Generation of Reactive Oxygen Species in the Vessel Wall, Is Associated With Progression of Coronary Atheroslerosis. *Circulation Res.* 2000; 86: 391-395

Cai H, Duarte N, Wilcken DE, Wang XL. NADH/NADPH oxidase p22 phox C242T polymorphism and coronary artery disease in the Australian population. *Eur J Clin Invest* 1999 Sep; 29(9): 744-8

Canaud B, Cristol JP, Morena M. Imbalance of oxidants and antioxidants in haemodialysed patients. *Blood Purif.* 1999; 17: 99-106

Cantarella G, Lempereur L, Presta M, Ribatti D, Lombardo G, Lazarovici P, Zappala G, Pafumi C, Bernardini R. Nerve growth factor-endothelial cell interaction leads to angiogenesis in vitro and in vivo. *FASEB J* 2002 Aug; 16(10): 1307-9

Celermajer DS, Sorensen KE, Gooch VM, Spiegelhalter DJ, Miller OI, Sullivan ID, Lloyd JK, Deanfield JE. Non-invasive detection of endothelial dysfunction in children and adults at risk of atherosclerosis. *Lancet.* 1992 Nov 7; 340(8828): 1111-5.

Celermajer DS, Sorensen KE, Bull C, Robinson J, Deanfield JE. Endothelium-dependent dilation in the systemic arteries of asymptomatic subjects relates to coronary risk factors and their interaction. *J Am Coll Cardiol.* 1994 Nov 15; 24(6): 1468-74

Chakravarti A, Li CC, Buetow KH. Estimation of the marker gene frequency and linkage disequilibrium from conditional marker data. *Am J Hum Genet.* 1984 Jan; 36(1): 177-86

Chaldakov GN, Stankulov IS, Fiore M, Ghenev PI, Aloe L. Nerve growth factor levels and mast cell distribution in human coronary atherosclerosis. *Atherosclerosis* 2001 Nov; 159(1): 57-66

Chan NN, Colhoun HM, Vallance P. Cardiovascular risk factors as determinants of endothelium-dependent and endothelium-independent vascular reactivity in the general population. J Am Coll Cardiol. 2001 Dec;38(7):1814-20.

Chan NN, Vallance P, Colhoun HM. Endothelium-Dependent and -Independent Vascular Dysfunction in Type 1 Diabetes. Role of Conventional Risk Factors, Sex, and Glycemic Control. *Arterioscler Thromb Vasc Biol.* 2003 Jun 1; 23(6): 1048-54

Charles IG, Chubb A, Gill R, Clare J, Lowe PN, Holmes LS, Page M, Keeling JG, Moncada S, Riveros-Moreno V. Cloning and expression of a rat neuronal nitric oxide synthase coding sequence in a baculovirus/insect cell system. *Biochem Biophys Res Commun* 1993 Nov 15; 196(3): 1481-9

Charles IG, Scorer CA, Moro MA, Fernandez C, Chubb A, Dawson J, Foxwell N, Knowles RG, Baylis SA. Expression of human nitric oxide synthase isozymes *Methods Enzymol.* 1996; 268: 449-60

Chester AH, Borland JAA, Buttery LDK, Mitchell JA, Cunningham DA, Hafizi S, Hoare GS, Springall DR, Polak JM, Yacoub MH. Induction of nitric oxide synthase in human vascular smooth muscle: interactions between proinflammatory cytokines. *Cardiovascular Res.* 1998; 38: 814-821

Cimato TR, Tang J, Xu Y, Guarnaccia C, Herschman HR, Pongor S, Aletta JM. Nerve growth factor-mediated increases in protein methylation occur predominantly at type I arginine methylation sites and involve protein arginine methyltransferase 1. *J Neurosci Res* 2002 Feb 15; 67(4): 435-42

Clarke S. Protein methylation. *Curr Opin Cell Biol* 1993 Dec; 5(6): 977-83

Clarkson P, Celermajor DS, Powe AJ, Donald AE, Henry RMA, Deanfield JE. Endothelium-Dependent Dilatation is Impaired in Young Healthy Subjects with a Family History of Premature Coronary Disease. *Circulation* 1997; 96: 3378-3383

Cockell AP, Poston L. Flow-mediated vasodilatation is enhanced in normal pregnancy but reduced in preeclampsia. *Hypertension* 1997 Aug; 30(2 Pt 1): 247-51

Colhoun HM, Rubens MB, Underwood RS, Fuller JH. The Effect of Type1 Diabetes Mellitus on the Gender Difference in Coronary Artery Calcification. *J Am Coll Cardiol.* 2000; 36: 2160-7

Cornhill JF, Roach MR. A quantitative study of the localization of atherosclerotic lesions in the rabbit aorta. *Atherosclerosis* 1976 May-Jun; 23(3): 489-501

Cross J, Donald A, Vallance P J, Deanfield J E, Woolfson R G, MacAllister R J. Dialysis improves endothelial function in humans. *Nephrol Dial Transplant* 2001 16; 1823-1829

Danesh J, Collins R, Peto R. Lipoprotein(a) and coronary heart disease. Meta-analysis of prospective studies. *Circulation.* 2000 Sep 5;102(10):1082-5

Dawson SJ, Wiman B, Hamsten A, Green F, Humphries S, Henney AM. The two allele sequences of a common polymorphism in the promoter of the plasminogen activator inhibitor-1 (PAI-1) gene respond differently to interleukin-1 in HepG2 cells. *J Biol Chem* 1993 May 25; 268(15): 10739-45

Dawson TM, Dawson V. Nitric Oxide Synthase: Role as a Transmitter/Mediator in the Brain and Endocrine System. *Ann. Rev. Med.* 1996; 47: 219-27

de Boer M, de Klein A, Hossle JP, Segar R, Corbeel L, Weening RS, Roos D. Cytochrome b558-negative, autosomal recessive chronic granulatomous disease: two new mutations in the cytochrome b558 light chain of the NADPH oxidase (p22-phox). *Am J Hum Genet* 1992; 51(5): 1127-1135

De Keulenaer GW, Alexander RW, Ushio-Fukai M, Ishizaka N, Griendling KK. Tumour necrosis factor alpha activates a p22phox-based NADH oxidase in vascular smooth muscle. *Biochem J* 1998 Feb 1; 329 (Pt 3): 653-7

Diamondstone LS, Tollerud DJ, Fuchs D, Wachter H, Brown LM, Maloney E, Kurman CC, Nelson DL, Blattner WA. Factors influencing serum neopterin and beta 2-microglobulin levels in a healthy diverse population. *J Clin Immunol.* 1994 Nov;14(6):368-74

Dinauer MC, Pierce EA, Burns GA, Curnutte JT, Orkin SH. Human neutrophil cytochrome b light chain (p22-phox). Gene structure, chromosomal location, and mutations in cytochrome-negative autosomal recessive chronic granulomatous disease. *J Clin Invest* 1990; 86(5): 1729-37

Dinauer MC, Pierce EA, Erickson RW, Muhlebach TJ, Messner H, Orkin SH, Seger RA, Curnutte JT. Point mutation in the cytoplasmic domain of the neutrophil p22-phox cytochrome b subunit is associated with a nonfunctional NADPH oxidase and chronic granulomatous disease. *Proc Natl Acad Sci U S A* 1991 Dec 15; 88(24): 11231-5

Dostch J, Hogen N, Nyul Z, Hanze J, Knerr I, Kirschbaum M, Rascher W. Increase of endothelial nitric oxide synthase and endothelin-1 mRNA expression in human placenta during pregnancy. *Eur J Obst and Gynecol and reproductive biology* 2001; 97: 163-167

Duch DS, Smith GK. Biosynthesis and function of tetrahydrobiopterin. *J. Nutr. Biochem.* 1991; 2: 411-423

Duncan DD, Stupakoff A, Hedrick SM, Marcu KB, Siu G. A Myc-associated zinc finger protein binding site is one of four important functional regions in the CD4 promoter. *Mol Cell Biol* 1995 Jun; 15(6): 3179-86

Eichner JE, Dunn ST, Perveen G, Thompson DM, Stewart KE, Stroehla BC. Apolipoprotein E polymorphism and cardiovascular disease: a HuGE review. *Am J Epidemiol* 2002 Mar 15; 155(6): 487-95

Fei J, Viedt C, Soto U, Elsing C, Jahn L, Kruezer J. Endothelin-1 and Smooth Muscle Cells. Induction of Jun Amino-Terminal Kinase Through an Oxygen Radical-Sensitive Mechanism. *Arterioscler Thromb Vasc Biol* 2000; 20: 1244-1249

Field LL. Genetic linkage and association studies of Type I diabetes: challenges and rewards. *Diabetologia.* 2002 Jan; 45(1): 21-35

Fleck C, Janz A, Schweitzer F, Karge E, Schwertfeger M, Stein G. Serum concentrations of asymmetric (ADMA) and symmetric (SDMA) dimethylarginine in renal failure patients. *Kidney Int Suppl.* 2001 Feb; 78: S14-8

Foley RN, Parfrey PS, Sarnak MJ. Cardiovascular disease and morbididty in ESRD. *J Nephrol.* 1998a Sep-Oct; 11 (5): 239-245

Foley RN, Parfrey PS, Sarnak MJ. Epidemiology of cardiovascular disease in chronic renal disease. *J Am Soc Nephrol.* 1998b Dec; 9 (12 suppl): S16-23

Forstermann U, Closs EI, Pollock JS, Nakane M, Schwarz P, Gath I, Kleinert H. Nitric oxide synthase isozymes. Characterisation, purification, molecular cloning and functions. *Hypertension* 1994; Vol 23: 1121-1131

Fujiwara N, Osanai T, Kamada T, Katoh T Takahashi K, Okumura K. Study on the relationship between plasma nitrite and nitrate level and salt sensitive in human hypertension. *Circulation* 2000; 101: 856-861

Fukai T, Galis ZS, Meng XP, Parthasarathy S, Harrison DG. Vascular expression of extracellular superoxide dismutase in atherosclerosis. *J Clin Invest* 1998 May 15; 101(10): 2101-11

Fukai T, Folz RJ, Landmesser U, Harrison DG. Extracellular superoxide dismutase and cardiovascular disease. *Cardiovascular Res* 2002 Aug 1; 55(2): 239-49

Fukuda Y, Teragawa H, Matsuda K, Yamagata T, Matsuura H, Chayama K. Tetrahydrobiopterin restores endothelial function of coronary arteries in patients with hypercholesterolaemia. *Heart.* 2002 Mar;87(3):264-9

Fukui T, Ishizaka N, Rajagopalan S, Laursen JB, Capers Q 4th, Taylor WR, Harrison DG, de Leon H, Wilcox JN, Griendling KK. p22phox mRNA expression and NADPH oxidase activity are increased in aortas from hypertensive rats. *Circulation Res* 1997 Jan; 80(1): 45-51

Furchgott R F, Zawadski J V. The Obligatory Role of Endothelial Cells in the Relaxation of Arterial Smooth Muscle be Acetylcholine. *Nature* 1980; Vol 288: 373-376

Gaeta G, De Michele M, Cuomo S, Guarini P, Foglia MC, Bond G, Trevisan M. Arterial abnormalities in the offspring of patients with premature myocardial infarction. *New Engl J Med* 2000 Vol 343; 12: 840-846

Gardemann A, Mages P, Katz N, Tillmanns H, Haberbosch W. The p22 phox A640G gene polymorphism but not the C242T gene variation is associated with coronary heart disease in younger individuals. *Atherosclerosis* 1999 Aug; 145(2): 315-23

Garland CJ, Plane F, Kemp BK, Cocks TM. Endothelium-dependent hyperpolarization: a role in the control of vascular tone. *Trends Pharmacol Sci.* 1995 Jan;16(1):23-30

Geiszt M, Kopp JB, Varnai P, Leto TL. Identification of renox, an NAD(P)H oxidase in kidney. *Proc Natl Acad Sci U S A* 2000 Jul 5; 97(14): 8010-4

Ghosh DK, Abu-Soud HM, Stuehr DJ. Domains of Macrophage NO Synthase Have Divergent Roles in Forming and Stabilizing the Active Dimeric Enzyme. *Biochemistry.* 1996 35; 1444-1449

Gimbrone MA Jr, Topper JN, Nagel T, Anderson KR, Garcia-Cardena G. Endothelial dysfunction, hemodynamic forces, and atherogenesis. *Ann N Y Acad Sci* 2000 May; 902: 230-9 discussion 239-40

Ginsberg HN. Insulin resistance and cardiovascular disease. *J Clin Invest.* 2000 vol 106; 4: 453-458

Giovanelli J, Campos KL, Kaufman S. Tetrahydrobiopterin, a cofactor for rat cerebellar nitric oxide synthase, does not function as a reductant in the oxygenation of arginine. *Proc. Natl. Acad. Sci. USA* 1991 88: 7091-7095

Gokce N, Keaney JF Jr, Hunter LM, Watkins MT, Nedeljkovic ZS, Menzoian JO, Vita JA. Predictive value of noninvasively determined endothelial dysfunction for long-term cardiovascular events in patients with peripheral vascular disease. *J Am Coll Cardiol.* 2003 May 21;41(10):1769-75

Golstein S, Czapski G. The reactio of NO^- with O_2^- and HO^{2-}: A pulse radiolysis study. *Free Radical Biol and Med.* 1995; 19: 505-510

Goonasekera C D A, Rees D D, Woolard P, Frend A, Shah V, Dillon M J. Nitric oxide synthase inhibitors and hypertension in children and adolescents. *J Hypertens* 1997 15: 901-909

Gordon D, Reidy MA, Benditt EP, Schwartz SM. Cell proliferation in human coronary arteries. *Proc Natl Acad Sci U S A* 1990 Jun; 87(12): 4600-4

Gorlach A, Brandes RP, Nguyen K, Amidi M, Dehghani F, Busse R. A gp91phox containing NADPH oxidase selectively expressed in endothelial cells is a major source of oxygen radical generation in the arterial wall. *Circulation Res* 2000 Jul 7; 87(1): 26-32

Griendling KK, Minieri CA, Ollerenshaw JD, Alexander RW. Angiotensin II stimulates NADH and NADPH oxidase activity in cultured vascular smooth muscle cells. *Circulation Res* 1994 Jun; 74(6): 1141-8

Griendling KK, Ushio-Fukai M. Redox control of vascular smooth muscle proliferation. *J Lab Clin Med* 1998 Jul; 132(1): 9-15

Griendling K K, Sorescu D, Ushio-Fukai M. NADPH Oxidase. Role in cardiovascular biology and disease. *Circulation Res* 2000 86; 494-501

Gutlich M, Jaeger E, Rucknagel KP, Werner T, Rodl W, Ziegler I, Bacher A. Human GTP cyclohydrolase I: only one out of three cDNA isoforms gives rise to the active enzyme. *Biochem J* 1994 Aug 15; 302 (Pt 1): 215-21

Guzik TJ, West NEJ, Black E, McDonald D, Ratnatunga C, Pillai R, Channon K. Functional Effect of the C242T Polymorphism in the NADPH Oxidase p22phox Gene on Vascular Superoxide Production in Atherosclerosis *Circulation.* 2000a; 102: 1744-1747

Guzik TJ, West NE, Black E, McDonald D, Ratnatunga C, Pillai R, Channon KM. Vascular superoxide production by NAD(P)H oxidase: association with endothelial dysfunction and clinical risk factors. *Circulation Res* 2000b May 12; 86(9): E85-90

Haffner SM, D'Agostino R, Mykkanen L, Tracy R, Howard B, Rewers M, Selby J, Savage P, Saad M. Insulin Sensitivity in Subjects with Type 2 Diabetes. *Diabetes Care* 1999 22; 562-568

Hall AV, Antoniou H, Wany Y, Cheung AH, Arbus AM, Olson SL, Lu WC, Kau CH, Marsden PA. Structural Organisation of the Human Neuronal Nitric Oxide Synthase Gene (*NOS1*). *J Biol Chem.* 1994 269: 33082-33090

Harada T, Kagamiyama H, Hatakeyama K. Feedback regulation mechanisms for the control of GTP cyclohydrolase I activity. *Science* 1993 Jun 4; 260(5113): 1507-10

Hardy GH. Mendelian Proportions in a mixed Popluation. *Science* 1908 Vol 28; 706: 49-50

Hatakeyama K, Inoue Y, Harada T, Kagamiyama H. Cloning and sequencing of cDNA encoding rat GTP cyclohydrolase I. The first enzyme of the tetrahydrobiopterin biosynthetic pathway. *J Biol Chem* 1991 Jan 15; 266(2): 765-9

Hattori Y, Gross SS. GTP cyclohydrolase I mRNA is induced by LPS in vascular smooth muscle: characterization, sequence and relationship to nitric oxide synthase. *Biochem Biophys Res Commun.* 1993 Aug 31; 195(1): 435-41

Hattori Y, Nakanishi N, Akimoto K, Yoshida M, Kasai K. HMG-CoA reductase inhibitor increases GTP cyclohydrolase I mRNA and tetrahydrobiopterin in vascular endothelial cells. *Arterioscler Thromb Vasc Biol.* 2003 Feb 1;23(2):176-82

Heinloth A, Heermeier K, Raff U, Wanner C, Galle J. Stimulation of NADPH oxidase by oxidized low-density lipoprotein induces proliferation of human vascular endothelial cells. *J Am Soc Nephrol.* 2000 Oct; 11(10): 1819-25

Heitzer T, Just H, Munzel T. Antioxidant vitamin C improves endothelial dysfunction in chronic smokers. *Circulation.* 1996 94; 6-9

Heitzer T, Brockhoff C, Mayer B, Warnholtz A, Mollnau H, Henne S, Meinertz T, Munzel T. Tetrahydrobiopterin improves endothelium-dependent vasodilation in chronic smokers : evidence for a dysfunctional nitric oxide synthase. *Circ Res.* 2000 Feb 4;86(2):E36-41

Heller R, Munscher-Paulig F, Graner R, Till U. L-Ascorbic acid potentiates nitric oxide synthesis in endothelial cells. *J Biol. Chem.* 1999 Vol. 274; No 12: 8254-8260

Heller R, Unbehaun A, Schellenberg B, Mayer B, Werner-Felmayer G, Werner ER. L-ascorbic acid potentiates endothelial nitric oxide synthesis via a chemical stabilization of tetrahydrobiopterin. *J Biol Chem.* 2001 Jan 5; 276(1): 40-7

Hingorani AD, Liang CF, Fatibene J, Lyon A, Monteith S, Parsons A, Haydock S, Hopper RV, Stephens NG, Shaughnessy KM, Brown MJ. A common Variant of the Endothelial Nitric Oxide Synthase (Glu298 Asp) Is a Major Risk Factor for Coronary Artery Disease in the UK. *Circulation.* 1999 100; 1515-1520

Hishikawa K, Luscher TF. Pulsatile stretch stimulates superoxide production in human aortic endothelial cells. *Circulation* 1997 Nov 18; 96(10): 3610-6

Hirayama K, Kapatos G. Regulation of GTP cyclohydrolase I gene expression and tetrahydrobiopterin content by nerve growth factor in cultures of superior cervical ganglia. *Neurochem Int* 1995 Aug; 27(2): 157-61

Hobbs HH, Brown MS, Goldstein JL. Molecular genetics of the LDL receptor gene in familial hypercholesterolemia. *Hum Mutat* 1992; 1(6): 445-66

Holden DP, Fickling SA, Whitley GS, Nussey SS. Plasma concentrations of asymmetric dimethylarginine, a natural inhibitor of nitric oxide synthase, in normal pregnancy and preeclampsia. *Am J Obstet Gynecol.* 1998 Mar;178(3):551-6

Hori T, Matsubara T, Ishibashi T, Higuchi K, Ochiai S, Takemoto M, Imai S, Nakagawa I, Ozaki K, Hatada K, Mezaki T, Tsuchida K, Nasuno A, Nishio M, Aizawa Y. Relationship between endothelial dysfunction and nitric oxide production in young male smokers. *J Cardiol.* 2001 Jul; 38(1): 21-8

Hornig B, Arakawa N, Kohler C, Drexler H. Vitamin C improves endothelial function of conduit arteries in patients with chronic heart failure. *Circulation.* 1998 Feb 3; 97(4): 363-8

Ichinose H, Ohye T, Takahashi E, Seki N, Hori T, Segawa M, Nomura Y, Endo K, Tanaka H, Tsuji S, et al. Hereditary progressive dystonia with marked diurnal fluctuation caused by mutations in the GTP cyclohydrolase I gene. *Nat Genet.* 1994 Nov; 8(3): 207-9

Ichinose H, Ohye T, Matsuda Y, Hori T, Blau N, Burlina A, Rouse B, Matalon R, Fujita K, Nagatsu T. Characterisation of mouse and human GTP Cyclohydrolase1 genes. Mutations in patients with GTP Cyclohydrolase 1 deficiency. *J Biol. Chem.* 1995 Vol. 270; 10062-10071.

Ignarro L J, Buga G M, Wood K S, Byrns R E, Chaudhuri G. Endothelium-derrived relaxing factor produced and released from artery and vein is nitric oxide. *Proc. Natl. Acad. Sci. USA.* 1987 Vol. 84; 9265-9269.

Imaizumi T, Hirooka Y, Masaki H, Harada S, Momohara M, Tagawa T, Takeshita A. Effects of L-arginine on forearm vessels and responses to acetylcholine. *Hypertension,* 1992 Vol 20: 511-517

Inoue N, Kawashima S, Kanazawa K, Yamada S, Akita H, Yokoyama M. Polymorphism of the NADH/NADPH oxidase p22 phox gene in patients with coronary artery disease. *Circulation* 1998 Jan 20; 97(2): 135-7

International Human Genome Sequencing Consortium. Initial Sequencing and Analysis of the Human Genome. *Nature* 2001Vol. 409; 860-921

Ito A, Tsoa P, Adimoolam S, Kimoto M, Ogawa T, Cooke JP. Novel mechanism for endothelial dysfunction. Dysregulation of dimethylarginine dimethylaminohydrolase *Circulation* 1999 99; 3092-3095

Ito D, Murata M, Watanabe K, Yoshida T, Saito I, Tanahashi N, Fukuuchi Y. C242T polymorphism of NADPH oxidase p22 PHOX gene and ischemic cerebrovascular disease in the Japanese population. *Stroke.* 2000 Apr; 31(4): 936-9

Jeerooburkhan N, Jones LC, Bujac S, Cooper JA, Miller GJ, Vallance P, Humphries SE, Hingorani AD. Genetic and environmental determinants of plasma nitrogen oxides and risk of ischemic heart disease. *Hypertension* 2001 Nov; 38(5): 1054-61

Joannides R, Haefeli WE, Linder L, Richard V, Bakkali EH, Thuillez C, Luscher TF. Nitric oxide is responsible for flow-dependent dilatation of human peripheral conduit arteries in vivo. *Circulation.* 1995 Mar 1;91(5):1314-1319

Jones LC, Tran CTL, Leiper JM, Hingorani AD, Vallance P. Common genetic variation in a basal promoter element alters DDAH2 expression in endothelial cells. *Biochem and Biophys Res Comm.* 2003;310(3):836-843.

Kakimoto Y, Akazawa S. Isolation and identification of N-G,N-G- and N-G,N'-G-dimethyl-arginine, N-epsilon-mono-, di-, and trimethyllysine, and glucosylgalactosyl- and galactosyl-delta-hydroxylysine from human urine. *J Biol Chem* 1970 Nov 10; 245(21): 5751-8

Kalisch BE, Bock NA, Davis WL, Rylett RJ. Inhibitors of nitric oxide synthase attenuate nerve growth factor-mediated increases in choline acetyltransferase expression in PC12 cells. *J Neurochem* 2002 May; 81(3): 624-35

Karantzoulis-Fegaras F, Antoniou H, Lai SL, Kulkarni G, D'Abreo C, Wong GK, Miller TL, Chan Y, Atkins J, Wang Y, Marsden PA. Characterization of the human endothelial nitric-oxide synthase promoter. *J Biol Chem* 1999 Jan 29; 274(5): 3076-93

Katusic ZS, Stelter A, Milstien S. Cytokines stimulate GTP cyclohydrolase I gene expression in cultured human umbilical vein endothelial cells. *Arterioscler Thromb Vasc Biol* 1998 Jan; 18(1): 27-32

Kaye DM, Vaddadi G, Gruskin SL, Du XJ, Esler MD. Reduced myocardial nerve growth factor expression in human and experimental heart failure. *Circulation Res* 2000 Apr 14; 86(7): E80-4

Kaye DM, Parnell MM, Ahlers BA. Reduced myocardial and systemic L-arginine uptake in heart failure. *Circulation Res* 2002 Dec 13; 91(12): 1198-203

Keavney B, McKenzie C, Parish S, Palmer A, Clark S, Youngman L, Delepine M, Lathrop M, Peto R, Collins R. Large-scale test of hypothesised associations between the angiotensin-converting-enzyme insertion/deletion polymorphism and myocardial infarction in about 5000 cases and 6000 controls. International Studies of Infarct Survival (ISIS) Collaborators. *Lancet.* 2000 Feb 5; 355(9202): 434-42

Keith M, Geranmayegan A, Sole MJ. Increased oxidative stress in patients with congestive heart failure. *J Am Coll Cardiol* 1998 31: 1352-1356

Kessler P, Bauersachs J, Busse R, Schini-Kerth VB. Inhibition of inducible nitric oxide synthase restores endothelium-dependent relaxations in proinflammatory mediator-induced blood vessels. *Arterioscler Thromb Vasc Biol* 1997 Sep; 17(9): 1746-55

Kielstein JT, Boger RH, Bode-Boger SM, Frolich JC, Haller H, Ritz E, Fliser D. Marked increase of asymmetric dimethylarginine in patients with incipient primary chronic renal disease. *J Am Soc Nephrol* 2002 Jan; 13(1): 170-6

Kikuchi H, Hikage M, Miyashita H, Fukumoto M. NADPH oxidase subunit, gp91(phox) homologue, preferentially expressed in human colon epithelial cells. *Gene* 2000 Aug 22; 254(1-2): 237-43

Klatt P, Schmidt M, Leopold E, Schmidt K, Werner E, Mayer B. The pteridine binding site of brain nitric oxide synthase. Tetrahydrobiopterin binding kinetics, specificity, and allosteric interaction with the substrate domain. *J. Biol Chem*, 1994 269: 13861-13866

Klatt P, Schmidt K, Lehner D, Glatter O, Bachinger H, Mayer B. Structural analysis of porcine brain nitric oxide synthase reveals a role for tetrahydrobiopterin and L-arginine in the formation of an SDS-resistant dimmer. *EMBO J*, 1995 14: 3687-3695

Koide S, Kugiyama K, Sugiyama S, Nakamura S, Fukushima H, Honda O, Yoshimura M, Ogawa H. Association of polymorphism in glutamate-cysteine ligase catalytic subunit gene with coronary vasomotor dysfunction and myocardial infarction. *J Am Coll Cardiol.* 2003 Feb 19;41(4):539-45

Kojda G, Harrison D. Interactions between NO and reactive oxygen species: pathophysiological importance in atherosclerosis, hypertension, diabetes and heart failure. *Cardiovasc Res.* 1999 Aug 15; 43(3): 562-71

Konishi H, Tanaka, M, Takemura Y, Matsuzaki H, Ono Y, Kikkawa, U, Nishizuka Y. Activation of protein kinase C by tyrosine phosphorylation in response to H_2O_2. *Proc. Natl. Acad. Sci. USA.* 1997; 94: 11233-11237

Kurioka S, Koshimura K, Murakami Y, Nishiki M, Kato Y. Reverse correlation between urine nitric oxide metabolites and insulin resistance in patients with type 2 diabetes mellitus. *Endocr J.* 2000 Feb; 47(1): 77-81.

Kuzkaya N, Weissmann N, Harrison DG, Dikalov S. Interactions of peroxynitrite, tetrahydrobiopterin, ascorbic acid, and thiols: implications for uncoupling endothelial nitric-oxide synthase. *J Biol Chem.* 2003 Jun 20; 278(25):22546-54. Epub 2003 Apr 10

Landmesser U, Merten R, Spiekermann S, Buttner K, Drexler H, Hornig B. Vascular extracellular superoxide dismutase activity in patients with coronary artery disease: relation to endothelium-dependent vasodilation. *Circulation* 2000 May 16; 101(19): 2264-70

Langenstroer P, Pieper GM. Regulation of spontaneous EDRF release in diabetic rat aorta by oxygen free radicals. *Am J Physiol*, 1992 263: H257-H265.

Lansink M, Koolwijk P, van Hinsbergh V, Kooistra T. Effect of steroid hormones and retinoids on the formation of capillary-like tubular structures of human microvascular endothelial cells in fibrin matrices is related to urokinase expression. *Blood* 1998 Aug 1; 92(3): 927-38

Lapize C, Pluss C, Werner ER, Huwiler A, Pfeilschifter J. Protein kinase C phosphorylates and activates GTP cyclohydrolase I in rat renal mesangial cells. *Biochem Biophys Res Commun* 1998 Oct 29; 251(3): 802-5

Laursen JB, Somers M, Kurz S, McCann L, Warnholtz A, Freeman BA, Tarpey M, Fukai T, Harrison DG. Endothelial regulation of vasomotion in apoE-deficient mice: implications for interactions between peroxynitrite and tetrahydrobiopterin. *Circulation.* 2001 Mar 6;103(9): 1282-8

Leeson CPM, Hingorani AD, Mullen MJ, Jeerooburkhan N, Kattenhorn M, Cole TJ, Muller DPR, Lucas A, Humphries SE, Deanfield JE. Glu298Asp Endothelial Nitric Oxide Synthase Gene Polymorphism Interacts With Environmental and Dietary Factors to Influence Endothelial Function. *Circulation Res.* 2002 90: 1153-1158

Leiper J, Sanya Maria J, Chubb A, MacAllister RJ, Charles IG, Whitley G, valance P. Identification of Two Human Dimethylarginine Dimethylaminohydrolases with Distinct Tissue Distribution and Homology to Microbial Arginine Deiminases. *Biochem J.* 1999 343; Pt.1: 209-214

Leiper J, Murray-Rust J, McDonald N, Vallance P. S-nitrosylation of dimethylarginine dimethylaminohydrolase regulates enzyme activity: further interactions between nitric oxide synthase and dimethylarginine dimethylaminohydrolase. *Proc Natl Acad Sci U S A* 2002 Oct 15; 99(21): 13527-32

Levine GN, Frei B, Koulouris SN, Gerhard MD, Keaney JF Jr, Vita JA. Ascorbic acid reverses endothelial vasomotor dysfunction in patients with coronary artery disease. *Circulation.* 1996 Mar 15; 93(6): 1107-13

Linscheid P, Schaffner A, Blau N, Schoedon G. Regulation of 6-pyruvoyltetrahydropterin synthase activity and messenger RNA abundance in human vascular endothelial cells. *Circulation* 1998 Oct 27; 98(17): 1703-6

Libby P, Aikawa M, Schonbeck U. Cholesterol and atherosclerosis. *Biochemica et Biophysica Acta* 2000 1529: 299-309

Lopez-Sanchez N, Frade JM. Control of the cell cycle by neurotrophins: lessons from the p75 neurotrophin receptor. *Histol Histopathol* 2002 Oct; 17(4): 1227-37

MacAllister RJ, Rambausek MH, Vallance P, Williams D, Hoffmann KH, Ritz E. Concentration of dimethyl-L-arginine in the plasma of patients with end-stage renal failure. *Nephrol Dial Transplant.* 1996 Dec; 11(12): 2449-52

Maeda T, Yoshimura T, Okamura H. Asymmetric dimethylarginine, an endogenous inhibitor of nitric oxide synthase, in maternal and fetal circulation. *J Soc Gynecol Investig.* 2003 Jan-Feb; 10(1): 2-4.

Maier W, Cosentino F, Lutolf RB, Fleisch M, Seiler C, Hess OM, Meier B, Luscher TF. Tetrahydrobiopterin improves endothelial function in patients with coronary artery disease. *J Cardiovasc Pharmacol.* 2000 Feb;35(2):173-8

Malatino LS, Benedetto FA, Mallamaci F, Tripepi G, Zoccali C, Parlongo S, Cutrupi S, Marino C, Panuccio V, Garozzo M, Candela V, Bellanuova I, Cataliotti A, Rapisarda F, Fatuzzo P, Bonanno G, Seminara G, Stancanelli B, Tassone F, Labate C Smoking,

blood pressure and serum albumin are major determinants of carotid atherosclerosis in dialysis patients. CREED Investigators. Cardiovascular Risk Extended Evaluation in Dialysis patients. *J Nephrol* 1999 Jul-Aug; 12(4): 256-60

Marenberg ME, Risch N, Berkman LF, Floderus B, de Faire U. Genetic susceptibility to death from coronary heart disease in a study of twins. *N Engl J Med* 1994 Apr 14; 330(15): 1041-6

Marsden PA, Schappert KT, Chen HS, Flowers M, Sundell CL, Wilcox JN, Lamas S, Michel T. Molecular cloning and characterization of human endothelial nitric oxide synthase. *FEBS Lett* 1992 Aug 3; 307(3): 287-93

Marsden PA, Heng HHQ, Scherer SW, Stewart RJ, Hall AV, Shi XM, Tsui LC, Schappert K. Structure and Chromosomal Lacalization of the Human Constitutive Endothelail Nitric Oxide Synthase Gene. *J Biol Chem* 1993; 268: 17478-17488.

Mazumder B, Seshadri V, Fox PL. Translational control by the 3'-UTR: the ends specify the means. *Trends Biochem Sci* 2003 Feb;28(2):91-8

McDonald KK, Zharikov S, Block ER, Kilberg MS. A caveolar complex between the cationic amino acid transporter 1 and endothelial nitric-oxide synthase may explain the "arginine paradox". *J Biol Chem* 1997 Dec 12; 272(50): 31213-6

McGill HC Jr, Herderick EE, McMahan CA, Zieske AW, Malcolm GT, Tracy RE, Strong JP. Atherosclerosis in youth. *Minerva Pediatr* 2002 Oct; 54(5): 437-47

McLean JR, Krishnakumar S, O'Donnell JM. Multiple mRNAs from the Punch locus of Drosophila melanogaster encode isoforms of GTP cyclohydrolase I with distinct N-terminal domains. *J Biol Chem* 1993 Dec 25; 268(36): 27191-7

McManus R, Moloney M, Borton M, Finch A, Chuan Y, Lawlor E, Weir DG, Kelleher D. Assciation of Celiac Disease with Microsatellite Polymorphisms Close to the Tumor Nectrosis Factor Genes. *Human Immunology* 1996; 45: 24-31

Meade TW, Mellows S, Brozovic M, Miller GJ, Chakrabarti RR, North WR, Haines AP, Stirling Y, Imeson JD, Thompson SG. Haemostatic function and ischaemic heart disease: principal results of the Northwick Park Heart Study. *Lancet* 1986 Sep 6; 2(8506): 533-7

Mehta J L, Lopez L M, Chen L, Cox OE. Alterations in nitric oxide synthase activity, superoxide anion generation and platelet aggregation in systemic hypertension, and effects of celiprolol. *Am J Cardiol*, 1994 74: 901-905

Mehta S, Stewart DJ, Levy RD. The hypotensive effect of L-arginine is associated with increased expired nitric oxide in humans. *Chest.* 1996 Jun; 109(6): 1550-5

Meier B, Jesaitis AJ, Emmendorffer A, Roesler J, Quinn MT. The cytochrome b-558 molecules involved in the fibroblast and polymorphonuclear leucocyte superoxide-generating NADPH oxidase systems are structurally and genetically distinct. *Biochem J* 1993 Jan 15; 289 (Pt 2): 481-6

Melichar B, Gregor J, Solichova D, Lukes J, Tichy M, Pidrman V. Increased urinary neopterin in acute myocardial infarction. *Clin Chem* 1994 Feb;40(2):338-9

Miller SA, Dykes DD, Polesky HF. A simple salting out procedure for extracting DNA from human nucleated cells. *Nucleic Acids Res* 1988 Feb 11; 16(3): 1215

Miyamoto Y, Saito Y, Kajiyama N, Yoshimura M, Shimasaki Y, Nakayama M, Kamitani S, Harada M, Ishikawa M, Kuwahara K, Ogawa E, Hamanaka I, Takahashi N, Kaneshige T, Teraoka H, Akamizu T, Azuma N, Yoshimasa Y, Yoshimasa T, Itoh H, Masuda I, Yasue H, Nakao K. Endothelial nitric oxide synthase gene is positively associated with essential hypertension. *Hypertension* 1998 Jul; 32(1): -8

Moncada S, Higgs A. The L-arginine-nitric oxide pathway. *N Engl J Med* 1993 Dec 30; 329(27): 2002-12

Morawietz H, Weber M, Rueckschloss U, Lauer N, Hacker A, Kojda G. Upregulation of vascular NAD(P)H oxidase subunit gp91phox and impairment of the nitric oxide signal transduction pathway in hypertension. *Biochem Biophys Res Commun* 2001 Aug 3; 285(5): 1130-5

Moshage H, Kok B, Huizenga JR, Jansen PL. Nitrite and nitrate determinations in plasma: a critical evaluation. *Clin Chem.* 1995 Jun; 41(6 Pt 1): 892-6

Mugge A, Elwell JH, Peterson TE, Hofmeyer TG, Heistad DD, Harrison DG. Chronic treatment with polyethylene-glycolated superoxide dismutase partially restores endothelium-dependent vascular relaxations in cholesterol-fed rabbits. *Circulation Res* 1991 Nov; 69(5): 1293-300

Mulder HJ, van Geel PP, Schalij MJ, van Gilst WH, Zwinderman AH, Bruschke AV; PREFACE trial. DD ACE gene polymorphism is associated with increased coronary artery endothelial dysfunction: the PREFACE trial. *Heart.* 2003 May;89(5):557-8

Murad F. Cyclic guanosine monophosphate as a mediator of vasodilation. *J Clin Invest.* 1986 78; 1-5

Murad F, Ishii K, Forstermann U, Gorsky L, Kerwin JF Jr, Pollock J, Heller M. EDRF is an intracellular second messanger and autocoid to regulate cGMP synthesis in many cells. *Adv Second Messanger Phosphoprotein Res.* 1990 24; 441-448

Murr C, Widner B, Wirleitner B, Fuchs D. Neopterin as a marker for immune system activation. *Curr Drug Metab* 2002 Apr; 3(2): 175-87

Murray-Rust J, Leiper J, McAlister M, Phelan J, Tilley S, Santa Maria J, Vallance P, McDonald N. Structural insights into the hydrolysis of cellular nitric oxide synthase inhibitors by dimethylarginine dimethylaminohydrolase. *Nature Struct Biol* 2001 Aug; 8(8): 679-83

Najbauer J, Johnson BA, Young AL, Aswad DW. Peptides with sequences similar to glycine, arginine-rich motifs in proteins interacting with RNA are efficiently recognized

by methyltransferase(s) modifying arginine in numerous proteins. *J Biol Chem.* 1993 May 15; 268(14): 10501-9.

Nakai K, Habano W, Fujita T, Nakai K, Schnackenberg J, Kawazoe K, Suwabe A, Itoh C. Highly multiplexed genotyping of coronary artery disease-associated SNPs using MALDI-TOF mass spectrometry. *Hum Mutat.* 2002 Aug; 20(2):133-8

Nakayama M, Yasue H, Yoshimura M, Shimasaki Y, Kugiyama K, Ogawa H, Motoyama T, Saito Y, Ogawa Y, Miyamoto Y, Nakao K. T-786-->C mutation in the 5'-flanking region of the endothelial nitric oxide synthase gene is associated with coronary spasm. *Circulation* 1999 Jun 8; 99(22): 2864-70

Nakiki T, Nakayama M, Kato R. Inhibition by nitric oxide and nitric oxide-producing vasodilators of DNA synthesis in vascular smooth muscle cells. *Eur. J. Pharmac.* 1990 189; 347-353.

Nelson SH, Steinsland OS, Wang Y, Yallampalli C, Dong YL, Sanchez JM. Increased nitric oxide synthase activity and expression in the human uterine artery during pregnancy. *Circulation Res.* 2000 Sep 1; 87(5): 406-11

Niederwieser A, Blau N, Wang M, Joller P, Atares M, Cardesa-Garcia J. GTP cyclohydrolase I deficiency, a new enzyme defect causing hyperphenylalaninemia with neopterin, biopterin, dopamine, and serotonin deficiencies and muscular hypotonia. *Eur J Pediatr* 1984 Feb; 141(4): 208-14

Node K, Kitakaze M, Yoshikawa H, Kosaka H, Hori M. Reduced plasma concentrations of nitrogen oxide in individuals with essential hypertension. *Hypertension.* 1997 Sep; 30(3 Pt 1): 405-8.

Noor R, Mittal, S, Iqbal J. Superoxide dismutase-applications and relevance to human diseases. *Med Sci Monit.* 2002; 8(9): 210-215.

Oemar BS, Tschudi MR, Godoy N, Brovkovich V, Malinski T, Luscher TF. Reduced endothelial nitric oxide synthase expression and production in human atherosclerosis. *Circulation* 1998 Jun 30; 97(25): 2494-8

Ogawa T, Kimoto M, Watanabe H, Sasaoka K. Metabolism of NG,NG-and NG,N'G-dimethylarginine in rats. *Arch Biochem Biophys* 1987 Feb 1; 252(2): 526-37

Ogawa T, Kimoto M, Sasaoka K. Purification and properties of a new enzyme, NG, NG-dimethylarginine dimethylaminohydrolase, from rat kidney. *J Biol Chem* 1989 Jun 15; 264(17): 10205-9

Ohara Y, Peterson T E, Harrison D G. Hypercholesterolemia increases endothelial superoxide anion production. *J Clin Investigation,* 1993 91: 2546-2551

Palmer RMJ, Ferrige AG, Moncada S. Nitric oxide release accounts for the biological effects of endothelium-derived relaxing factor. *Nature.* 1987 Vol. 327, 524-526.

Parkos CA, Dinauer MC, Walker LE, Allen RA, Jesaitis AJ, Orkin SH. Primary structure and unique expression of the 22-kilodalton light chain of human neutrophil cytochrome b. *Proc. Nat. Acad. Sci.* 1988. 85: 3319-3323

Parks CL, Shenk T. The serotonin 1a receptor gene contains a TATA-less promoter that responds to MAZ and Sp1. *J Biol Chem* 1996 Feb 23;271(8):4417-30

Patterson C, Ruef J, Madamanchi NR, Barry-Lane P, Hu Z, Horaist C, Ballinger CA, Brasier AR, Bode C, Runge MS. Stimulation of a vascular smooth muscle cell NAD(P)H oxidase by thrombin. Evidence that p47(phox) may participate in forming this oxidase in vitro and in vivo. *J Biol Chem* 1999 Jul 9; 274(28): 19814-22

Perret F, Bovet P, Shamlaye C, Paccaud F, Kappenberger L. High prevalence of peripheral atherosclerosis in a rapidly developing country. *Atherosclerosis* 2000 Nov; 153(1): 9-21

Pettersson A, Hedner T, Milsom I. Increased circulating concentrations of asymmetric dimethylarginine (ADMA), an endogenous inhibitor of nitric oxide synthesis, in preeclampsia. *Acta Obstet Gynecol Scand.* 1998 77; 808-813

Peunova N, Enikolopov G. Nitric oxide triggers a switch to growth arrest during differentiation of neuronal cells. *Nature* 1995 May 4; 375(6526): 68-73

Pieper GM. Acute amelioration of diabetic endothelial dysfunction with a derivative of the nitric oxide synthase cofactor, tetrahydrobioptrin. *J Cardiovasc Pharmacol.* 1997 Vol 29(1); 8-15

Pou S, Pou WS, Bredt DS, Snyder SH, Rosen GM. Generation of Superoxide by Purified Nitric Oxide Synthase. *J. Biol. Chem.* 1992 Vol. 267; No. 34: pp24173-24176

Promoega-Protocols and Application Guide, Third Edition, 1996

Pullin CH, Wilson JF, Ashfield-Watt PA, Clark ZE, Whiting JM, Lewis MJ, McDowell IF. Influence of methylenetetrahydrofolate reductase genotype, exercise and other risk factors on endothelial function in healthy individuals. *Clin Sci* (Lond). 2002 Jan;102(1):45-50.

Radomski MW, Palmer RMJ, Moncada S. Comparaitive pharmacology of endothelium-derived relaxing factor, nitric oxide and prostacyclin in platelets. *Br. J. Phamacol.* 1987a 92: 181-187.

Radomski M W, Palmer R M J, Moncada S. Endogenous Nitric Oxide Inhibits Human Platelet Adhesion to Vascular Endothelium. *The Lancet.* 1987b Nov 7, 1057-1058.

Rapoport R M, Draznin M B, Murad F. Endothelium-dependent relaxation in rat aorta may be mediated through cyclic GMP-dependent protein phosphorylation. *Nature,* 1983 Vol 306; 174-176.

Resnick N, Gimbrone MA Jr. Hemodynamic forces are complex regulators of endothelial gene expression. *FASEB J* 1995 Jul; 9(10): 874-82

Rees DD, Palmer RMJ, Hodson HF, Moncada S. A specific inhibitor of nitric oxide formation from L-arginine attenuates endothelium-dependent relaxation. *Br J Pharmacol*, 1989 96: 418-424

Rhodes P, Leone AM, Francis PL, Struthers AD, Moncada S, Rhodes PM [corrected to Rhodes P. The L-arginine:nitric oxide pathway is the major source of plasma nitrite in fasted humans. *Biochem Biophys Res Commun.* 1995 Apr 17; 209(2): 590-6.

Ribas G, Neville M, Wixon J L, Cheng J, Campbell R D. genes Encoding Three New Members of the Leukocyte Antigen 6 Superfamily and a Novel Member if Ig Superfamily, Together with Genes Encoding the Regulatory Nuclear Chloride Ion Channel Protein (Hrncc) and a Nw-Nw- Dimethylarginine Dimethylaminohydrolase Homolgue, Are Found in a 30kb Segment of the MHC Class 111 Region. *The Journal of Immunology* 1999 163; 278-287

Ross R. The pathogenesis of atherosclerosis: a perspective for the 1990s. *Nature* 1993 Apr 29; 362(6423): 801-9

Rossaak JI, Van Rij AM, Jones GT, Harris EL. Association of the 4G/5G polymorphism in the promoter region of plasminogen activator inhibitor-1 with abdominal aortic aneurysms. *J Vasc Surg* 2000 May;31(5):1026-32

Rossi GP, Cesari M, Zanchetta M, Colonna S, Maiolino G, Pedon L, Cavallin M, Maiolino P, Pessina AC. The T-786C endothelial nitric oxide synthase genotype is a novel risk factor for coronary artery disease in Caucasian patients of the GENICA study. *J Am Coll Cardiol.* 2003 Mar 19;41(6):930-7

Sarkar R, Meinberg EG, Stanley JC, Gordon D, Clinton Webb R. Nitric oxide reversibly inhibits the migration of cultured vascular smooth muscle cells. *Circ Res*, 1996 78; 225-230

Sattar N, Greer IA. Pregnancy complications and maternal cardiovascular risk: opportunities for intervention and screening? *BMJ* 2002 Jul 20;325(7356):157-60

Savvidou MD, Vallance PJT Nicolaides KH, Hingorani AD. Endothelial Nitric Oxide Synthase Gene Polymorphism and Maternal Vascular Adaptation to Pregnancy. *Hypertension.* 2001; 38: 1289-1293

Savvidou MD, Hingorani AD, Tsikas D, Frolich JC, Vallance P, Nicolaides KH. Endothelial dysfunction and raised plasma concentrations of asymmetric dimethylarginine in pregnant women who subsequently develop pre-eclampsia. *Lancet.* 2003 May 3; 361(9368): 1511-7

Schachinger V, Britten MB, Zeiher AM. Prognostic impact of coronary vasodilator dysfunction on adverse long-term outcome of coronary heart disease. *Circulation.* 2000 Apr 25;101(16):1899-906

Schachinger V, Britten MB, Dimmeler S, Zeiher AM. NADH/NADPH oxidase p22 phox gene polymorphism is associated with improved coronary endothelial vasodilator function. *Eur Heart J* 2001 Jan; 22(1): 96-101

Schennach H, Murr C, Gachter E, Mayersbach P, Schonitzer D, Fuchs D. Factors influencing serum neopterin concentrations in a population of blood donors. *Clin Chem* 2002;48(4):643-5

Schmidt RJ, Baylis C. Total nitric oxide production is low in patients with chronic renal disease. *Kidney Int.* 2000 Sep; 58(3): 1261-6

Schumacher M, Halwachs G, Tatzber F, Fruhwald FM, Zweiker R, Watzinger N, Eber B, Wilders-Truschnig M, Esterbauer H, Klein W. Increased neopterin in patients with chronic and acute coronary syndromes. *J Am Coll Cardiol* 1997 Sep;30(3):703-7

Sellers A, Murphy G. Collagenolytic enzymes and their naturally occurring inhibitors. *Int Rev Connect Tissue Res* 1981; 9:151-90

Shiose A, Kuroda J, Tsuruya K, Hirai M, Hirakata H, Naito S, Hattori M, Sakaki Y, Sumimoto H. A novel superoxide-producing NAD(P)H oxidase in kidney. *J Biol Chem* 2001 Jan 12; 276(2): 1417-23

Sikkema JM, van Rijn BB, Franx A, Bruinse HW, de Roos R, Stroes ES, van Faassen EE. Placental superoxide is increased in pre-eclampsia. *Placenta* 2001 Apr; 22(4): 304-8

Smilde TJ, van Wissen S, Wollersheim H, Kastelein JJ, Stalenhoef AF. Genetic and metabolic factors predicting risk of cardiovascular disease in familial hypercholesterolemia. *Neth J Med* 2001 Oct; 59(4): 184-95

Smith GC, Pell JP, Walsh D. Pregnancy complications and maternal risk of ischaemic heart disease: a retrospective cohort study of 129,290 births. *Lancet.* 2001 Jun 23;357(9273):2002-6

Solzbach U, Hornig B, Jeserich M, Just H. Vitamin C improves endothelial dysfunction of epicardial coronary arteries in hypertensive patients. *Circulation.* 1997 Sep 2; 96(5): 1513-9.

Sorescu D, Weiss D, Lassegue B, Clempus RE, Szocs K, Sorescu GP, Valppu L, Quinn MT, Lambeth JD, Vega JD, Taylor WR, Griendling KK. Superoxide production and expression of nox family proteins in human atherosclerosis. *Circulation* 2002 Mar 26; 105(12): 1429-35

Stasia MJ, Lardy B, Maturana A, Rousseau P, Martel C, Bord igoni P, Demaurex N, Morel F. Molecular and functional characterization of a new X-linked chronic granulatomous disease variant ($X91^+$) case with a double missense mutation in the cytosolic gp91phox C-terminal tail. *Biochimica et Biophysica Acta* 2002; 1586: 316-330

Stroes E, Kastelein J, Cosentino F, Erkelens W, Wever R, Koomans H, Luscher T, Rabelink T. Tetrahydrobiopterin restores Endothelial Function in Hypercholesterolemia. *J. Clin Invest.* 1997 Vol. 99; Number 1: 41-46

Stroes ESG, Van Faassen EE, Yo M, Martasek P, Boer P, Govers R, Rabelink TJ. Folic Acid Reverts Dysfunction of Endothelial Nitric Oxide Synthase. *Circ Res* 2000 :86: 1129-1134

Stuehr DJ. Mammalian nitric oxide synthases. *Biochim Biophys Acta* 1999 May 5; 1411(2-3): 217-30

Stuhlinger MC, Abbasi F, Chu JW, Lamendola C, McLaughlin TL, Cooke JP, Reaven GM, Tsao PS. Relationship between insulin resistance and an endogenous nitric oxide synthase inhibitor. *JAMA* 2002 Vol.287; 11: 1420-1426.

Suh YA, Arnold RS, Lassegue B, Shi J, Xu X, Sorescu D, Chung AB, Griendling KK, Lambeth JD. Cell transformation by the superoxide-generating oxidase Mox1. *Nature* 1999 Sep 2; 401(6748): 79-82

Surdacki A, Nowicki M, Sandmann J, Tsikas D, Boeger RH, Bode-Boeger SM, Kruszelnicka-Kwaitkowska O, Franciszek D, Jacek S, Froelich JC. Reduced Urinary Excretion of Nitric Oxide Metabolites and Increased Plasma Levels of Asymmetric Dimethylarginine in Men with Essential Hypertension. *J. Cardiovasc. Pharmacol.* 1999 Vol.33(4): 652-658

Suwaidi JA, Hamasaki S, Higano ST, Nishimura RA, Holmes DR Jr, Lerman A. Long-term follow-up of patients with mild coronary artery disease and endothelial dysfunction. *Circulation.* 2000 Mar 7;101(9):948-54.

Tanaka S, Yashiro A, Nakashima Y, Nanri H, Ikeda M, Kuroiwa A. Plasma nitrite/nitrate level is inversely correlated with plasma low-density lipoprotein cholesterol level. *Clin Cardiol.* 1997 Apr; 20(4): 361-5

Tatchum-Tolum R, Schulz R, McNeill R, Khadour FH. Upregulation of neuronal nitric oxide synthase in skeletal muscle by swim training. *Am J Physiol Heart Circ Physiol,* 2000 279: H1757-H1766

Tatzber F, Rabl H, Koriska K, Erhart U, Puhl H, Waeg G, Krebs A, Esterbauer H. Elevated serum neopterin levels in atherosclerosis. *Atherosclerosis* 1991 Aug;89(2-3):203-8

Terashima M, Akita H, Kanazawa K, Inoue N, Yamada S, Ito K, Matsuda Y, Takai E, Iwai C, Kuragane H, Yoshida Y, Yokoyama M. Stromelysin Promoter 5A/6A Polymorphism Is Associated With Acute Myocardial Infarction. *Circulation* 1999 99: 2717-2719.

Tesauro M, Thompson WC, Rogliani P, Qi L, Chaudhary PP, Moss J. Intracellular processing of endothelial nitric oxide synthase isoforms associated with differences in severity of cardiopulmonary diseases: cleavage of proteins with aspartate vs. glutamate at position 298. *Proc Natl Acad Sci U S A.* 2000 Mar 14;97(6):2832-5

The International SNP Map Working Group. A map of human genome sequence variation containing 1.42 million single nucleotide polymorphisms. *Nature* 2001 409: 928-933
Thomson G. HLA disease associations: models for insulin dependent diabetes mellitus and the study of complex human genetic disorders. *Annu Rev Genet* 1988; 22: 31-50

Thony B, Blau N. Mutations in the GTP cyclohydrolase I and 6-pyruvoyl-tetrahydropterin synthase genes. *Hum Mutation.* 1997; 10(1): 11-20

Thony B, Auerbach G, Blau N. Tetrahydrobiopterin biosynthesis, regeneration and function. *Biochem J.* 2000 347, 1-16.

Ting HH, Timimi FK, Boles KS, Creager SJ, Ganz P, Creager MA. Vitamin C improves endothelium-dependent vasodilation in patients with non-insulin-dependent diabetes mellitus. *J Clin Invest.* 1996 Jan 1; 97(1): 22-8.

Ting HH, Timimi FK, Haley EA, Roddy MA, Ganz P, Creager MA. Vitamin C improves endothelium-dependent vasodilation in forearm resistance vessels of humans with hypercholesterolemia. *Circulation.* 1997 Jun 17; 95(12): 2617-22.

Togari A, Ichinose H, Matsumoto S, Fujita K, Nagatsu T. Multiple mRNA forms of human GTP cyclohydrolase I. *Biochem Biophys Res Commun* 1992 Aug 31; 187(1): 359-65

Topper JN, Gimbrone MA Jr. Blood flow and vascular gene expression: fluid shear stress as a modulator of endothelial phenotype. *Mol Med Today* 1999 Jan; 5(1): 40-6

Tousoulis D, Davies GJ, Tentolouris C, Crake T, Katsimaglis G, Stefanadis C, Toutouzas P. Effects of Changing the Availability of the Substrate for Nitric Oxide Synthase by L-Arginine Administration on Coronary Vasometer Tone in Angina Patients With Angiographically Narrowed and in Patients With Normal Coronary Arteries. *Am J Cardiol* 1998 Vol 82: 1110-1113

Tran CT, Fox MF, Vallance P, Leiper JM. Chromosomal localization, gene structure, and expression pattern of DDAH1: comparison with DDAH2 and implications for evolutionary origins. *Genomics* 2000 Aug 15; 68(1): 101-5

Tsukada T, Yokoyama K, Arai T, Takemoto F, Hara S, Yamada A, Kawaguchi Y, Hosoya T, Igari J. Evidence of association of the ecNOS gene polymorphism with plasma NO metabolite levels in humans. *Biochem Biophys Res Commun.* 1998 Apr 7; 245(1): 190-3.

Ueda S, Matsuoka H, Miyazaki H, Usui M, Okuda S, Imaizumi T. Tetrahydrobiopterin Restores Endothelial Function in Long-Term Smokers. *J Am Coll Cardio.* 2000; 35: 71-75

Usui M, Matsuoka H, Miyazaki H, Ueda S, Okuda S, Imaizumi T. Increased endogenous nitric oxide synthase inhibitor in patients with congestive heart failure. *Life Sci* 1998; 62(26): 2425-30

Vallance P, Collier J, Moncada S. Effects of endothelium-derived nitric oxide on peripheral arterial tone in man. *Lancet*, 1989 2: 997-1000

Vallance P, Leone A, Calver A, Collier J, Moncada S. Accumulation of an Endogenous Inhibitor of Nitric Oxide Synthesis in Chronic Renal Failure. *Lancet* 1992 339; 572-75.

Vallance P, Chan N. Endothelial function and nitric oxide: clinical relevance. *Heart* 2001 Mar; 85(3): 342-50

Van Heerebeek L, Meischl C, Stooker W, Meijer CJ, Niessen HW, Roos D. NADPH oxidase(s): new source(s) of reactive oxygen species in the vascular system? *J Clin Pathol* 2002 Aug;55(8): 561-8

Virchow R. Der ateromatose Prozess der Arterien. *Wein Med Wochenschr* 1856; 6: 852-1

Vasquez-Vivar J, Hogg N, Martasek P, Karoui H, Pritchard KA, Kalyanaraman B. Tetrahydrobiopterin-dependent inhibition of superoxide generation from neuronal nitric oxide synthase. *J Biol Chem*, 1999 Vol 274; 38: 26736-26742

Vita JA, Treasure CB, Nabel EG, McLenachan JM, Fish RD, Yeung AC, Vekshtein VI, Selwyn AP, Ganz P. Coronary vasomotor response to acetylcholine relates to risk factors for coronary artery disease. *Circulation.* 1990 Feb;81(2):491-7.

Wahbi N, Dalton RN, Turner C, Denton M, Abbs I, Swaminathan R. Dimethylarginines in chronic renal failure. *J Clin Pathol.* 2001 Jun; 54(6): 470-3

Wald DS, Law M, Morris JK. Homocysteine and cardiovascular disease: evidence on causality from a meta-analysis. *BMJ.* 2002 Nov 23; 325(7374): 1202.

Wang J, Stuehr DJ, Ikeda-Saito M, Rousseau DL. Haem coordination and structure of the catalytic site in nitric oxide synthase. *J Biol Chem*, 1993 268: 22255-22258

Wang J, Stuehr DJ, Rousseau DL. Tetrahydrobiopterin-deficient nitric oxide synthase has a modified haem environment and forms a cytochrome P-450 analogue. *Biochemistry*, 1995 34: 7080-7087.

Wang XL, Sim AS, Badenhop RF, McCredie RM, Wilcken DE. A smoking-dependent risk of coronary artery disease associated with a polymorphism of the endothelial nitric oxide synthase gene. *Nat Med.* 1996 Jan; 2(1): 41-5

Wang XL, Mahaney MC, Sim AS, Wang J, Wang J, Blangero J, Almasy L, Badenhop RB, Wilcken DE. Genetic contribution of the endothelial constitutive nitric oxide synthase gene to plasma nitric oxide levels. *Arterioscler Thromb Vasc Biol.* 1997 Nov; 17(11): 3147-53.

Weber C, Erl W, Pietsch A, Strobel M, Ziegler-Heitbrock HW, Weber PC. Antioxidants inhibit monocyte adhesion by suppressing nuclear factor-kappa B

mobilization and induction of vascular cell adhesion molecule-1 in endothelial cells stimulated to generate radicals. *Arterioscler Thromb* 1994 Oct; 14(10): 1665-73

Weinberg JB, Granger DL, Pisetsky DS, Seldin MF, Misukonis MA, Mason SN, Pippen AM, Ruiz P, Wood ER, Gilkeson GS. The role of nitric oxide in the pathogenesis of spontaneous murine autoimmune disease: increased nitric oxide production and nitric oxide synthase expression in MRL-lpr/lpr mice, and reduction of spontaneous glomerulonephritis and arthritis by orally administered NG-monomethyl-L-arginine. *J Exp Med* 1994 Feb 1; 179(2): 651-60

Weiss G, Willeit J, Kiechl S, Fuchs D, Jarosch E, Oberhollenzer F, Reibnegger G, Tilz GP, Gerstenbrand F, Wachter H. Increased concentrations of neopterin in carotid atherosclerosis. *Atherosclerosis* 1994 Apr;106(2):263-71

Werner-Felmayer G, Werner ER, Fuchs D, Hausen A, Reibnegger G, Wachter H. Tumour necrosis factor-alpha and lipopolysaccharide enhance interferon-induced tryptophan degradation and pteridine synthesis in human cells. *Biol Chem Hoppe Seyler* 1989 Sep;370(9):1063-9

Werner-Felmayer G, Werner ER, Fuchs D, Hausen A, Reibnegger G, Schmidt K, Weiss G, Wachter H. Pteridine biosynthesis in human endothelial cells. Impact on nitric oxide-mediated formation of cyclic GMP. *J Biol Chem* 1993 Jan 25; 268(3): 1842-6

Werner ER, Werner-Felmayer G, Fuchs D, Hausen A, Reibnegger G, Yim JJ, Pfleiderer W, Wachter H. Tetrahydrobiopterin biosynthetic activities in human macrophages, fibroblasts, THP-1, and T 24 cells. GTP-cyclohydrolase I is stimulated by interferon-gamma, and 6-pyruvoyl tetrahydropterin synthase and sepiapterin reductase are constitutively present. *J Biol Chem* 1990 Feb 25; 265(6): 3189-92

Wever RMF, Dam T, Rijn HJM, de Groot F, Rabelink TJ. Tetrahydrobiopterin regulates superoxide generation by recombinant endothelial nitric oxide synthase. *Biochem and Biophys Res Com,* 1997 237; 340-344.

Wheeler DC. Cardiovascular disease in patients with chronic renal failure. *Lancet* 1996 Dec 21-28; 348(9043): 1673-4

White JW Jr. Relative significance of dietary sources of nitrate and nitrite. *J Agric Food Chem.* 1975 Sep-Oct;23(5):886-91

Wilson BJ, Watson MS, Prescott GJ, Sunderland S, Campbell DM, Hannaford P, Smith WC. Hypertensive diseases of pregnancy and risk of hypertension and stroke in later life: results from cohort study. *BMJ.* 2003 Apr 19;326(7394):845.

Witter K, Werner T, Blusch JH, Schneider EM, Riess O, Ziegler I, Rodl W, Bacher A, Gutlich M. Cloning, sequencing and functional studies of the gene encoding human GTP cyclohydrolase I. *Gene* 1996 Jun 1; 171(2): 285-90

Witztum JL. The role of oxidized LDL in atherosclerosis. *Adv Exp Med Biol* 1991; 285:353-65

Xia Y, Tsau A, Berka, V, Zweier JL. Superoxide generation from endothelial nitric oxide synthase. A Ca^{2+}/ calmodulin-dependent and tetrahydrobiopterin regulatory process. *J Biol Chem*, 1998 Vol. 273; Issue 40: 25804-25808

Yamada M, Ariga T, Kawamura N, Ohtsu M, Imajoh-Ohmi S, Ohshika E, Tatsuzawa O, Kobayashi K, Sakiyama Y. Genetic studies of three Japanese patients with p22-phox-deficient chronic granulomatous disease: detection of a possible common mutant CYBA allele in Japan and a genotype-phenotype correlation in these patients. *Br J Haematol* 2000 Mar; 108(3): 511-7

Yamada Y, Izawa H, Ichihara S, Takatsu F, Ishihara H, Hirayama H, Sone T, Tanaka M, Yokota M. Prediction of the risk of myocardial infarction from polymorphisms in candidate genes. *N Engl J Med* 2002 Dec 12; 347(24): 1916-23

Ye S, Watts GF, Mandalia S, Humphries SE, Henney AM. Preliminary report: genetic variation in the human stromelysin promoter is associated with progression of coronary atherosclerosis. *Br Heart J* 1995 Mar;73(3):209-15

Ye S, Eriksson P, Hamsten A, Kurkinen M, Humphries SE, Henney AM. Progression of coronary atherosclerosis is associated with a common genetic variant of the human stromelysin-1 promoter which results in reduced gene expression. *J Biol Chem* 1996 May 31; 271(22):13055-60

Yoneyama T, Brewer JM, Hatakeyama K. GTP cyclohydrolase I feedback regulatory protein is a pentamer of identical subunits. Purification, cDNA cloning, and bacterial expression. *J Biol Chem* 1997 Apr 11; 272(15): 9690-6

Yoshimura M, Yasue H, Nakayama M, Shimasaki Y, Sumida H, Sugiyama S, Kugiyama K, Ogawa H, Ogawa Y, Saito Y, Miyamoto Y, Nakao K. A missense Glu298Asp variant in the endothelial nitric oxide synthase gene is associated with coronary spasm in the Japanese. *Hum Genet.* 1998 Jul; 103(1): 65-9.

Yoshimura T, Yoshimura M, Tabata A, Shimasaki Y, Nakayama M, Miyamoto Y, Saito Y, Nakao K, Yasue H, Okamura H. Association of the missense Glu298Asp variant of the nitric oxide synthase gene with severe preeclampsia. *J Soc Gynecol Investig.* 2000 7. 238-241.

Zarins CK, Giddens DP, Bharadvaj BK, Sottiurai VS, Mabon RF, Glagov S. Carotid bifurcation atherosclerosis. Quantitative correlation of plaque localization with flow velocity profiles and wall shear stress. *Circulation Res* 1983 Oct; 53(4): 502-14

Zdravkovic S, Wienke A, Pedersen NL, Marenberg ME, Yashin AI, De Faire U. Heritability of death from coronary heart disease: a 36-year follow-up of 20 966 Swedish twins. *J Intern Med* 2002 Sep; 252(3): 247-54

Zhang H, Schmeisser A, Garlichs CD, Plotze K, Damme U, Mugge A, Daniel WG. Angiotensin II-induced superoxide anion generation in human vascular endothelial cells: role of membrane-bound NADH-/NADPH-oxidases. *Cardiovascular Res* 1999 Oct; 44(1): 215-22

Zoccali C, Bode-Boger S, Mallamaci F, Benedetto F, Tripepi G, Malatino L, Cataliotti A, Bellanuova I, Fermo I, Frolich J, Boger R. Plasma concentration of asymmetrical dimethylarginine and mortality in patients with end-stage renal disease: a prospective study. *Lancet* 2001 Dec 22-29; 358(9299): 2113-7